U.S. Department
of Transportation
Federal Highway
Administration

October 1996

Seismic Design of Bridges Design Example No. 6

Three-Span Continuous CIP Concrete Box Bridge

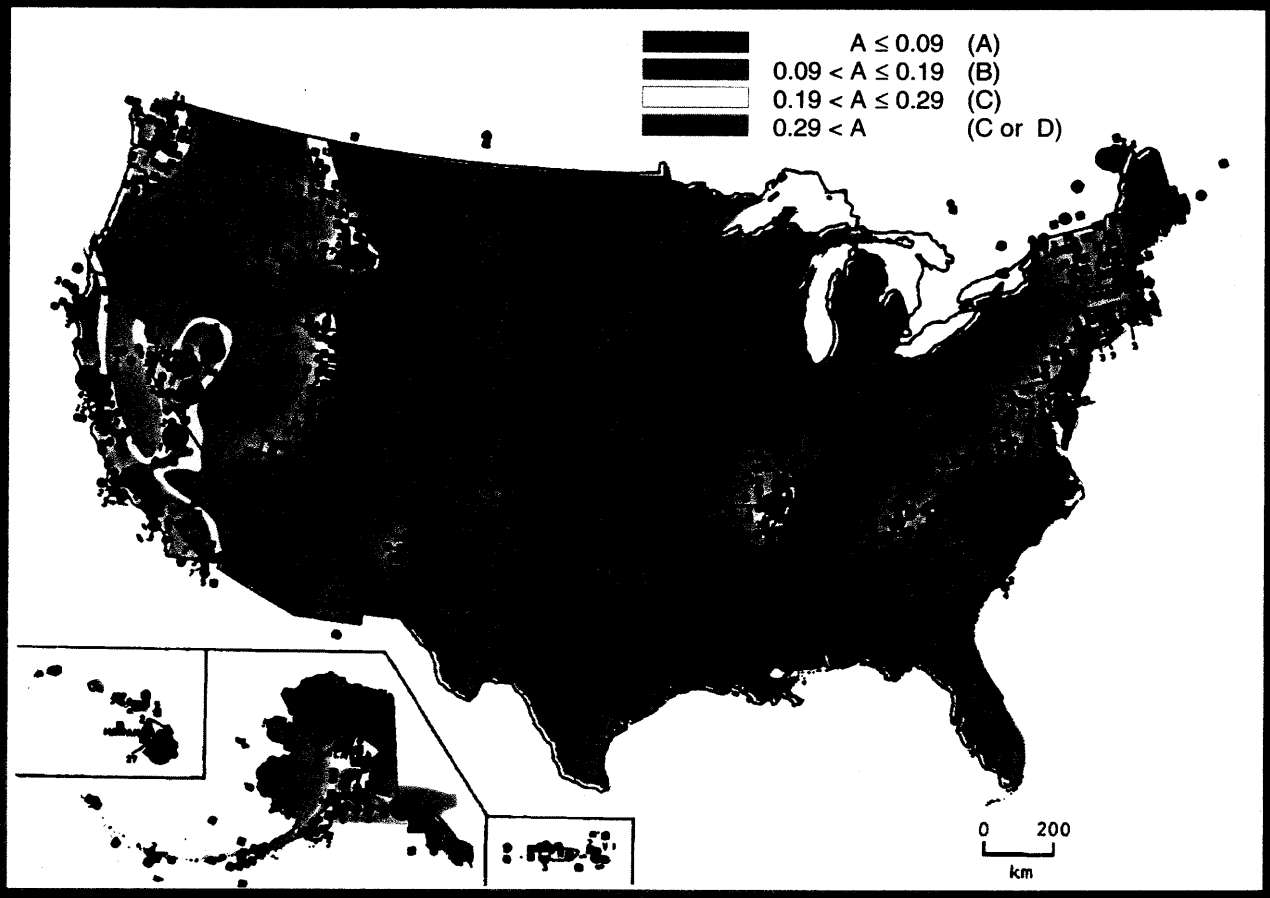

Publication No. FHWA-SA-97-011

Seismic Design Course

Design Example No. 6

Prepared for

U.S. Department of Transportation
Federal Highway Administration
Central Federal Lands Highway Division

September 1996

Prepared by

BERGER/ABAM Engineers Inc.
33301 Ninth Avenue South, Suite 300
Federal Way, Washington 98003-6395

Job No. A95013

ACKNOWLEDGMENTS

The Federal Highway Administration gratefully acknowledges the contributions to this project from the following individuals. Their efforts greatly assisted the project to meet the objective of providing training materials that meet the needs of the appliers of the AASHTO Bridge Seismic Design Specification.

Steering Group

Ian Buckle
John Clark
James Cooper
Edward Dortignac
James Gates
Hamid Ghasemi
Paul Grant
John Hooks
Dick Jobes
James Keeley
Gary Kasza
Antonio Nieves
Tom Pfister
Walter Podolny
Phil Rabb
Michael Whitney
Mark Whittemore
Philip Yen

Design Example Development

Robert Griebenow
James Guarre
Susan Johnson
Lee Marsh
Robert Mast
Chuck Spry
Warren Wilson

Many others contributed to this project by providing information and suggestions. Their efforts contributed greatly, and the Federal Highway Administration gratefully acknowledges their assistance.

PLEASE NOTE

Data, specifications, suggested practices, and drawings presented herein are based on the best available information, are delineated in accord with recognized professional engineering principles and practices, and are provided for general information only. None of the procedures suggested or discussed should be used without first securing competent advice regarding their suitability for any given application.

This document was prepared with the help and advice of FHWA, State, academic, and private engineers. The intent of this document is to aid practicing engineers in the application of the AASHTO seismic design specification. BERGER/ABAM and the United States Government assume no liability for its contents or use thereof.

TABLE OF CONTENTS

TABLE OF CONTENTS (continued)

LIST OF FIGURES (continued)

LIST OF FIGURES (continued)

LIST OF FIGURES (continued)

LIST OF FIGURES (continued)

LIST OF TABLES (continued)

LIST OF TABLES (continued)

LIST OF TABLES (continued)

Section I
Introduction

PURPOSE OF DESIGN EXAMPLE

This is the sixth in a series of seismic design examples developed for the FHWA. A different bridge configuration is used in each example. The bridges are in either Seismic Performance Category B or C sites. Each example emphasizes different features that must be considered in the seismic analysis and design process. The matrix below is a summary of the features of the first seven examples.

DESIGN EXAMPLE NO.	DESIGN EXAMPLE DESCRIPTION	SEISMIC CATEGORY	PLAN GEOMETRY	SUPER-STRUCTURE TYPE	PIER TYPE	ABUTMENT TYPE	FOUNDATION TYPE	CONNECTIONS AND JOINTS
1	Two-Span Continuous	SPC - C	Tangent Square	CIP Concrete Box	Three-Column Integral Bent	Seat Stub Base	Spread Footings	Monolithic Joint at Pier Expansion Bearing at Abutment
2	Three-Span Continuous	SPC - B	Tangent Skewed	Steel Girder	Wall Type Pier	Tall Seat	Spread Footings	Elastomeric Bearing Pads (Piers and Abutments)
3	Single-Span	SPC - C	Tangent Square	AASHTO Precast Concrete Girders	(N/A)	Tall Seat (Closed-In)	Spread Footings	Elastomeric Bearing Pads
4	Three-Span Continuous	SPC - C	Tangent Skewed	CIP Concrete	Two-Column Integral Bent	Seat	Spread Footings	Monolithic at Col. Tops Pinned Column at Base Expansion Bearings at Abutments
5	Nine-Span Viaduct with Four-Span and Five-Span Continuous Structs.	SPC - B	Curved Square	Steel Girder	Single-Column (Variable Heights)	Seat	Steel H-Piles	Conventional Steel Pins and PTFE Sliding Bearings
6	Three-Span Continuous	SPC - C	Sharply-Curved Square	CIP Concrete Box	Single Column	Monolithic	Drilled Shaft at Piers, Steel Piles at Abutments	Monolithic Concrete Joints
7	12-Span Viaduct with (3) Four-Span Structures	SPC - B	Tangent Square	AASHTO Precast Concrete Girders	Pile Bents (Battered and Plumb)	Seat	Concrete Piles and Steel Piles	Pinned and Expansion Bearings

REFERENCE AASHTO SPECIFICATIONS

The examples conform to the following specifications.

AASHTO Division I (herein referred to as "Division I")

Standard Specifications for Highway Bridges, American Association of State Highway and Transportation Officials, Inc., 15th Edition, as amended by the Interim Specifications-Bridges-1993 through 1995.

AASHTO Division I-A (herein referred to as "Division I-A" or the "Specification")

Standard Specifications for Highway Bridges, Division I-A, Seismic Design, American Association of State Highway and Transportation Officials, Inc., 15th Edition, as amended by the Interim Specifications-Bridges-1995.

FLOWCHARTS AND DESIGN STEPS

This third example follows the outline given in detailed flowcharts presented in Section II, Flowcharts. The flowcharts include a main chart, which generally follows the one currently used in AASHTO Division I-A, and several subcharts that detail the operations that occur for each Design Step.

The purpose of Design Steps is to present the information covered by the example in a logical and sequential manner that allows for easy referencing within the example itself. Each Design Step has a unique number in the left margin of the calculation document. The title is located to the right of the Design Step number. Where appropriate, a reference to either Division I or Division I-A of the AASHTO Specification follows the title.

An example is shown below.

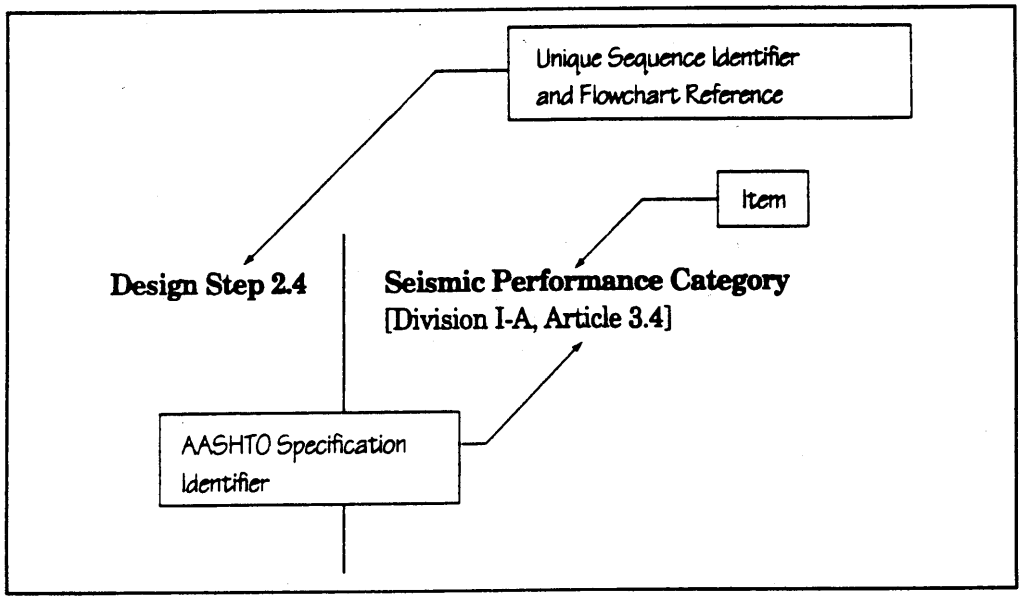

USE OF DIFFERENT TYPE FONTS

In the example, two primary type fonts have been used. One font, similar to the type used for textbooks, is used for all section headings and for commentary. The other, an architectural font that appears hand printed, is used for all primary calculations. The material in the architectural font is the essential calculation material and essential results.

An example of the use of the fonts is shown below.

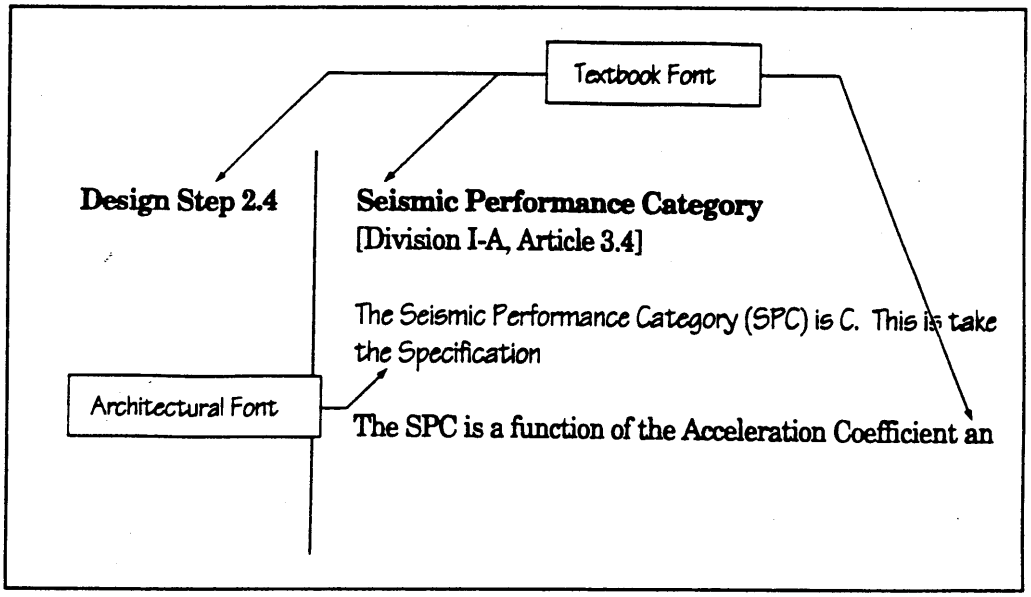

USE OF MATHCAD®

To provide consistent results and quality control, all calculations have been performed using the program Mathcad®.

The variables used in equations calculated by the program are defined before the equation, and the **definition** of either a variable or an equation is distinguished by a ':=' symbol. The **echo** of a variable or the result of a calculation is distinguished by a '=' symbol, i.e., no colon is used.

An example is shown below.

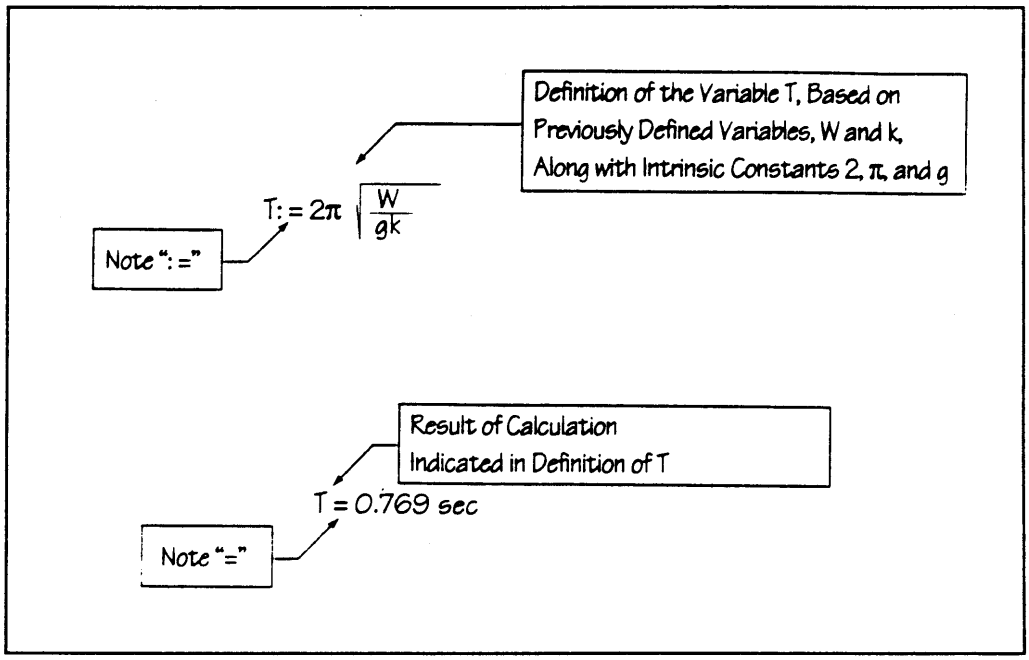

Note that Mathcad® carries the full precision of the variables throughout the calculations, even though the listed result of a calculation is rounded off. Thus, hand-calculated checks made using intermediate rounded results may not yield the same result as the number being checked.

Also, Mathcad® does not allow the superscript " ′ " to be used in a variable name. Therefore, the specified compressive strength of concrete is defined as f_c in this example (not f'_c).

Section II
Flowcharts

FLOWCHARTS

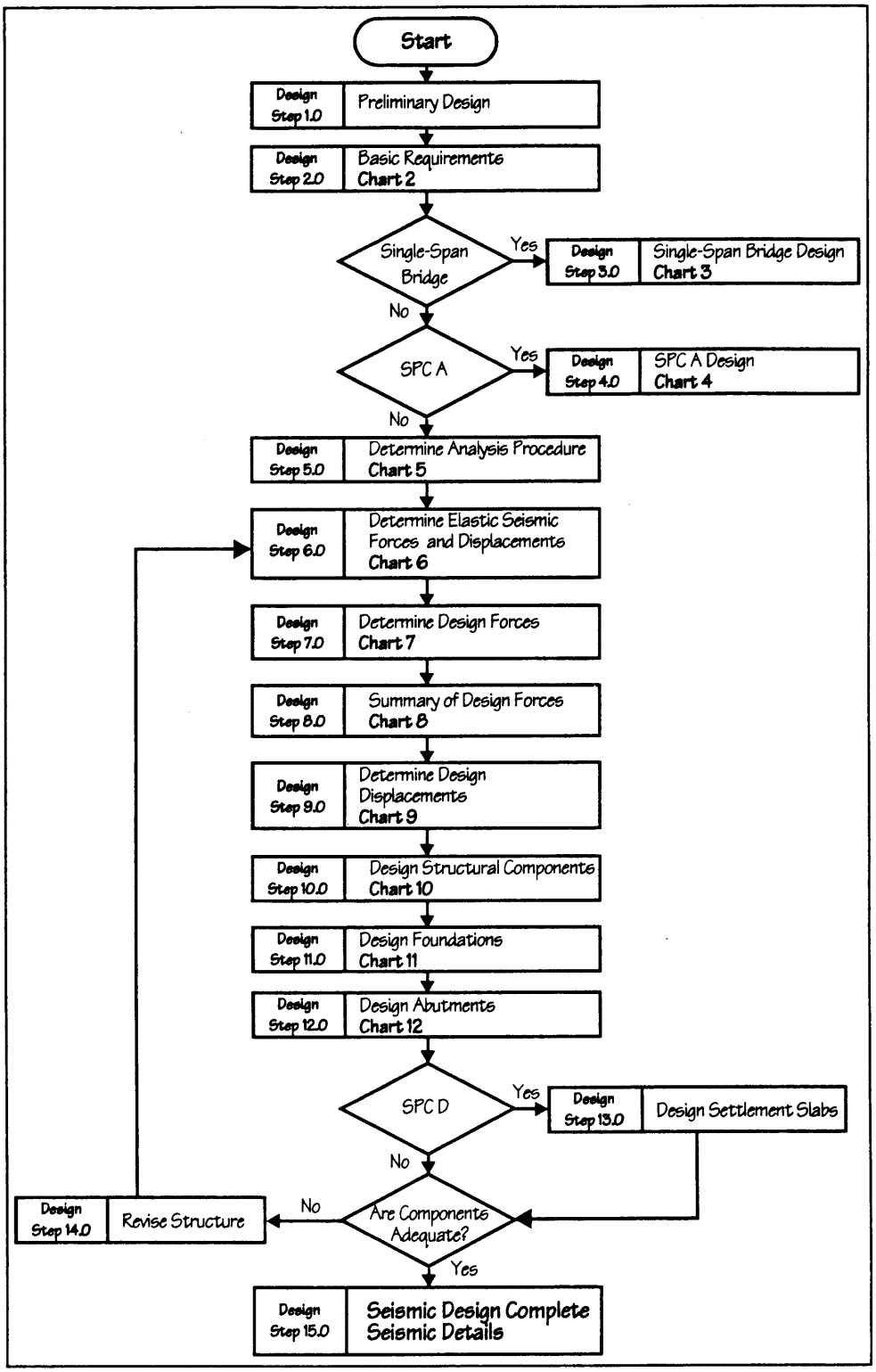

Main Flowchart — Seismic Design AASHTO Division I-A

FLOWCHARTS
(continued)

Key to Detailed Flowcharts

Design Step 1.0 — Not Focused on in Example No. 6/Not Included

Design Step 2.0 — Page 2-3

Design Step 3.0 — Not Applicable for Example No. 6

Design Step 4.0 — Not Applicable for Example No. 6

Design Step 5.0 — Page 2-4

Design Step 6.0 — Page 2-5

Design Step 7.0 — Page 2-6

Design Step 8.0 — Page 2-7

Design Step 9.0 — Page 2-8

Design Step 10.0 — Page 2-9

Design Step 11.0 — Page 2-10

Design Step 12.0 — Page 2-11

Design Step 13.0 — Not Required for Example No. 6

FLOWCHARTS
(continued)

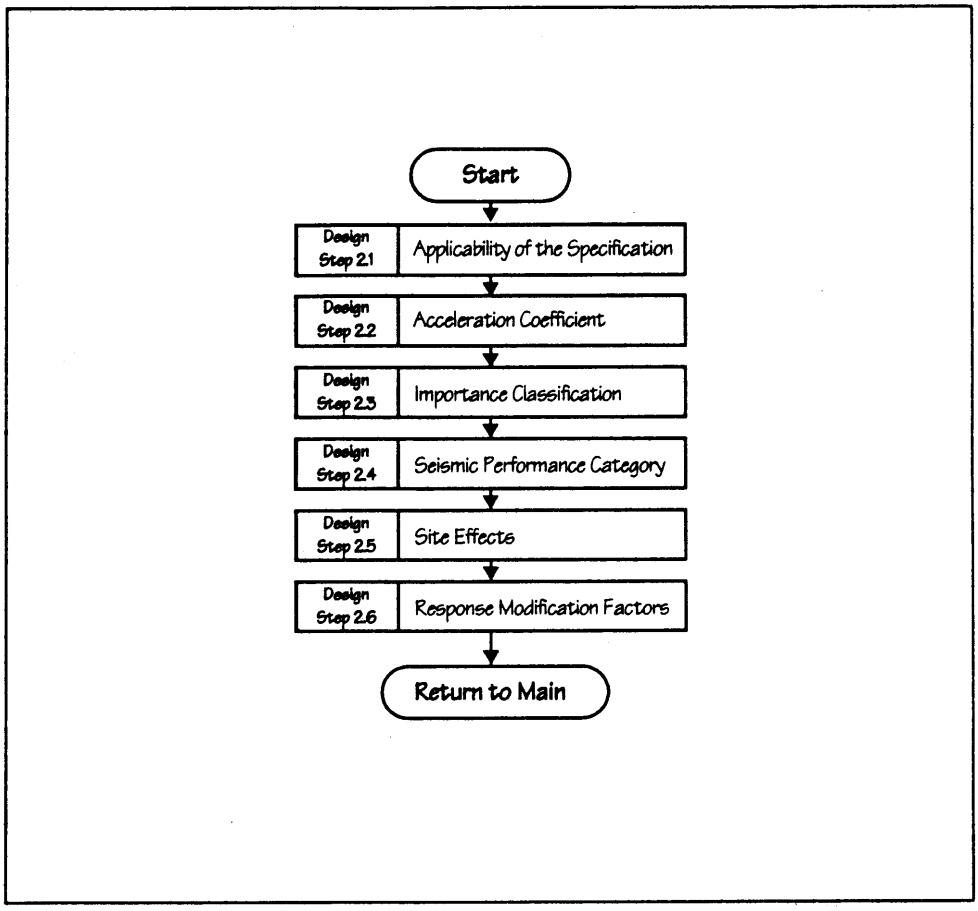

Chart 2 — Basic Requirements

FLOWCHARTS
(continued)

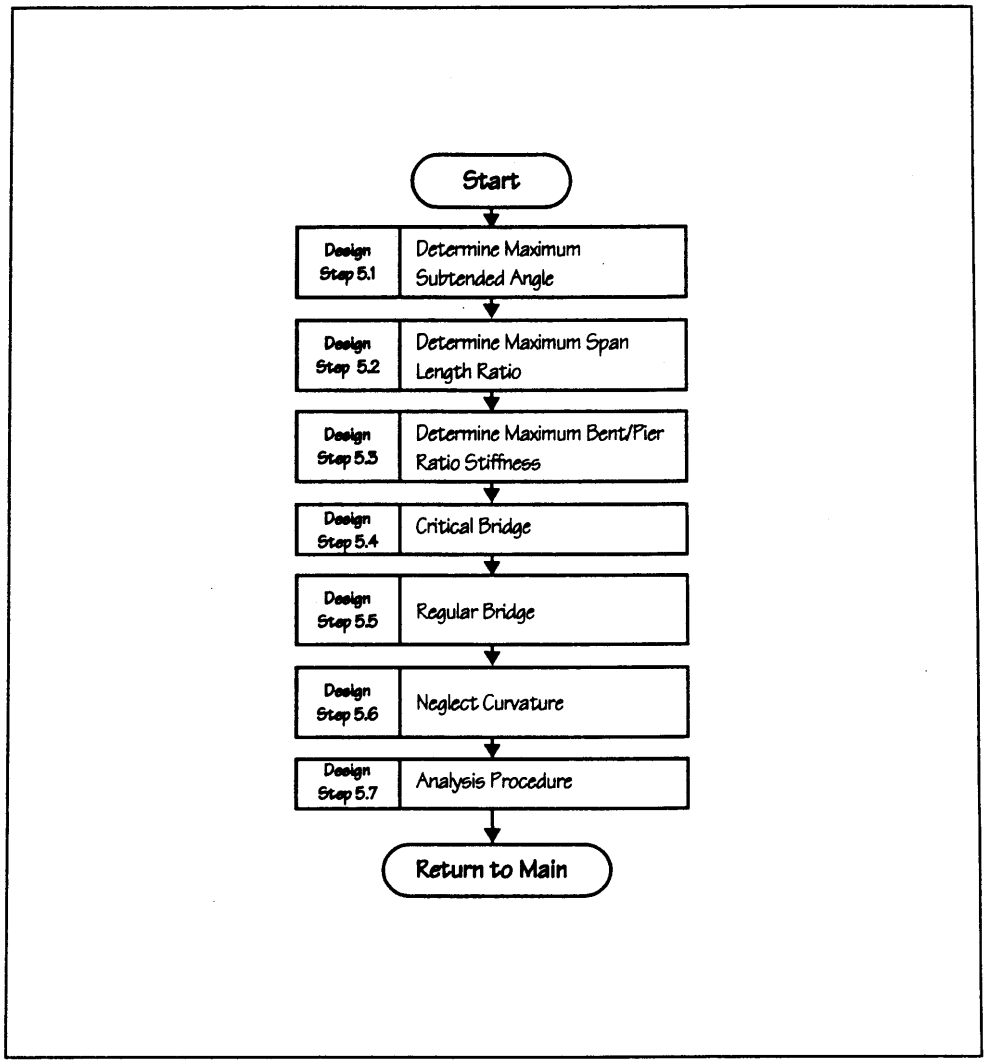

Chart 5 — Determine Analysis Procedure

FLOWCHARTS
(continued)

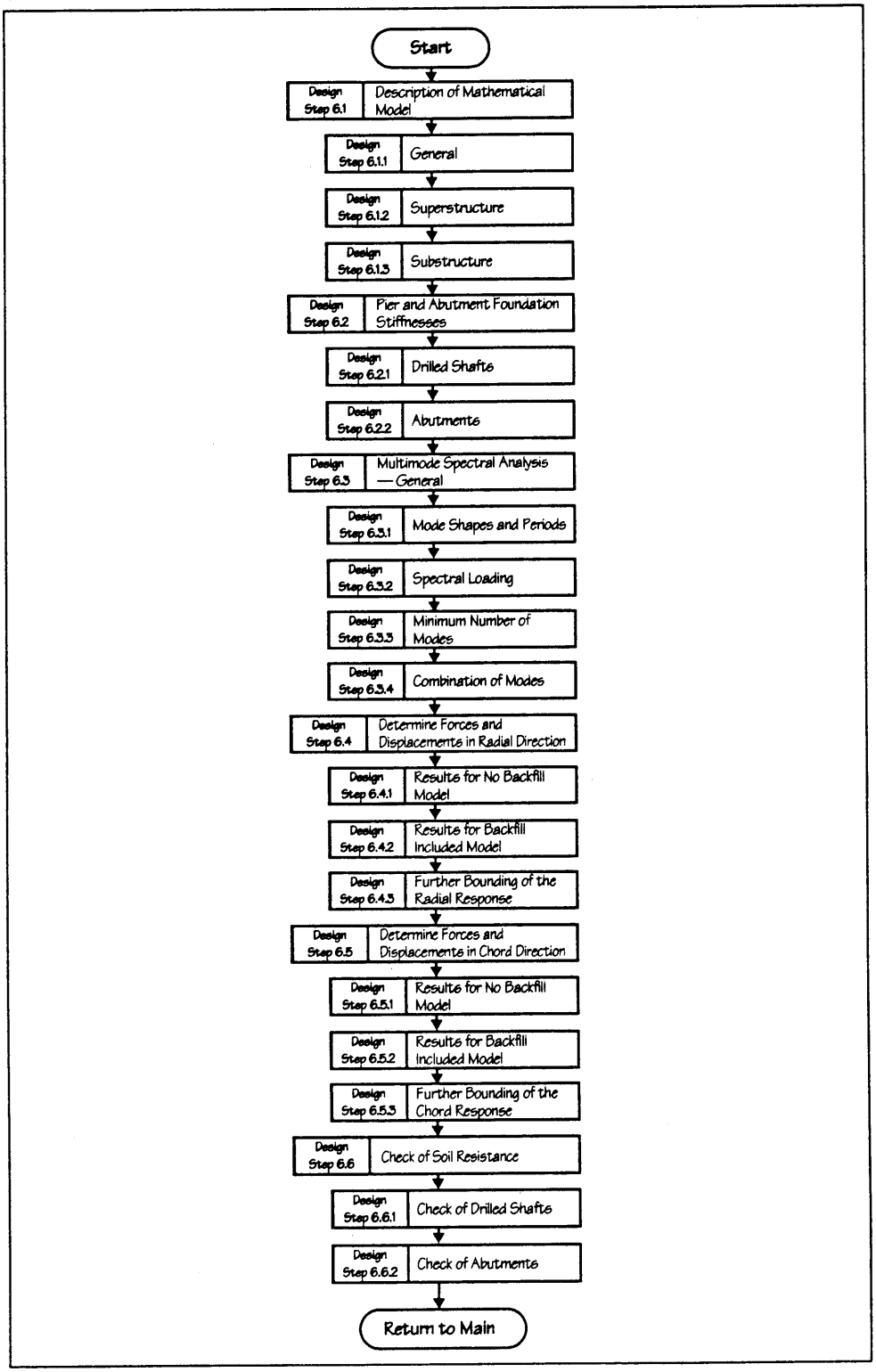

Chart 6 — Determine Elastic Seismic Forces and Displacements

FLOWCHARTS
(continued)

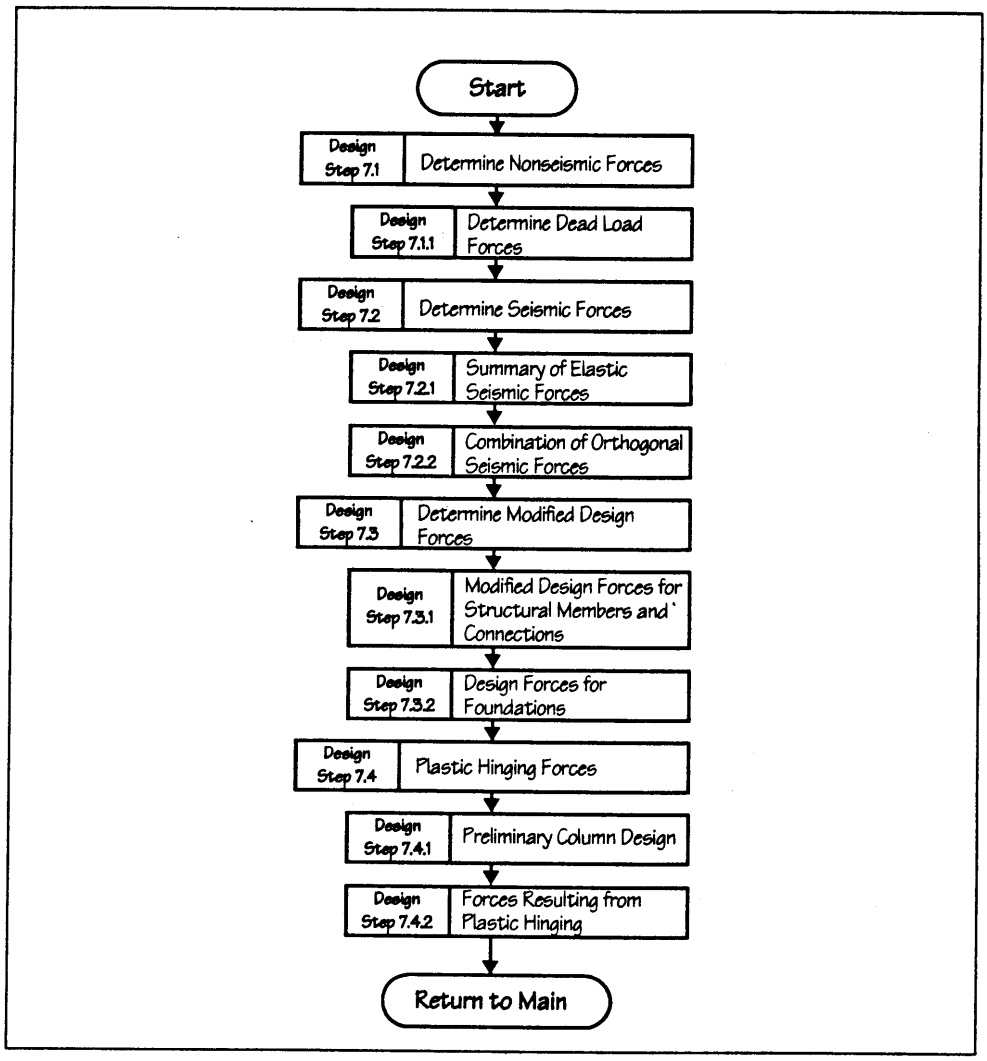

Chart 7 – Determine Design Forces

FLOWCHARTS
(continued)

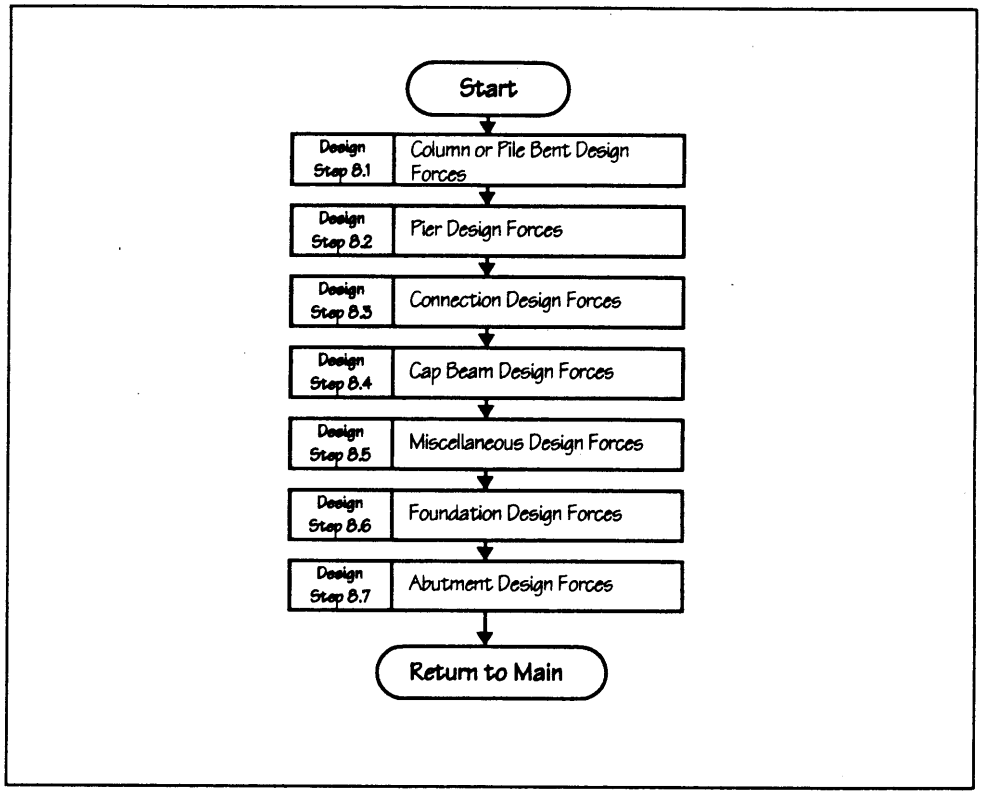

Chart 8 — Summary of Design Forces

FLOWCHARTS
(continued)

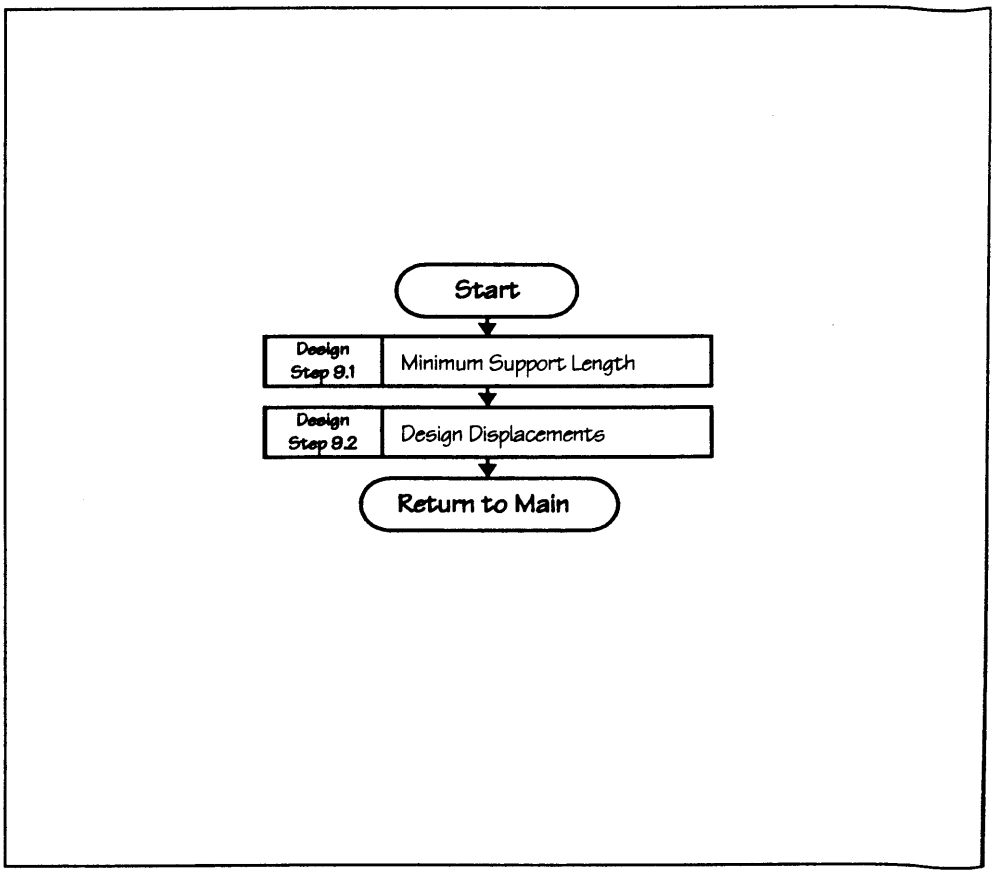

Chart 9 — Determine Design Displacements

FLOWCHARTS
(continued)

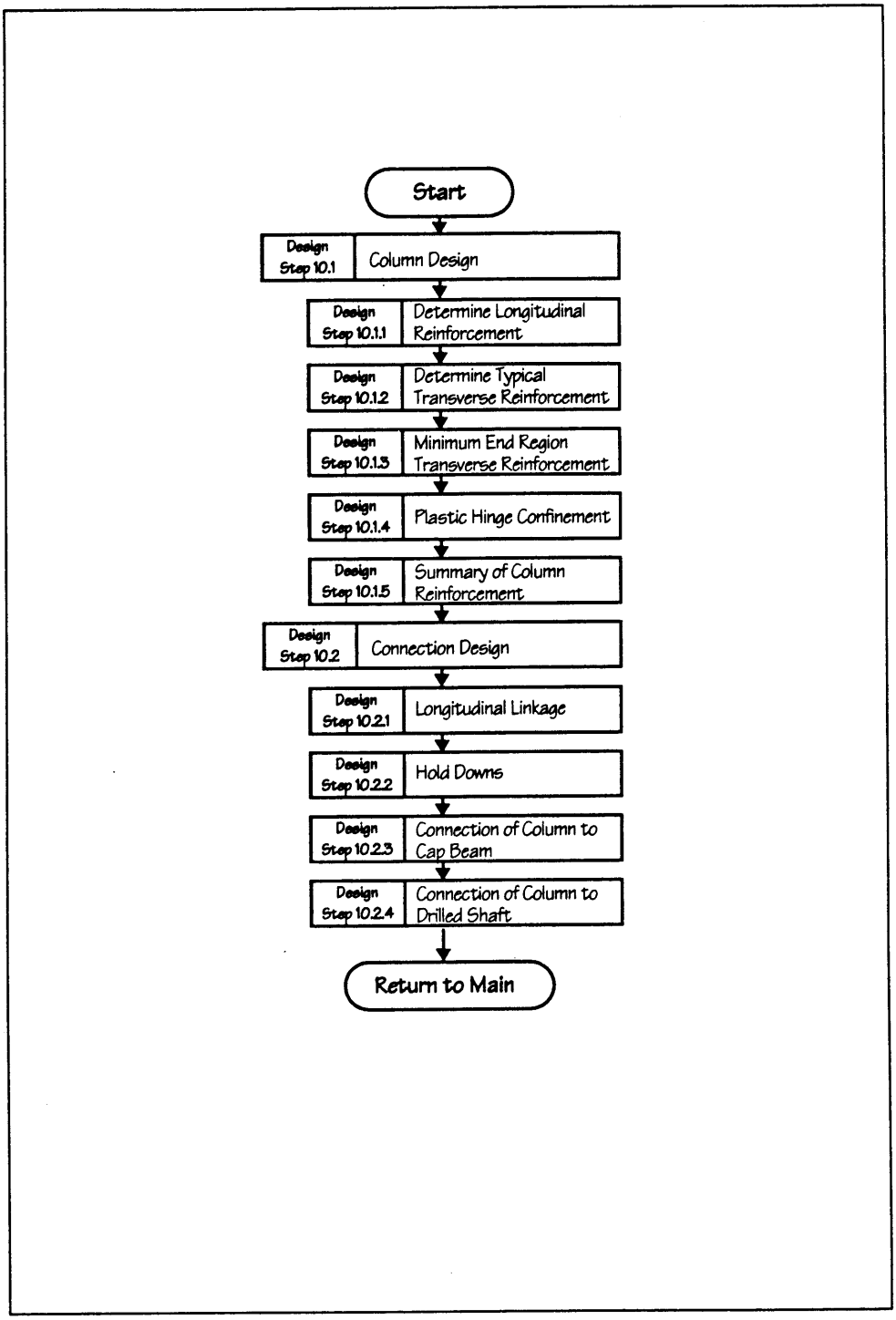

Chart 10 — Design Structural Components

FLOWCHARTS
(continued)

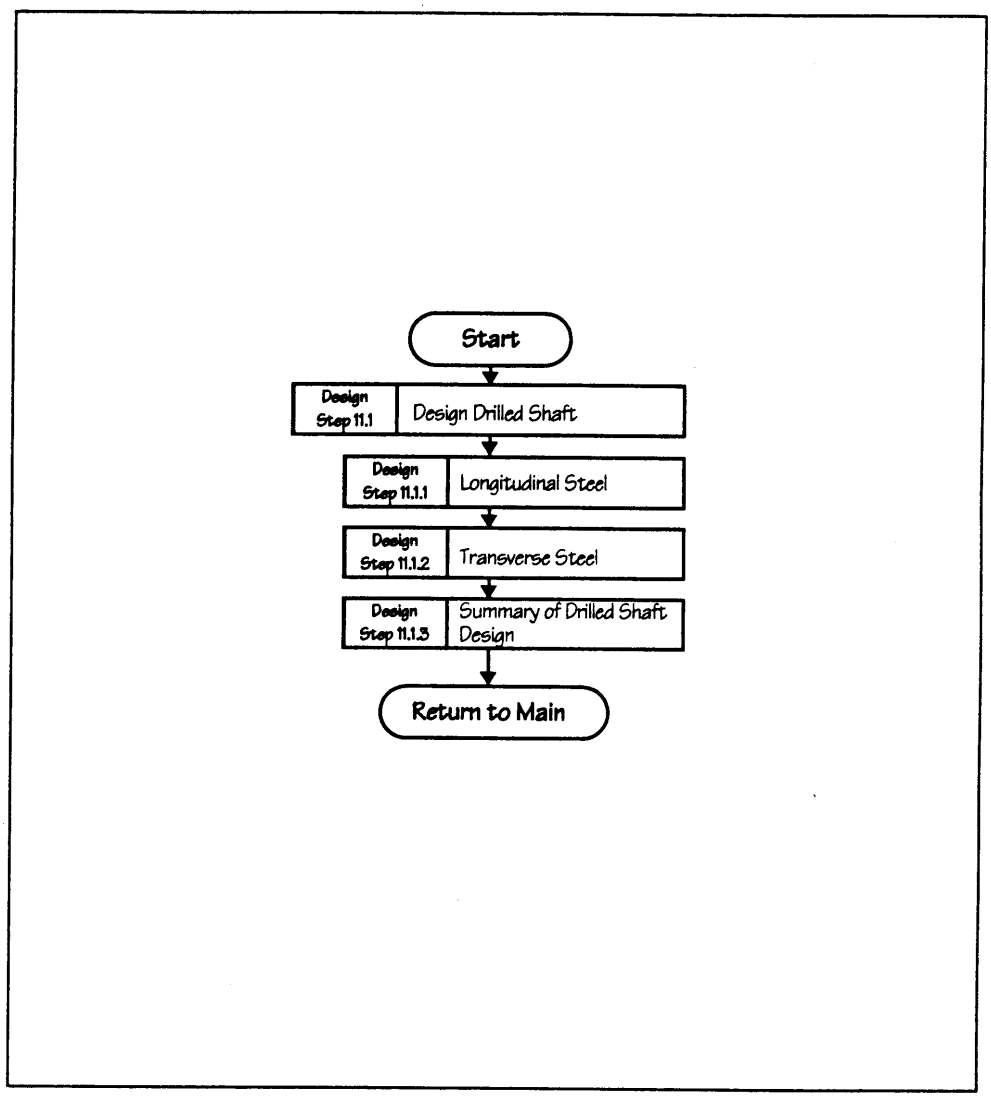

Chart 11 — Design Foundations

FLOWCHARTS
(continued)

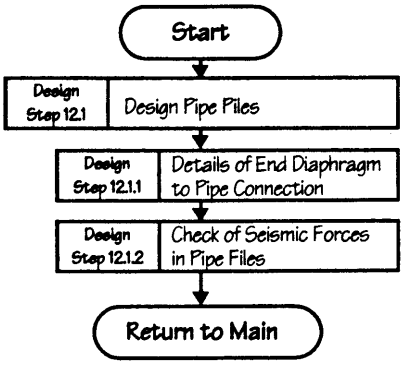

Chart 12 — Design Abutments

Section III
Analysis and Design

SECTION III ANALYSIS AND DESIGN

DATA

The bridge is to be built in the Northwestern United States in a seismic zone with an acceleration coefficient of 0.20g.

The configuration of the bridge is a three-span, concrete box girder superstructure supported on reinforced concrete columns founded on drilled shafts and on integral abutments founded on steel pipe piles. The bridge is located on a site underlain by a deep deposit of cohesionless material. Figure 1 (a to i) provides details of the configuration and Appendix A provides geotechnical information about the site.

The alignment of the roadway over the bridge is sharply curved, horizontally (104 degrees), but there is no vertical curve. The substructure elements are oriented at right angles to the bridge centerline at each substructure station.

REQUIRED

Design the bridge for seismic loading using the *Standard Specifications for Highway Bridges, Division I-A, Seismic Design,* American Association of State Highway and Transportation Officials, Inc., 15th Edition, as amended by the Interim Specifications-Bridges-1995.

FEATURES

ISSUES EMPHASIZED IN THIS EXAMPLE

- Effect of Significant Horizontal Curvature
- Drilled Shafts
- Integral Abutments with Piles
- Rectangular Column to Circular Shaft Detailing

BRIDGE DATA
(continued)

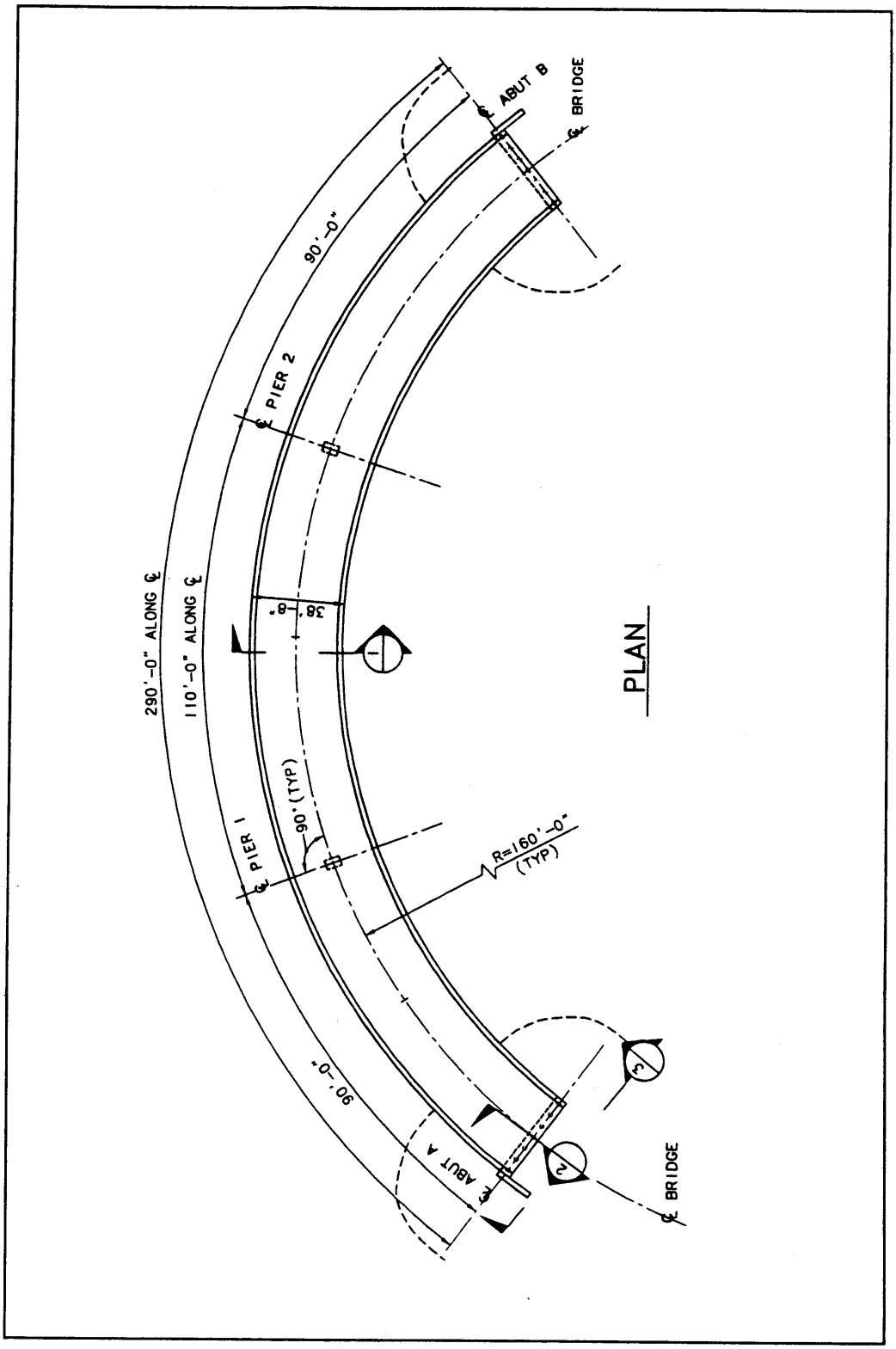

Figure 1a — Bridge No. 6 - Plan

BRIDGE DATA
(continued)

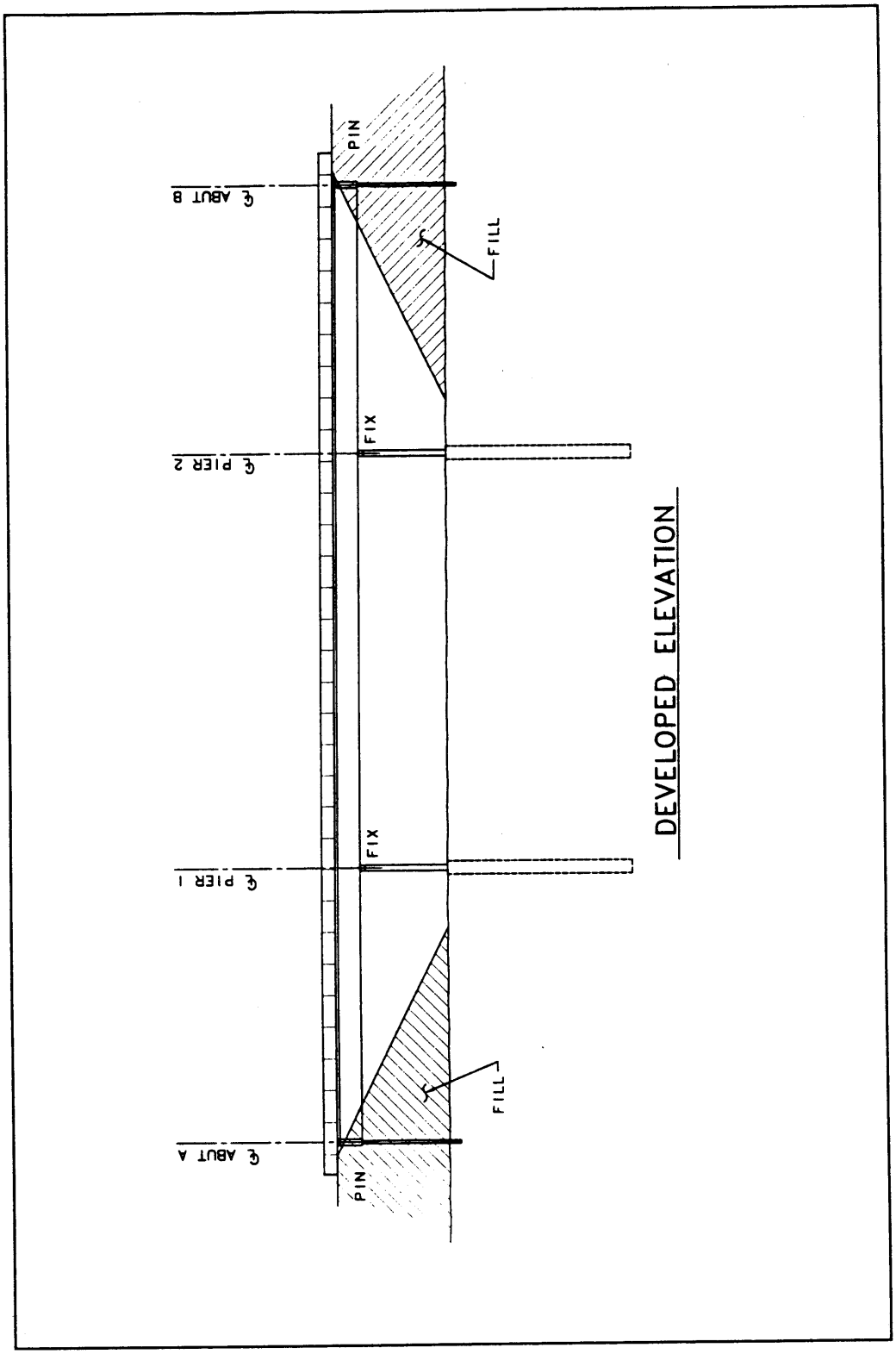

Figure 1b — Bridge No. 6 - Developed Elevation

BRIDGE DATA
(continued)

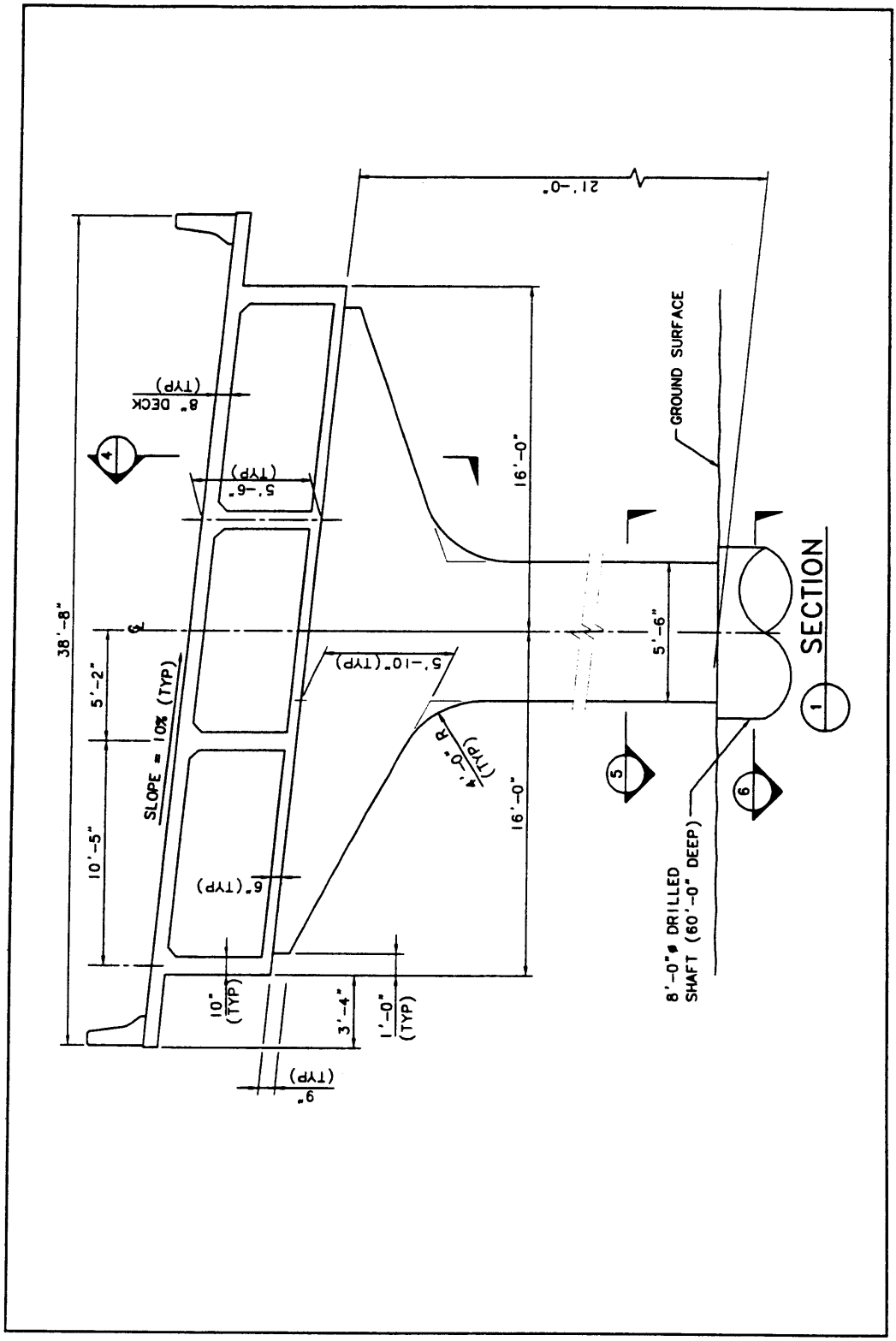

Figure 1c — Bridge No. 6 - Section at Pier

BRIDGE DATA
(continued)

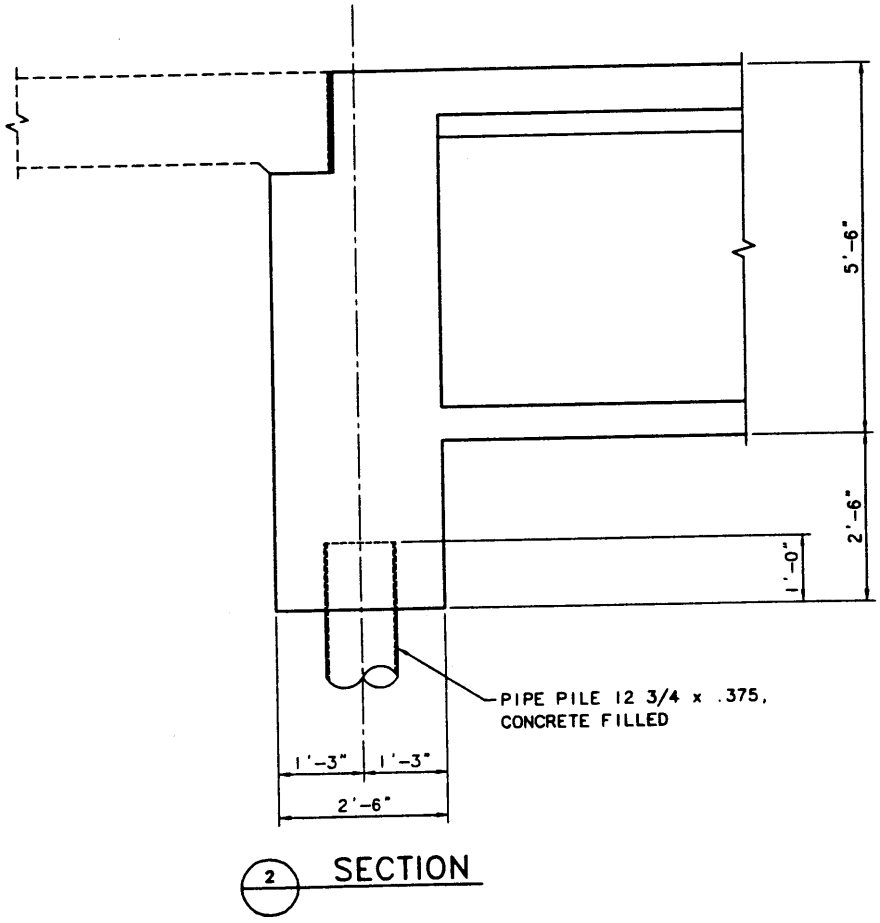

Figure 1d — Bridge No. 6 - Section at Abutment

BRIDGE DATA
(continued)

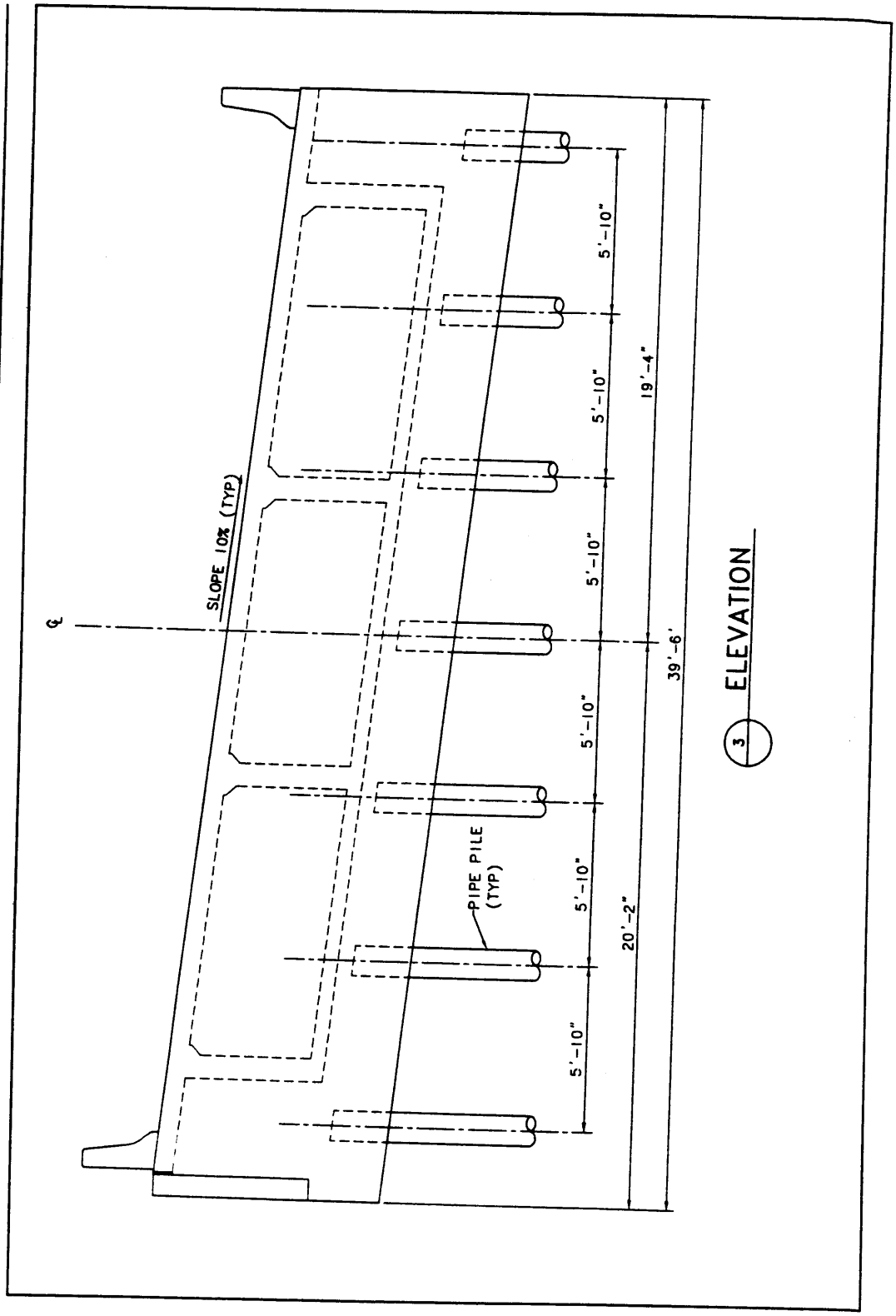

Figure 1e — Bridge No. 6 - End Elevation at Abutment

BRIDGE DATA
(continued)

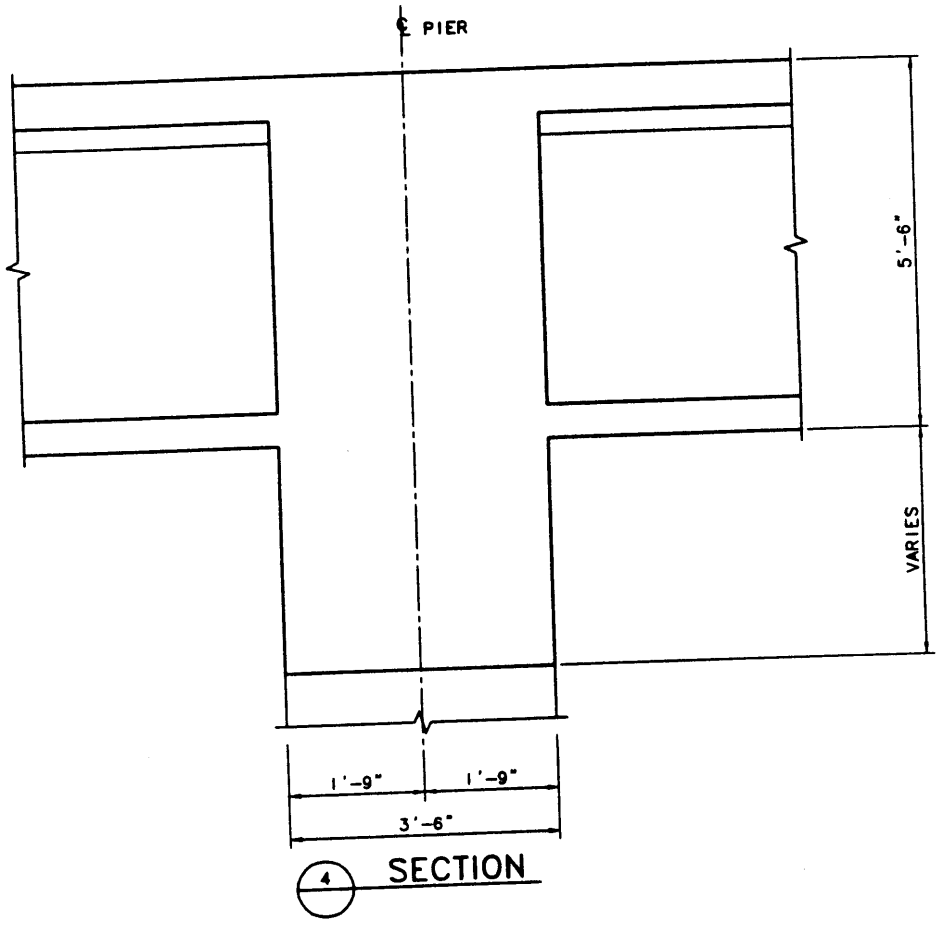

Figure 1f — Bridge No. 6 - Section through Integral Cap Beam

BRIDGE DATA
(continued)

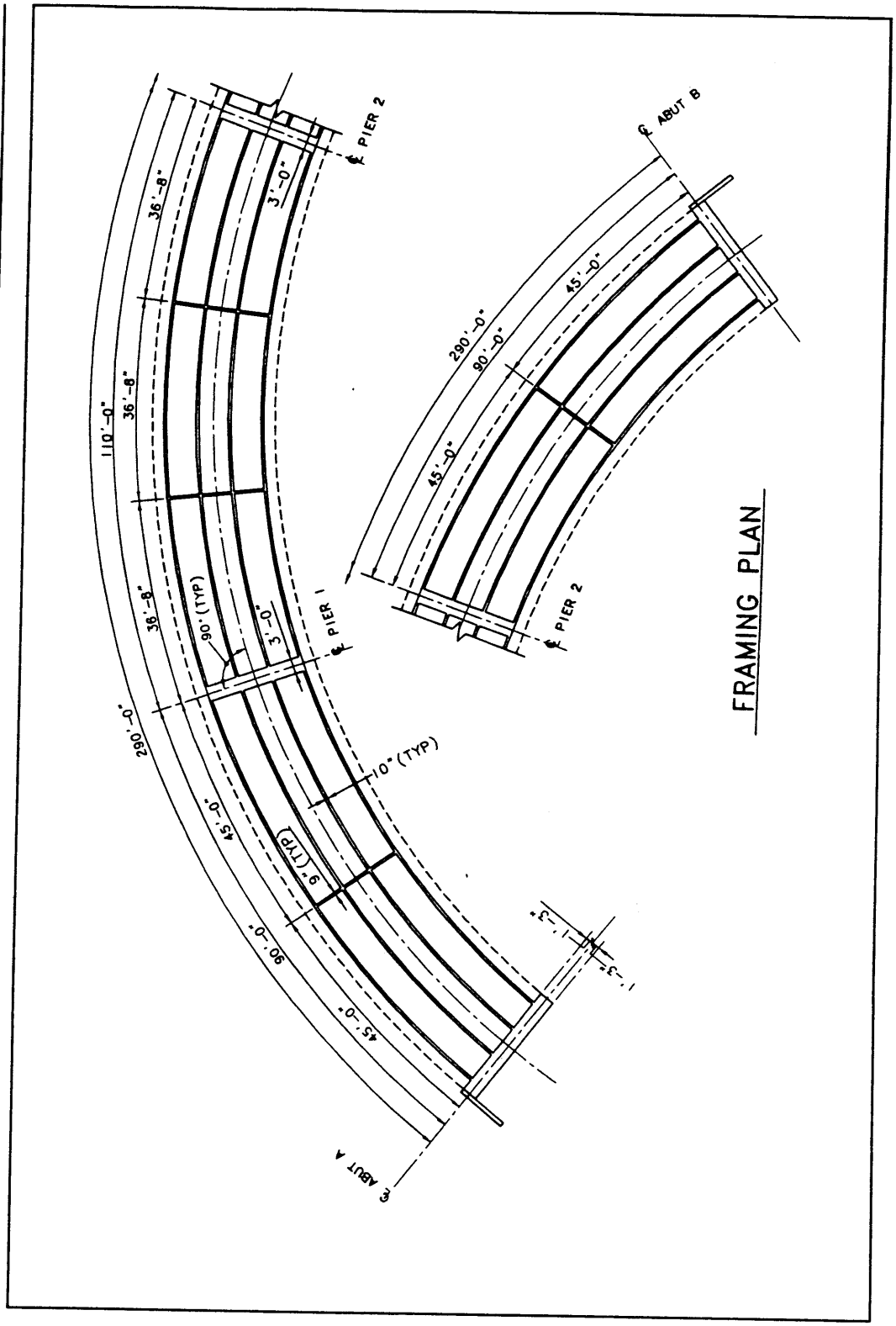

Figure 1g — Bridge No. 6 - Framing Plan

BRIDGE DATA
(continued)

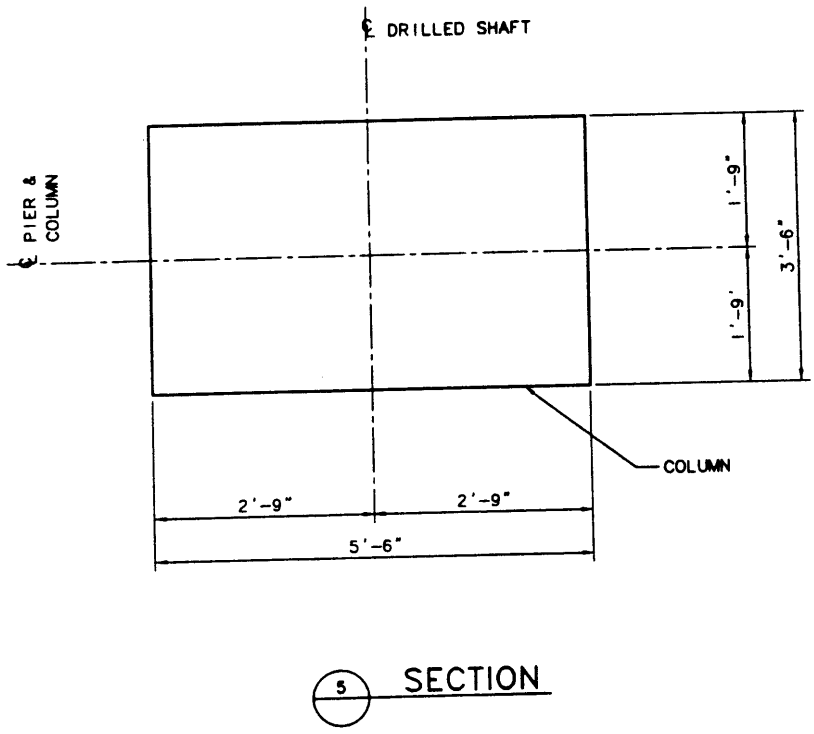

Figure 1h — Bridge No. 6 - Horizontal Section Through Column

BRIDGE DATA
(continued)

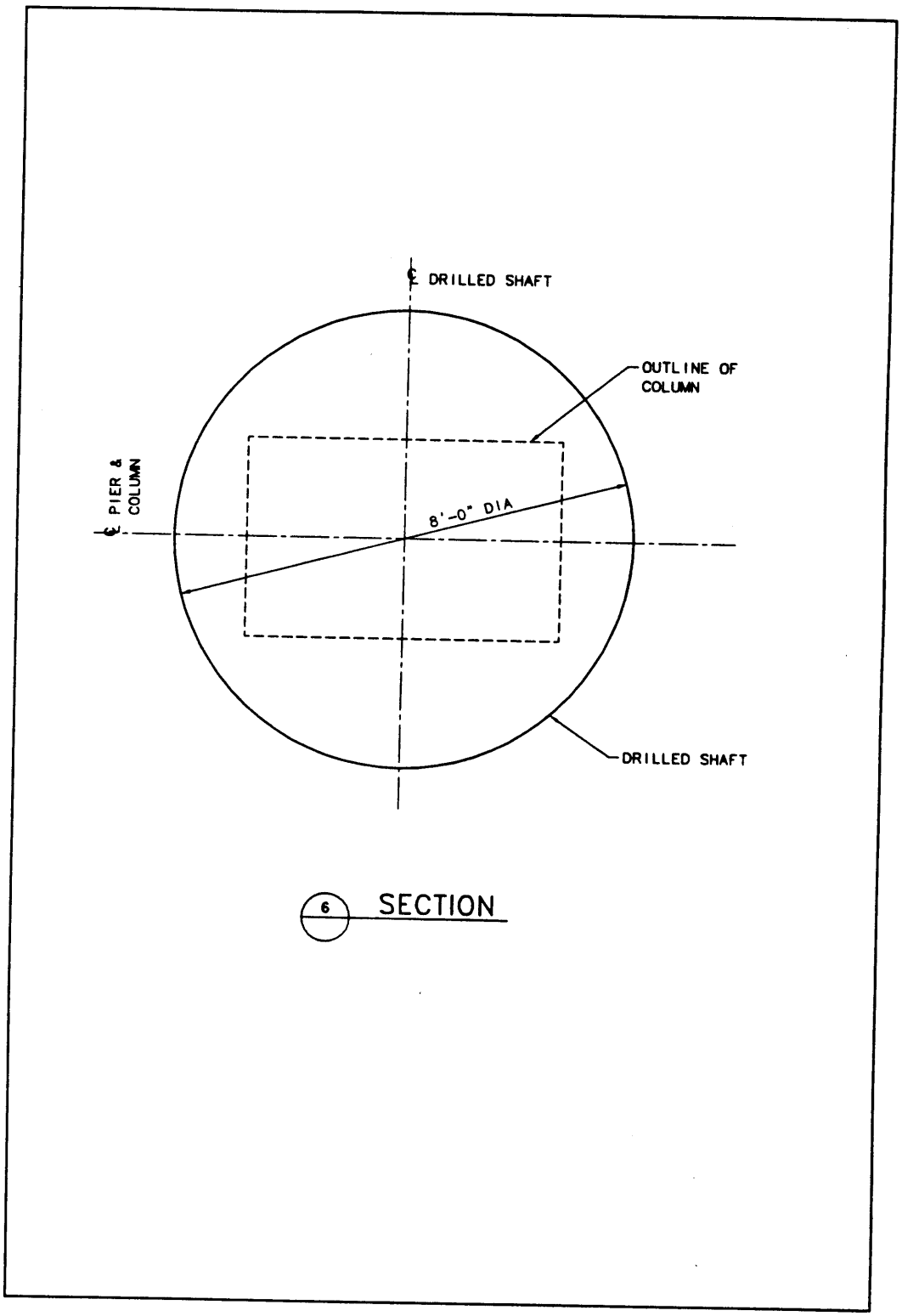

Figure 1i — Bridge No. 6 - Horizontal Section Through Drilled Shaft

SOLUTION

DESIGN STEP 1

PRELIMINARY DESIGN

The gravity load design established a preliminary configuration of the bridge and preliminary sizes of the members.

Because the bridge has such a sharp curve, the soil effects behind the abutments cannot be properly considered by a single elastic analysis; therefore, several models were used to bound the response. Earthquake loading must be considered in two orthogonal directions (Division I-A, Section 3.8), which for this bridge will be taken along the chord between the two abutments and along a line perpendicular to the chord — called the radial direction for this example (Figure 2).

For movement in the radial earthquake direction, the soil behind the abutment end walls is not effective when the bridge is moving away from the approach fills. For movement in the opposite direction, the soil behind the abutment is effective. This behavior is nonlinear, since "compression only" springs would have to be used to model such behavior. Because all the analyses performed in this example will be linear elastic, the actual response can only be bounded.

Bounding for the radial earthquake loading is accomplished by considering the worst-case behavior of two models: one without the abutment soil effects and one with the abutment soil. The same two models may also be used for bounding the chord earthquake loading.

Such bounding of the response should be considered both in preliminary hand calculations of the response and in the more complex computer-based calculations that typically follow.

DESIGN STEP 1
(continued)

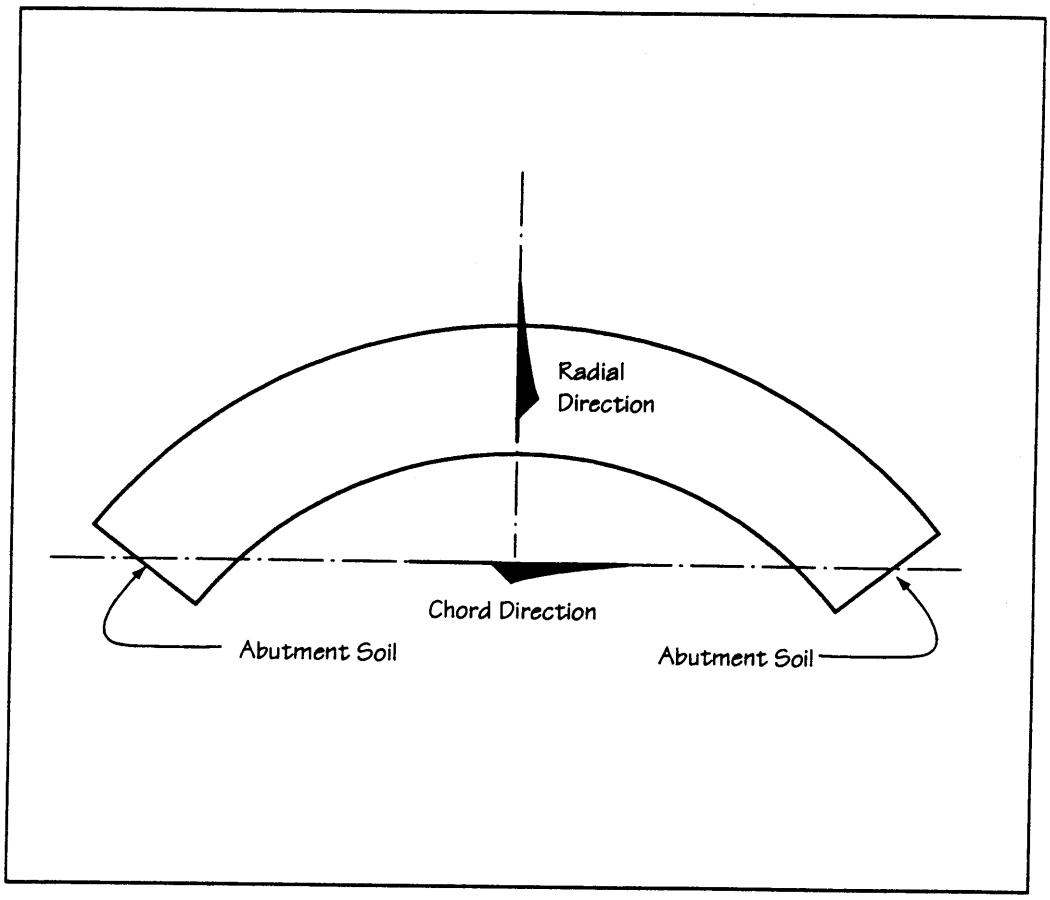

Figure 2 — Earthquake Loading Directions

DESIGN STEP 2 BASIC REQUIREMENTS

Design Step 2.1 Applicability of Specification

[Division I-A, Article 3.1]

The bridge has three spans that total 290 feet along the centerline. The end spans are 90 feet, the center span is 110 feet, and the bridge superstructure is a concrete box girder. Because no span is longer than 500 feet and the construction is conventional, the Specification applies.

Design Step 2.2 Acceleration Coefficient

[Division I-A, Article 3.2]

The bridge is sited in an area where the Acceleration Coefficient, A, is 0.20.

Design Step 2.3 Importance Classification

[Division I-A, Article 3.3]

The Importance Classification (IC) of this bridge is taken to be II. It is assumed not to be essential for use following an earthquake.

Design Step 2.4 Seismic Performance Category

[Division I-A, Article 3.4]

The Seismic Performance Category (SPC) is C, as taken from Table 1 of the Specification.

Design Step 2.5 Site Effects

[Division I-A, Article 3.5]

The site conditions affect the design through a coefficient based on the soil profile. In this case, SOIL PROFILE TYPE II corresponds to a deep cohesionless material.

The Site Coefficient, S, for this type of soil is 1.2 per Table 2 of the Specification. See Appendix A for more a detailed discussion.

Design Step 2.6

Response Modification Factors

[Division I-A, Article 3.7]

Since this bridge is classified as SPC C, appropriate Response Modification Factors (R Factors) must be selected for later use in establishing appropriate design force levels.

In this case, Table 3 of the Specification gives the following R Factors.

R = 3 For the columns, since a single column is used at the intermediate support locations

R = 1.0 For connections that transfer forces between the superstructure and substructure except at the abutments, and for connections between the column and the drilled shaft

R = 0.8 For connections at the abutments

These factors will be used to ensure that inelastic effects are restricted to elements that can be designed to provide reliable, ductile response that can be inspected after an earthquake to assess damage, and that can be repaired relatively easily.

The foundations do not fit this constraint, and will be designed to experience smaller or no inelastic effects. The foundations should be able to resist the probable forces that can be delivered by the piers without incurring any damage. For SPC C and D bridges, this objective is accomplished by designing the foundations to withstand the plastic hinging forces likely to be developed in the columns.

In some cases, meeting the objective outlined above may not be practical, and limited inelastic action may occur in the foundation. For instance, with drilled shafts it is not always possible to prevent plastic hinging from occurring in the shaft. This may occur particularly when there is a sharp change in stiffness in layered soils, where plastic hinging may form near the area of transition from soft to stiff soil. In cases where hinging is apt to occur in the shaft, it is reasonable to allow limited inelasticity, on the basis that such hinging is spread over a substantial length of the shaft. Thus, any damage is spread throughout a relatively large volume of material, thereby, minimizing its effect on long-term performance. In this context, limited yielding may be construed as ductility demands of 2 or less.

DESIGN STEP 3 SINGLE-SPAN BRIDGE DESIGN

Not applicable.

DESIGN STEP 4 SEISMIC PERFORMANCE CATEGORY A DESIGN

Not applicable.

DESIGN STEP 5 DETERMINE ANALYSIS PROCEDURE

Design Step 5.1 Determine Maximum Subtended Angle
[Division I-A, Article 4.2]

The bridge is curved in the horizontal plane, and as shown in Figure 1, the curve radius is 160 feet. The beginning and end of the curve are off of the bridge; thus, the entire length of the bridge is on the curve. The length of the bridge, measured along the centerline, is 290 feet. The subtended angle is then calculated as

$$\Delta_{sa} := \frac{290 \cdot ft}{2 \cdot \pi \cdot 160 \cdot ft} \cdot 360 \cdot deg \qquad \Delta_{sa} = 104 \cdot deg$$

Design Step 5.2 Determine Maximum Span Length Ratio
[Division I-A, Article 4.2]

The maximum span length ratio is 1.22 = 110 ft/90 ft.

Design Step 5.3 Determine Maximum Bent/Pier Stiffness Ratio
[Division I-A, Article 4.2]

The piers are identical; thus, the ratio of their stiffnesses is 1.

Design Step 5.4 Critical Bridge
[Division I-A, Article 4.2.3]

Assume that the bridge is not critical.

Design Step 5.5 Regular Bridge
[Division I-A, Article 4.2]

Table 5 of the Specification gives the requirements for determining whether a bridge is regular. The requirements are based on limiting values of the parameters determined in the steps above.

The bridge is not regular, since the subtended angle of the curve exceeds 90 degrees. The span length ratio is less than 2, and maximum pier stiffness ratio is less than 4; thus it is the curve alone that makes the bridge "not regular."

Design Step 5.6

Neglect Curvature

[Division I-A, Article 4.2.2]

The bridge cannot be analyzed as if it were straight, because the bridge is not regular and the subtended angle exceeds 30 degrees.

Design Step 5.7

Analysis Procedure

[Division I-A, Article 4.2]

Because this is not a single-span bridge, and is not classified as SPC A, the analysis requirements of Article 4 must be satisfied. Table 4 of the Specification is used to select the minimum analysis requirements.

From Table 4 of the Specification, Procedure 3 — the Multimode Spectral Method — must be used to analyze the structure.

The analysis requirements of this method are minimum that may be used; alternatively, the Time-History Method (Procedure 4) could be used in lieu of Procedure 3.

For this example, Procedure 3 is used for the analysis.

DESIGN STEP 6

DETERMINE ELASTIC SEISMIC FORCES AND DISPLACEMENTS

Design Step 6.1

Description of Mathematical Model

Design Step 6.1.1

General

[Division I-A, Article 4.5.2]

The structural analysis program SAP90 Version 6.0 Beta (CSI, 1994) was used for the analyses. The mathematical model used is shown in Figure 3 and includes a single line of frame elements for the superstructure and a single line of elements for the piers, which include the full length of the drilled shafts. The drilled shafts are restrained by sets of uniformly spaced elastic springs oriented in two orthogonal directions. In the model, the abutments, which are supported on pipe piles, are supported by elastic springs.

As discussed in Design Step 1, Preliminary Design, the actual seismic response of the bridge can only be bounded due to the "compression only" resistance of the abutment backfill and the large curvature of the bridge. To bound the response, two versions of the model will be considered. The first includes only the pipe pile resistance for the abutment springs, and is called the "No Backfill Model." The second adds the abutment backfill resistance to the pipe pile contribution, and is called the "Backfill Included Model." The No Backfill Model is expected to provide larger overall displacements, owing to its higher flexibility, and is also expected to yield larger intermediate pier forces. For this behavior, the No Backfill Model will control the design of the intermediate piers.

Design Step 6.1.2

Superstructure

a) Geometry

The superstructure has been modeled using eight elements per span to provide a reasonable representation of the curve. The work lines of the elements are located along the centroid of the superstructure box girder.

As shown in Figure 3, the superstructure has been collapsed into a single line of 3-D frame elements. Each span is split into eight elements to provide appropriate representation of the stiffness and mass distribution due to the sharp curve.

Design Step 6.1.2 (continued)

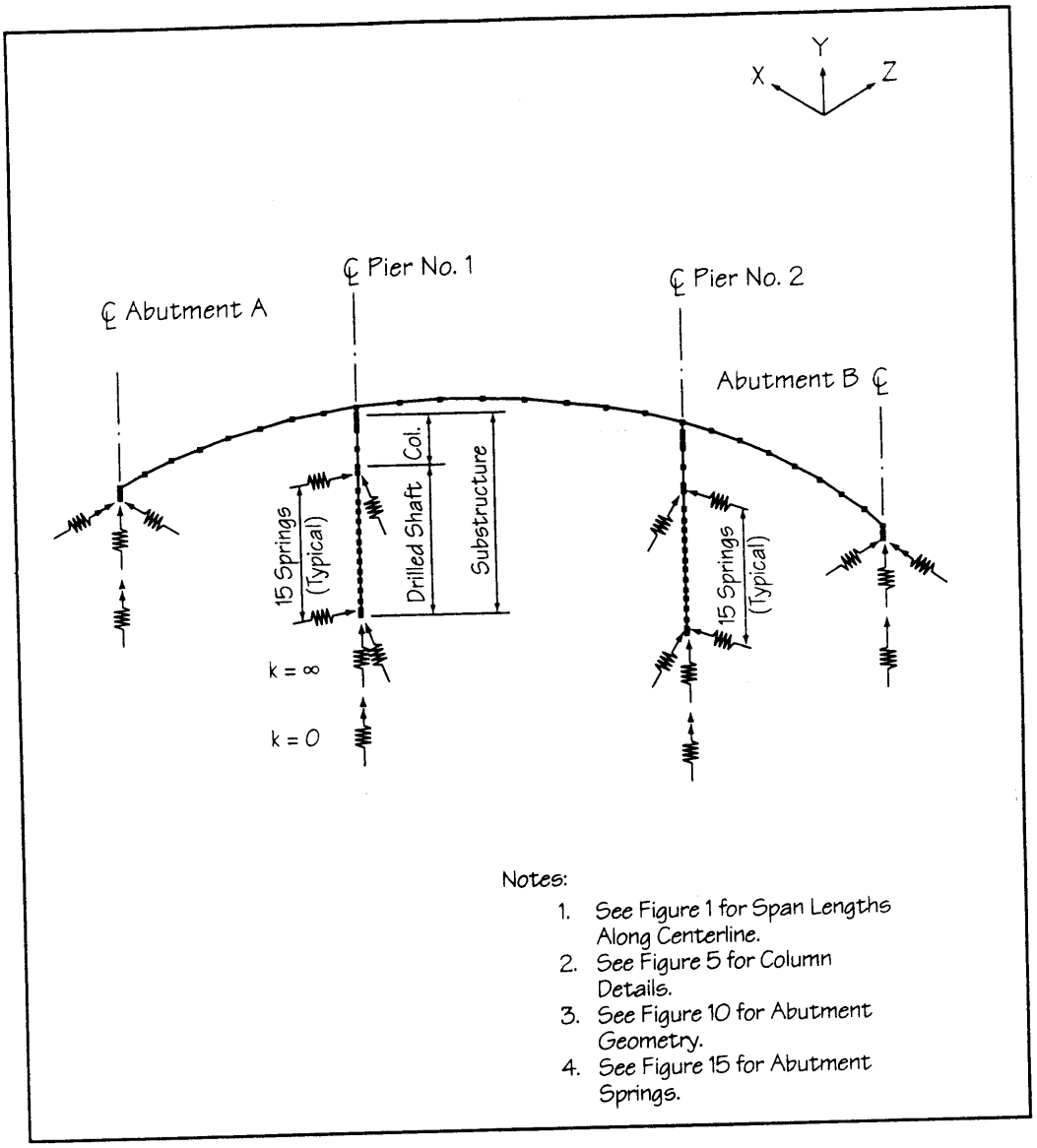

Figure 3 — Structural Model of Bridge

This is a reasonable approach for most bridges that have regular geometry, particularly box girders. There is no rule for determining the number of elements to use along the length of each span for a curved bridge. For a straight bridge, each span might be split into four elements; however, the analyst may consider using more for a sharply curved structure.

The seismic analysis "stick" model is used primarily to account for the forces in the substructure and foundation elements. So, the fact that it may not be as accurate for determining internal superstructure forces

Design Step 6.1.2 (continued)

exerted by other load types is not a concern. Such a simplified model may, however, be useful for checking static load case results from more elaborate superstructure models. Many designers use a "stick" model for the seismic analysis, and further discussion of setting up the seismic model is given by FHWA (1987) and Caltrans (1989).

b) Properties

The properties of the superstructure elements have been calculated neglecting the effect of the 10 percent superelevation. The properties are listed below. The weights listed are those that must be added to the SAP90 model. This program can calculate the weight and mass of the individual elements, but additional mass that is not associated with the elements themselves must be added separately.

$A_s := 56.2 \cdot ft^2$ Cross-sectional area of superstructure.

$I_{sh} := 250 \cdot ft^4$ Moment of inertia about horizontal axis

$I_{sv} := 6800 \cdot ft^4$ * Moment of inertia about vertical axis

$J_s := 777 \cdot ft^4$ Torsional constant of superstructure

$W_{ed} := 119 \cdot kip$ Weight of end diaphragms at abutment

$W_{pd} := 79 \cdot kip$ Weight of pier diaphragms or cap beams

$W_{id} := 15 \cdot kip$ Weight of intermediate diaphragms

$w_b := 0.9 \cdot \frac{kip}{ft}$ Weight of barriers per unit length

* Note that I_{sv}, the moment of inertia about a vertical axis, was specified as 6800 ft^4 instead of 6526 ft^4. This incorrect value has been used in all calculations. It was not corrected, because it only produces a small and insignificant error, less than 1 percent.

Design Step 6.1.2 (continued)

The calculation of the superstructure cross-sectional area, moments of inertia, and centroidal depths are shown in Table 1. The calculation of the torsional constant for the box girder is given below, and the dimensions are taken from Figure 4. The method is taken from *Roark's Formulas for Stress and Strain*, Young (1989), Table 20, Case 15, "Any Thin Tube."

$L_{mb} := (32 \cdot 12 - 10) \cdot in$ Length of median boundary, as shown in Figure 4

$L_{mb} = 374 \cdot in$

$H_{mb} := (5.5 \cdot 12 - 4 - 3) \cdot in$ Height of median boundary

$H_{mb} = 59 \cdot in$

$A_{mb} := L_{mb} \cdot H_{mb}$ Area enclosed by the median boundary

$A_{mb} = 153 \cdot ft^2$

$$J := \frac{4 \cdot A_{mb}^2}{\frac{H_{mb}}{10 \cdot in} + \frac{H_{mb}}{10 \cdot in} + \frac{L_{mb}}{6 \cdot in} + \frac{L_{mb}}{8 \cdot in}}$$ Torsional Constant

$J = 777 \cdot ft^4$

The denominator is the summation of the individual side lengths divided by their thicknesses. The sides are the flanges and webs through which the median boundary, shown in Figure 4, passes. The source equation in Roark and Young shows an integral in the denominator, but this degenerates into the summation given above for the case where the sides have constant thicknesses.

This calculation considers the actual multicell box as a single-cell box comprised only of the perimeter elements. This approach is an approximation that greatly simplifies the calculations. If the actual multicell torsion constant is calculated, three simultaneous equations must be solved, and the result turns out to be less than 1 percent larger than the single-cell result. The calculation of the multicell torsion constant, if desired, can be made using the method outlined by Heins (1975).

Design Step 6.1.2 (continued)

Table 1
Superstructure Property Calculation

Centroid and Moment of Inertia About Horizontal Axis

Item	Width	Height	Number	Es / Ec	A, area	Lever, y	Ay	Io	d	Ad²	Iy
deck	38.67	0.667	1	1	25.79	0.333	8.59	0.96	2.04	107.44	108.40
webs	0.833	4.333	4	1	14.44	2.833	40.90	5.65	-0.46	3.04	8.69
soffit	32	0.5	1	1	16.00	5.25	84.00	0.33	-2.88	132.34	132.68
									2.374		
					56.23 ft²		133.49 ft³				249.77 ft⁴

NA depth = 28.49 in. from top I_{sh} = 250 ft⁴

Centroid and Moment of Inertia About Vertical Axis

Item	Width	Height	Number	Es / Ec	A, area	Lever, y	Ay	Io	d	Ad²	Iy
deck	0.667	38.67	1	1	25.79	0.000	0.00	3214.16	0.00	0.00	3214.16
soffit	0.5	32	1	1	16.00	0.000	0.00	1365.33	0.00	0.00	1365.33
web 1	4.333	0.833	1	1	3.61	15.583	56.25	0.21	-15.58	876.47	876.68
web 2	4.333	0.833	1	1	3.61	5.167	18.65	0.21	-5.17	96.36	96.57
web 3	4.333	0.833	1	1	3.61	-5.167	-18.65	0.21	5.17	96.36	96.57
web 4	4.333	0.833	1	1	3.61	-15.583	-56.25	0.21	15.58	876.47	876.68
					56.23 ft²		0.00 ft³				6525.99 ft⁴

NA depth = 0.00 in. from right side I_{sv} = 6526 ft⁴

Design Step 6.1.2 (continued)

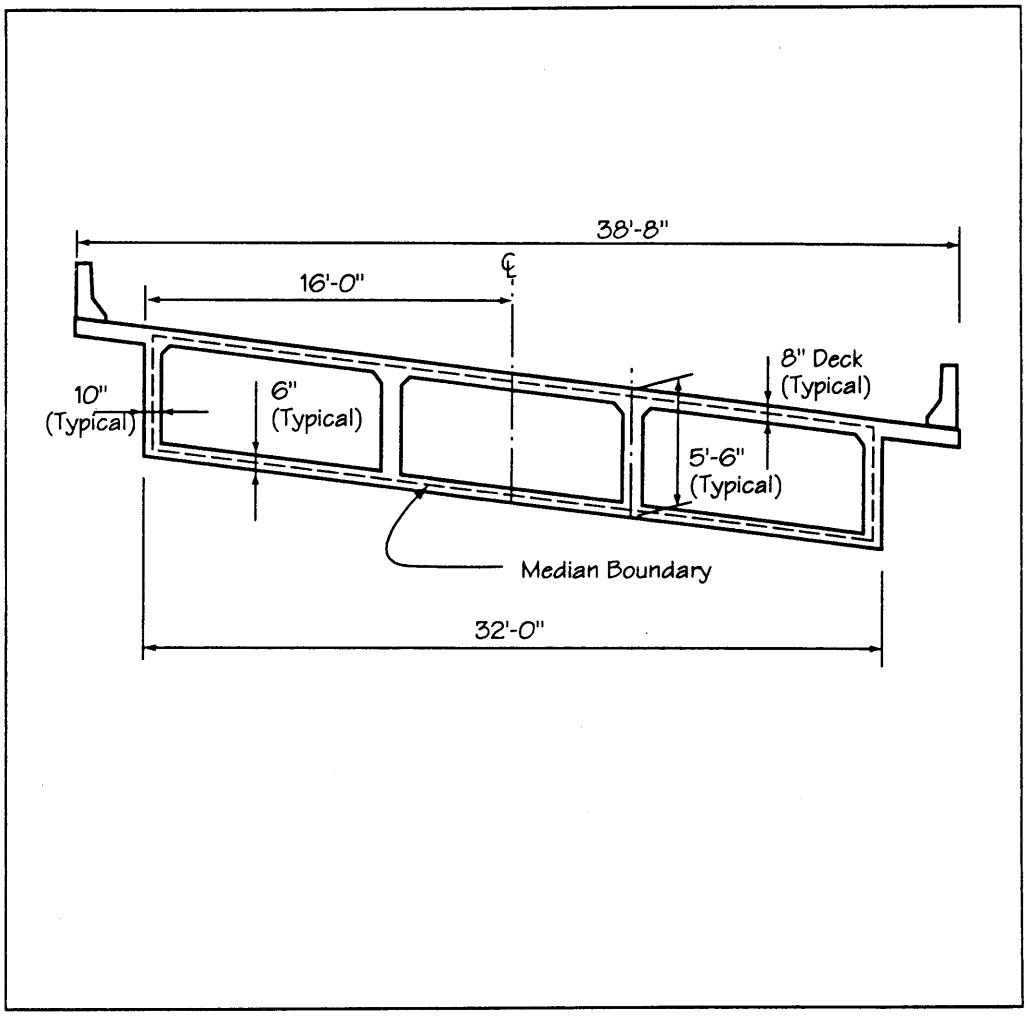

Figure 4 — Calculation of Torsion Properties

Design Step 6.1.3

Substructure

The single line of elements representing each pier has been divided into elements with nodes at each change in cross section, as shown in Figure 5. A rigid link is used to model the stiff part of the column that is located in the cap beam of the superstructure. The flare at the top of the column is modeled using three elements, which are each two feet high and 3.5 feet thick. The width of the elements varies from 10 feet to 28 feet. The lower portion of the column is modeled with two elements, and the drilled shaft is modeled with 16 elements, each 4 feet long, except for the top and bottom elements, which are made 2 feet long in order to keep the tributary length of the foundation springs the same. The development of the springs is discussed in Design Step 6.2.1.

The piers and abutments are oriented radially; thus, these substructure elements are rotated in the model to properly account for the position of the pier on the curve. Figure 6 shows the direction of the first two local axes of each structure element with arrows. In SAP90, the first local axis is always directed along the length of the member. The second axis is oriented orthogonally to the first axis. As is seen in the figure, the pier elements are oriented in the radial direction. This figure was taken from an output plot made by SAP90. It is always useful to use such plotting capabilities to check the orientation of the elements. The "I" shape used in the figure is simply an icon to show the orientation of the elements' cross sections.

The properties for the substructure elements were not input directly, instead they were calculated by SAP90, based on the input cross-sectional dimensions. The calculated properties include both the stiffness and the mass of the piers.

The mass of the elements was calculated based on the specified cross sectional area and the densities of the elements. The program calculates the mass tributary to each node, and then lumps that mass at the node. The mass of the drilled shaft was not included, since it is located entirely below grade. The difference between the concrete density and the density of the displaced soil is not great enough to warrant assigning mass to the foundation. This mass was excluded by assigning zero density to the elements representing the drilled shaft.

Design Step 6.1.3 (continued)

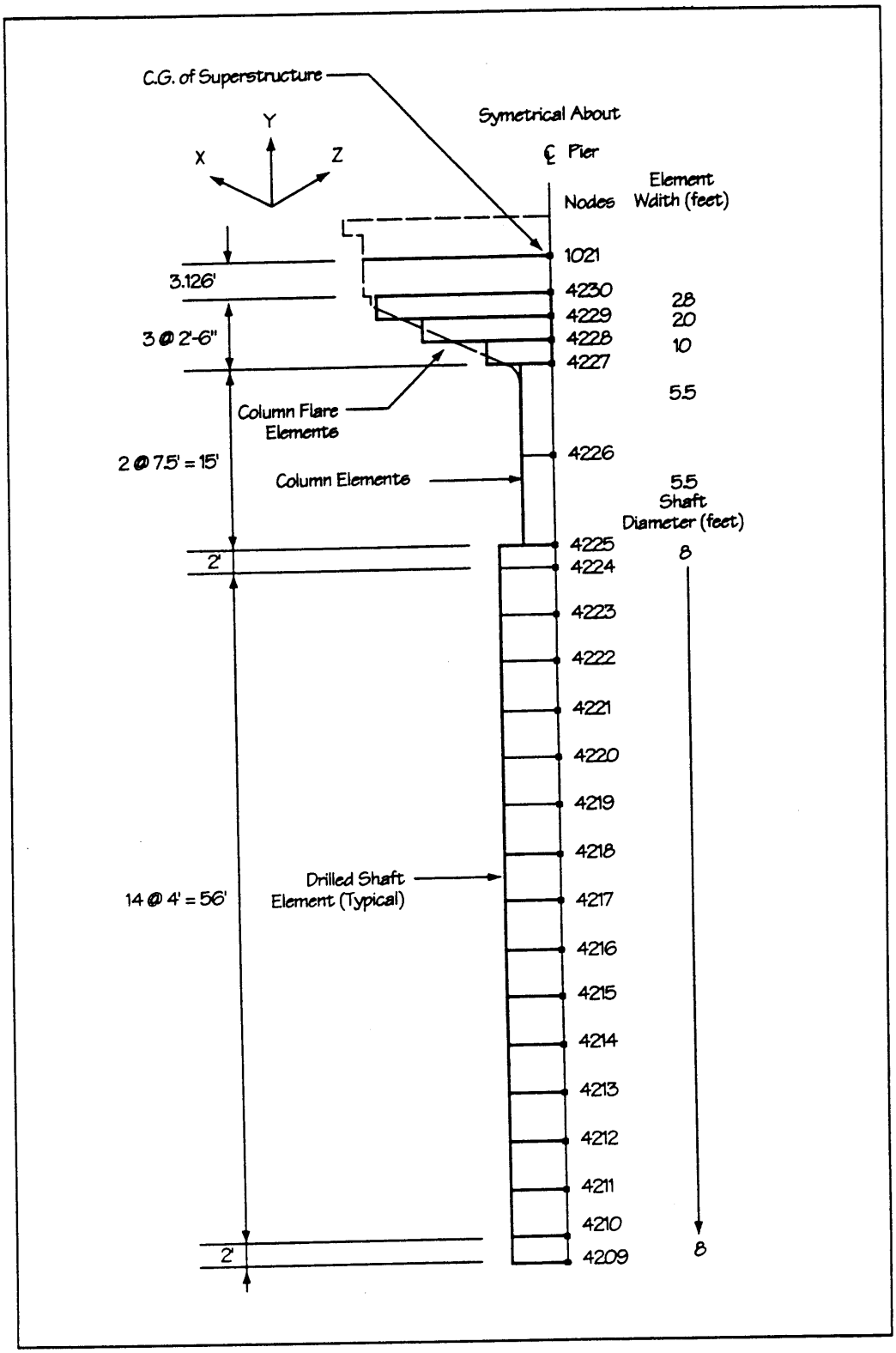

Figure 5 — Pier Geometry and Element Layout

Design Step 6.1.3 (continued)

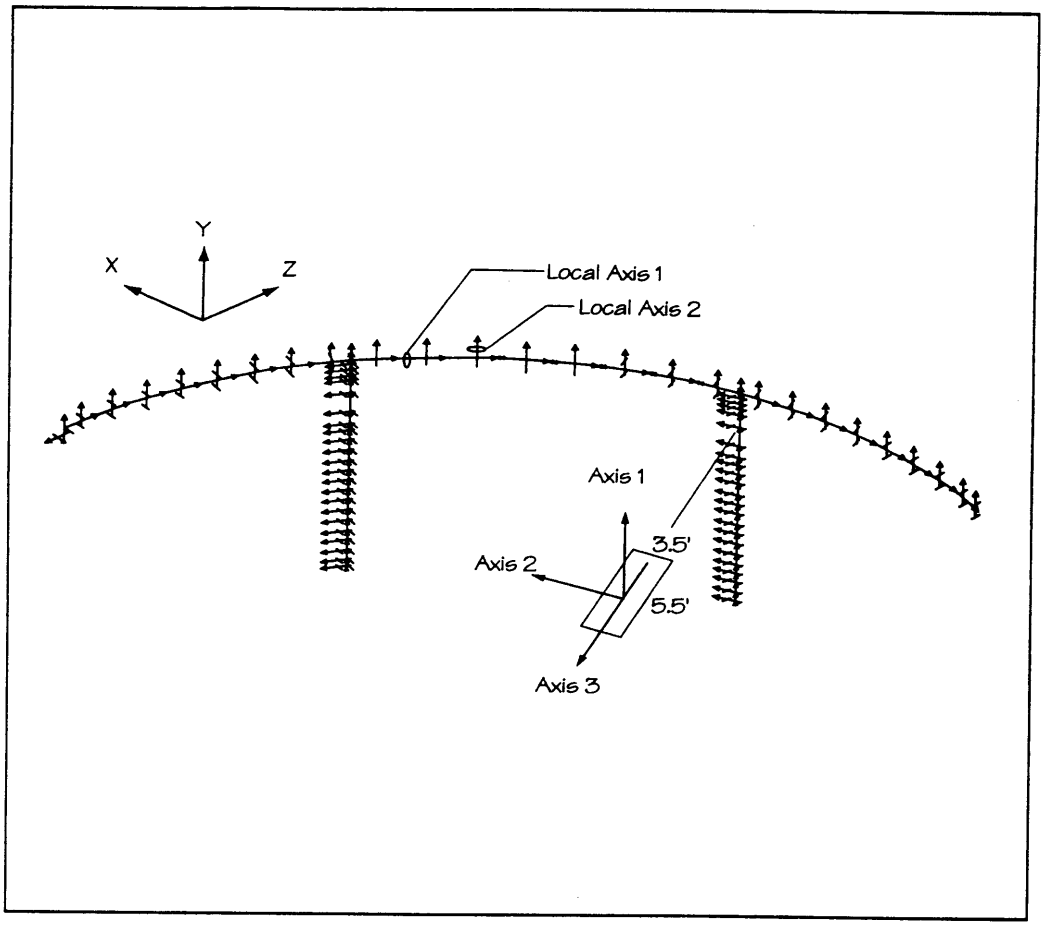

Figure 6 – Orientation of Member Local Axes

Design Step 6.2

Pier and Abutment Foundation Stiffnesses

Design Step 6.2.1

Drilled Shafts

a) General

The drilled shafts can be modeled by one of several techniques, which are illustrated in Figure 7. A discussion of each technique is given by FHWA (1987), and only brief descriptions are given here. Additional information on drilled shafts is available in *Drilled Shafts* (FHWA, 1988).

The simplest method is the equivalent cantilever, whose length is selected to provide approximately the same tip stiffness as the actual system. Charts are available to provide guidance in the selection of the cantilever length. Additionally, a separate length is often used for estimating the maximum moment in the drilled shaft itself. The method works best when the column and the drilled shaft have the same diameter.

The equivalent base spring method simply replaces the actual shaft-soil system with an equivalent system of springs attached to the base of the column. This method can work well if the coupling between translation and rotation of the shaft at the ground level are accounted for in the development of the equivalent springs. In general, this coupling will require that a "6 x 6" stiffness matrix be used to represent the spring constants. In other words, simple independent springs are not sufficiently accurate to model the coupled behavior of the shaft. Many analysis programs now allow the user to specify "6 x 6" matrices to represent such coupled spring supports. The method is iterative if the soil behavior is nonlinear; thus those spring constants must be selected that best represent the actual nonlinear behavior. Good coordination between structural and geotechnical engineers is essential to the development of reasonable spring values.

In addition to the FHWA publication listed above, Conner and Grant (1995) provide detailed discussion of the application of the equivalent cantilever and equivalent base spring methods. Their paper also includes guidance on how to handle nonlinear soil behavior with the two methods.

Design Step 6.2.1 (continued)

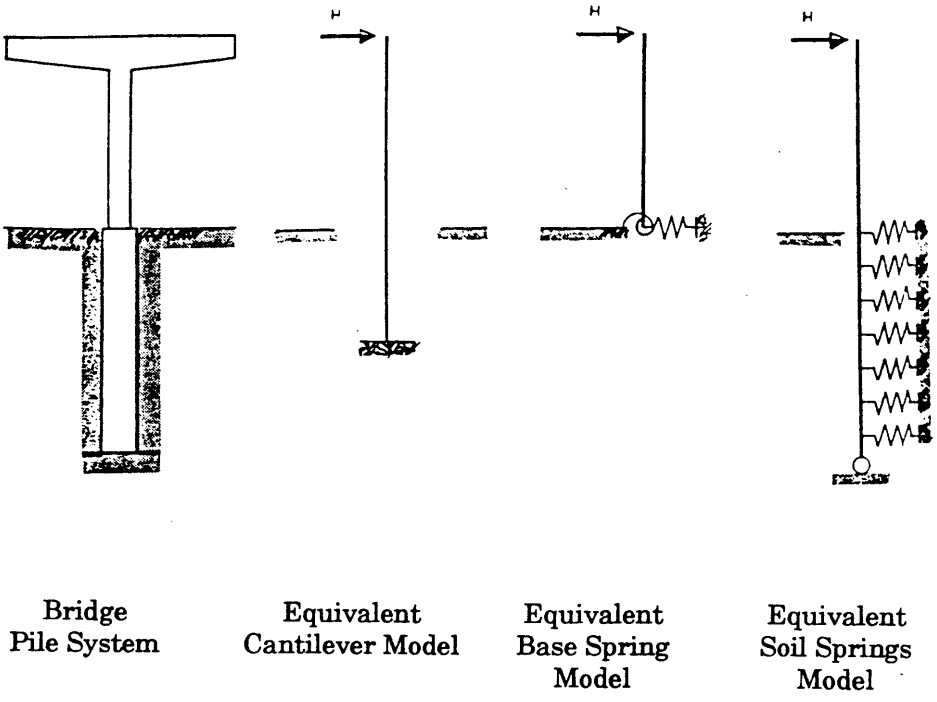

Reference: FHWA-IP-87-6, Seismic Design and Retrofit Manual for Highway Bridges, May 1987

Figure 7 — Methods of Modeling Drilled Shafts

The third method is the equivalent soil springs model, in which the drilled shaft is included in the structural model and the soil is modeled as a series of springs connected to the drilled shaft at even intervals. Such an approach circumvents the approximation process of the previous two methods, and so it directly gives reasonable stiffnesses and reasonable internal forces in the shaft. The method also allows the presence of layered materials and the water table to be directly included. The chief disadvantage of the method is the increase in computer time required, since each spring and each shaft portion between soil springs must be modeled with separate elements.

Design Step 6.2.1 (continued)

For this design, the equivalent soil springs method is selected for the substructure. This is a reasonable approach for this example, because only two drilled shafts are present. If a large number of shafts are present, then modeling of each individual shaft may yield too large a model to be practical.

The soil springs at each depth are calculated using a coefficient of horizontal subgrade reaction that increases linearly with depth and is inversely proportional to the cross sectional dimension of the shaft. The methodology is discussed in the following section. It is based on work described by Terzagi (1955), and it forms the basis of the lateral pile behavior described in the NAVFAC DM7.02 (1986) document.

Expanded discussion of lateral pile (or shaft) behavior and the methodology used can be found in *Pile Foundation Analysis and Design* by Poulos and Davis (1980) and in *Foundation Analysis* by Scott (1981). Also, more in-depth treatment of the topic can be found in the user's manual to the program LPILE, Reese and Wang (1993). This program is widely used to analyze pile and drilled shaft foundations in which the soil behaves either elastically or inelastically under lateral loading.

b) Development of Lateral Springs for Drilled Shaft

A sufficient number of springs should be used along the length of the shaft, such that the response of the system is not sensitive to the number of springs used. In general, more springs are better, but only to the point where the results no longer change with increased numbers of springs. Additionally, the springs near the surface are usually the most important for characterizing the response; thus a closer spacing may be used in that region. However, there is usually not enough time to fully explore this design aspect. Thus, springs spaced at about half the diameter of the shaft are recommended.

Use 15 springs spaced at 4 feet on center along the length of the drilled shaft. Since the shaft is 60 feet in length, begin the springs at 2 feet below the top of the shaft, and end the springs at 2 feet from the bottom of the shaft. These 15 springs will thus attach to nodes 4210 to 4224, as shown in Figure 5 for Pier 1. The initial and final 2-foot segments serve to make all the spring constants based on a 4-foot tributary length of column. Note that springs with the same stiffness constant are required in two orthogonal directions, so that the stiffness of the soil acting against the shaft is the same in all horizontal directions.

Design Step 6.2.1 (continued)

The method for calculating the horizontal spring constants is based on the variables and equation given below. The stiffness of the soil is based on the water table extending all the way to the ground surface. Note that the example calculation is given for a spring that is 30 feet below the surface.

$n_h := 15 \cdot pci$

$n_h = 25.92 \cdot kcf$

Constant of horizontal subgrade reaction based on soil type (water table at surface)

$z := 30 \cdot ft$ Depth from surface to spring location

$D := 8 \cdot ft$ Diameter of the drilled shaft

$k_h := \frac{n_h \cdot z}{D}$ $k_h = 97.2 \cdot kcf$ Coefficient of horizontal subgrade reactionat z; in this case, 30 feet

$H_{trib} := 4 \cdot ft$ Height of tributary soil for spring

$k_{30} := k_h \cdot D \cdot H_{trib}$

$k_{30} = 3110 \cdot \frac{kip}{ft}$

Horizontal spring constant at 30 feet of depth; this is also the spring constant for the spring attached to Node 4217 of Figure 5

A full listing of the spring constants used along the length of the shaft is given in Table 2.

Design Step 6.2.1 (continued)

Table 2
Lateral Spring Constants for Drilled Shaft

Horizontal z (ft)	Coefficient of Horizontal Subgrade Reaction k_h (kcf)	Spring Constant k_i (k/ft)
2	6.5	207
6	19.4	622
10	32.4	1,037
14	45.4	1,452
18	58.3	1,866
22	71.3	2,281
26	84.2	2,696
30	97.2	3,110
34	110.2	3,525
38	123.1	3,940
42	136.1	4,355
46	149.0	4,769
50	162.0	5,184
54	175.0	5,599
58	187.9	6,013

c) Discussion of Nonlinear Effects

The resistance of the soil is strain dependent, and thus the soil can exhibit significant nonlinear behavior if the soil loading is high enough. For this reason, the spring constants developed in the previous section are only valid provided that the lateral soil pressures do not exceed certain thresholds.

To deal with this phenomenon from an analytical viewpoint, idealizations of the actual behavior must be used. One such idealization that has been applied to this problem is passive failure theory. If the soil contact stress is high enough, then a passive failure wedge, as shown in Figure 8, may develop. When this occurs, the resistance of the soil in the failed zone no longer increases with displacement.

Design Step 6.2.1 (continued)

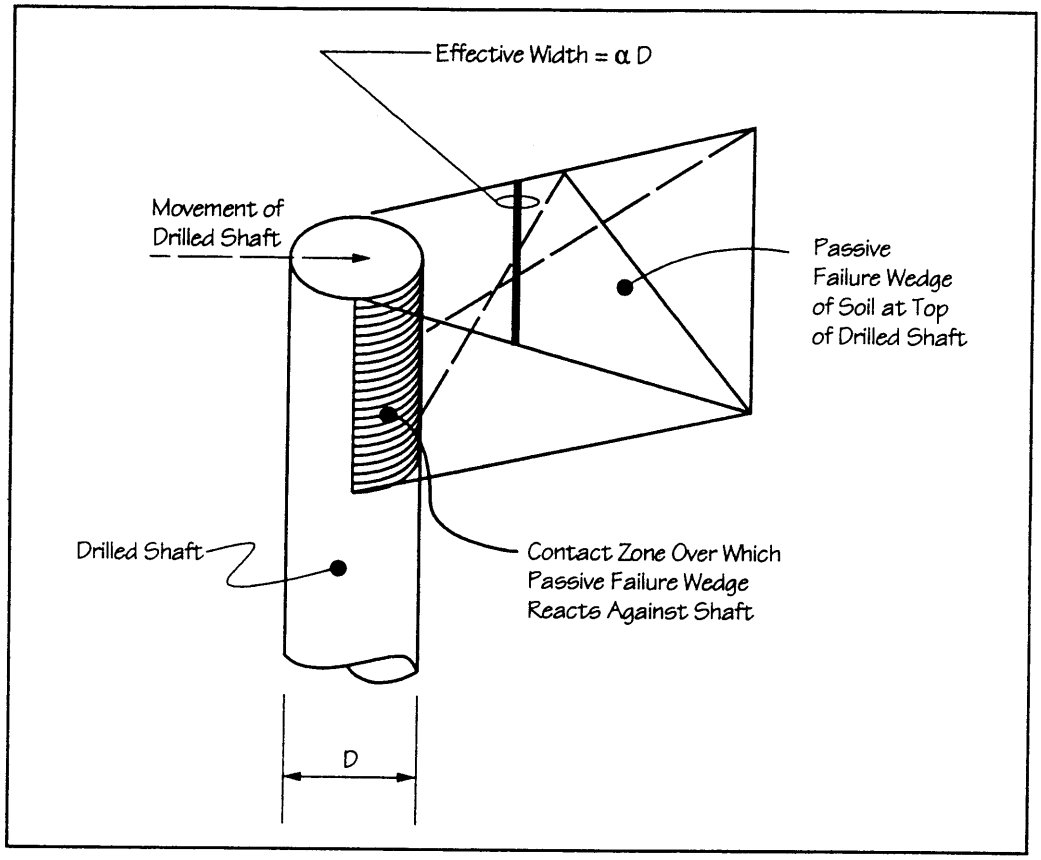

Figure 8 — Passive Failure Wedge of Soil

A force-displacement representation of this phenomenon is shown in Figure 9, which illustrates the response of one of the idealized soil springs at a depth "z" from the surface. The actual response of this spring is a nonlinear smoothly varying curve; however, this can be approximated by using a bilinear curve as shown. Each soil spring along the length of the shaft has a unique stiffness and capacity. The stiffness may be taken as that listed in the previous section, and the capacity or passive resistance can be calculated using the Rankine Method.

As an example, the available passive resistance at 30 feet of depth is calculated below.

$\gamma := 60 \cdot pcf$	Unit weight of the submerged soil; the water table is at the soil surface
$z = 30 \cdot ft$	Depth to spring in question

Design Step 6.2.1 (continued)

$\phi := 34 \cdot deg$ Angle of internal friction

$PP := \gamma \cdot z \cdot \left(\tan\left(45 \cdot deg + \frac{\phi}{2} \right) \right)^2$ Passive resistance as a pressure

$PP = 6.37 \cdot ksf$

The stress in the soil can be calculated from the soil spring force obtained from the multimode spectral analysis. This calculation is accomplished by dividing the force by the tributary length of shaft and by the effective width of the soil. The effective width may be taken as a larger width than that of the shaft, to account for the wedge-shaped passive failure zone that would develop adjacent to the shaft (see Figure 8). In this example, the effective width is taken as twice the shaft diameter, based on the geotechnical consultant's recommendation for this Type II soil. However, this effective width may not be unique for all soil types or for other lateral capacity methods (i.e., methods other than Rankine's).

If the lateral stress in the soil at the effective width exceeds the passive resistance, then the soil spring constant can be reduced as shown in Figure 9. The lateral analysis is then re-performed and the results checked. The stiffnesses are adjusted until the stiffnesses and resistances converge.

When such iteration is required, it is important to distinguish between the elastic seismic forces and the actual (or probable) forces. This distinction is necessary because the soil springs should be based on the actual forces that will be transferred. However, a check can be made using the elastic forces, and if the soil springs remain elastic for these forces, then they will work for the actual forces. A more detailed discussion of this issue is given by Conner and Grant (1995).

For this example, the elastic soil spring forces will be checked against the soil capacities first. If nonlinear action is not indicated by the check, no alterations will be required. If significant nonlinear action is indicated, then the proper soil spring stiffnesses, which correspond to the full elastic forces, must be iteratively determined. These stiffnesses may be lower bounds to the actual stiffness, because the elastic forces are larger than the forces corresponding to plastic hinging.

Design Step 6.2.1 (continued)

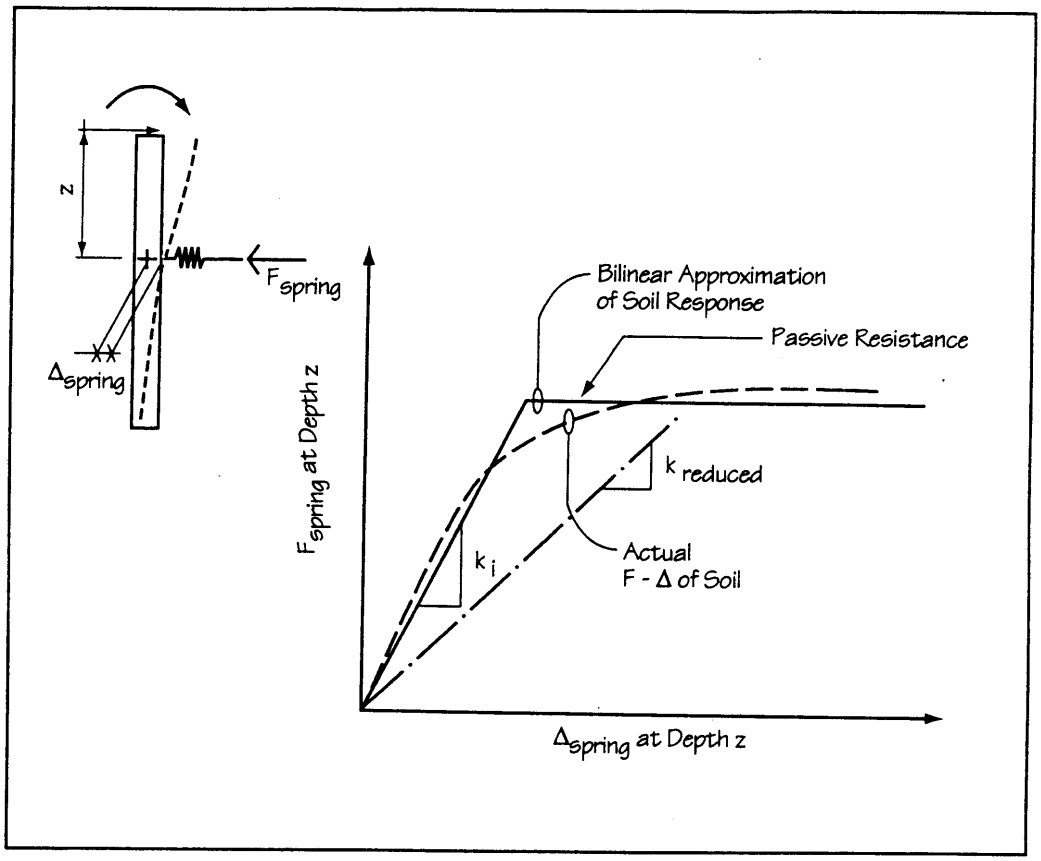

Figure 9 — Nonlinear Soil Response

An estimate of the actual soil stiffness can then be made by interpolating — via judgment — an intermediate soil stiffness for each nonlinear spring. This process results in an equivalent linear model that applies only for a given intensity of loading. While this might seem to be an overly restrictive way to handle soil nonlinearity, it does allow the use of linear elastic analysis methods, such as multimode spectral analysis.

d) Vertical Supports at Base of Shaft

As shown in Figure 3, vertical movement of the drilled shaft is restrained by an infinitely stiff spring at the base of the shaft. Actual vertical resistance occurs via skin friction and end bearing. However, for this analysis, the simplification of restraining only the base of the shaft is felt to be reasonable. Likewise, torsional movement of the shaft would be resisted by skin friction. However, no torsional restraint was used in this model, as shown in Figure 3. The response is not sensitive to lack of torsional restraint in the shaft, and this can be demonstrated by simple bounding analyses.

Design Step 6.2.2

Abutments

a) General

The abutments are modeled with rigid links that extend downward from the superstructure centroid to the approximate force transfer point located between the piles and the end diaphragm. This arrangement is shown in Figure 10. The springs that represent the piles are connected to the lowermost nodes (e.g. node 4101), and the springs that represent the abutment backfill, which is considered in the bounding of response, are connected to the middle nodes (e.g. node 4102).

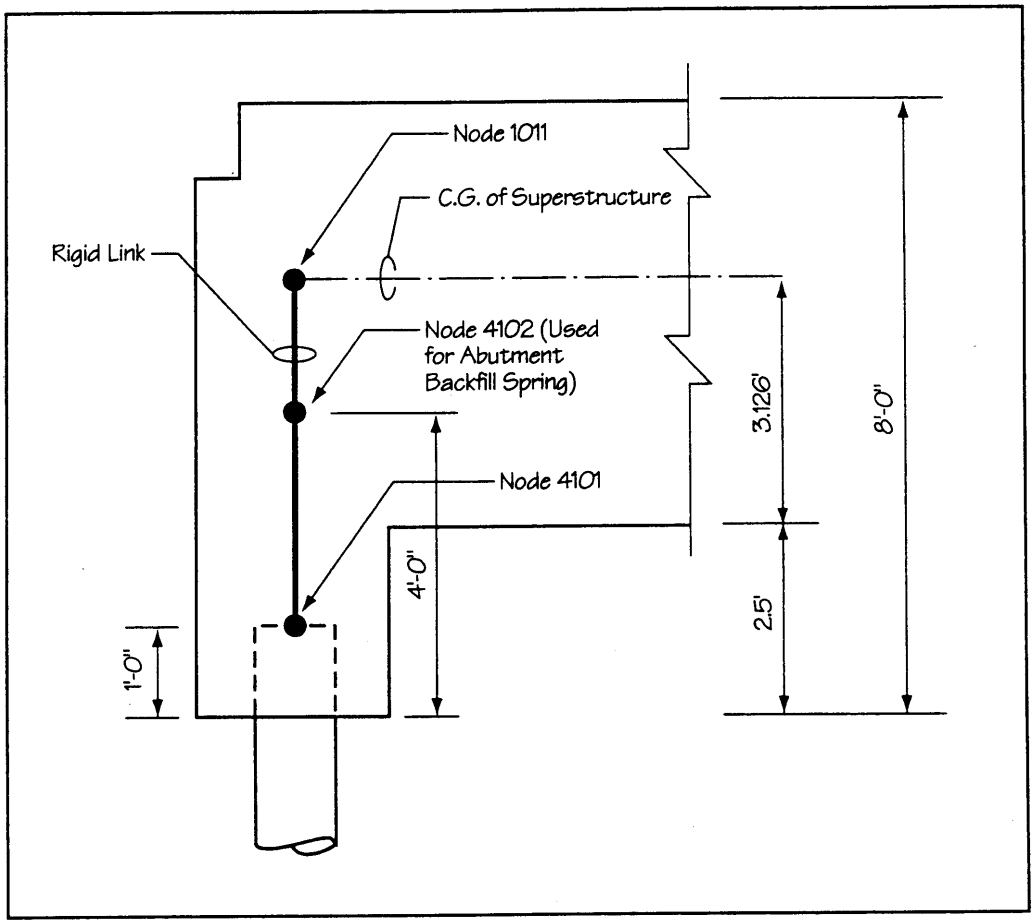

Figure 10 — Abutment Geometry

Design Step 6.2.2 (continued)

b) Pipe Piles

General. The methods used for determining the stiffness relations for a drilled shaft can also be used for piles. A common practice is to model piles using equivalent springs. The spring constants can be developed using a model of the pile similar to the one used for the drilled shaft in this example. This can either be done directly by the analyst, or by using commercially available programs such as LPILE, Reese and Wang (1993). These methods are most effective when the subsurface conditions are well established. A simpler approach, which is sufficient for many applications, is that outlined by NAVFAC DM7.02 (1986) — here called the DM7 Method. Any of the three methods should give identical results for the same input, provided the soil remains linear elastic.

The DM7 Method is used in this example to calculate the abutment pipe pile spring constants. DM7 considers two forms of pile rotational restraint: pinned at the top of the pile and fixed at the top of the pile. The top may be either at the ground surface or above it. The connection between the end diaphragm and the steel pipe pile for this example is considered more nearly pinned than fixed.

The fixity of the pile head (top of the pile) has a significant effect on the stiffness of the pile, similar to that obtained by restraining the tip of a cantilever from rotating during loading. Since the superstructure is relatively stiff, the details of the connection between the pile and the pile cap (or in this case, the abutment end wall) largely determine whether the pile is fixed, pinned, or in between. A fixed head condition requires either deep (several diameters) embedment of the pile into the abutment or a sufficient number of reinforcing bars connecting the pile and the abutment. In this case, the embedment is only 1 foot (as shown in Figure 1d), and only a few bars that are centered in the concrete fill of the pile will be used. The design of these bars is addressed in Design Step 12.1.1.

The DM7 Method is applied for pinned-top piles by using the information provided in Figures 11, 12, and 13. Based on the soil compressive strength or density, the coefficient of variation of lateral subgrade reaction "f" for the DM7 Method is determined. Note that the parameter "f" in the DM7 Method is the same as the parameter "n_h" used with the drilled shafts. (The terminology for the DM7 Method has been used in the description herein.) Then the four-step procedure shown in Figure 12 is used to calculate the deflection for a known load, as well as the moment and shear in the pile. The plots shown in Figure 13 are used to determine the coefficients for deflection, moment, and shear.

Design Step 6.2.2 (continued)

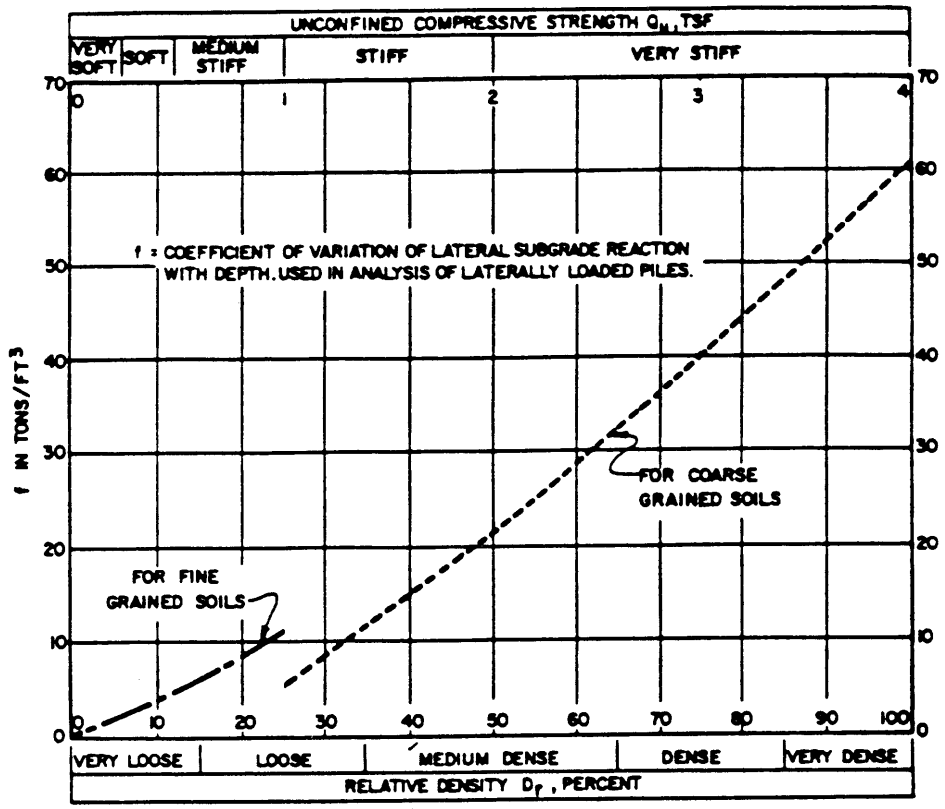

From: NAVFAC DM7.02 (1986)

Figure 11 — Coefficient of Variation of Lateral Subgrade Reaction

Design Step 6.2.2 (continued)

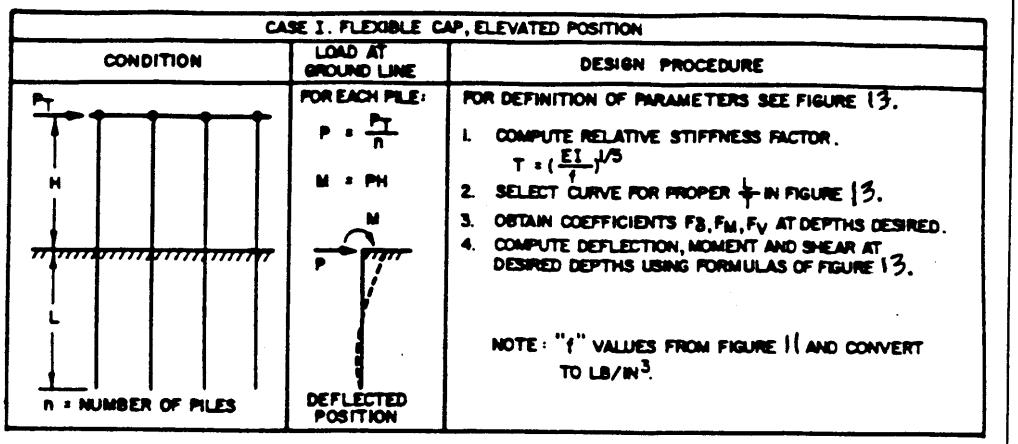

From: NAVFAC DM7.02 (1986)

Figure 12 — Design Procedure for Laterally Loaded Piles

Design Step 6.2.2 (continued)

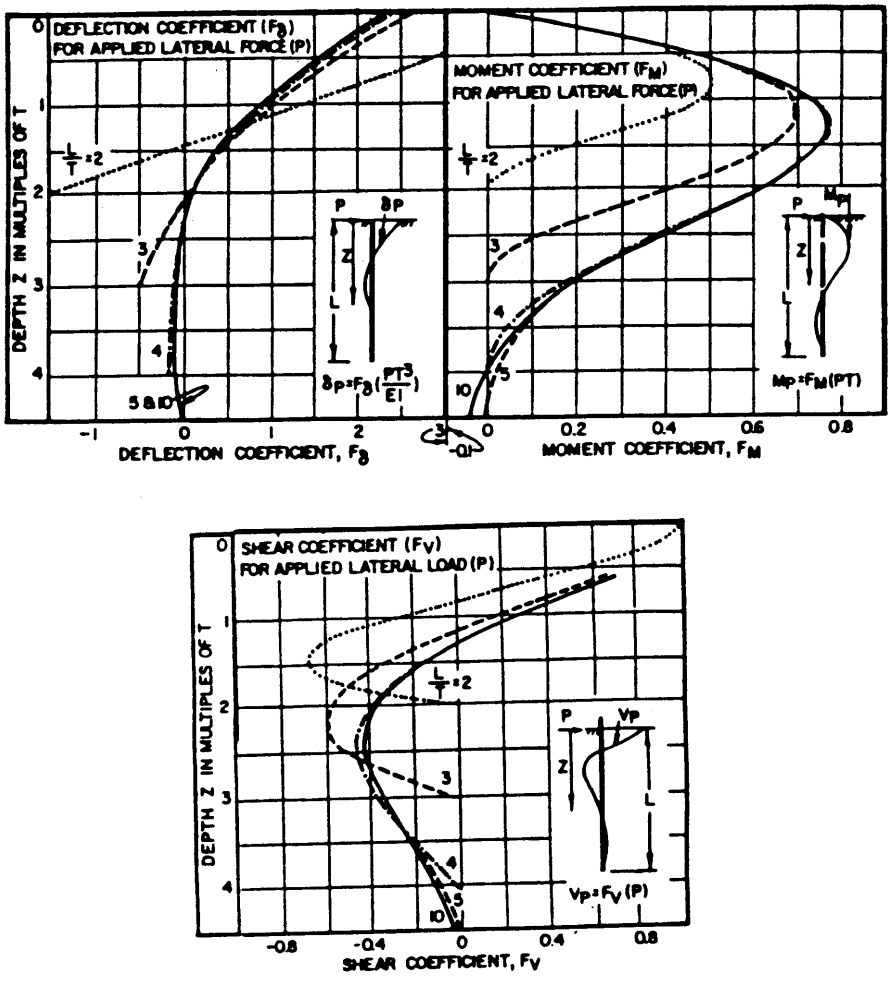

Case I. Flexible Cap or Hinged End Condition

From: NAVFAC DM7.02 (1986)

Figure 13 — Influence Values for Pile with Applied Lateral Load and Moment

Design Step 6.2.2 (continued)

The stiffness of the soil surrounding the pipe piles is based on the approach fills being of a similar material to the site soil. However, it has been assumed that the water table is not located in the fill itself during the design earthquake. Due to this constraint, the soil stiffness of the fill is larger than that of the site. The length of the piles is sufficient to penetrate the fill; thus, the piles are surrounded effectively by materials of two different stiffnesses. However, the material nearest the head of the pipe has the strongest influence on the lateral stiffness. Therefore, the properties of the fill are assumed effective along the entire length of pile.

The spring constants of the piles are calculated in the following sections.

Horizontal Longitudinal Stiffness. The stiffness of the pile in the longitudinal direction is determined by multiplying the stiffness of a single pile by the total number of piles at the abutment. There is no accounting for group effects, since the loading is perpendicular to the line of piles. Recall, from Figure 1e, that there are seven 12-inch nominal steel pipe piles in a single line at each abutment.

The first step in calculating the translational stiffness is to determine the value of T, which is based on the subgrade modulus f, and E and I for the pile. From Figure 11, the subgrade modulus selected for the approach fill material is 20 tcf. The pile will be filled with concrete to prevent buckling of the wall; thus for the stiffness calculation, the worst case for force in the pile will result from the use of the composite steel and concrete pile.

$f := 20 \cdot \frac{tons}{ft^3}$ Subgrade modulus

$f = 23.148 \cdot pci$

$I_{pipe} := 279 \cdot in^4$ Moment of inertia of a 12-inch standard weight steel pipe AISC (1989)

$I_{conc} := \frac{\pi \cdot 12^4}{64} \cdot \frac{1}{8} \cdot in^4$ Moment of inertia of the concrete in terms of equivalent steel; the modular ratio is 8

$I := I_{pipe} + I_{conc}$ $I = 406 \cdot in^4$

Design Step 6.2.2 (continued)

$E_s := 29000 \cdot ksi$ Young's modulus of steel

$$T_{long} := \left(\frac{E_s \cdot I}{f}\right)^{\frac{1}{5}} \qquad T_{long} = 55.1 \cdot in$$ From Figure 12

The coefficients given in the plots of Figure 13 are based on the quotient L/T.

$L := 40 \cdot ft$ Total length of pile

$$\frac{L}{T_{long}} = 8.7$$

From Figure 13, the coefficients for deflection and moment corresponding to an applied shear are taken from the top two plots.

$F_\delta := 2.3$ Deflection coefficient at the ground surface

$F_M := 0.77$ Moment coefficient (maximum); this will be used to check the moment in the pile

From the equations given at the lower right corner of the graph for deflection coefficient F_δ of Figure 13

$$K_I := \frac{E_s \cdot I}{F_\delta \cdot T_{long}^3} \qquad K_I = 367 \cdot \frac{kip}{ft}$$

$$K_{long} := 7 \cdot K_I \qquad K_{long} = 2569 \cdot \frac{kip}{ft}$$

Horizontal Transverse Stiffness. The stiffness of the piles in the transverse direction is reduced for group effects, because the piles are close enough to one another to reduce their stiffnesses. The reduction is based on the spacing of the piles and is applied to the constant of horizontal subgrade reaction. The reduction factors are given in Table 3.

Design Step 6.2.2 (continued)

Table 3
Group Effect Reduction Factors

Pile Spacing in Direction of Loading D = Pile Diameter	Subgrade Reaction Reduction Factor R
8D	1.00
6D	0.70
4D	0.40
3D	0.25

From: NAVFAC DM7.02 (1986)

$s := \frac{5.83 \cdot ft}{12.75 \cdot in}$ $s = 5.5$ Spacing of the piles in terms of pile diameters, approximately 6D in this case

$R := 0.7$ Approximate reduction factor from the table

$T_{trans} := \left(\frac{E_s \cdot I}{f \cdot R}\right)^{\frac{1}{5}}$ $T_{trans} = 59.2 \cdot in$

$\frac{L}{T_{trans}} = 8.1$

From Figure 13

$F_\delta := 2.3$ Deflection coefficient at the ground surface

$F_M := 0.77$ Moment coefficient (maximum); this will be used to check the moment in the pile

Design Step 6.2.2 (continued)

From the equations given at the lower right corner of the graph for deflection $F\delta$ in Figure 13

$$K_t := \frac{E_s \cdot I}{F_\delta \cdot T_{trans}^3} \qquad K_t = 296 \cdot \frac{kip}{ft}$$

$$K_{trans} := 7 \cdot K_t \qquad K_{trans} = 2074 \cdot \frac{kip}{ft}$$

The method used for including the group effect stiffness reduction is only one of several ways that this effect may be included. Table 3 is taken from the DM7.02 document, and the reduction to the horizontal subgrade reaction suggested by the table is used here to be consistent with the DM7 Method. It should be recognized that the soil modulus effects the lateral stiffness by the 3/5 power in the DM7 Method. This is seen from the equations given in Figures 12 and 13. Other methods apply the correction for group action to the individual pile stiffness, directly. Further discussion of this issue may be found in Scott (1981) and Poulus and Davis (1980). Important points are: 1) to coordinate closely with the geotechnical engineer to ensure that appropriate lateral stiffness methods are applied and 2) to ensure consistency by using the recommended reduction for a given lateral stiffness method, since the manner in which the researchers report and interpret data may vary.

Vertical Stiffness. The vertical or axial stiffness of the piles themselves should be included because the axial stiffnesses of the drilled shafts are included.

The piles are friction piles and the skin friction in this case may be assumed to be uniformly distributed along the pile. Also, the bottoms of the piles are assumed not to deflect downwards. The geotechnical engineer should be consulted on the adequacy of this assumption. Based on these assumptions, it can be shown that the axial stiffness is given by 2AE/L.

$A_s := 14.60 \cdot in^2$ Area of steel pipe

$A_{conc} := \frac{\pi \cdot (12 \cdot in)^2}{4} \cdot \frac{1}{8}$ Area of concrete in equivalent steel

Design Step 6.2.2 (continued)

$A_{conc} = 14.14 \cdot in^2$

$L = 40 \cdot ft$ Length of pile

$$K_v := \frac{2 \cdot \left(A_s + A_{conc}\right) \cdot E_s}{L} \qquad K_v = 41669 \cdot \frac{kip}{ft} \text{ per pile}$$

$$K_{vert} := 7 \cdot K_v \qquad K_{vert} = 2.917 \cdot 10^5 \cdot \frac{kip}{ft}$$

Rotation About Vertical Axis. Rotation about the vertical axis of the abutment is resisted by lateral deflection of the piles in the longitudinal direction. Thus the longitudinal stiffness of the piles is used to develop this rotational stiffness. The rotational stiffness is the moment developed about the vertical axis when a unit rotation is imposed about the axis. It can be shown that the rotational stiffness is the summation of "$K_l \, d^2$" for all the piles. The behavior is similar to that of a bolt group subjected to an applied moment.

Recall from the longitudinal translation stiffness section the stiffness of an individual pile.

$$K_l = 367 \cdot \frac{kip}{ft}$$

The calculation is based on assuming that the piles are all connected by a rigid link, as shown in Figure 14. The group is then subjected to a unit rotation about a vertical axis, and the moment required to produce the rotation is calculated. This moment is equal to the rotational stiffness, since the rotation is unity.

For spacing the seven piles, determination of the distances from the centroid of each pile is required. The centroid or center of stiffness of the group is the geometric center by symmetry. Thus, the center pile of the group of seven is not effective in resisting rotation.

Design Step 6.2.2 (continued)

Note that this calculation ignores the contribution from torsion of the individual piles, since it is so small as to be insignificant.

$d_1 := 5.833 \cdot ft$

$d_2 := 2 \cdot d_1$

$d_3 := 3 \cdot d_1$

Distances from the group centroid to individual piles on one side of the centroid

$K_{rv} := 2 \cdot K_I \cdot \left[(d_1)^2 + (d_2)^2 + (d_3)^2 \right]$

Rotational stiffness about vertical axis

The factor 2 is used for symmetry. There are actually six piles that contribute to the rotational stiffness.

$K_{rv} = 3.496 \cdot 10^5 \cdot \frac{kip \cdot ft}{rad}$

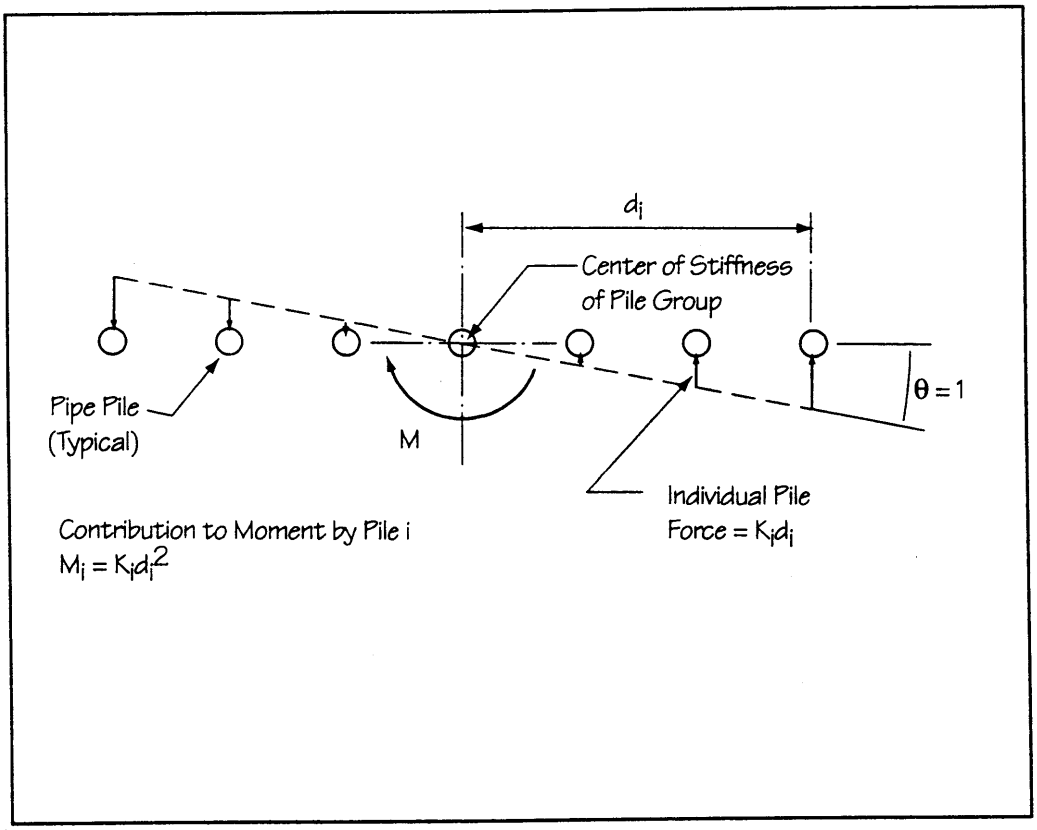

Figure 14 — Calculation Details of Rotational Stiffness

Design Step 6.2.2 (continued)

Rotation About Longitudinal Axis. The rotation about the longitudinal axis of the superstructure is resisted by axial forces developed in the piles. Thus, the axial stiffness of the piles is used to develop the rotational stiffness. The method is essentially the same as that used for determining rotation about the vertical axis, and the stiffness under upward loading is assumed to be the same as that under downward loading.

$$K_v = 41669 \cdot \frac{kip}{ft}$$

For spacing the seven piles, determination of the distances from the centroid of each pile is required. The centroid or center of stiffness of the group is the geometric center by symmetry. Thus, the center pile of the group of seven is not effective in resisting rotation.

$d_1 := 5.833 \cdot ft$

$d_2 := 2 \cdot d_1$

$d_3 := 3 \cdot d_1$

Distances from the group centroid to individual piles on one side of the centroid

$$K_{rl} := 2 \cdot K_v \cdot \left[(d_1)^2 + (d_2)^2 + (d_3)^2 \right]$$

Rotational stiffness about longitudinal axis

The factor 2 is used for symmetry. There are actually six piles that contribute to the rotational stiffness.

$$K_{rl} = 3.97 \cdot 10^7 \cdot \frac{kip \cdot ft}{rad}$$

Rotation About Transverse Axis. Because the tops of the piles are assumed to be pins, no rotational stiffness will be used about this axis.

c) Stiffness of Backfill

For the bounding case, in which the backfill is considered effective, a spring constant must be developed for the soil. The Caltrans (1989) method for determining the spring constants for abutment backwalls will be used.

Design Step 6.2.2 (continued)

Caltrans recommends starting with a stiffness of 200 kip/in/ft of wall for an 8-foot-high wall, provided a well-compacted material is used for backfill. If the wall has a different height, the basic stiffness may be prorated linearly. There is some concern that this stiffness may be too high, thus, the designer may wish to reduce the starting value. For this example, the use of a high value for bounding the solution is conservative.

Recall, from Figure 1d, that the height of the abutment backwall or end diaphragm is 8 feet. Use the 200 kip/in/ft directly. Also recall that the total width is 39.5 feet. This width includes a small wingwall on the outside of the curve. However, the wingwall is so small that it is not considered in the seismic analysis. The width can be reduced to account for the wingwall, although the stiffness is not such a precise number that such adjustments are necessary.

$$K_{back} := 200 \cdot \frac{kip}{in \cdot ft} \cdot (39.5 \cdot ft) \cdot \left(12 \cdot \frac{in}{ft}\right)$$

$$K_{back} = 9.48 \cdot 10^4 \cdot \frac{kip}{ft}$$ Stiffness of backfill

Because the backfill is considered effective only in compression, the backfill spring is normally considered to be effective at only one end of the bridge at any one point in time. To incorporate this nonlinear behavior into a linear elastic analysis, the typical practice has been to assign half of the abutment stiffness to a spring at either end of the bridge (FHWA, 1987). While this practice works for a straight bridge, it does not work for a sharply curved bridge such as this one. In this case, both abutments will be effective in resisting lateral forces when the bridge is moving in a radial direction (see Figure 2) towards the abutments. So the full spring value is assigned to each end in the bounding model.

d) Summary of the Abutment Spring Values

In the previous sections, the spring constants attributable to the abutment foundations have been developed. The values are summarized in Table 4, and the locations and orientations of the springs are explained in Figure 15.

Design Step 6.2.2 (continued)

Table 4
Spring Constants for Abutment Springs

K_{long} (kip/ft) Longitudinal Translation	2,569
K_{trans} (kip/ft) Transverse Translation	2,074
K_{vert} (kip/ft) Vertical Translation	291,700
K_{rv} (kip-ft/rad) Rotation About Vertical Axis	349,600
K_{rl} (kip-ft/rad) Rotation About Longitudinal Axis	39,700,000
K_{rt} (kip-ft/rad) Rotation About Transverse Axis	0
K_{back} (kip/ft) Translation Into Backfill	94,800
Translation Away From Backfill	0

Design Step 6.2.2 (continued)

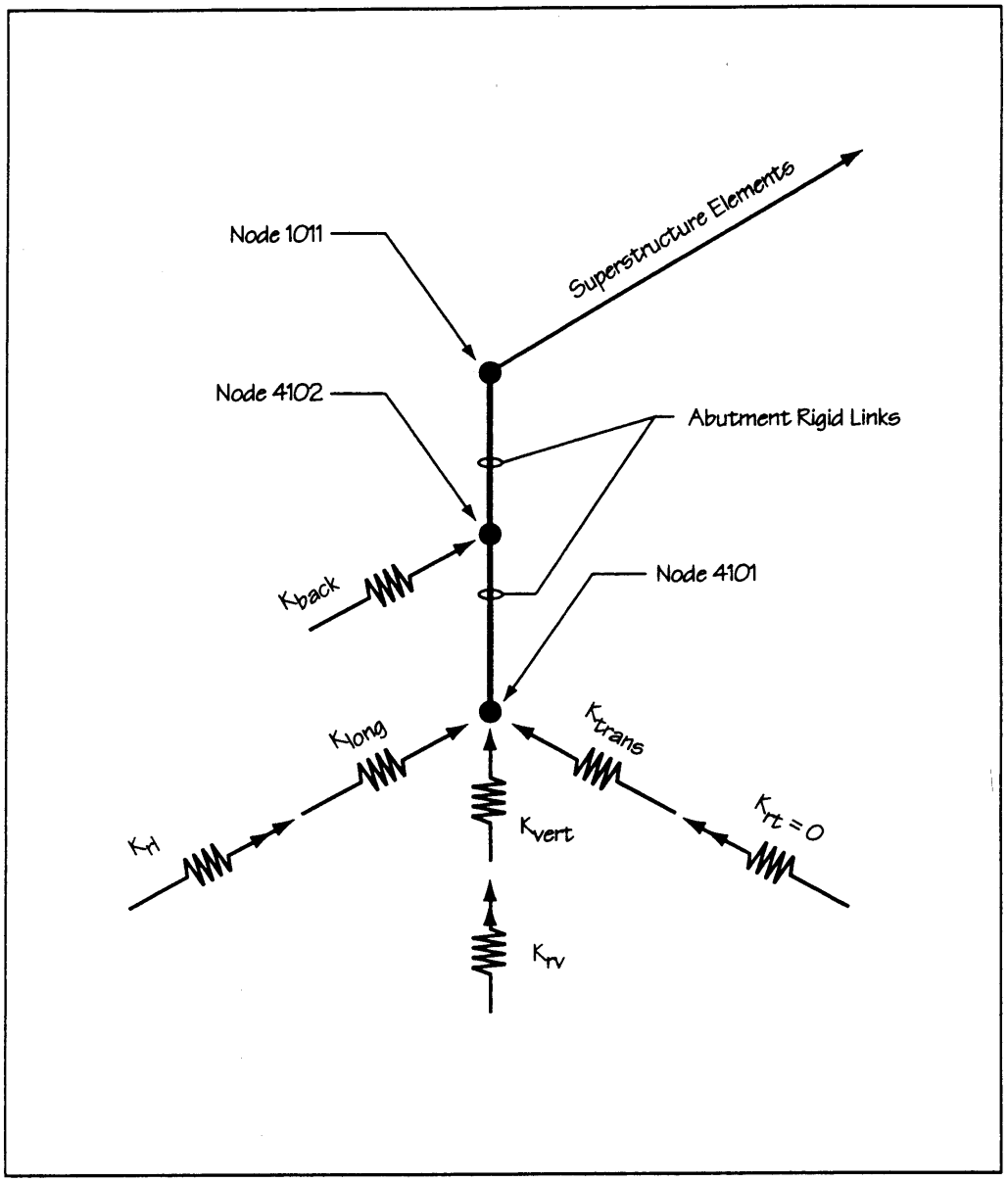

Figure 15 — Soil Spring Configuration at Abutments

Design Step 6.3

Multimode Spectral Analysis - General

Design Step 6.3.1

Mode Shapes and Periods
[Division I-A, Article 4.5.3]

The structure has been modeled using eight elements per span. The model includes elements for both the piers and the drilled shafts, and springs for the pipe piles at the abutment. Ten vibration modes have been determined for use in the multimodal spectral analysis, which involves the superposition of individual modal responses to estimate the overall structural seismic response.

SAP90 will determine the vibration periods and shapes for each of the vibration modes of the structure. The number of modes is dependent on the number of masses, the number of constrained degrees of freedom, and the number of foundation restraints for the system. Typically determination of all the modes is not required to obtained a reasonable estimate of the dynamic response. By using only a few modes, instead of all the modes, a substantial savings of computer time can be realized. Such savings can be important for large models. However, enough modes need to be determined so that the modal superposition, which provides the estimates of forces and displacements, is sufficiently accurate.

The first 10 natural periods of vibration for the No Backfill model are given in Table 5, and the vibration shapes for the first three modes are shown in Figure 16. Additionally, the participating mass for the first 10 modes is given in Table 6.

The first 10 periods for the Backfill Included model are given in Table 7, and the vibration shapes for Modes 1, 5, and 7 of the Backfill Included model are shown in Figure 17. Finally, the participating mass for the Backfill Included model is given in Table 8.

Design Step 6.3.1 (continued)

Table 5
Modal Periods and Frequencies for the No Backfill Model

PROGRAM SAP90, VERSION BETA6.00 FILE:b6sh15p.OUT
C Bridge 6 FHWA

E I G E N V A L U E S A N D F R E Q U E N C I E S

MODE	PERIOD (TIME)	FREQUENCY (CYC/TIME)	FREQUENCY (RAD/TIME)	EIGENVALUE (RAD/TIME)**2
1	0.689725	1.449854	9.109698	82.986604
2	0.671630	1.488915	9.355126	87.518386
3	0.543369	1.840371	11.563391	133.712005
4	0.292762	3.415741	21.461735	460.606057
5	0.245319	4.076331	25.612344	655.992144
6	0.205738	4.860540	30.539673	932.671636
7	0.173398	5.767078	36.235622	1313.020
8	0.101009	9.900088	62.204090	3869.349
9	0.082104	12.179735	76.527530	5856.463
10	0.061448	16.274000	102.252556	10455.585

Design Step 6.3.1 (continued)

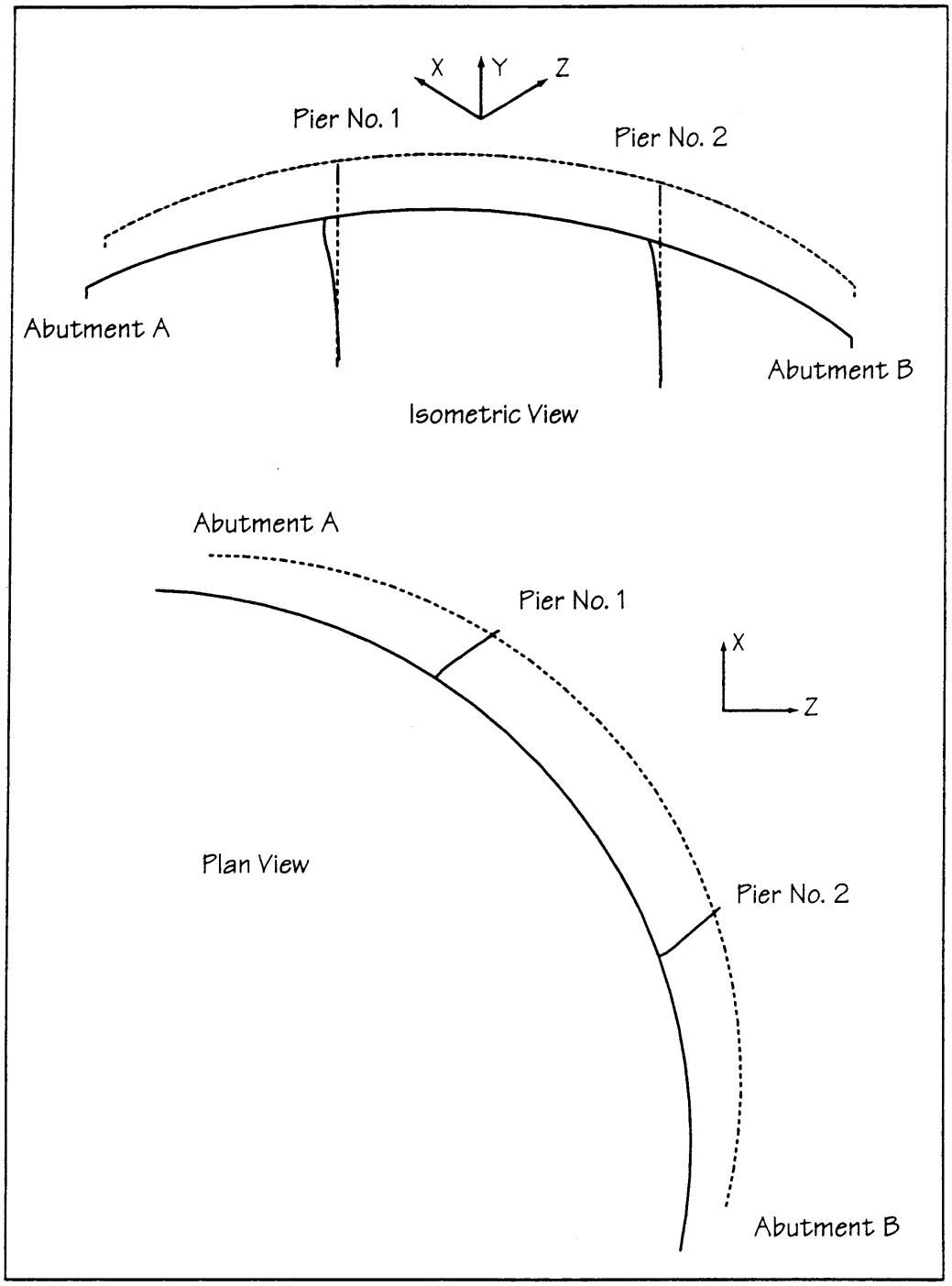

Figure 16a — Vibration Shape for Mode 1, No Backfill

Design Step 6.3.1 (continued)

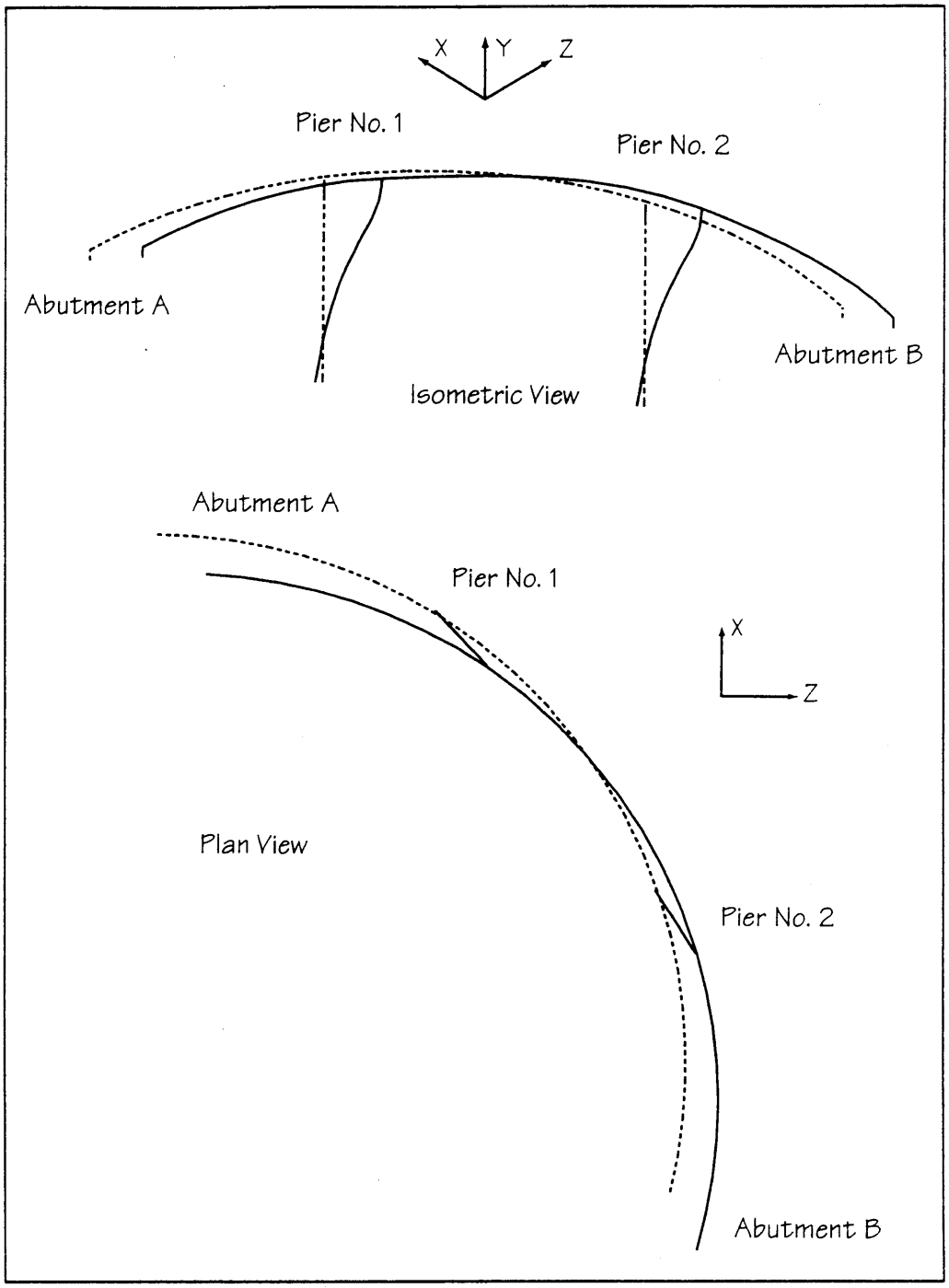

Figure 16b — Vibration Shape for Mode 2, No Backfill

Design Step 6.3.1 (continued)

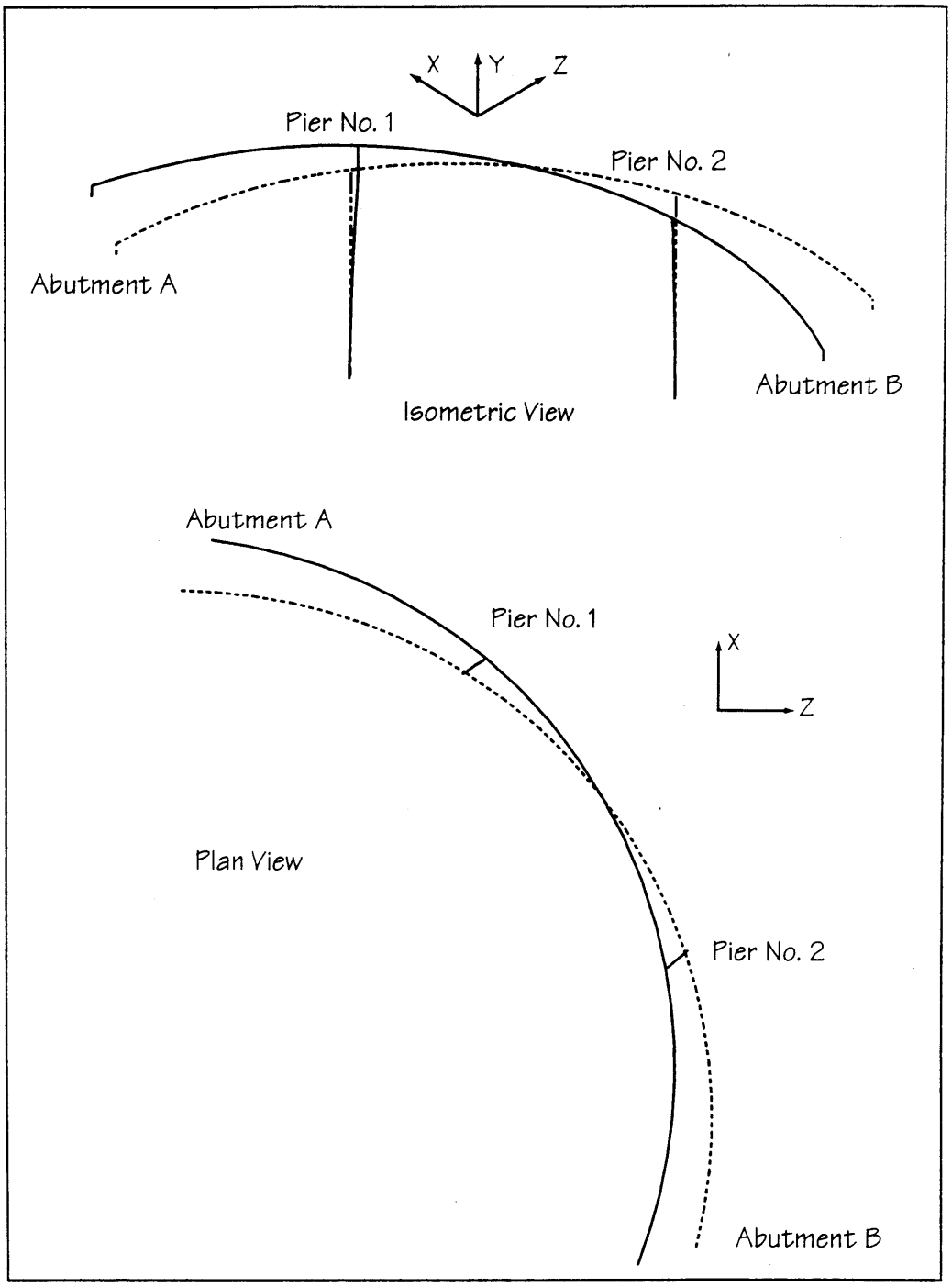

Figure 16c — Vibration Shape for Mode 3, No Backfill

Design Step 6.3.1 (continued)

Table 6
Participating Mass for the No Backfill Model

PROGRAM SAP90, VERSION BETA6.00 FILE:b6sh15p.OUT
C Bridge 6 FHWA

M O D A L P A R T I C I P A T I N G M A S S

MODE	PERIOD	INDIVIDUAL MODE (PERCENT)			CUMULATIVE SUM (PERCENT)		
		UX	UY	UZ	UX	UY	UZ
1	0.689725	37.7001	0.0055	61.6939	37.7001	0.0055	61.6939
2	0.671630	60.7736	0.0000	37.1182	98.4737	0.0055	98.8121
3	0.543369	1.1500	0.0000	0.7228	99.6237	0.0055	99.5350
4	0.292762	0.0261	0.0649	0.0425	99.6498	0.0705	99.5775
5	0.245319	0.1081	0.0023	0.1763	99.7579	0.0728	99.7538
6	0.205738	0.0590	0.0000	0.0362	99.8169	0.0728	99.7900
7	0.173398	0.0027	65.9654	0.0043	99.8196	66.0381	99.7943
8	0.101009	0.0019	0.0000	0.0012	99.8215	66.0381	99.7955
9	0.082104	0.0164	0.0000	0.0101	99.8379	66.0381	99.8056
10	0.061448	0.0003	4.1289	0.0010	99.8383	70.1670	99.8066

T O T A L U N R E S T R A I N E D M A S S A N D L O C A T I O N

DIRECTION	MASS	X	Y	Z
UX	104.199250	84.734461	-0.634382	108.100301
UY	104.199250	84.734461	-0.634382	108.100301
UZ	104.199250	84.734461	-0.634382	108.100301

Table 7
Modal Periods and Frequencies for the Backfill Included Model

PROGRAM SAP90, VERSION BETA6.00 FILE:b6abtspr.OUT
C Bridge 6 FHWA

E I G E N V A L U E S A N D F R E Q U E N C I E S

MODE	PERIOD (TIME)	FREQUENCY (CYC/TIME)	FREQUENCY (RAD/TIME)	EIGENVALUE (RAD/TIME)**2
1	0.607773	1.645352	10.338052	106.875329
2	0.294328	3.397575	21.347592	455.719702
3	0.255566	3.912878	24.585340	604.438965
4	0.208915	4.786642	30.075362	904.527379
5	0.202529	4.937564	31.023627	962.465451
6	0.170320	5.871285	36.890371	1360.899
7	0.138258	7.232858	45.445387	2065.283
8	0.100828	9.917926	62.316164	3883.304
9	0.082216	12.163090	76.422947	5840.467
10	0.062534	15.991310	100.476364	10095.500

Design Step 6.3.1 (continued)

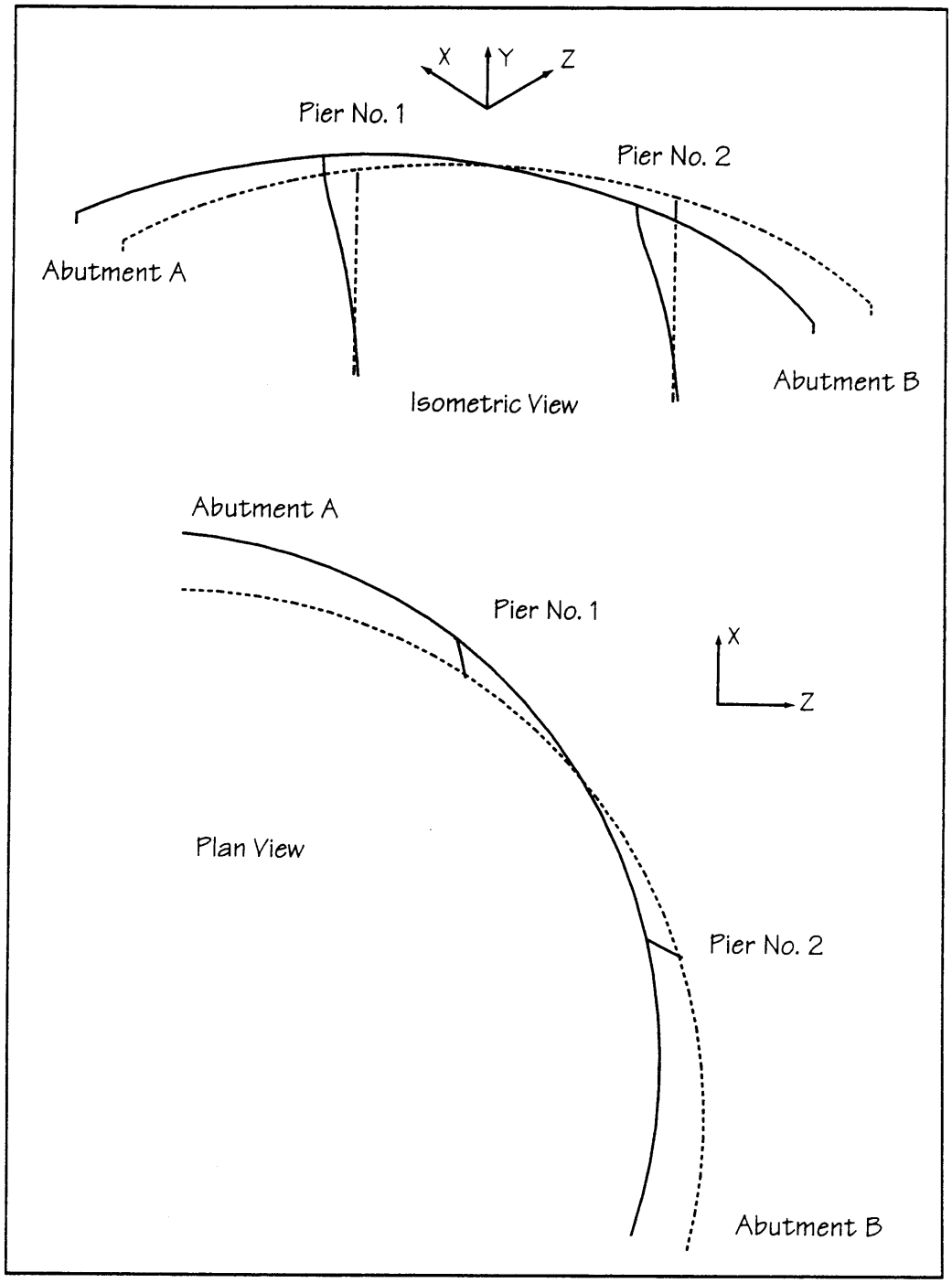

Figure 17a — Vibration Shape for Mode 1, Backfill Included

Design Step 6.3.1 (continued)

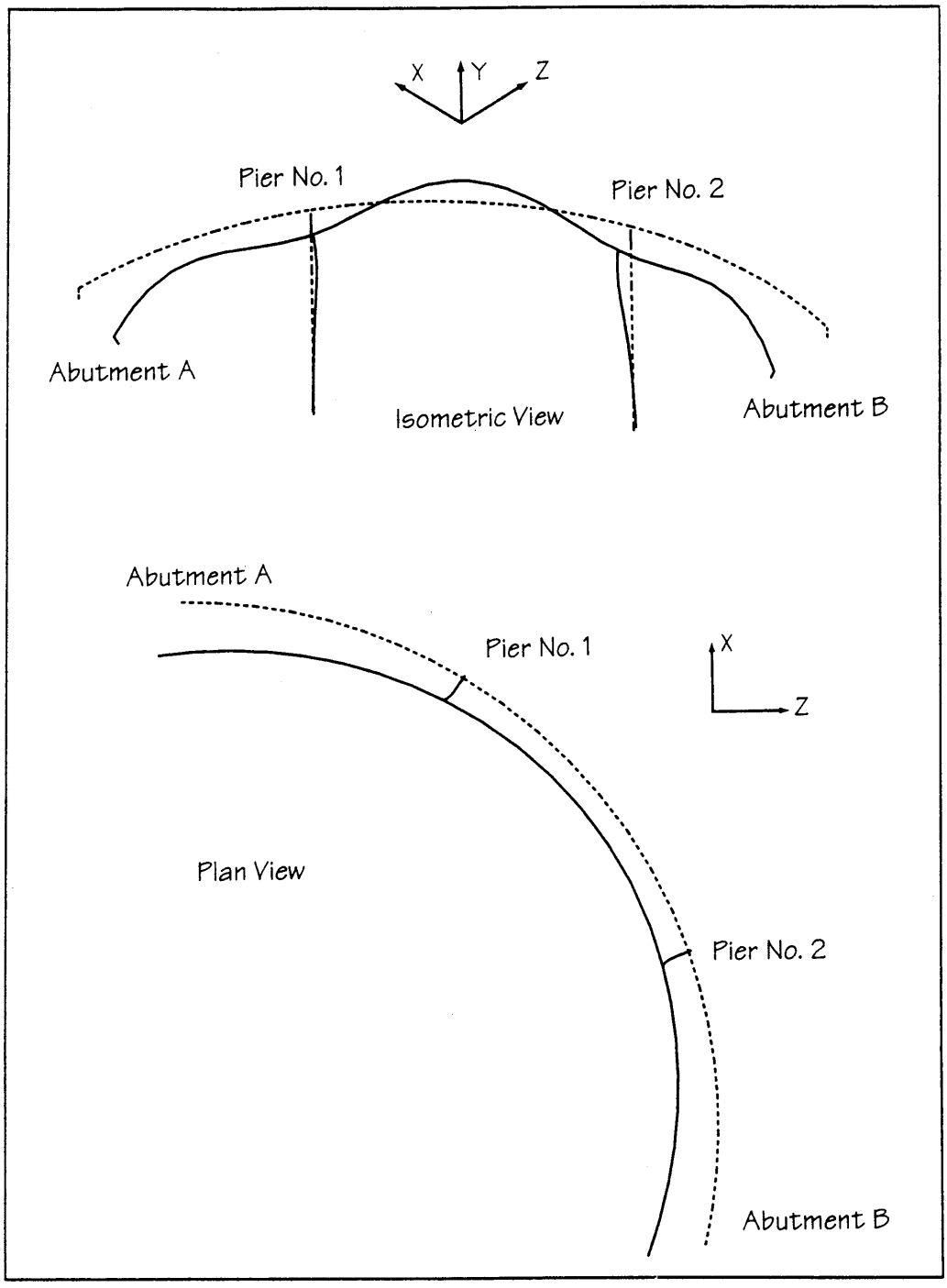

Figure 17b — Vibration Shape for Mode 5, Backfill Included

Design Step 6.3.1 (continued)

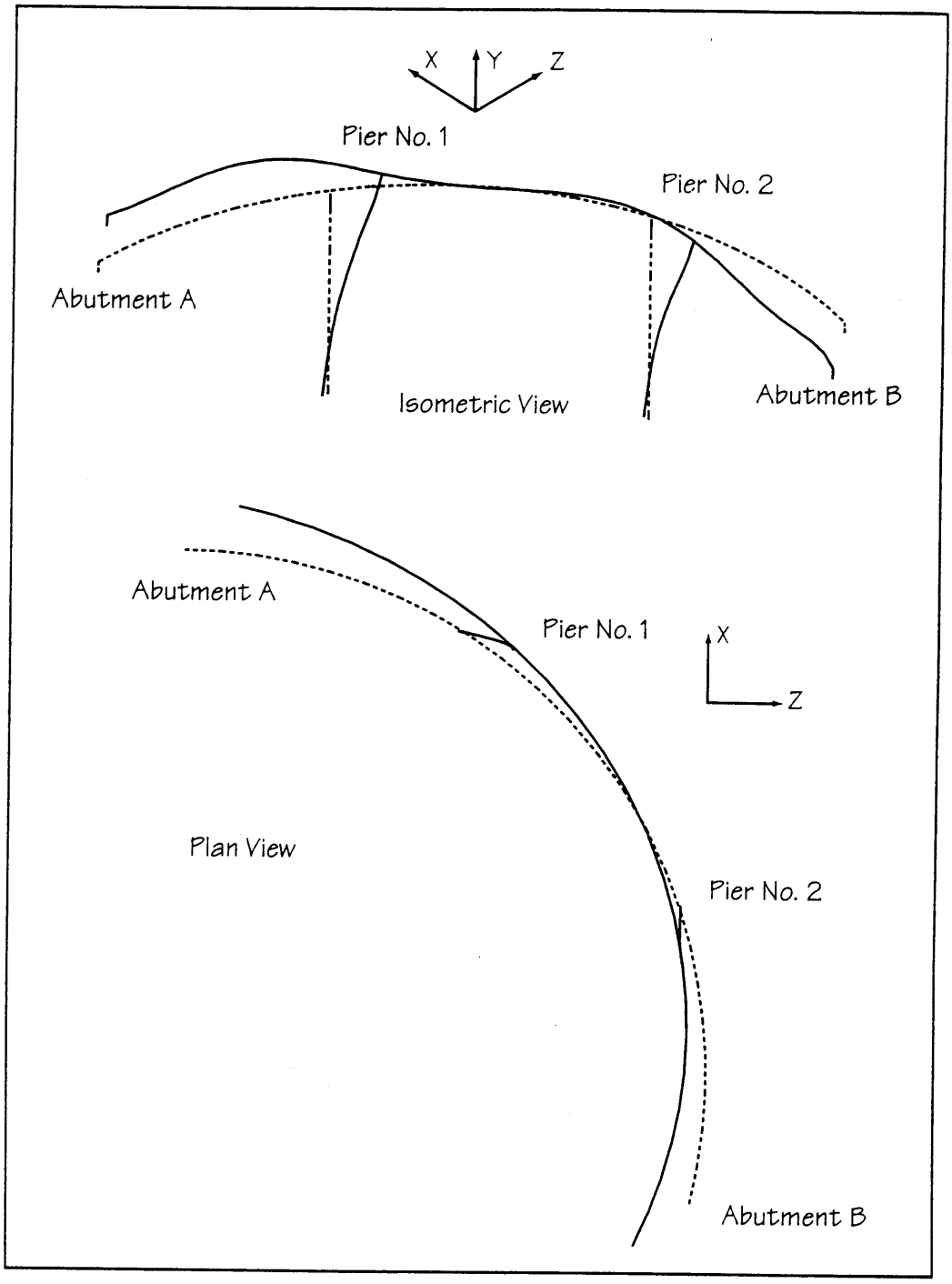

Figure 17c — Vibration Shape for Mode 7, Backfill Included

Design Step 6.3.1 (continued)

Table 8
Participating Mass for the No Backfill Included Model

PROGRAM SAP90, VERSION BETA6.00 FILE:b6abtspr.OUT
C Bridge 6 FHWA

M O D A L P A R T I C I P A T I N G M A S S

MODE	PERIOD	INDIVIDUAL MODE (PERCENT)			CUMULATIVE SUM (PERCENT)		
		UX	UY	UZ	UX	UY	UZ
1	0.607773	43.1823	0.0000	26.4633	43.1823	0.0000	26.4633
2	0.294328	0.7917	0.0129	1.2917	43.9740	0.0129	27.7550
3	0.255566	6.0058	0.1696	9.8198	49.9799	0.1825	37.5748
4	0.208915	1.0265	0.0000	0.6405	51.0063	0.1825	38.2153
5	0.202529	26.8852	7.2360	43.8393	77.8915	7.4185	82.0546
6	0.170320	3.7395	59.4455	6.1051	81.6310	66.8640	88.1597
7	0.138258	17.4515	0.0000	10.6919	99.0825	66.8640	98.8516
8	0.100828	0.1045	0.0000	0.0621	99.1870	66.8640	98.9137
9	0.082216	0.0397	0.0000	0.0243	99.2267	66.8641	98.9380
10	0.062534	0.0159	2.6294	0.0326	99.2425	69.4935	98.9706

T O T A L U N R E S T R A I N E D M A S S A N D L O C A T I O N

DIRECTION	MASS	X	Y	Z
UX	104.199250	84.734461	-0.634382	108.100301
UY	104.199250	84.734461	-0.634382	108.100301
UZ	104.199250	84.734461	-0.634382	108.100301

The analyst should carefully review the periods, mode shapes, and participating mass for the models, since these items provide a characterization of the structural model inclusive of the stiffnesses, mass and restraints. In this review, most significant errors that may have occurred in the model development can be found.

For this model the fundamental periods of vibration can be checked by hand, even though the structure is irregular in geometry. These checks are made in the section following this discussion. Note that even though the structure is sharply curved, the superstructure is quite stiff in the transverse bending directions, and therefore behaves almost as a rigid body in the first translational modes. This means that the hand checks can be made with the understanding that all the flexibility resides in the substructure, much as would be done for a straight bridge.

Inspection of the first two mode shapes, Figures 16a and 16b, corroborate the statement made above regarding nearly rigid motion of the

Design Step 6.3.1 (continued)

superstructure. As can be seen, the first two modes for the No Backfill model are translational modes in the 'radial' and 'chord' directions, as defined in Figure 2. Note, from Table 5, that the periods of vibration of these two modes are quite close. This should be expected, since the substructure elements, due to their symmetric orientation (rotations) relative to the radial and chord directions, should produce similar overall lateral stiffness in all directions. Table 6, which gives the participating mass, indicates that these first two modes are the primary translational modes, since the two combined contribute over 98 percent of the participating mass.

The third mode is primarily a rotational mode, and because it has very little net translation is associated with it, the participating mass is quite small.

Hand Check ✓ Check No. 1 Fundamental Period of Vibration — Translation in Radial Direction

This check assumes that the soil behind the abutments is not effective, and therefore the check compares with the model for the case where the bridge is moving away from the abutment soil.

The mass (weight) and the stiffness of the bridge are the two primary values needed to calculate the period. For the check, the superstructure will be assumed to be rigid, and all the flexibility is associated with the piers and the pile foundations at the abutments.

Weight Calculation. The weight is calculated first, and is based on the cross-sectional area and individual element weights listed in Design Step 6.1.2 (b).

$$W_{super} := \left(56.2 \cdot ft^2\right) \cdot (0.150 \cdot kcf) \cdot (290 \cdot ft)$$

$$W_{super} = 2445 \cdot kip$$

$W_{pd} := 79 \cdot kip$ Pier diaphragm weight

$W_{id} := 15 \cdot kip$ Intermediate diaphragm weight

$W_{ed} := 119 \cdot kip$ End diaphragm weight

Design Step 6.3.1 (continued)

$W_b := \left(0.9 \cdot \frac{kip}{ft}\right) \cdot (290 \cdot ft)$ Barrier weight

$W_b = 261 \cdot kip$

Estimate the weight of the upper half (10.5 feet) of each pier (use Figure 5).

$W_{up} := (0.15 \cdot kcf) \cdot ((28 \cdot ft + 20 \cdot ft + 10 \cdot ft) \cdot 2 \cdot ft + 5.5 \cdot ft \cdot 4.5 \cdot ft) \cdot 3.5 \cdot ft$

$W_{up} = 74 \cdot kip$

There are two pier diaphragms, three intermediate diaphragms, and two end diaphragms.

$W_{seismic} := W_{super} + 2 \cdot W_{pd} + 3 \cdot W_{id} + 2 \cdot W_{ed} + W_b + 2 \cdot W_{up}$

$W_{seismic} = 3294 \cdot kip$

At this point, the mass of the SAP90 model may be checked by comparing the mass listed in Table 6 against the value just determined.

$W_{SAP} := \left(104.199 \cdot kip \cdot \frac{sec^2}{ft}\right) \cdot 32.2 \cdot \frac{ft}{sec^2}$

$W_{SAP} = 3355 \cdot kip$

The value of the total weight just calculated does not include the weight of the lower 10.5 feet of the pier. This number is calculated below and added into the total weight to provide "apples-to-apples" comparison.

$W_{lp} := (0.150 \cdot kcf) \cdot (5.5 \cdot ft \cdot 3.5 \cdot ft) \cdot 10.5 \cdot ft$

$W_{lp} = 30 \cdot kip$

Design Step 6.3.1 (continued)

$W_{bridge} := W_{seismic} + 2 \cdot W_{lp}$

$W_{bridge} = 3355 \cdot kip$

Note that this value identically matches the SAP value. So the SAP input for mass is considered correct.

Stiffness Calculation. Two determinations are required for the stiffness of the No Backfill model: the abutment pile stiffness and the drilled shaft stiffness. To determine that a completely independent check is made, none of the stiffnesses previously determined will be used.

a) Abutment Pile Stiffness

The method described in FHWA (1987) and shown in Figure 18 is used to determine an equivalent cantilever length for the piles. In this calculation, no adjustment for group action is made.

Recall the following information regarding the piles and soil.

$E_s := 29000 \cdot ksi$ Young's Modulus of Steel

$I_{pile} := 406 \cdot in^4$ Moment of inertia of pile (includes the concrete fill)

$n_h := 23 \cdot pci$ Constant of horizontal subgrade reaction of approach fills (also equals 'f' used for DM7)

$$L_s := 1.8 \cdot \left(\frac{E_s \cdot I_{pile}}{n_h} \right)^{\frac{1}{5}}$$ Equivalent cantilever length for stiffness calculations in inches

$L_s = 99 \cdot in$

$$k_{pile} := \frac{3 \cdot E_s \cdot I_{pile}}{L_s^3} \cdot \left(12 \cdot \frac{in}{ft} \right) \qquad k_{pile} = 432 \cdot \frac{kip}{ft}$$

Design Step 6.3.1 (continued)

$k_{abut} := 7 \cdot k_{pile}$ $\quad k_{abut} = 3027 \cdot \frac{kip}{ft}$

Note that this value is about 25 to 50 percent higher than the stiffnesses listed in Table 4.

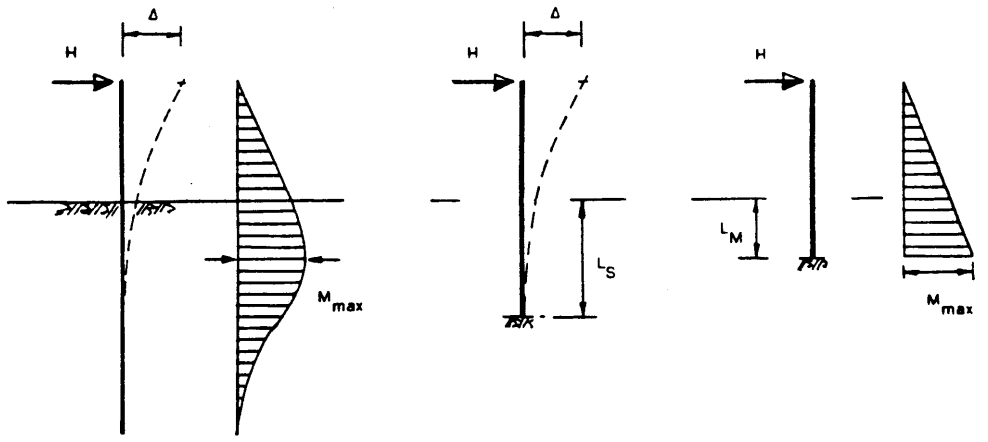

	L_S	L_M
Cohesive Soil Constant K_h	$1.4\sqrt[4]{\frac{EI}{K_h}}$	$0.44\sqrt[4]{\frac{EI}{K_h}}$
Cohesionless Soil Constant n_h	$1.8\sqrt[5]{\frac{EI}{n_h}}$	$0.78\sqrt[5]{\frac{EI}{n_h}}$

Reference: FHWA-IP-87-6, Seismic Design and Retrofit Manual for Highway Bridges, May 1987

Figure 18 — Equivalent Cantilever Method Using Relative Stiffness Factors

As a side note, the expression for L_S described in Figure 18 can be equated to the stiffness calculated by the DM7 Method using Figures 11, 12, and 13. This can be accomplished by recognizing that the quantity raised to the 1/5 power in the L_S expression is T in the DM7 Method. If the stiffness of the equivalent cantilever is equated to the stiffness from DM7,

Design Step 6.3.1 (continued)

the constant, which is listed as 1.8 in Figure 18, can be determined, directly.

The DM7 stiffness is

$$k := \frac{E \cdot I}{F_\delta \cdot T^3}$$

The same stiffness calculated as an equivalent cantilever of length αT is

$$k := \frac{3 \cdot E \cdot I}{(\alpha \cdot T)^3}$$

Note that the length of the cantilever L_s is αT in this expression. If the two equations for k are set equal to one another, and like terms canceled, then the following expression for α results.

$$\alpha := \left(F_\delta \cdot 3\right)^{\frac{1}{3}}$$

If F_δ at the ground surface ($z = 0$) is 2.3, as is the case for L/T values greater than 3 (see Figure 13), then α is

$$\alpha := (2.3 \cdot 3)^{\frac{1}{3}} \qquad \alpha = 1.9$$

This number is nearly identical to the 1.8 value listed in Figure 18. This is more than coincidental, because the two methods are based on the same principles. The difference that arises, 1.8 versus 1.9, is undoubtedly due to round-off that has occurred in the presentation of the two methods' results.

b) Stiffness of Drilled Shaft and Column

The stiffness of the shafts is calculated using Figure 18 again. The properties of the shaft and of the soil are the required input. Because the column and the shaft have different cross sections, the equivalent cantilever length of the drilled shaft will be determined separately and combined with the column to form an approximate system stiffness.

Design Step 6.3.1 (continued)

Calculate the shaft moment of inertia.

$$I_{shaft} := \frac{\pi \cdot (8 \cdot ft)^4}{64} \qquad I_{shaft} = 201.1 \cdot ft^4$$

Assume the concrete modulus is

$$E_c := 519000 \cdot ksf$$

The constant of horizontal subgrade reaction is also required, and as described in Design Step 6.2.1, the constant is

$$n_h := 15 \cdot pci \qquad n_h = 25.92 \cdot kcf$$

From the equation given in Figure 18 for cohesionless soil

$$L_s := 1.8 \cdot \left(\frac{E_c \cdot I_{shaft}}{n_h} \right)^{\frac{1}{5}} \qquad L_s = 37.7 \cdot ft$$

So the effective depth of the drilled shaft, when considered a cantilever, is 37.7 feet.

The column stiffness is also required to estimate the stiffness of the system. However, the stiffness of the column differs in each direction due to the unequal side dimensions; therefore, take an average value for the stiffness calculation. This average value will be assumed to apply in all directions, and as a result, the skew angle of the columns to the radial and chord directions will not be directly included in the stiffness calculation.

$$I_{cw} := \frac{5.5 \cdot ft \cdot (3.5 \cdot ft)^3}{12}$$

Weak direction column moment of inertia

$$I_{cw} = 19.7 \cdot ft^4$$

Design Step 6.3.1 (continued)

$$I_{cs} := \frac{3.5 \cdot ft \cdot (5.5 \cdot ft)^3}{12}$$ Strong direction column moment of inertia

$$I_{cs} = 48.5 \cdot ft^4$$

$$I_{avg} := \frac{I_{cw} + I_{cs}}{2}$$ Average column moment of inertia

$$I_{avg} = 34.1 \cdot ft^4$$

The column and the drilled shaft stiffnesses need to be combined in some rational manner in order to estimate the composite stiffness of the system. A simple approach is shown in Figure 19, where the intersection of the column and the shaft is considered to be an inflection point. Also, the column is assumed to be fixed against rotation at its top (soffit of the superstructure), and the shaft is assumed fixed at 37.7 feet below its intersection with the column, which is also the surface of the ground.

The location of the assumed inflection point is arbitrary, and can be varied by the designer to best represent the actual structure. Obviously some judgment is required. The model of the column is essentially two cantilevers that meet at the inflection point. Therefore, the stiffness of this system is simply a parallel combination of the two cantilever stiffnesses. This can be easily shown.

The lengths of the cantilevers are

$L_t := 21 \cdot ft$ Top cantilever (column)

$L_b := 37.7 \cdot ft$ Bottom cantilever (drilled shaft)

$$k_{top} := \frac{3 \cdot E_c \cdot I_{avg}}{L_t^3} \qquad k_{top} = 5731 \cdot \frac{kip}{ft}$$

$$k_{bot} := \frac{3 \cdot E_c \cdot I_{shaft}}{L_b^3} \qquad k_{bot} = 5842 \cdot \frac{kip}{ft}$$

Design Step 6.3.1 (continued)

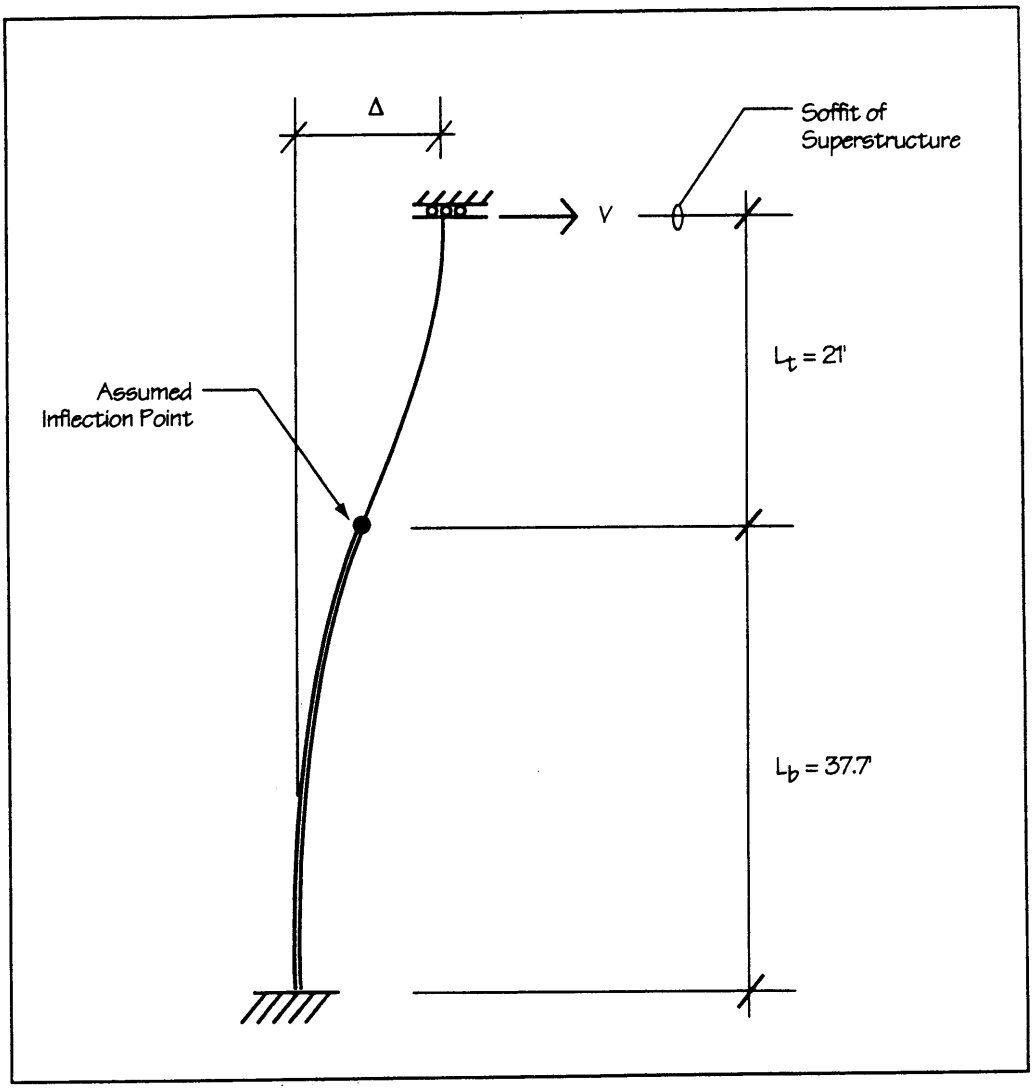

Figure 19 — Simplified Model of Column and Drilled Shaft

The parallel combination of top and bottom stiffnesses is

$$k_{pier} := \frac{1}{\left(\frac{1}{k_{top}} + \frac{1}{k_{bot}}\right)} \qquad k_{pier} = 2893 \cdot \frac{kip}{ft}$$

Design Step 6.3.1 (continued)

c) Total Stiffness

The total stiffness of the bridge substructure elements is derived from the addition of the abutment contributions and the pier contributions.

$$k_{total} := 2 \cdot k_{abut} + 2 \cdot k_{pier}$$

$$k_{total} = 11840 \cdot \frac{kip}{ft}$$

Recall that the stiffnesses of the abutment piles did not include group effects and are thus the same in all directions. Also, the average of the column weak and strong direction stiffnesses have been used to determine the pier stiffnesses. Thus the total estimated stiffness is effectively independent of loading direction. This simplification of the actual system allows the stiffness to be calculated easily and without consideration of the orientation of the substructure elements.

Period Calculation. Because the approximations of stiffness give the same stiffness in all directions, the radial period of vibration and the chord period estimates will be identical.

Recall the weight and the acceleration due to gravity.

$$W_{seismic} = 3294 \cdot kip \qquad g = 32.174 \cdot \frac{ft}{sec^2}$$

$$T := 2 \cdot \pi \cdot \sqrt{\frac{W_{seismic}}{g \cdot k_{total}}} \qquad \text{Period of vibration}$$

$$T = 0.584 \cdot sec$$

The periods from SAP90 for the No Backfill model are 0.690 second and 0.671 second for the radial and chord directions, respectively. These represent 18 and 15 percent differences with the hand calculation. Given that the hand value is completely independent of the SAP90 values, the check looks quite reasonable.

Design Step 6.3.1 (continued)

At this point, the designer should evaluate whether the period calculated by hand and that given by the analysis program are close enough. If a simple order-of-magnitude check is being made, the period just determined is certainly adequate. However, if the designer wishes to make a closer check on the SAP90 program results, then several improvements to the hand check can be made. Such improvements may simply entail using values for stiffness that more nearly match the SAP90 results. The purpose of doing this is to determine whether matching the stiffnesses can resolve the differences between the hand period and the computer model period. If it can, then there are probably no major flaws in the SAP90 model, and the designer's confidence in the computer results is justified.

One way of improving the period estimate for this example is to adjust the abutment stiffnesses to better reflect the values given in Table 4 for the two horizontal translational directions. For instance, inspection of the table values indicates that an average abutment stiffness might be about 2300 kips/ft. If the period calculation is repeated with this value, the hand check should produce a longer period, since the abutment contribution to stiffness drops.

$$k_{revised} := 2 \cdot \left(2300 \cdot \frac{kip}{ft} \right) + 2 \cdot k_{pier}$$

Where $k_{pier} = 2893 \cdot \frac{kip}{ft}$

$$T_{revised} := 2 \cdot \pi \cdot \sqrt{\frac{W_{seismic}}{g \cdot k_{revised}}} \qquad T_{revised} = 0.624 \cdot sec$$

Indeed the period estimate is more accurate, and the relative differences are 10 and 7 percent, respectively.

Further improvement can be made in the period estimate by using a stiffness for the drilled shaft that is taken directly from the SAP90 results. Obviously the checking process is then no longer independent of the SAP90 model, but this refinement of the estimate does allow an assessment of the source of the difference between the hand check and the SAP90 results.

The stiffness of the drilled shaft alone, when subjected to the earthquake spectral forces, can be estimated from the shear transferred between the

Design Step 6.3.1 (continued)

column and the shaft and the displacements of the top of the shaft. These results will be reported and discussed in Design Step 6.4 for earthquake loading in the radial direction of the bridge. In that design step, Table 9 reports the transverse and longitudinal shears at the top of the shaft as 272 kips and 113 kips, respectively. Also in Design Step 6.4, Table 11 reports the displacements (translation) of the top of the shaft as 0.074 and 0.030 foot for the two directions. From these forces and displacements the stiffness can be calculated as shown below.

$$k_{shaft} := \frac{\sqrt{(272\cdot kip)^2 + (113\cdot kip)^2}}{\sqrt{(0.074\cdot ft)^2 + (0.030\cdot ft)^2}}$$

$$k_{shaft} = 3689\cdot\frac{kip}{ft}$$

By combining this stiffness in parallel with the column stiffness k_{top} previously determined, a new estimate of the pier stiffness can be made.

Recall that $k_{top} = 5731\cdot\frac{kip}{ft}$

$$k_{pier} := \frac{1}{\left(\frac{1}{k_{top}} + \frac{1}{k_{shaft}}\right)} \qquad k_{pier} = 2244\cdot\frac{kip}{ft}$$

The revised estimate of the total bridge stiffness is then

$$k_{revised} := 2\cdot\left(2300\cdot\frac{kip}{ft}\right) + 2\cdot\left(k_{pier}\right)$$

$$k_{revised} = 9088\cdot\frac{kip}{ft}$$

Design Step 6.3.1 (continued)

The revised period is then

$$T_{revised} := 2\cdot\pi\cdot\sqrt{\frac{W_{seismic}}{g\cdot k_{revised}}} \qquad T_{revised} = 0.667\cdot sec$$

It can be seen that this value is now much closer to the periods calculated by SAP90 (within 1 to 3 percent). The closer agreement between the hand check and the SAP90 results is an indication that the stiffness differences between the two models generally corresponds to the differences between period estimates.

Design Step 6.3.2

Spectral Loading
[Division I-A, Article 3.6.2]

The input response spectra for this bridge is shown in Figure 20. The curve shown in the figure is given by the equation for C_{sm} shown below.

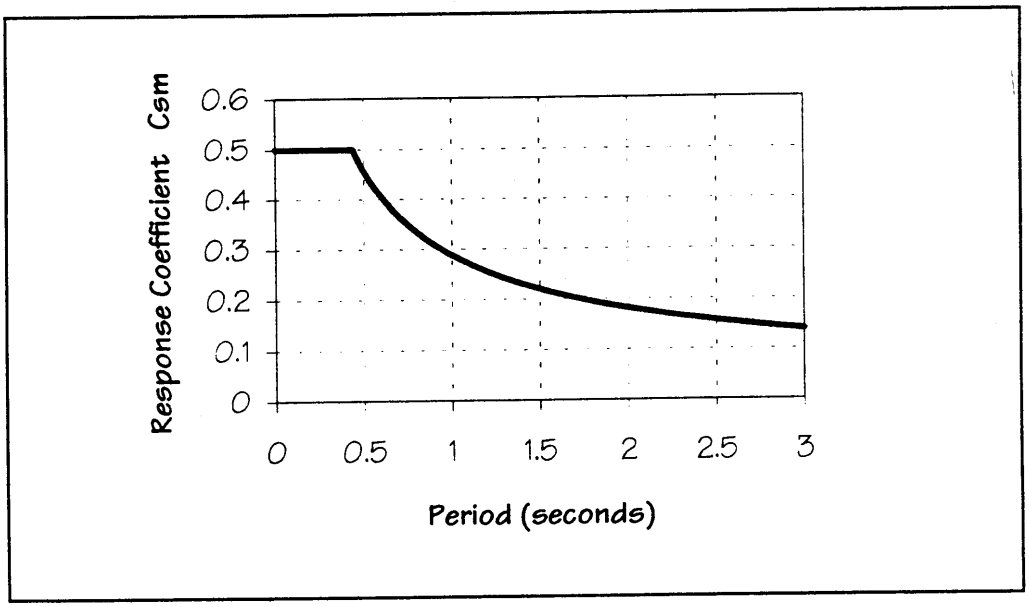

Figure 20 — Relationship Between Elastic Seismic Response Coefficient and Period

$$C_{sm} := \frac{1.2\cdot A\cdot S}{T_m^{\frac{2}{3}}} \le 2.5\cdot A$$

Division I-A
Eqn (3-2)

Design Step 6.3.2

where

A is the acceleration coefficient.
S is the site coefficient.
T_m is the period.

A design response spectrum must be input to provide loading for the models. This spectrum is specified in Section 3.6.2 of Division I-A, and it applies in both the transverse and longitudinal directions. Equation 3-2 of Division I-A, together with the equation's corresponding upper limit of two and a half times A, effectively define the spectrum as a function of period T. This fact can be seen in Figure 20 for this bridge. Most programs require period-spectrum data pairs to be input. Thus, the user must calculate the C_{sm} values that will define a smooth function within the analysis software. (C_{sm} is the modal analysis version of C_s.) The range used must cover the entire range of expected periods for the structure.

Some programs allow the user to control interpolation between the input points. The typical choice is linear interpolation on an arithmetic scale or linear interpolation on a log-log scale. Logarithmic interpolation results in a curvilinear representation between data points on an arithmetic scale. Therefore, the user should be aware of how the program will interpolate so that a smooth representation of the input spectrum is obtained, and the spectrum obtained is what the user expects. Regardless of how the interpolation is done, use of small increments between input points will ensure that the proper spectral values are used by the program.

Design Step 6.3.3

Minimum Number of Modes
[Division I-A, Articles 4.5.4]

Ten modes have been included to provide an accurate estimate of the response and internal forces for both the No Backfill and Backfill Included models.

As mentioned above, most dynamic response can be adequately characterized without using all the vibration modes. The minimum number of modes required is specified in Division I-A, Article 4.5.4 as three times the number of spans, which in this case is nine modes.

The two sets of analyses for this bridge used 10 modes each, as shown in Tables 7 and 8.

Design Step 6.3.3

It can be seen from the tables that it is much easier to capture a high percentage of participating mass — say over 90 percent — when the restraint of the heaviest part of the structure is relatively low. For instance, in the No Backfill model the restraint for translation at the abutments is relatively low, since only the pipe piles provide restraint there. Consequently, only the first two modes are required to capture over 98 percent of the mass as shown in Table 7. On the other hand, the restraint provided by the backfill soil increases the frequency of the translational modes in the Backfill Included model; so the first seven modes are required to capture over 98 percent participating mass, as shown in Table 8.

The effect of the foundation restraint on participating mass, seen in the two tables, is typical. Often the presence of stiff foundation restraints means that more modes will be required to obtain a given level of mass participation. This phenomenon is the result of the stiff restraints not allowing much movement of the mass that is immediately adjacent to the restraint.

For this bridge, the effect of the restraints is seen primarily with the abutment springs and not with the drilled shaft springs. Recall that the mass of the drilled shaft was not included in the model, since the difference between the density of concrete and that of soil is not large. Since the mass of the shaft was not included, obtaining nearly full mass participation required only a few modes. If the mass of the shaft had been included, many more modes would have been required to get the same level of mass participation. One might wonder if the structure forces are significantly in error, due to the omission of the shaft mass. Actually, however, the forces transmitted between the column and the shaft would not be changed much at all by including more modes and the shaft mass. The main difference would be in the forces in the shaft, because they would be changed according to the inertial effects induced. However, this change would generally be small relative to the magnitude of the forces transferred from the columns and superstructure.

Design Step 6.3.4

Combination of Modes
[Division I-A, Articles 4.5.5]

The Complete Quadratic Combination (CQC) technique has been used to combine the modal results.

This combination accounts statistically for the fact that the maximum response does not occur simultaneously for all modes. It also accounts for the coupling that can occur between modal responses when two or more modes have nearly the same period. Note that for the No Backfill model, the first two modes have nearly identical periods, and they provide most of the response, since their mass participation is quite high. Thus, the CQC technique is particularly applicable to this bridge.

Design Step 6.4

Determine Forces and Displacements in Radial Direction

[Division I-A, Articles 3.8 and 4.5]

The Multimode Spectral Method of analysis was used to determine the internal seismic forces, reactions, and displacements for earthquake loading in a direction perpendicular to the chord of the bridge. This direction is called the radial direction.

Article 3.8 discusses the directions for which earthquake loadings are to be considered for curved bridges. The two orthogonal directions that should be used are one parallel to the chord and one perpendicular to the chord. See Figure 2.

Design Step 6.4.1

Results for No Backfill Model

a) Forces

The force results of the radial direction analysis for the model that does not include the backfill are given in Tables 9 and 10 for the substructure and the soil springs, respectively. Figure 21 provides a key to the force directions given in the two tables. Additionally, Table 11 provides the shear forces in the drilled shafts. Note that results are given only for Abutment A and Pier No. 1, since the results are essentially identical for both abutments and both piers. Also note that the transverse and longitudinal directions given in Figure 21 refer to the orientation relative to the superstructure at the station in question.

The symmetry of the results about the center of the bridge can be used as a further check of the model. For this bridge, the entire structure and its boundary conditions are symmetric about the center of the bridge, and the loading is symmetric. Therefore the results must be symmetric, and if they are not, then the model should be checked for input errors.

Figures 22a through 22d show the shear and moment diagrams for the pier in the longitudinal and transverse directions.

Design Step 6.4.1 (continued)

Table 9
Response for Multimode Spectral Method
Radial Direction/No Backfill

Support/Location		Radial Earthquake/No Backfill Model Forces and Moments in Substructure					
		Traneverse		Longitudinal		Vertical	
		Shear (kips)	Moment (kip-ft)	Shear (kips)	Moment (kip-ft)	Axial (kips)	Moment (kip-ft)
Abutment A	Pile Group	151	4,546	288	0	78	87
	Backfill	--	--	0	--	--	--
Pier No. 1	Top of Column	246	4,115	103	1,813	82	0
	Base of Flare	264	2,596	110	1,178	82	0
	Base of Column	272	1,405	113	494	82	0
	Maximum in Shaft (Depth in Feet)	272 (0')	4,990 (22')	113 (0')	2,009 (22')	82 (0')	--

Design Step 6.4.1 (continued)

Table 10
Radial Earthquake/No Backfill Model

Radial Earthquake/No Backfill Model		
	Soil Forces	
Depth (feet)	Transverse (kips)	Longitudinal (kips)
2	15.3	6.3
6	39.5	16.2
10	55.7	22.8
14	64.6	26.5
18	67.3	27.7
22	64.6	26.6
26	55.7	23.8
30	47.5	19.7
34	34.6	14.4
38	19.6	8.3
42	2.7	1.4
46	15.9	6.3
50	36.6	14.8
54	59.6	24.2
58	85.3	34.8

Design Step 6.4.1 (continued)

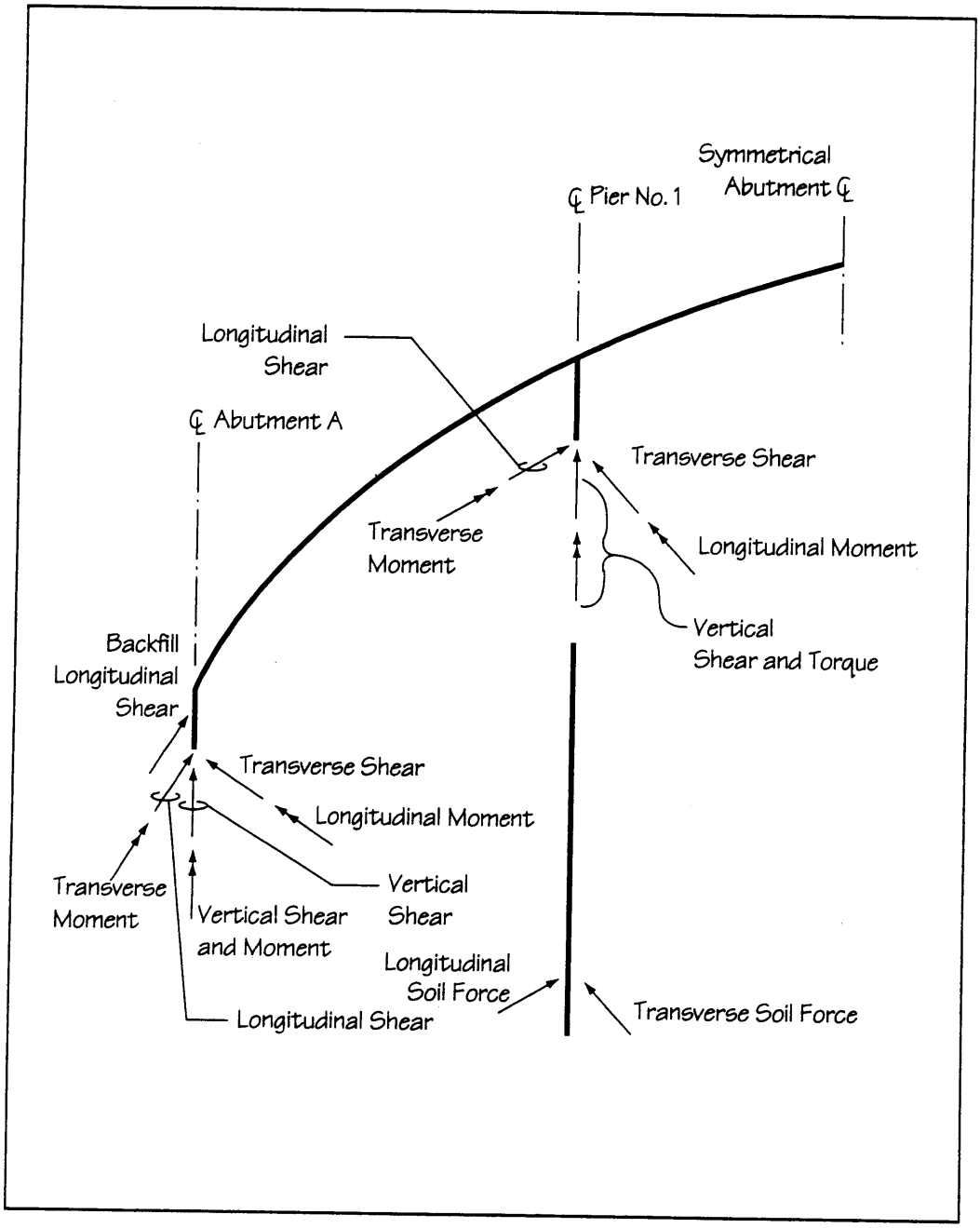

Figure 21 — Key to Substructure Forces

Design Step 6.4.1 (continued)

Table 11
Shear Forces in Shaft for Radial Earthquake

Depth (ft)	V_{tr} (kips)	V_{lr} (kips)
2	272	113
6	256	107
10	217	91
14	161	68
18	97	42
22	29	14
26	35	13
30	93	36
34	140	56
38	175	70
42	195	79
46	197	80
50	181	74
54	145	59
58	85	35
60	0	0

V_{tr} = Shear in Transverse Direction for Radial Earthquake
V_{lr} = Shear in Longitudinal Direction for Radial Earthquake

Design Step 6.4.1 (continued)

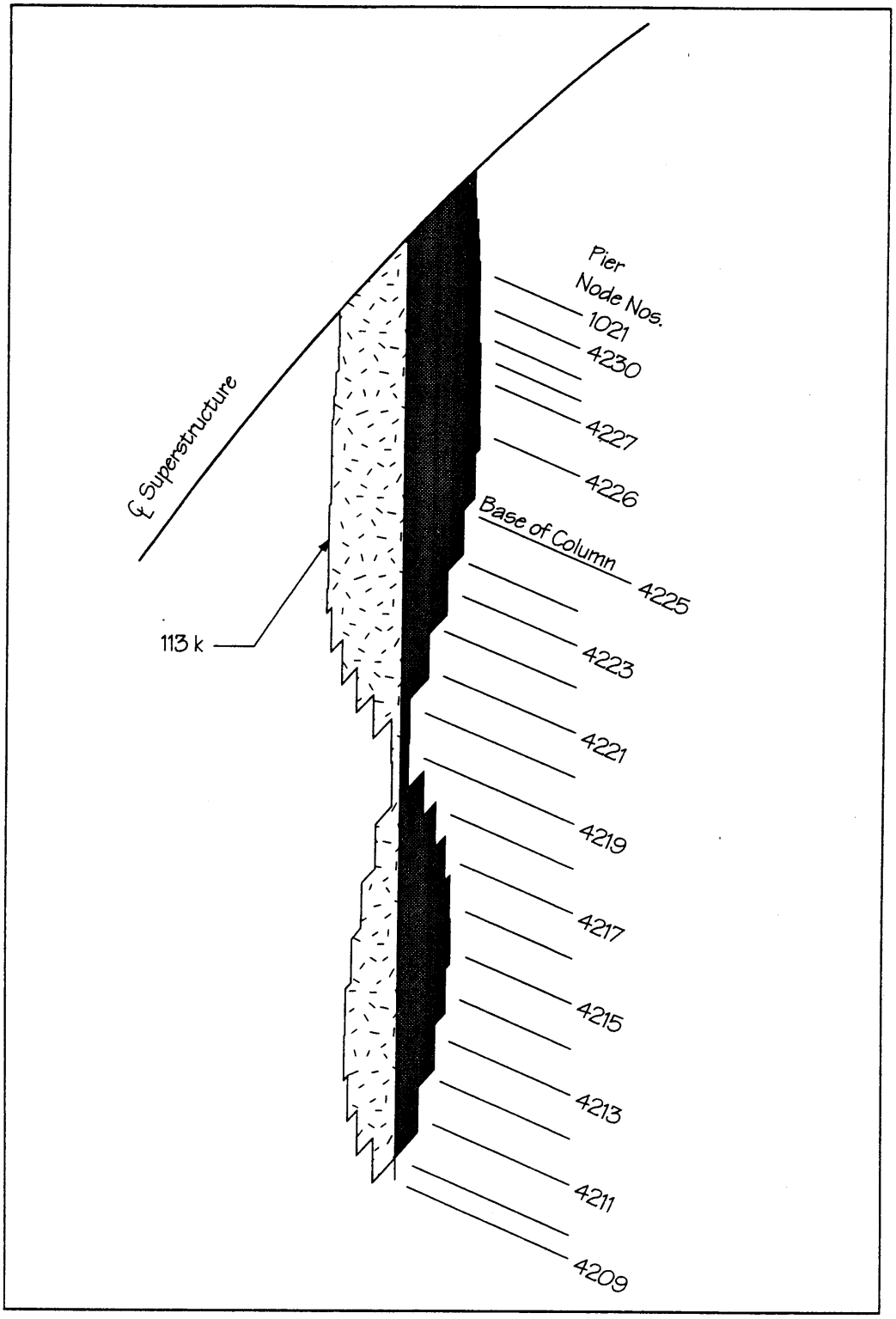

Figure 22a — Pier No. 1 Longitudinal Shear Radial Earthquake

Design Step 6.4.1 (continued)

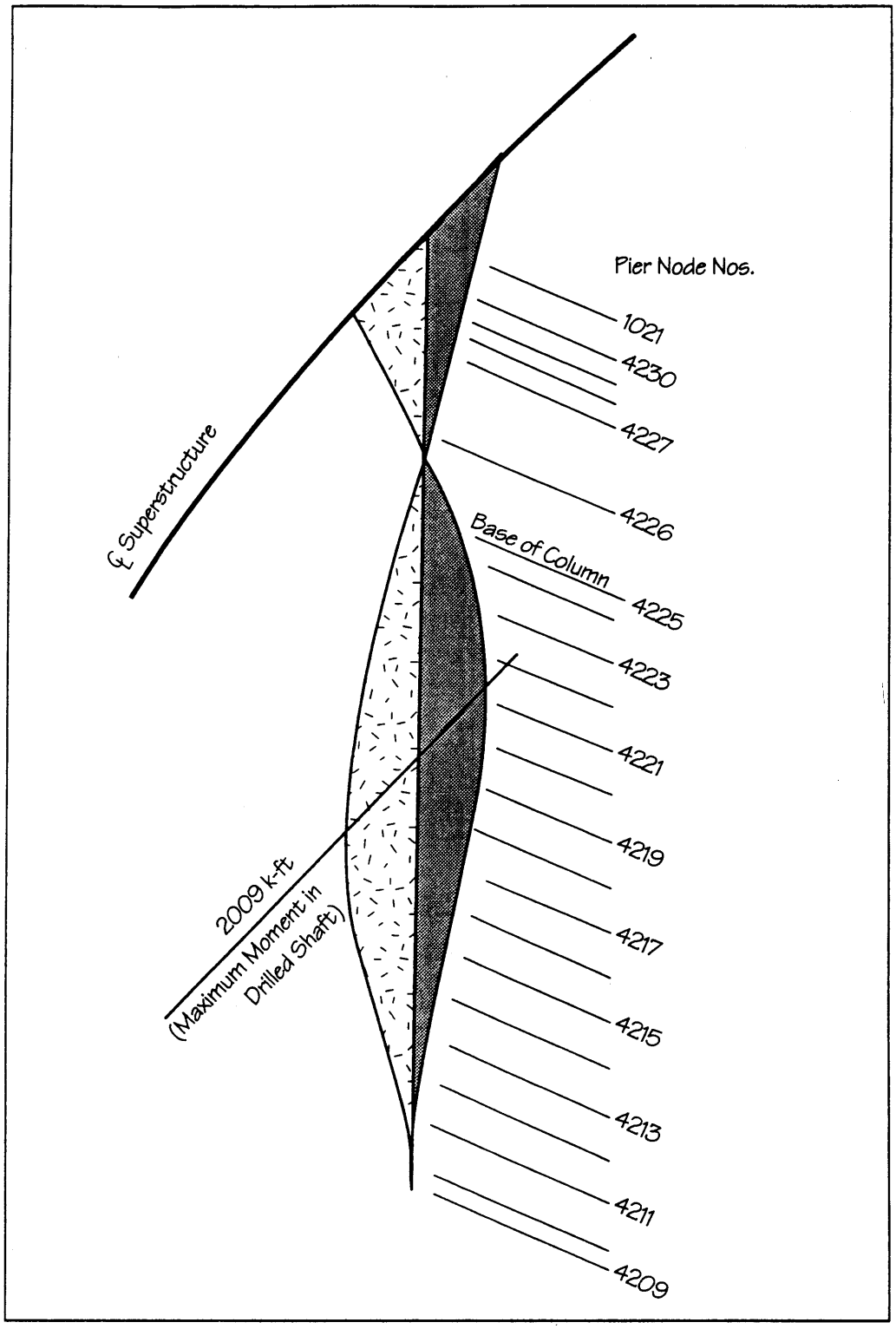

Figure 22b — Pier No. 1 Longitudinal Moment Radial Earthquake

Design Step 6.4.1 (continued)

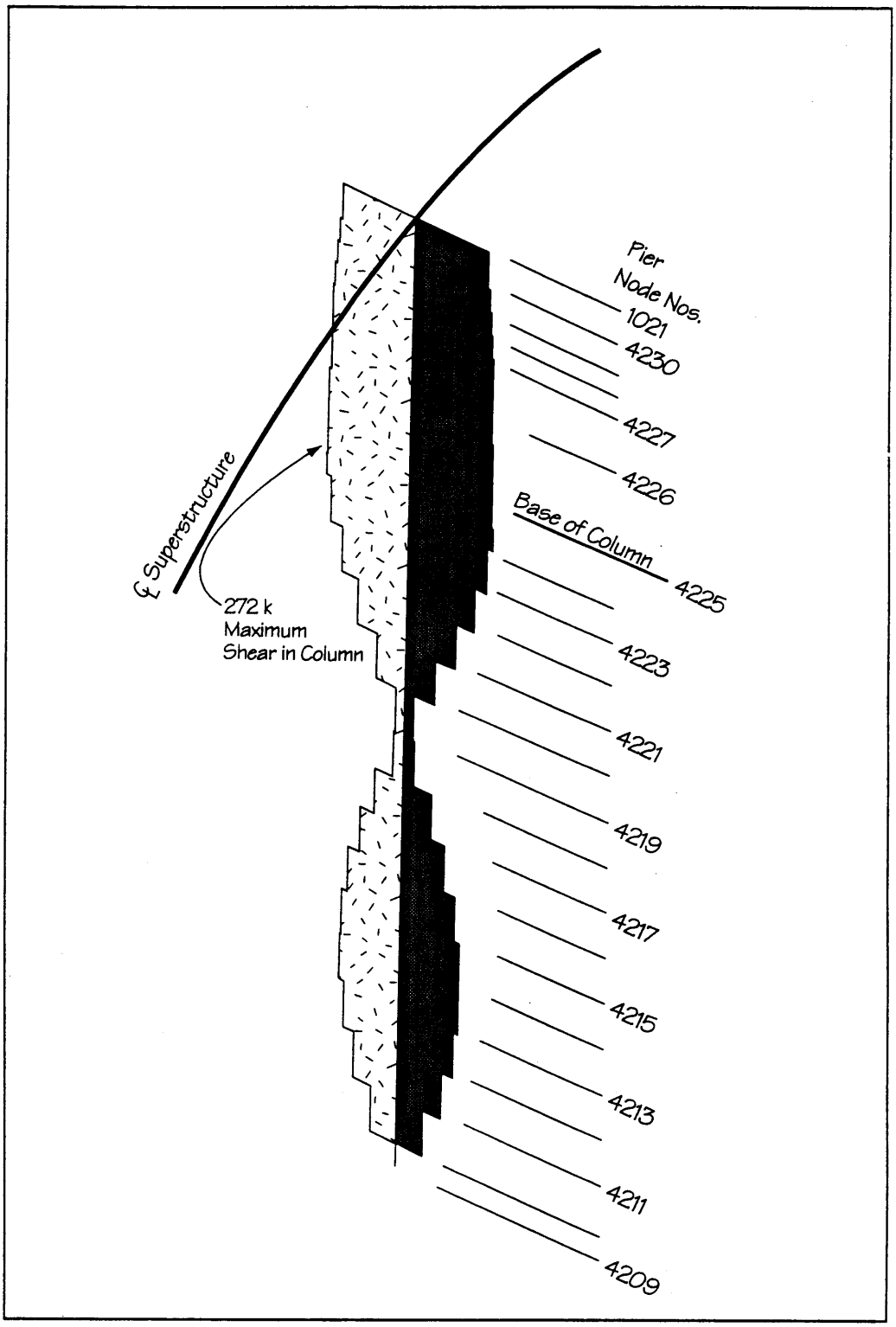

Figure 22c — Pier No. 1 Transverse Shear Radial Earthquake

Design Step 6.4.1 (continued)

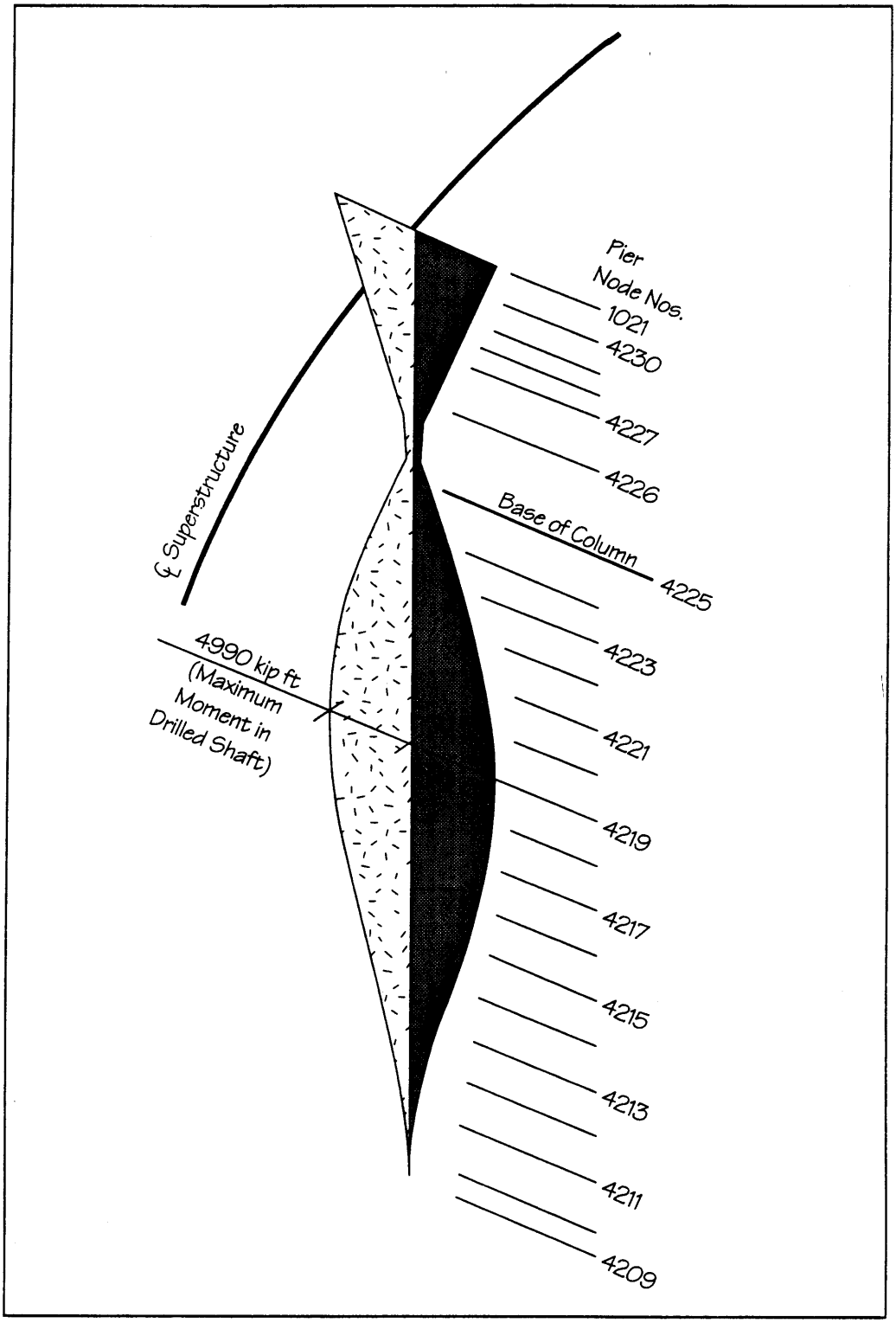

Figure 22d — Pier No. 1 Transverse Moment Radial Earthquake

Design Step 6.4.1 (continued)

b) Displacements

The displacements for the No Backfill Model are given in Table 12, and a key to the locations for which displacements are given (and their directions) is provided in Figure 23. The radial and chord directions are parallel to the earthquake loading directions, and the tangential and longitudinal directions are parallel to the pier directions of the same name.

An enlarged view of the deflected shape of one pier is given in Figure 24.

The seemingly peculiar shape shown in Figure 24 can be attributed to the fact that all displacements for a response spectrum analysis are shown as positive. Thus the 'kink' in the lower portion of the drilled shaft is due to this plotting feature and is not physical. Also, the nearly horizontal line at the top of the figure is present to connect the superstructure and the pier deformed shapes, which happen to have positive directions defined in different directions. So the analyst should not suspect an error when inspecting the plots.

Table 12
Radial Earthquake Displacements

Radial Earthquake/No Backfill Model		
Superstructure Displacement		
Location	Radial (feet)	Chord (feet)
Abut. A	0.134	0.012
Pier No. 1	0.149	0.001
Midspan	0.153	0
Pier No. 2	0.149	0.001
Abut. B	0.134	0.012
Pier Displacement		
Location	Tangential (feet)	Longitudinal (feet)
Column to Shaft	0.074	0.03

Design Step 6.4.1 (continued)

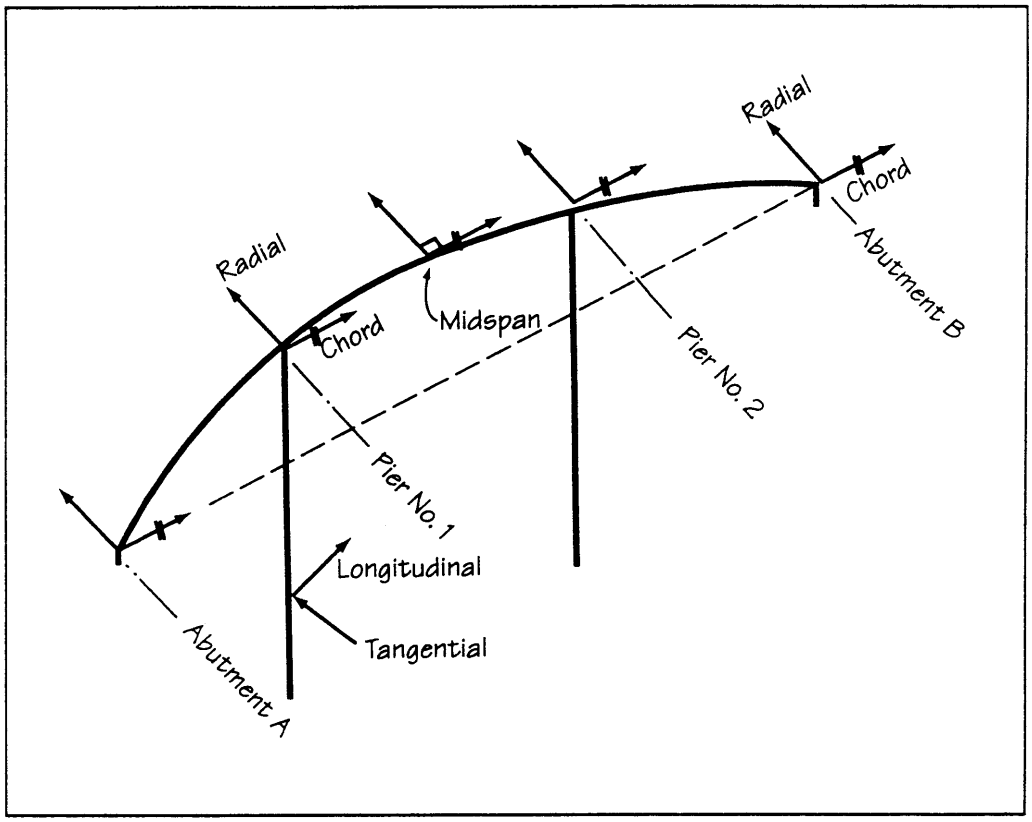

Figure 23 — Key to Displacements

Design Step 6.4.1 (continued)

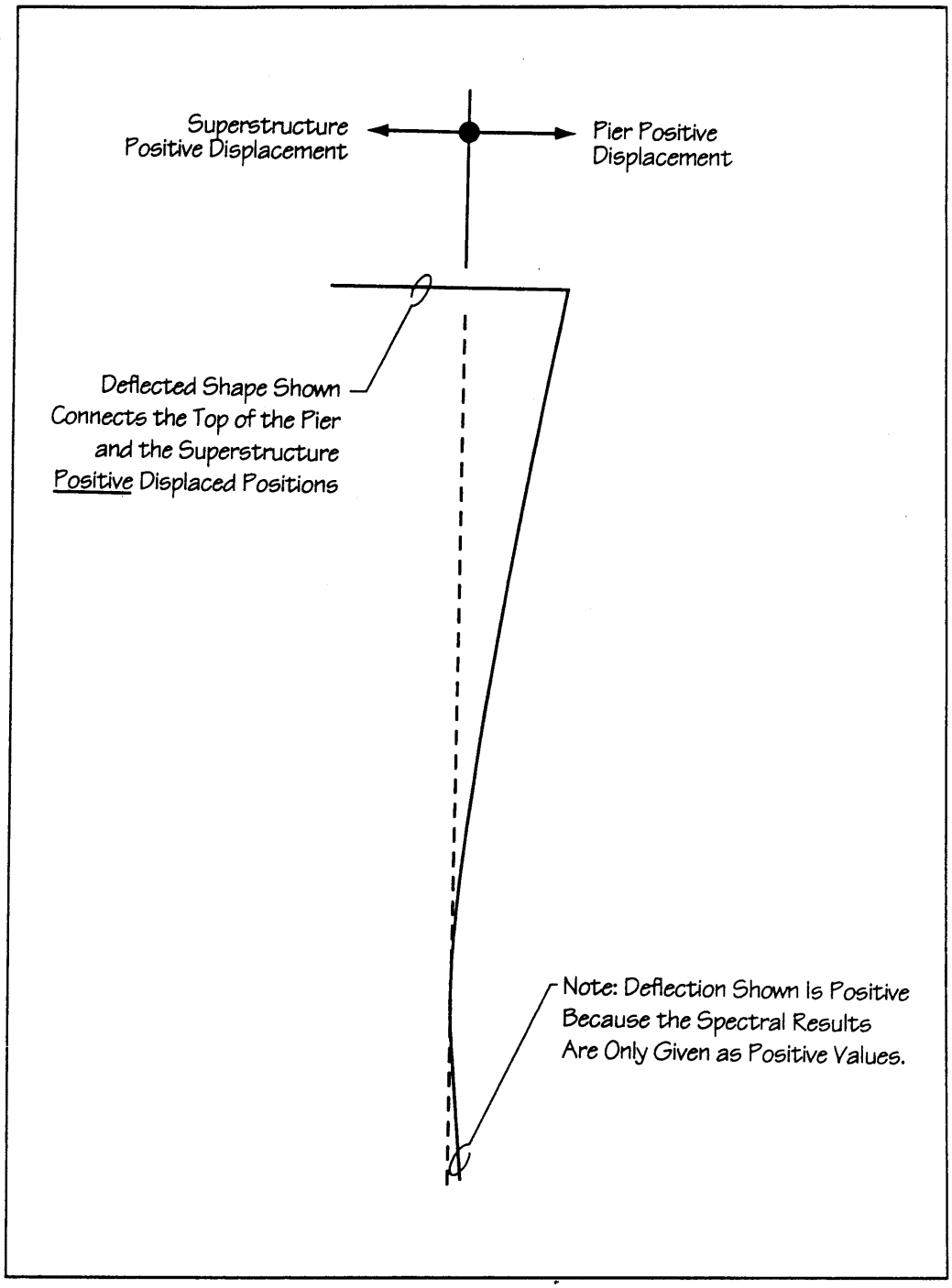

Figure 24 — Deformed Shape of Column and Drilled Shaft for Radial Earthquake

Design Step 6.4.2

Results for Backfill Included Model

a) Forces

The substructure forces and soil spring forces for radial earthquake loading are given in Tables 13 and 14.

b) Displacements

The displacements for the radial earthquake are given in Table 15.

c) Discussion

The reason for using a model that included the backfill at the abutment was to obtain a bounding solution for the case where the bridge is moving into or towards the soil during an earthquake. Obviously it is expected that the forces in the structure will be less if the soil behind the abutment assists in resisting lateral loadings. Indeed this is the case, as can be seen upon comparison of both the force and displacement results for the No Backfill and Backfill Included Models. The magnitudes of both the forces and the displacements are reduced by an order of magnitude when the soil behind the abutment is mobilized.

For the design of the bridge substructure elements, exclusive of the abutment end diaphragm, the internal forces and displacements developed in the No Backfill Model will control for the design of the substructure, for loading in the radial direction.

It should be recalled that the actual response of the bridge is only approximated by the two models considered. In fact, the actual response is nonlinear, since the abutments act only when the structure moves towards the soil backfill. Thus a linear elastic program and a response spectrum analysis can only bound the actual response. If a nonlinear program is used to analyze this structure, a time history analysis would have to be used to estimate the actual response.

Design Step 6.4.2 (continued)

Table 13
Response for Multimode Spectral Method
Radial Direction/Backfill Included

Support/Location		Radial Earthquake/Backfill Included Model Forces and Momente in Substructure					
		Transverse		Longitudinal		Vertical	
		Shear (kips)	Moment (kip-ft)	Shear (kips)	Moment (kip-ft)	Axial (kips)	Moment (kip-ft)
Abutment A	Pile Group	46	661	18	0	57	97
	Backfill	--	--	756	--	--	--
Pier No. 1	Top of Column	7	404	11	362	205	0
	Base of Flare	24	330	15	287	206	0
	Base of Column	32	73	18	86	207	0
	Maximum in Shaft (Depth in Feet)	32 (0')	513 (22')	18 (0')	232 (22')	207 (0')	--

Design Step 6.4.2 (continued)

Table 14
Radial Earthquake/Backfill Included Model

Radial Earthquake/Backfill Included Model		
	Soil Forces	
Depth (feet)	Transverse (kips)	Longitudinal (kips)
2	1.7	0.8
6	4.3	2.1
10	6.1	3.1
14	7.2	3.6
18	7.5	3.8
22	7.3	3.7
26	6.5	3.4
30	5.4	2.9
34	4	2.2
38	2.4	1.4
42	0.5	0.5
46	1.5	0.6
50	3.8	1.8
54	6.3	3
58	9.2	4.5

Table 15
Radial Earthquake Displacements

Radial Earthquake/Backfill Included		
Superstructure Displacement		
Location	Radial (feet)	Chord (feet)
Abut. A	0.018	0.015
Pier No. 1	0.015	0.002
Midspan	0.017	0
Pier No. 2	0.015	0.002
Abut. B	0.018	0.015
Pier Displacement		
Location	Tangential (feet)	Longitudinal (feet)
Column to Shaft	0.009	0.004

Design Step 6.4.3

Further Bounding of the Radial Response

It is well known that the actual response of a bridge due to earthquake loading often is large enough to cause significant cracking and potential yielding of the substructure elements. Consequently, analyses which bound the actual response may be used to estimate the sensitivity of the response to softening of the structural elements. Yielding is handled very approximately through the R Factors, but cracking should also be considered. A simple approach is to run additional analyses using cracked section properties for those substructure elements likely to be cracked, and to determine the effect on response.

Typically the gross cross section results would be used for an upper bound on the structure forces and the reduced cross section results would be used as an upper bound on structure displacements.

For this structure, the column portions of Pier Nos. 1 and 2 are modified to include cracking by reducing the moments of inertia to 50 percent of the gross section values. This is a widely used value for approximating the cracked stiffness. The No Backfill Model is reanalyzed using these reduced properties. The stiffnesses of the drilled shafts and of the pipe piles are left unchanged.

a) Forces

The force results are given in Tables 16 and 17.

b) Displacements

The displacement results are given in Table 18.

c) Discussion

Comparison of the gross section results and the reduced section results shows that the forces at the intermediate piers are slightly reduced and those at the abutments are very slightly increased. Likewise the displacements are increased by a very small amount when the reduced column section properties are used. The small difference is probably due to the high relative stiffness of the abutments. In this case, the gross section results for both forces and displacements will be used for design.

Design Step 6.4.3 (continued)

Table 16
Response for Multimode Spectral Method
Radial Direction/No Backfill/Half Column I

Support/Location		Radial Earthquake/No Backfill Model/Reduced Column I Forces and Moments in Substructure					
		Transverse		Longitudinal		Vertical	
		Shear (kips)	Moment (kip-ft)	Shear (kips)	Moment (kip-ft)	Axial (kips)	Moment (kip-ft)
Abutment A	Pile Group	153	4,377	291	90	71	90
	Backfill	--	--	0	--	--	--
Pier No. 1	Top of Column	242	3,857	92	1,455	76	0
	Base of Flare	260	2,362	99	884	76	0
	Base of Column	268	1,581	103	624	76	0
	Maximum in Shaft	268	5,076	103	1,958	76	--
	(Depth in Feet)	(0')	(22')	(0')	(22')	(0')	

Design Step 6.4.3 (continued)

Table 17
Radial Earthquake/No Backfill/Half Column I

Radial Earthquake/No Backfill/Half Column I		
	Soil Forces	
Depth (feet)	Transverse (kips)	Longitudinal (kips)
2	15.4	5.9
6	39.6	15.2
10	55.8	21.4
14	64.6	24.8
18	67.2	25.8
22	64.5	24.7
26	57.5	22
30	47.1	18.1
34	34.2	13.1
38	19.1	7.3
42	2.2	0.8
46	16.4	6.4
50	37.1	14.3
54	60.1	23.1
58	85.8	33

Table 18
Radial Earthquake Displacements

Radial Earthquake/Half Column I		
Superstructure Displacement		
Location	Radial (feet)	Chord (feet)
Abut. A	0.135	0.012
Pier No. 1	0.151	0.001
Midspan	0.155	0
Pier No. 2	0.151	0.001
Abut. B	0.135	0.012
Pier Displacement		
Location	Tangential (feet)	Longitudinal (feet)
Column to Shaft	0.079	0.03

Design Step 6.5

Determine Forces and Displacements in Chord Direction
[Division I-A, Articles 3.8 and 4.5]

The Multimode Spectral Method of analysis was used to determine the internal seismic forces, reactions, and displacements for earthquake loading in a direction parallel to the chord of the bridge.

Design Step 6.5.1

Results for No Backfill Model

a) Forces

The force results of the chord direction analysis for the model that does not include the backfill are given in Tables 19 and 20 for the substructure and the soil springs, respectively. Table 21 provides the shear forces in the drilled shafts. As with the radial loading, results are given only for Abutment A and Pier No. 1, because the results are essentially identical for both abutments and both piers.

b) Displacements

The displacements for the No Backfill Model are given in Table 22.

Table 19
Response for Multimode Spectral Method
Chord Direction/No Backfill

Support/Location		Chord Earthquake/No Backfill Model Forces and Momente in Substructure					
		Transverse		Longitudinal		Vertical	
		Shear (kips)	Moment (kip-ft)	Shear (kips)	Moment (kip-ft)	Axial (kips)	Moment (kip-ft)
Abutment A	Pile Group	181	1,538	256	0	38	102
	Backfill	--	--	0	--	--	--
Pier No. 1	Top of Column	87	1,816	281	5,048	50	0
	Base of Flare	93	1,281	301	3,314	50	0
	Base of Column	96	126	310	1,253	50	0
	Maximum in Shaft (Depth in Feet)	96 (0')	1,459 (22')	310 (0')	5,416 (22')	50 (0')	--

Design Step 6.5.1 (continued)

Table 20
Chord Earthquake/No Backfill Model

Chord Earthquake/No Backfill Model		
	Soil Forces	
Depth (feet)	Transverse (kips)	Longitudinal (kips)
2	4.8	17
6	12.6	43.9
10	17.9	62
14	20.9	72.1
18	21.9	75.2
22	21.3	72.4
26	19.2	64.9
30	16.1	53.6
34	12	39.3
38	7.2	22.7
42	1.8	3.9
46	4.2	16.9
50	10.9	39.9
54	18.4	65.6
58	26.8	94.4

Design Step 6.5.1 (continued)

Table 21
Shear Forces in Shaft for Chord Earthquake

Depth (ft)	V_{tc} (kips)	V_{lc} (kips)
2	96	310
6	91	293
10	78	249
14	60	187
18	39	115
22	17	40
26	4	32
30	23	97
34	39	151
38	51	190
42	59	213
46	60	217
50	56	200
54	45	160
58	27	94
60	0	0

V_{tc} = Shear in Transverse Direction for Chord Earthquake
V_{lc} = Shear in Longitudinal Direction for Chord Earthquake

Design Step 6.5.1 (continued)

Table 22
Chord Earthquake Displacements

Chord Earthquake/No Backfill Model		
Superstructure Displacement		
Location	Radial (feet)	Chord (feet)
Abut. A	0.032	0.128
Pier No. 1	0.013	0.14
Midspan	0	0.142
Pier No. 2	0.013	0.14
Abut. B	0.032	0.128
Pier Displacement		
Location	Tangential (feet)	Longitudinal (feet)
Column to Shaft	0.025	0.087

Design Step 6.5.2

Results for Backfill Included Model

a) Forces

The force results of the chord direction analysis for the model that includes the backfill are given in Tables 23 and 24 for the substructure and the soil springs, respectively.

b) Displacements

The displacements for the Backfill Included Model are given in Table 25.

c) Discussion

The forces in the substructure are reduced, in an overall sense, by including the abutment soil restraint. "Overall" refers to the resultant of the longitudinal and transverse forces, and it is the resultant forces that are smaller. On the other hand, the transverse component is larger for the Backfill Included Model than for the No Backfill Model. This is the result of several primary modes (Modes 1 and 7 shown in Figure 17) having a rotational component of movement coupled with translation. Thus, even though the

Design Step 6.5.2 (continued)

translation is the primary response developed during the earthquake, some rotation of the bridge will always accompany the translation. Such a coupling between translations and rotations occurs whenever the center of mass and the center of stiffness (or rigidity) are not coincident. For this model, neither quantity has been directly calculated; however, if they were calculated the two centers would not be coincident.

Note also that the longitudinal force developed in the backfill for this loading case is 388 kips, compared with 756 kips for loading in the radial direction. This substantial difference is probably the result of the combined translation and rotation discussed above. Due to this coupling, the superstructure tends to 'skip' laterally off of the abutment backfill as the chord direction earthquake loading is applied. Figure 17a for Mode 1 illustrates this behavior.

Since the overall forces are less for the Backfill Included Model, the results of the No Backfill Model will be used for design.

Table 23
Response for Multimode Spectral Method
Chord Direction/Backfill Included

Support/Location		Chord Earthquake/Backfill Included Model Forces and Moments in Substructure					
		Transverse		Longitudinal		Vertical	
		Shear (kips)	Moment (kip-ft)	Shear (kips)	Moment (kip-ft)	Axial (kips)	Moment (kip-ft)
Abutment A	Pile Group	284	2,400	11	0	40	203
	Backfill	--	--	388	--	--	--
Pier No. 1	Top of Column	135	2,844	120	2,179	74	0
	Base of Flare	145	2,012	131	1,436	74	0
	Base of Column	150	194	136	552	74	0
	Maximum in Shaft (Depth in Feet)	150 (0')	2,291 (22')	136 (0')	2,371 (22')	74 (0')	--

Design Step 6.5.2 (continued)

Table 24
Chord Earthquake/Backfill Included Model

Chord Earthquake/Backfill Included Model		
	Soil Forces	
Depth (feet)	Transverse (kips)	Longitudinal (kips)
2	7.6	7.4
6	19.8	19.2
10	28.1	27.1
14	32.9	31.5
18	34.5	32.9
22	33.5	31.7
26	30.2	28.4
30	25.2	23.4
34	18.9	17.2
38	11.4	9.9
42	2.9	1.7
46	6.6	7.4
50	17.1	17.5
54	28.9	28.7
58	42.1	41.3

Table 25
Chord Earthquake Displacements

Chord Earthquake/Backfill Included		
Superstructure Displacement		
Location	Radial (feet)	Chord (feet)
Abut. A	0.084	0.108
Pier No. 1	0.038	0.077
Midspan	0	0.07
Pier No. 2	0.038	0.077
Abut. B	0.084	0.108
Pier Displacement		
Location	Tangential (feet)	Longitudinal (feet)
Column to Shaft	0.039	0.038

Design Step 6.5.3

Further Bounding of the Chord Response

As with the radial loading analysis, the column moments of inertia were reduced to 50 percent of the gross cross section values and the analysis was repeated.

a) Forces

The force results of the chord direction analysis for the reduced stiffness model are given in Tables 26 and 27 for the substructure and the soil springs, respectively.

b) Displacements

The displacements for the reduced stiffness model are given in Table 28.

c) Discussion

As for the radial loading, the results are hardly changed when the column stiffness is reduced. Thus, the gross section property results will be used for design.

Table 26
Response for Multimode Spectral Method
Chord Direction/No Backfill/Half Column I

Support/Location		Chord Earthquake/No Backfill Model/Reduced Column I Forces and Moments in Substructure					
		Transverse		Longitudinal		Vertical	
		Shear (kips)	Moment (kip-ft)	Shear (kips)	Moment (kip-ft)	Axial (kips)	Moment (kip-ft)
Abutment A	Pile Group	182	1,381	272	0	34	120
	Backfill	--	--	0	--	--	--
Pier No. 1	Top of Column	82	1,515	257	4,070	35	0
	Base of Flare	87	1,012	276	2,484	35	0
	Base of Column	90	312	285	1,709	35	0
	Maximum in Shaft (Depth in Feet)	90 (0')	1,528 (22')	285 (0')	5,421 (22')	35 (0')	--

Design Step 6.5.3 (continued)

Table 27
Chord Earthquake/No Backfill/Half Column I

Chord Earthquake/No Backfill/Half Column I		
	Soil Forces	
Depth (feet)	Transverse (kips)	Longitudinal (kips)
2	4.8	16.4
6	12.5	42.2
10	17.7	59.5
14	20.6	68.9
18	21.5	71.6
22	20.8	68.7
26	18.6	61.2
30	15.4	50.2
34	11.4	36.3
38	6.6	20.3
42	1.3	2.3
46	4.7	17.6
50	11.3	39.6
54	18.6	64.1
58	26.9	91.5

Table 28
Chord Earthquake Displacements

Chord Earthquake/Half Column I		
Superstructure Displacement		
Location	Radial (feet)	Chord (feet)
Abut. A	0.038	0.132
Pier No. 1	0.016	0.146
Midspan	0	0.148
Pier No. 2	0.016	0.146
Abut. B	0.038	0.132
Pier Displacement		
Location	Tangential (feet)	Longitudinal (feet)
Column to Shaft	0.025	0.084

Design Step 6.6

Check of Soil Resistance

Before proceeding with the design of the substructure and foundation elements, the soil resistance at each foundation element should be checked to determine if nonlinear soil behavior is likely. If the behavior is nonlinear, then the model should be adjusted to incorporate the soil softening, and the analysis should be reperformed. This process is repeated until convergence is obtained between the soil forces and the corresponding displacements.

The designer should keep in mind that the elastic seismic forces may be somewhat larger than the actual forces, due to the possibility of yielding in the columns. Therefore, some judgment is required when deciding upon an appropriate level of convergence; absolute convergence of the results is often not required. Additionally, the soil near the top of the shaft is critical to overall response, although some nonlinearity may be allowed in that zone without necessitating reanalyzing the structure, provided it is limited in depth. Some designers allow nonlinearity to occur over a depth equal to about twice the shaft diameter before reanalyzing the structure. For large shaft diameters such as at this site, allowing nonlinearity over about twice the shaft diameter would not be desirable, and a limit of 5 feet or so in depth would be reasonable. When such nonlinear soil response is indicated by the check, the geotechnical engineer should be consulted for guidance regarding refinement of the analysis.

Design Step 6.6.1

Check of Drilled Shafts

The controlling results, i.e., the No Backfill Model results, will be checked for nonlinearity of the soil forces using the method outlined in Section 6.2.1(c). In that section the maximum passive soil pressure that could be developed was calculated for the soil spring at 30 feet of depth.

The soil spring input data for the check is taken from Tables 10 and 20, for the radial and chord earthquake loading directions. The check is made after the two earthquake loadings have been combined as described in Division I-A, Article 3.9. This article requires that 100 percent of one direction's loading must be considered, simultaneously with 30 percent of the other direction's loading.

The results of the check are given in Table 29. The LC1 load case represents 100 percent loading in the chord direction and 30 percent in the radial, and LC2 represents 30 percent in the chord direction and 100 percent in the radial. The value in the column labeled R is the resultant soil spring force for

Design Step 6.6.1 (continued)

the given load case. This force is then divided by the tributary height of the spring and the effective width of the soil, which is twice the shaft diameter, to obtain the soil stress σ. Recall that this step was discussed in Section 6.2.1(c). To calculate the factor of safety (FS) against movement of the soil, the passive resistance capacity is divided by the soil stress demand.

As seen in the two columns labeled FS in Table 29, no nonlinear action is expected for the shaft, since the factors of safety all exceed unity.

Table 29
Drilled Shaft Soil Spring Capacity Check

Depth	Chord Direction		Radial Direction		Passive	LC1			LC2		
z	F_{lc}	F_{tc}	F_{lr}	F_{tr}	Pressure, PP	R_1	σ_1	FS_1	R_2	σ_2	FS_2
(ft)	(kips)	(kips)	(kips)	(kips)	(ksf)	(kips)	(ksf)		(kips)	(ksf)	
2	17	4.8	6.3	15.3	0.42	21.10	0.33	1.29	20.25	0.32	1.34
6	43.9	12.6	16.2	39.5	1.27	54.55	0.85	1.49	52.30	0.82	1.56
10	62	17.9	22.8	55.7	2.12	77.05	1.20	1.76	73.78	1.15	1.84
14	72.1	20.9	26.5	64.6	2.97	89.61	1.40	2.12	85.67	1.34	2.22
18	75.2	21.9	27.7	67.3	3.82	93.52	1.46	2.61	89.35	1.40	2.74
22	72.4	21.3	26.6	64.6	4.67	90.09	1.41	3.32	85.87	1.34	3.48
26	64.9	19.2	23.8	55.7	5.52	80.49	1.26	4.39	75.16	1.17	4.70
30	53.6	16.1	19.7	47.5	6.37	66.80	1.04	6.10	63.39	0.99	6.43
34	39.3	12	14.4	34.6	7.22	49.03	0.77	9.42	46.32	0.72	9.97
38	22.7	7.2	8.3	19.6	8.06	28.38	0.44	18.18	26.49	0.41	19.48
42	3.9	1.8	1.4	2.7	8.91	5.05	0.08	113.03	4.14	0.06	137.94
46	16.9	4.2	6.3	15.9	9.76	20.82	0.33	30.01	20.59	0.32	30.35
50	39.9	10.9	14.8	36.6	10.61	49.44	0.77	13.74	48.02	0.75	14.14
54	65.6	18.4	24.2	59.6	11.46	81.39	1.27	9.01	78.52	1.23	9.34
58	94.4	26.8	34.8	85.3	12.31	117.20	1.83	6.72	112.68	1.76	6.99

Constants

soil density, γ = 60 pcf — height of spring, h = 4 ft

friction angle, ϕ = 34 degrees — effective width, w = 16 ft

Definitions

F_{lc} = Spring Force in Longitudinal Direction for Chord Earthquake

F_{tc} = Spring Force in Transverse Direction for Chord Earthquake

R_1 = Spring Force Resultant for Load Case, LC1

F_{lr} = Longitudinal Force for Radial Earthquake

F_{tr} = Transverse Force for Radial Earthquake

R_2 = Resultant for Load Case, LC2

Formulae

$$PP = \gamma\, z \tan^2(45 + \phi/2)$$

$$R_1 = ((1.0\ F_{lc} + 0.3\ F_{lr})^2 + (1.0\ F_{tc} + 0.3\ F_{tr})^2)^{1/2}$$

$$R_2 = ((0.3\ F_{lc} + 1.0\ F_{lr})^2 + (0.3\ F_{tc} + 1.0\ F_{tr})^2)^{1/2}$$

$$\sigma_1 = R_1 / (h\,w) \qquad FS_1 = PP / \sigma_1$$

$$\sigma_2 = R_2 / (h\,w) \qquad FS_2 = PP / \sigma_2$$

Design Step 6.6.2

Check of Abutments

a) Pipe Piles

The pipe piles should be checked for excessive soil forces and excessive deflections. The DM7 Method used to determine the soil spring values does not give a direct means to calculate soil stresses. However, the displacements can be used as an indicator.

Tables 12 and 22 indicate that roughly 0.14 foot (1.7 inches) of lateral displacement is expected at the abutments. This is a rather large displacement for the soil immediately adjacent to the tops of the piles to accommodate without developing some nonlinear behavior.

Because DM7 does not directly address this issue, the displacement obtained should be checked by the geotechnical engineer (geotech), and if a reduction in stiffness is appropriate, new springs can be developed in consultation with the geotech. Typically, the geotech can run 'LPILE' (Reese and Wang, 1993) or a similar program to determine new estimates of the pile stiffnesses. Then the analyses can be rerun until convergence of the input and required stiffness is obtained.

For this example, the original springs are used for the design.

To give an idea of the sensitivity of the overall structure response to the abutment pipe pile stiffnesses, the No Backfill Model was rerun with the lateral stiffnesses at the abutments reduced to 50 percent of their original values. The results of this exercise are given in Tables 30 and 31 for the radial earthquake forces and displacements, respectively. The values listed are expressed as changes from those obtained previously for the No Backfill Model; these changes are given as fractions of the original values. It can be seen from the tables that the forces and displacements at Pier Nos. 1 and 2 are increased by only about 20 percent.

DM7 does state that it is assumed that the lateral load does not exceed about one-third of the ultimate lateral load capacity, as limited by the soil. The geotechnical engineer should be requested to develop this capacity.

Design Step 6.6.2 (continued)

Table 30
Response for Multimode Spectral Method
Radial Direction/Reduced Abutment Spring

Support/Location		Radial Earthquake/Reduced Abutment Springs — Changes in Forces and Moments in Substructure					
		Transverse		Longitudinal		Vertical	
		Shear (fraction)	Moment (fraction)	Shear (fraction)	Moment (fraction)	Axial (fraction)	Moment (fraction)
Abutment A	Pile Group	0.71	1.11	0.62	0.	1.08	0.16
	Backfill	--	--	0.	--	--	--
Pier No. 1	Top of Column	1.23	1.2	1.19	1.15	1.05	0.
	Base of Flare	1.2	1.2	1.17	1.14	1.05	0.
	Base of Column	1.19	1.21	1.17	1.23	1.05	0.
	Maximum in Shaft (Depth in Feet)	1.19 (0')	1.2 (22')	1.17 (0')	1.17 (22')	1.05 (0')	--

Table 31
Changes in Radial Earthquake Displacements

Radial Earthquake/Reduced Abut. Spr.		
Superstructure Displacement		
Location	Radial (fraction)	Chord (fraction)
Abut. A	1.3	0.33
Pier No. 1	1.19	0.3
Midspan	1.18	1.
Pier No. 2	1.19	0.3
Abut. B	1.29	0.33
Pier Displacement		
Location	Tangential (feet)	Longitudinal (feet)
Column to Shaft	1.27	1.27

Design Step 6.6.2 (continued)

b) Backfill Soil

For the analyses that considered the backfill soil to be effective, the maximum force developed in the backfill should be checked against the maximum soil capacity. This limit is taken as 7.7 ksf for well-compacted backfill, as discussed by Caltrans (1989).

From Tables 13 and 23, the maximum soil forces are 756 kips and 388 kips for the radial and chord earthquakes. If 100 percent of the radial loading and 30 percent of the chord loading are used, a maximum force of 872 kips is obtained. The area of the abutment endwall is 316 square feet, which is based on 8 feet of height and 39.5 feet of width. The 872 kips force acting over 316 square feet of wall produces 2.8 ksf of soil stress demand in the backfill. Obviously this is less than the 7.7 ksf allowed, thus no correction is required.

DESIGN STEP 7 DETERMINE DESIGN FORCES

Design Step 7.1 Determine Nonseismic Forces

Design Step 7.1.1 Determine Dead Load Forces

The dead load forces are summarized in Table 32 below. The forces shown in the table were determined using the same spine model of the bridge (Figure 3) that was used for determining the seismic forces.

Table 32
Dead Load Forces

Support/Location		Dead Load Analysis/No Backfill Model Forces and Moments in Substructure					
		Transverse		Longitudinal		Vertical	
		Shear (kips)	Moment (kip-ft)	Shear (kips)	Moment (kip-ft)	Axial (kips)	Moment (kip-ft)
Abutment A	Pile Group	3	874	9	0	314	0
	Backfill	--	--	0	--	--	--
Pier No. 1	Top of Column	5	92	2	26	1,137	0
	Base of Flare	5	61	2	16	1,198	0
	Base of Column	5	17	2	10	1,241	0
	Maximum in Shaft (Depth in Feet)	5 (0')	87 (22')	2 (0')	33 (22')	1,241 (0')	--

Design Step 7.2

Determine Seismic Forces

Design Step 7.2.1

Summary of Elastic Seismic Forces

The full elastic seismic forces for earthquake loading along each of the principal axes (radial and chord) are shown in Tables 9 and 19, respectively, for the No Backfill Model.

Design Step 7.2.2

Combination of Orthogonal Seismic Forces
[Division I-A, Article 3.9]

Before the seismic forces are combined with the dead load to create the modified design forces, the seismic forces along the two principal axes must be combined in load combinations LC1 and LC2 (without dead load).

The definitions of load combinations LC1 and LC2 are as follows.

LC1 = 100 percent of the Chord Analysis Results + 30 percent of the Radial Analysis Results

LC2 = 30 percent of the Chord Analysis Results + 100 percent of the Radial Analysis Results

Note that all the forces in LC1 and LC2 are the full elastic seismic forces.

These forces are combinations using the full elastic seismic results, and have not yet been modified by the R Factor. At this stage, the designer could elect to check for these forces combined with dead load, if other load cases such as stream flow control the size of the substructure.

For example, in Pier No. 1, the transverse shear at the base of the column for LC1 is derived as follows.

$V = (1.0 * V_{CT}) + (0.3 * V_{RT})$
$V = (1.0 * 272) + (0.3 * 96) = 300$ kips

The forces used in the calculations are listed in Tables 9 and 19. V_{CT} refers to the shear induced in the column in the direction transverse to the superstructure under chord earthquake loading. Similarly, V_{RT} refers to the shear in the transverse direction due to radial earthquake loading.

Design Step 7.2.2 (continued)

All other forces for the LC1 and LC2 loading combinations are calculated similarly, and the results are given in Tables 33 and 34.

Table 33
Orthogonal Seismic Force Combination LC1

Support/Location		Load Case LC1 Forces (LC1 = 1.0*EQchord + 0.3*EQradial)					
		Transverse		Longitudinal		Vertical	
		Shear (kips)	Moment (kip-ft)	Shear (kips)	Moment (kip-ft)	Axial (kips)	Moment (kip-ft)
Abutment A	Pile Group	227	2,902	342	0	62	128
	Backfill	--	--	0	--	--	--
Pier No. 1	Top of Column	161	3,051	312	5,591	74	0
	Base of Flare	172	2,060	334	3,667	74	0
	Base of Column	177	548	344	1,401	74	0
	Maximum in Shaft (Depth in Feet)	177 (0')	2,956 (22')	344 (0')	6,019 (22')	74 (0')	--

Table 34
Orthogonal Seismic Force Combination LC2

Support/Location		Load Case LC2 Forces (LC2 = 0.3*EQchord + 1.0*EQradial)					
		Transverse		Longitudinal		Vertical	
		Shear (kips)	Moment (kip-ft)	Shear (kips)	Moment (kip-ft)	Axial (kips)	Moment (kip-ft)
Abutment A	Pile Group	206	5,007	365	0	89	118
	Backfill	--	--	0	--	--	--
Pier No. 1	Top of Column	272	4,659	188	3,327	97	0
	Base of Flare	292	2,981	201	2,172	97	0
	Base of Column	300	1,443	206	870	97	0
	Maximum in Shaft (Depth in Feet)	300 (0')	5,428 (22')	206 (0')	3,634 (22')	97 (0')	--

Design Step 7.3

Determine Modified Design Forces

[Division I-A, Article 7.2.1(A)]

For Seismic Performance Category C, the modified seismic design forces for structural members and connections are determined by dividing the elastic seismic forces by the appropriate Response Modification Factor R. The modified design forces for the foundations are determined by dividing the elastic seismic forces by unity. The design forces obtained from Division I-A replace the Group VII load combination found in Table 3.22.1A of Division I. These modified design forces, along with the forces developed as a result of plastic hinging in the substructure, are used to design the various components of the bridge.

The design forces use the R Factor to "modify" or reduce the elastic seismic forces. This reduction is appropriate for structural systems that possess enough ductility to endure the inelastic demands likely to occur in the reduced strength system. As outlined in Section 1.1 of Division I-A, the design philosophy is to restrict inelastic effects and/or damage to parts of the bridge where such effects are readily detectable following a large earthquake. The implication here is that inelastic action should not occur in the foundations.

The columns are the elements that are allowed to perform inelastically in a large earthquake, since they can be detailed to provide adequate ductility. This inelastic action is expected to be in the form of plastic hinges. Therefore the only forces that are reduced by the R Factor are the column moments. To be conservative, the shear and the axial forces are not reduced. However, as discussed in Design Step 8, the final design shear and axial forces are the smaller of the elastic forces, and those corresponding to plastic hinging.

Design Step 7.3.1

Modified Design Forces for Structural Members and Connections

The Specification makes a distinction between the forces for members and connections verses the design forces for foundations calculated in Design Step 7.3.2. Use Equation (7-1) in Division I-A to calculate the maximum forces in each member.

$$Group\ Load = 1.0\ (D + B + SF + E + EQM)$$ Division I-A Eqn (7-1)

In this equation, forces B, SF, and E are buoyancy, stream flow, and earth forces, respectively. D and EQM forces are the dead load and earthquake

Design Step 7.3.1 (continued)

forces, respectively. For this example the B, SF, and E forces are assumed to be zero.

If only the dead and earthquake loads are present, then Equation 7-1 reduces to

Group Load = 1.0 (D + EQM)

Where EQM = (LC1 or LC2 forces) divided by R

a) Response Modification Reduction Factor, R
[Division I-A, Article 3.7, Table 3]

The R Factor is used to modify EQM, and applies to specific forces for specific members. The decision of which R value to apply to each member is a critical one, since the R values, to a great extent, affect the locations and magnitude of the expected damage.

In this example, R reduces the seismic column moments. Recall that R was determined in Design Step 2.6. A summary of the R values used to modify EQM is presented below.

R = 3.0 For design of the pier column portion

R = 1.0 For connections that transfer forces between the superstructure and substructure, except at the abutments, and for connections between the column and the drilled shaft

R = 0.8 For connections at the abutments

b) Calculate the Design Forces with EQM

Once the R values have been established, the value of EQM can be calculated.

The design forces for the columns are given in Table 35. The R values used are given above the table.

As an example of the calculations used to generate the table, the transverse moment at the top of the column for LC1 is derived as follows.

M = (D + EQ/R)
M = (92 + 3051/3) = 1109 k-ft

Design Step 7.3.1 (continued)

All other forces in the tables are calculated similarly.

The R Factors have been applied only to moments and not to shear and axial forces, in accordance with the provisions of Division I-A for SPC C structures.

Table 35
Modified Design Forces at Structural Members
LC1 and LC2 in Group Load

Group LC1 = 1.0*Dead Load + 1.0*LC1 / R R = 3.0 Single Column Moments

Group LC2 = 1.0*Dead Load + 1.0*LC2 / R R = 1.0 Shear and Axial Force

Support/Location		Modified Design Forces — Forces and Moments in Column Portion of Pier No. 1					
		Transverse		Longitudinal		Vertical	
		Shear (kips)	Moment (kip-ft)	Shear (kips)	Moment (kip-ft)	Axial (kips)	Moment (kip-ft)
LC1	Top of Column	166	1,109	314	1,890	1,211	0
	Base of Flare	177	748	336	1,238	1,272	0
	Base of Column	182	199	346	477	1,315	0
LC2	Top of Column	277	1,645	189	1,136	1,234	0
	Base of Flare	297	1,055	202	740	1,295	0
	Base of Column	306	498	208	300	1,338	0

Design Step 7.3.2

Design Forces for Foundations [Division I-A, Article 7.2.1(B)]

Use Equation (7-2) in Division I-A to calculate the maximum forces in the foundations.

Group Load = 1.0 (D + B + SF + E + EQF) — Division I-A Eqn (7-2)

For this example, the forces B, SF, and E are assumed to be zero. Therefore, only D and EQF forces are combined in this section.

a) Response Modification Reduction Factor, R [Division I-A, Article 7.2.1(B)]

R = 1 for calculating the design forces in the foundation.

b) Calculate the Design Forces with EQF

Table 36 summarizes the combination of D and EQF forces.

For example, the maximum moment in the drilled shaft in the transverse direction, using LC1, is derived as follows.

M = (D + EQ/R)
M = (87 + 2,956/1.0) = 3043 k-ft

All other forces in the table are calculated similarly.

Design Step 7.3.2 (continued)

Table 36
Modified Design Forces for Foundations

Group LC1 = 1.0*Dead Load + 1.0*LC1 / R

Group LC2 = 1.0*Dead Load + 1.0*LC2 / R

R = 1.0 Foundations

		Modified Design Forces					
		Forces and Moments in Piles and Drilled Shafts					
		Transverse		Longitudinal		Vertical	
Support/Location		Shear (kips)	Moment (kip-ft)	Shear (kips)	Moment (kip-ft)	Axial (kips)	Moment (kip-ft)
LC1	Abut. A Piles	229	3,776	351	0	375	128
	Pier No. 1 Shaft	182	3,043	346	6,052	1,315	--
LC2	Abut. A Piles	208	5,881	374	0	403	118
	Pier No. 1 Shaft	306	5,515	208	3,666	1,338	--

Design Step 7.4

Plastic Hinging Forces

Before the forces due to plastic hinging can be calculated, the preliminary longitudinal column reinforcement must be determined.

Design Step 7.4.1

Preliminary Column Design
[Division I-A, Article 7.6.2 (A and B)]

The previous design step derived the Seismic Group Loads to be used in the seismic design of the bridge. This design step focuses on the preliminary design of the Pier No. 1 column. Both the longitudinal and transverse reinforcement in the column will be designed for the seismic load case.

Depending on the Seismic Performance Category, the column may be controlled by dead load combined with seismic loads or other loads such as live loads or stream flow loads. This example deals only with the seismic load combinations.

Division I-A, Article 7.6.2(B) mentions moment magnification in the columns. Currently, the magnitude and method of computing magnified moments for seismic loadings are under review by AASHTO. Some engineers refer to the Division I, Article 8.16.5; others feel that moment magnification during seismic loadings should not be included for concrete columns.

For concrete columns, a good method of approximation to account for a magnified moment is to multiply the maximum axial load in the column by the full elastic deflection at the column top. This additional moment is then added to the primary seismic moment before designing the reinforcement. Because the columns in this example are stiff, and the effect is small enough to be insignificant, magnification has been ignored.

a) Summary of Modified Design Forces for the Preliminary Column Design
[Division I-A, Article 7.2.3]

Table 35 gives the modified forces for load cases LC1 and LC2. There are three locations that may control the design of the column: the top of the column, the base of the flare, and the bottom of the column. The forces at each of these locations have been reported in the table.

At this point in the design, the designer should conceptually select the reinforcement layout for the column. Due to the flare at the top of the column, the manner in which the top is reinforced will have a bearing on

Design Step 7.4.1 (continued)

the behavior of the column and its strength at various points along its height.

For this example, the longitudinal reinforcement will be continued from the lower part of the column through the flare and into the superstructure. Only minimum (temperature and shrinkage) steel will be used to reinforce the flare.

By inspection, it can be seen that the controlling forces in the column will be at the base of the flare, since the top-of-column forces are only slightly larger and the forces at the bottom are quite small. Thus the longitudinal steel design strategy will be to design the column based on the forces at the flare, and to check the column, neglecting the flare, at the top. This approach is conservative.

From Table 35, the controlling forces for LC1 and LC2 for the base of the flare are

$P_{u1} := 1272 \cdot kip$ Axial force for LC1

$Mt_{u1} := 748 \cdot kip \cdot ft$ Transverse moment for LC1

$Ml_{u1} := 1238 \cdot kip \cdot ft$ Longitudinal moment for LC1

$P_{u2} := 1295 \cdot kip$ Axial force for LC2

$Mt_{u2} := 1055 \cdot kip \cdot ft$ Transverse moment for LC2

$Ml_{u2} := 740 \cdot kip \cdot ft$ Longitudinal moment for LC2

b) Calculate the ϕ Factor for Use with M_u

Division I-A, 7.6.2(B) specifies a ϕ factor that varies from 0.9 to 0.5 depending on the axial load. Because the lower bound of ϕ equals 0.5 when the axial stress exceeds $0.2*f'_c$, column charts that use a lower bound of ϕ equal to 0.7 are not applicable.

For this example problem, the nominal capacity of the column is plotted as P_n, M_n without a ϕ factor. Therefore, the factored loads must be divided by ϕ before being plotted on the capacity chart. See Figure 25 for the general curves for design capacity, nominal capacity, and plastic capacity.

Design Step 7.4.1 (continued)

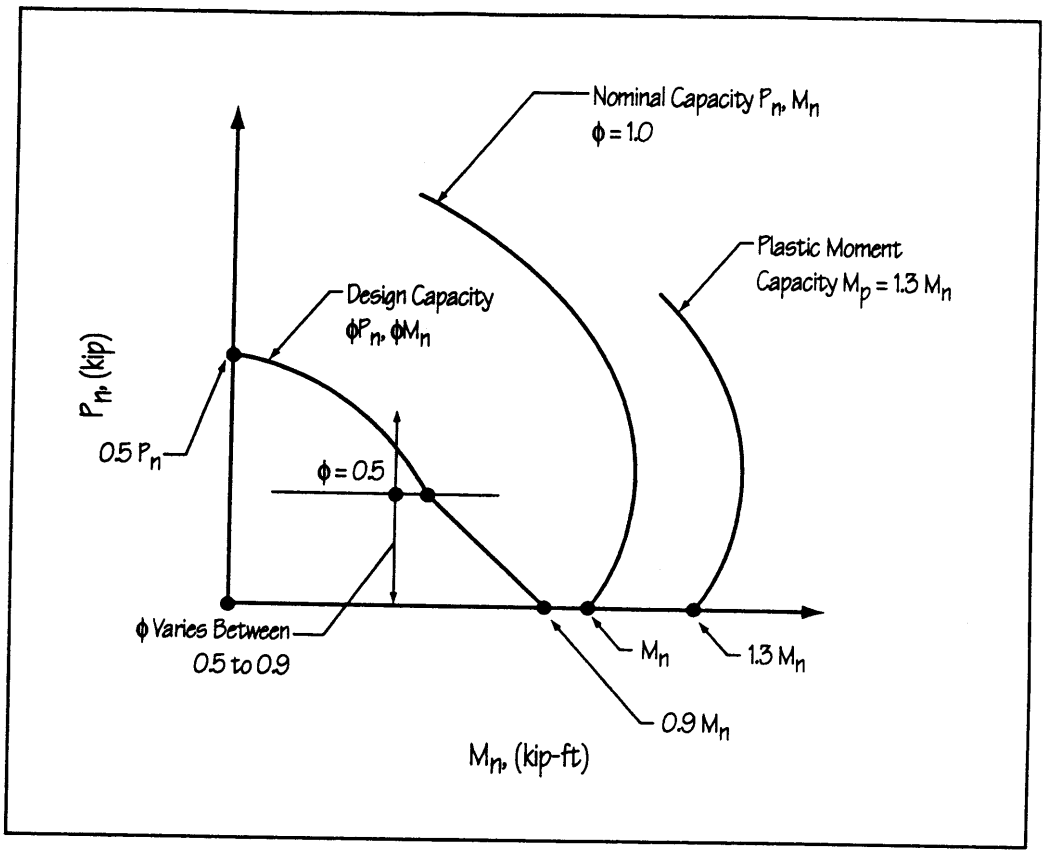

Figure 25 —Column Interaction Curves, General

Compute the axial stress for the highest of the two axial loads. Because the loads are so close, use the same ϕ factor with both load cases.

$$A_g := (3.5 \cdot ft \cdot 5.5 \cdot ft) \cdot \left(144 \cdot \frac{in^2}{ft^2}\right)$$ Area of column

$$A_g = 2772 \cdot in^2$$

$$\sigma_u := \frac{P_{u2}}{A_g} \qquad \sigma_u = 467 \cdot psi$$

Per Division I-A, Article 7.6.2(B), $\phi = 0.5$ when the maximum axial stress exceeds $0.2 * f'_c$, and varies linearly from 0.5 to 0.9 for stresses less than $0.2 * f'_c$. See Figure 26.

Design Step 7.4.1 (continued)

$f_c := 4000 \cdot psi$ $\quad 0.2 \cdot f_c = 800 \cdot psi$

Because the applied axial force is less than 800 psi, the value of ϕ is greater than 0.5.

$$\phi := 0.9 - \frac{\sigma_u}{0.2 \cdot f_c} \cdot (0.9 - 0.5) \qquad \phi = 0.67$$

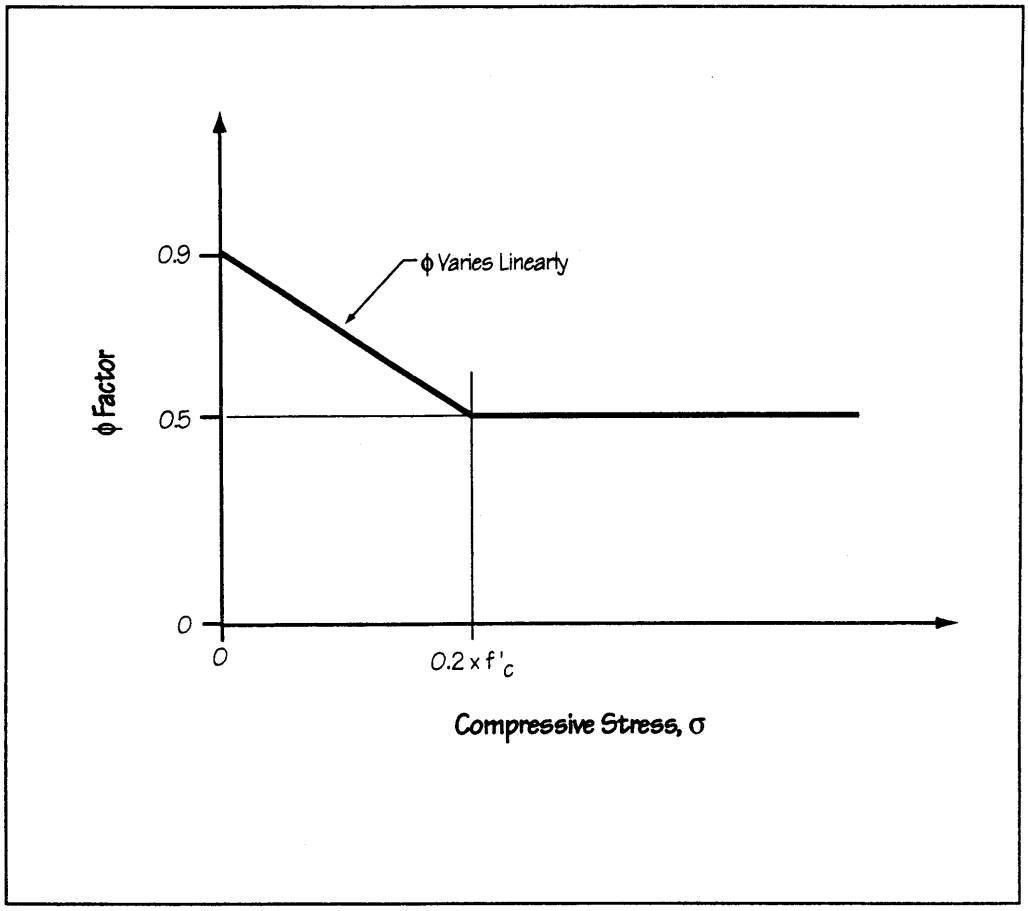

Figure 26 — ϕ Factor versus Compressive Stress

c) Calculate the P_u / ϕ and M_u / ϕ Forces and Plot on the P_n, M_n Column Capacity Curve

Using the value of ϕ just determined, the required forces for the column design can be calculated as follows.

Design Step 7.4.1 (continued)

For load case LC1

$\frac{P_{u1}}{\phi} = 1909 \cdot kip$ Required axial strength

$\frac{Mt_{u1}}{\phi} = 1122 \cdot ft \cdot kip$ Required transverse flexural strength

$\frac{Ml_{u1}}{\phi} = 1858 \cdot ft \cdot kip$ Required longitudinal flexural strength

For load case LC2

$\frac{P_{u2}}{\phi} = 1943 \cdot kip$ Required axial strength

$\frac{Mt_{u2}}{\phi} = 1583 \cdot ft \cdot kip$ Required transverse flexural strength

$\frac{Ml_{u2}}{\phi} = 1110 \cdot ft \cdot kip$ Required longitudinal flexural strength

The application of the strength reduction factor ϕ in this example is based on Article 8.16.4.2.4 of Division I. While the seismic provisions of Division I-A provide alternate values for the ϕ factor for SPC C and D, the provisions imply that the application of the factor is identical to that specified in Division I. In Division I, the nominal strength interaction diagram is reduced "radially" by the ϕ factor. This means that both the axial strength P_n and the flexural strength M_n are reduced by the same ϕ factor to obtain the design strengths ϕP_n and ϕM_n, as shown qualitatively in Figure 25.

Some designers prefer to apply the ϕ factor only to the nominal moment strengths when the axial loads are in the tension controlled region (below the balance point of the interaction diagram). Since the moment strength increases with axial load, the process of not applying the ϕ factor to the axial load effectively uses a nominal flexural strength that is smaller than

Design Step 7.4.1 (continued)

would result if ϕ were used with the axial load. In design, this practice will result in more reinforcement than if the standard Division I practice is used. Stated differently, the practice is similar to using a slightly smaller R Factor for determining the required moment strengths.

The practice of using ϕ only with the moment is more conservative than the standard practice, although probably only slightly so. However, the practice is not consistent with the philosophy of the ϕ factor, in which ϕ is meant to account for potential material, member, or system understrength.

d) Select the Preliminary Longitudinal Reinforcement

Try the minimum longitudinal steel (1 percent) for the 3.5- by 5.5-foot column. This corresponds to 22 #10 bars. The resulting biaxial interaction diagram plotted at the design axial force level is shown in Figure 27a. Also shown are the load points for LC1 and LC2.

Note that the ϕ factor is unity for the curve shown, and the ϕ factor is included in the loads that are plotted.

Obviously the capacity of the column with 1 percent steel exceeds that required by a substantial amount. If only the seismic loads govern the column, then the column size could be reduced. However, for this example the column size will not be changed.

Design Step 7.4.1 (continued)

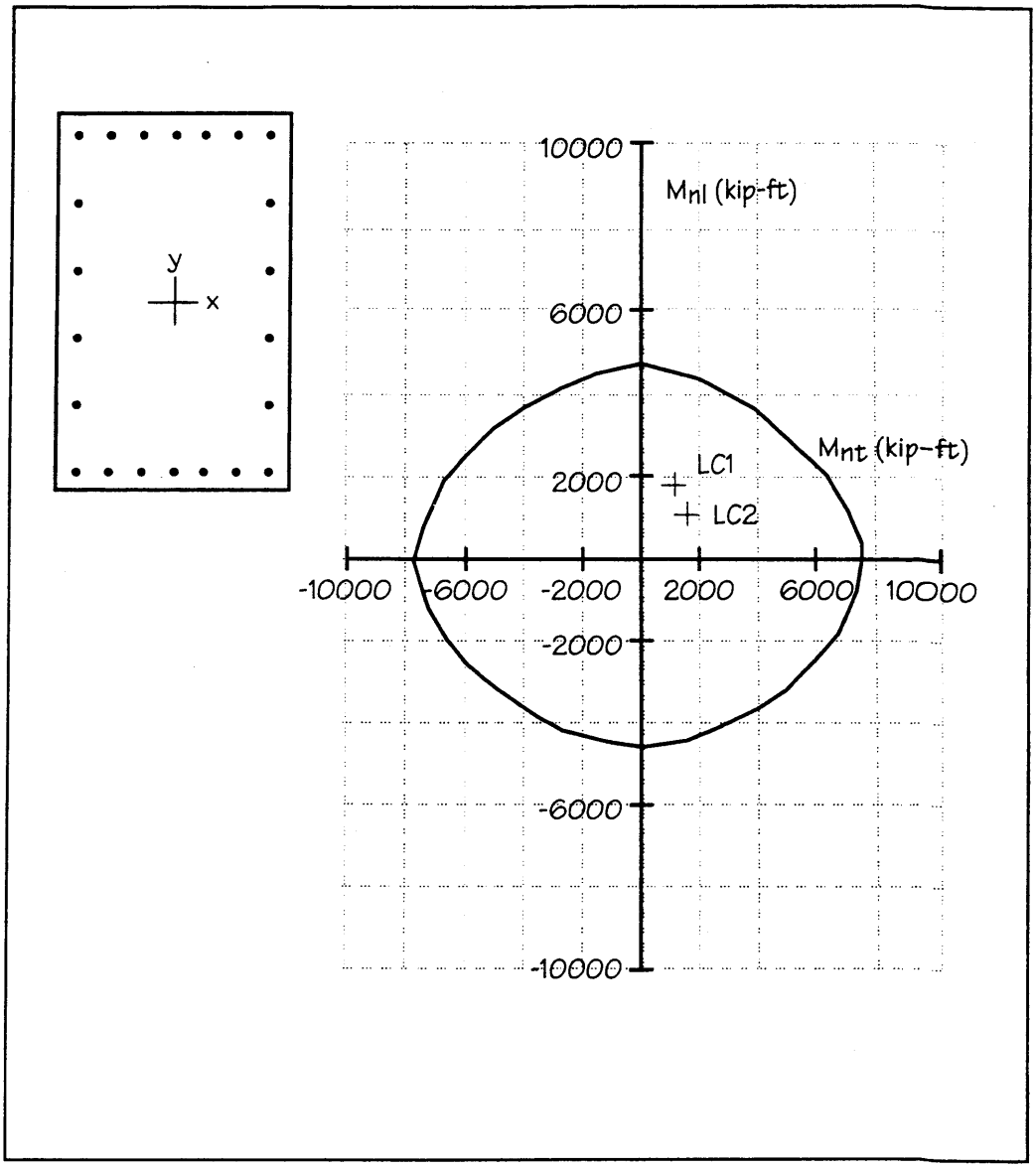

Figure 27 — Load Cases at Base of Flare

Design Step 7.4.1 (continued)

e) Check the Other Column Sections

Consideration of the other cross sections, for which forces are listed in Table 35, indicates that the forces at the bottom of the column will not control the design. However, the loading at the top of the column will be checked for the basic 3.5- by 5.5-foot cross section, neglecting the flare. If the loads check for this cross section, they will certainly check for the larger sections in the flare.

The axial stress acting on the 3.5- by 5.5-foot cross section must be determined to set the ϕ factor.

$$\sigma_{LC1} := \frac{1211 \cdot kip}{A_g} \qquad \sigma_{LC1} = 437 \cdot psi$$

$$\sigma_{LC2} := \frac{1234 \cdot kip}{A_g} \qquad \sigma_{LC2} = 445 \cdot psi$$

It can be shown that ϕ is equal to 0.68 for these two axial loads. Thus, the required loads can be calculated using ϕ as before.

$$\phi := 0.68$$

For load case LC1 at the top of the column

$$P_{top1} := \frac{1211 \cdot kip}{\phi} \qquad P_{top1} = 1781 \cdot kip$$

$$Mt_{top1} := \frac{1109 \cdot kip \cdot ft}{\phi} \qquad Mt_{top1} = 1631 \cdot ft \cdot kip$$

$$Ml_{top1} := \frac{1890 \cdot kip \cdot ft}{\phi} \qquad Ml_{top1} = 2779 \cdot ft \cdot kip$$

Design Step 7.4.1 (continued)

For load case LC2 at the top of the column

$$P_{top2} := \frac{1234 \cdot kip}{\phi} \qquad P_{top2} = 1815 \cdot kip$$

$$Mt_{top2} := \frac{1645 \cdot kip \cdot ft}{\phi} \qquad Mt_{top2} = 2419 \cdot ft \cdot kip$$

$$Ml_{top2} := \frac{1136 \cdot kip \cdot ft}{\phi} \qquad Ml_{top2} = 1671 \cdot ft \cdot kip$$

Because the axial forces are so close to one another, the 1781 value is used for both load cases to simplify the check. This approach allows both load points to be plotted on the same graph, which appears in Figure 28. It can be seen that the section is capable of resisting these loads.

Design Step 7.4.1 (continued)

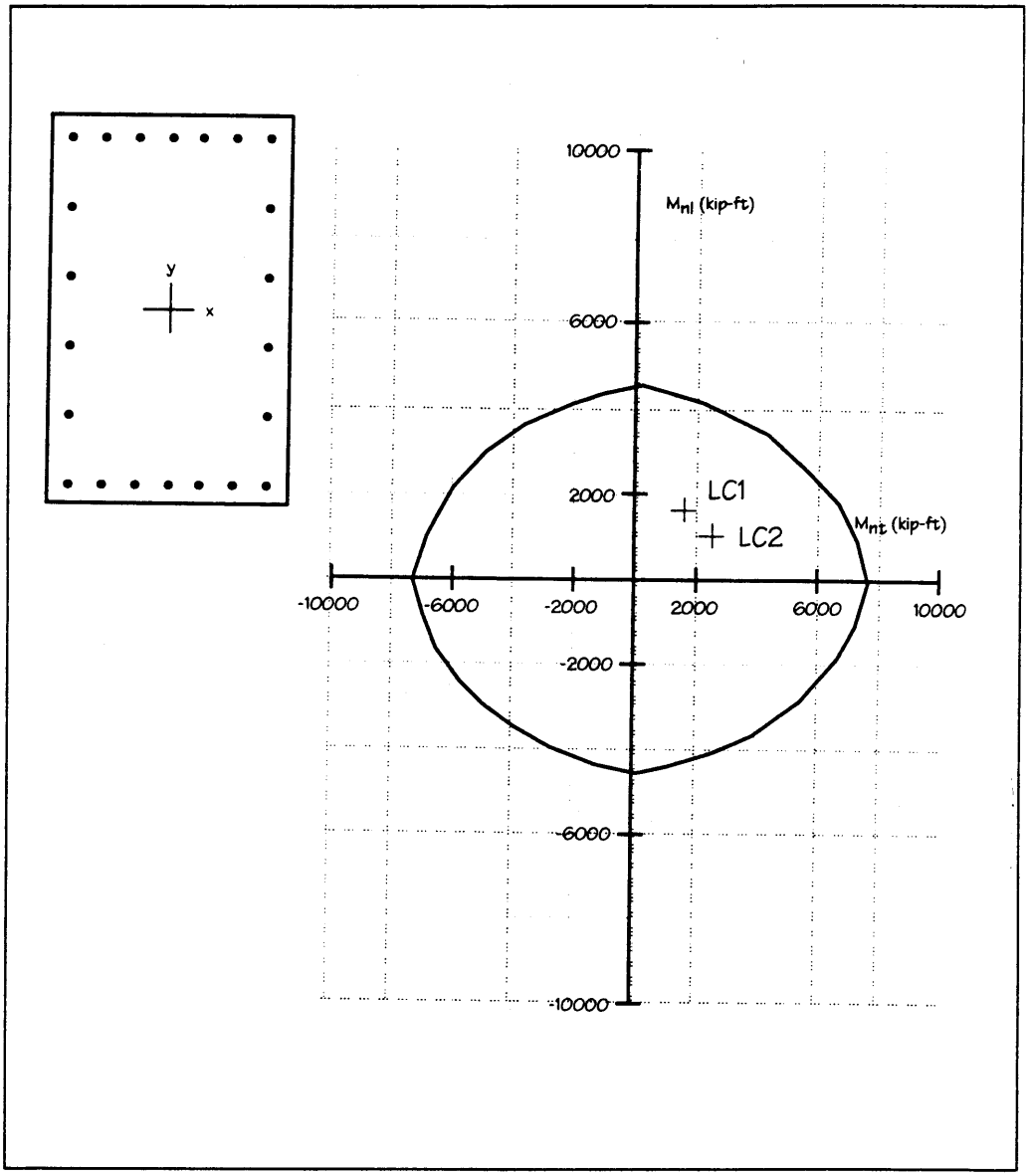

Figure 28 — Load Cases at Top of Column

Design Step 7.4.2

Forces Resulting from Plastic Hinging
[Division I-A, Article 7.2.2(A)]

After the column longitudinal reinforcement has been determined, the shear forces resulting from plastic hinging in the column must be computed before the transverse reinforcement can be established. Determination of the plastic hinging forces at the top and bottom of the column is also necessary to establish the connection forces transferred to the cap beam and foundation.

Plastic hinging forces are calculated for bridges in Seismic Categories C and D. When the columns are allowed to form a plastic hinge at the top and bottom of the column during a design level earthquake, the hinge acts as a "fuse" to limit the forces transferred to some of the bridge components. This fuse limits the forces transferred into both the footing at the bottom of the column and the cap beam at the top of the column. It also limits the shear (and sometimes the axial force) that the column has to be designed for. The Specification does allow the above components to be designed without calculating the plastic hinging forces. Typically, the plastic hinging forces are less than the elastic forces in Seismic Categories C and D.

Because the column longitudinal steel is sized to meet the minimum steel requirements, the flexural strength of the column will be somewhat larger than that required. Thus the elastic seismic forces may be smaller than the actual plastic hinging forces.

Article 7.2.2(A) of Division I-A covers the determination of plastic hinging forces for single columns. The critical force is the shear associated with plastic hinging, and this force is typically the sum of the plastic moments at the top and bottom of the column, divided by the column height. However, for a column/drilled shaft system it is possible for plastic hinging to occur in the shaft, below the ground surface, and not at the column-to-shaft connection. This hinging can occur in spite of the fact that the design forces for the drilled shaft will be based on the elastic or unmodified seismic forces. Often it is physically impossible and impractical to prevent plastic hinging from occurring in the shaft itself. Usually, however, as in this case, no significant damage is expected in the shaft as a result of the design ground motion.

The actual plastic hinging mechanism for a column/shaft system is not easily predicted. In fact, the plastic mechanism depends on the soil stiffness along the shaft, including nonlinear effects; on the relative

Design Step 7.4.2 (continued)

flexural strengths of the column and shaft, and on the restraint offered by the superstructure to the top of the column.

As can be seen from Figures 22(b) and 22(d), for purely elastic response, the moment at the base of the column is somewhat smaller than the maximum shaft moment. From the elastic moment distribution, it can be inferred that if the column and shaft have nearly identical flexural strengths, then hinging will probably occur in the shaft. On the other hand, if the column is somewhat weaker in flexure than the shaft, then hinging may occur at the base of the column. Obviously, both the column and shaft longitudinal steel contents must be known before the actual behavior can be predicted.

Since potential soil nonlinear behavior also affects the distribution of column and shaft moments, either a trial-and-error equilibrium approach or a full nonlinear (pushover) analysis is required to determine the correct plastic mechanism. The trial-and-error approach is based on "trying out" different mechanisms and determining the required internal and reaction forces to satisfy equilibrium. The actual mechanism is then the one that requires the smallest lateral load. This is the well-established 'upper-bound theorem' of plasticity (Gaylord et. al., 1992). A pushover analysis is more comprehensive and actually tracks the formation of plastic hinges and soil nonlinearity, adjusting the structure stiffness as the analysis proceeds. Thus the results are not only the final plastic mechanism, but also the sequence of yielding up to the formation of a mechanism. Typically, a full pushover analysis is not performed during the seismic design of a non-critical bridge. Instead of a pushover analysis, the program LPILE can often be used to determine much of the information needed to assess the plastic mechanism of a column/drilled shaft system.

For this column, plastic hinging is probably unlikely since the nominal strength of the column with minimum longitudinal steel greatly exceeds the seismic load combinations LC1 and LC2, as shown in Figures 27 and 28. Thus the elastic forces could control the design of the column for shear. However, to provide for potential overload and to prevent the possibility of a brittle failure of the column in shear, the column will be designed to carry the shear corresponding to development of a plastic mechanism.

For loading in the transverse column direction, hinging will occur at the base of the flare; however, for longitudinal loading, hinging could occur near the top of the column, depending on the relative strength of the column cross sections. It is conservative for the shear design to assume that hinging will occur at

Design Step 7.4.2 (continued)

the base of the flare. This approach will satisfy the requirements of Article 7.2.2(A) for flared columns.

As discussed above, plastic hinging will probably occur in the shaft and not at the column-to-shaft connection. However, an upper-bound column shear corresponding to hinging occurring at the base of the column can be used. According to the upper-bound plasticity theorem, this shear will be larger than the actual shear and will therefore be conservative. This approach avoids having to calculate the actual mechanism just to design the column for shear. In fact, as will be seen in Design Step 10.1.3, the potential hinging zones cover most of the column length, and the required confinement steel in these zones will also accommodate the upper-bound shear force.

Article 7.2.2(A) of Division I-A gives two steps for calculating the plastic hinging forces for single columns.

Step 1. Determine the column overstrength plastic moment capacities using a 1.3 factor for reinforced concrete sections.

For this example the nominal flexural strengths of the column, assuming a ϕ of unity, have been determined and are shown in Figures 29a and 29b for the sections at the base of the flare and the bottom of the column, respectively. The figures show the biaxial interaction diagram at a load contour equal to the axial earthquake load, since this is the axial load most likely to be present if the seismic loading occurs. In the figures, M_{nt} is the moment capacity for bending in the transverse plane and M_{nl} is the capacity in the longitudinal plane.

From the figures, the transverse plastic moment capacity at the base of the flare is 6700 kip-ft and the longitudinal capacity is 4050 kip-ft. At the bottom of the column, the capacities are 6750 and 4100 kip-ft, respectively.

Note that even though the design loads are biaxial and not aligned along the principal axes of the column, the plastic hinging determination is conducted along the principal axes.

The specification suggests using a ϕ factor of 1.3 for the calculation of the moment overstrength capacity. In this example, the results for a ϕ of 1.0 are simply multiplied by 1.3, for clarity.

Design Step
7.4.2
(continued)

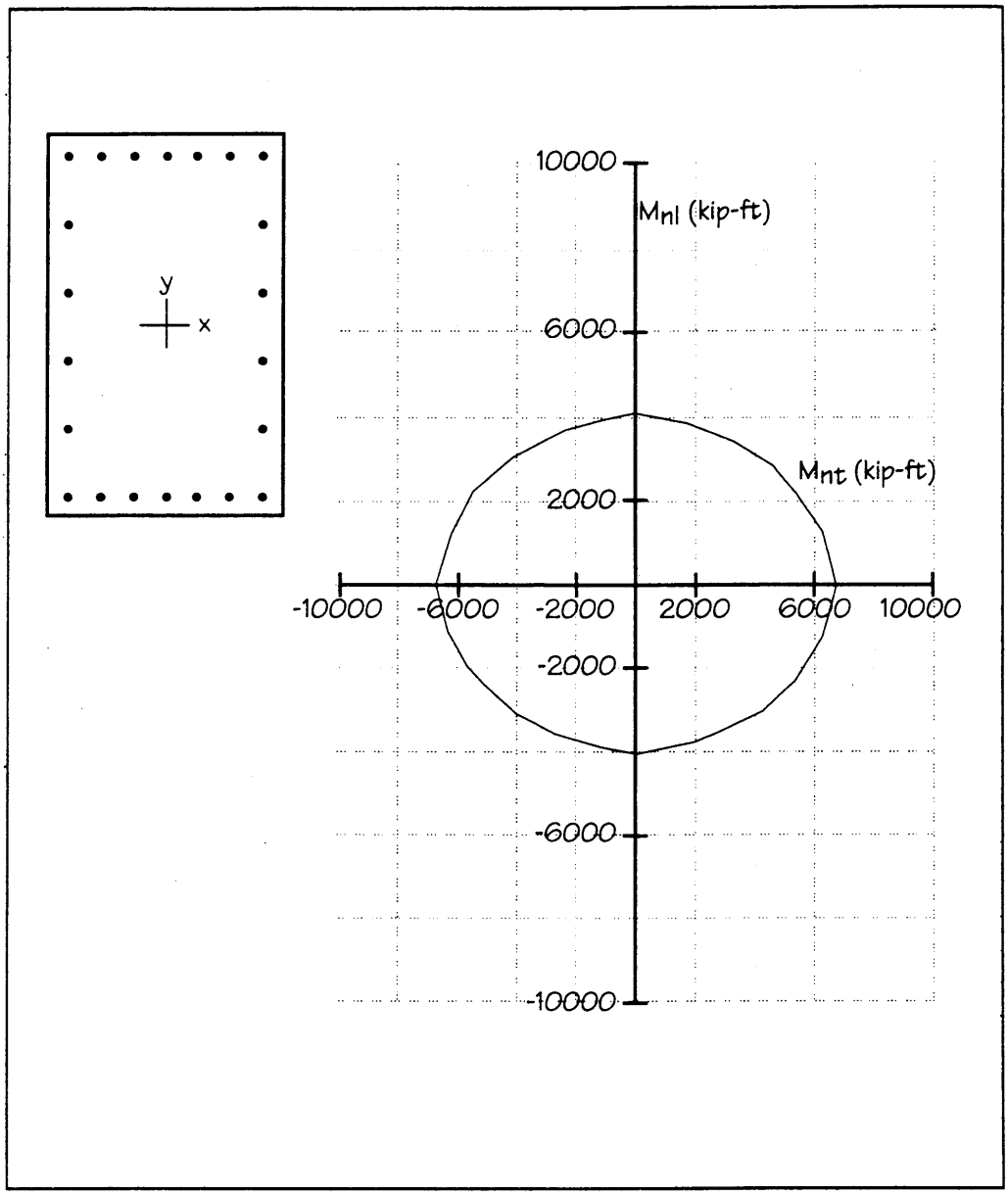

Figure 29a — Moment Capacities at Base of Flare

Design Step 7.4.2 (continued)

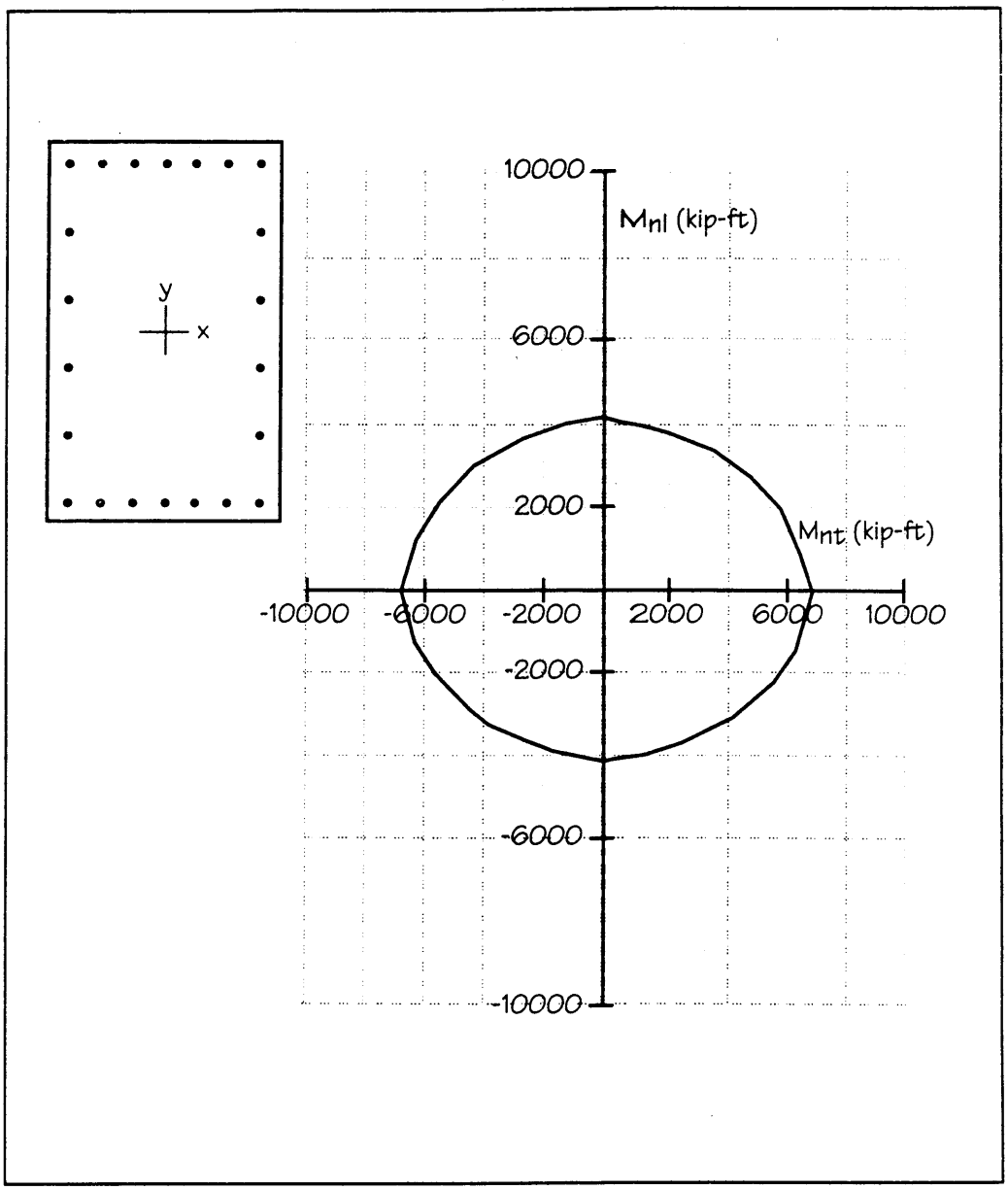

Figure 29b — Moment Capacities at Base of Column

Design Step 7.4.2 (continued)

Step 2. Calculate the column shear force corresponding to the attainment of plastic hinging at the most likely locations within the column.

As discussed above, hinges will be assumed at the base of the flare and at the bottom of the column. The clear distance between these locations is 15 feet. Thus, the plastic hinging shears are

$Vp_t = 1.3 * (6700 + 6750) / 15 = 1166$ kips

$Vp_l = 1.3 * (4050 + 4100) / 15 = 706$ kips

For the case of a single-column pier, the axial forces corresponding to plastic hinging are essentially equal to the elastic axial forces.

DESIGN STEP 8

SUMMARY OF DESIGN FORCES

Design Step 8.1

Column or Pile Bent Design Forces
[Division I-A, Article 7.2.3]

The selection of design forces, used to design the column reinforcement for seismic loads, is outlined in Division I-A, Article 7.2.3. A selection is made between the modified elastic forces and the forces associated with plastic hinging.

a) Axial Forces per Division I-A, Article 7.2.3(a)

Use either the modified forces calculated in Design Step 7.3.1 (same as elastic forces because R = 1) or the plastic hinging forces calculated in Design Step 7.4.2. For a single-column pier, the two axial forces are identical.

Modified Elastic Forces

Load Case LC1

Top of the column	P = 1211 kips	
Base of the flare	P = 1272 kips	
Bottom of the column	P = 1315 kips	

Load Case LC2

Top of the column	P = 1234 kips	
Base of the flare	P = 1295 kips	← Use
Bottom of the column	P = 1338 kips	← Use

b) Moments per Division I-A, Article 7.2.3(b)

Use the modified moments calculated in Design Step 7.3.1

Load Case LC1

Top of the column	M_t = 1109 kip-ft	M_l = 1890 kip-ft
Base of the flare	M_t = 748 kip-ft	M_l = 1238 kip-ft ← Use
Bottom of the column	M_t = 346 kip-ft	M_l = 477 kip-ft

Design Step 8.1 (continued)

Load Case LC2

Top of the column	M_t = 1645 kip-ft	M_l = 1136 kip-ft
Base of the flare	M_t = 1055 kip-ft	M_l = 740 kip-ft
Bottom of the column	M_t = 498 kip-ft	M_l = 300 kip-ft

c) Shear Forces per Division I-A, Article 7.2.3(c)

Use either the modified forces calculated in Design Step 7.3.1 (same as elastic forces, because R = 1), or the plastic hinging forces calculated in Design Step 7.4.2.

Modified Elastic Forces (Use the maximum over the height of the column.)

Load Case LC1

Bottom of the column	V_t = 182 kip	V_l = 346 kip

Load Case LC2

Bottom of the column	V_t = 306 kip-ft	V_l = 208 kip
Hinging Forces	Vp_t = 1166 kips	← Use
	Vp_l = 706 kips	← Use

Even though the elastic shear forces are much smaller than plastic hinging forces, use the hinging forces for design.

This approach provides a fail-safe load path should the abutment piles not perform as intended. Furthermore, using the hinging shear makes the possibility of brittle shear failure very remote.

Design Step 8.2

Pier Design Forces

Not applicable.

Design Step 8.3 **Connection Design Forces**
[Division I-A, Article 7.2.5]

Design Step 8.3.1 Longitudinal Linkage Connections
[Division I-A, Article 7.2.5(A)]

There are no linkage connections; therefore, provisions are not applicable.

Design Step 8.3.2 Hold-Down Devices
[Division I-A, Article 7.2.5(B)]

Not applicable.

Design Step 8.3.3 Column and Pier Connection to Cap Beam
[Division I-A, Article 7.2.5(C)]

Not addressed in this example.

Design Step 8.3.4 Column Connection to Foundation
[Division I-A, Article 7.2.5(C)]

The recommended connection design force between the column and foundation are the forces developed at the bottom of the column due to column hinging. These forces are the same as in Design Step 8.3.3.

Design Step 8.4 **Cap Beam Design Forces**

Not addressed in this example.

Design Step 8.5 **Miscellaneous Design Forces**

Not applicable.

Design Step 8.6 **Foundation Design Forces**
[Division I-A, Article 7.2.6]

The design forces for the drilled shaft may be either the full elastic forces or the forces corresponding to plastic hinging.

a) Modified Design Forces for Foundations
[Division I-A, Article 7.2.1(B)]

These forces were calculated in Design Step 7.3.2 and are summarized in Table 36. Note that R = 1.0 represents the full elastic seismic forces.

Design Step 8.6 (continued)

b) Forces from Column Plastic Hinging
[Division I-A, Article 7.2.2]

The plastic hinging forces were calculated in Design Step 7.4.

Since the plastic hinging forces are so much larger than the elastic forces, use the elastic forces given in Table 36 for design of the drilled shaft.

Design Step 8.7

Abutment Design Forces
[Division I-A, Article 7.2.7]

The primary abutment elements that are designed in this example are the pipe piles.

The design forces for the pipe piles are the full elastic forces listed in Table 36.

DESIGN STEP 9 — DETERMINE DESIGN DISPLACEMENTS

[Division I-A, Article 7.3]

Design Step 9.1 — Minimum Support Length

[Division I-A, Article 7.3.1]

Not applicable.

Design Step 9.2 — Design Displacements

The displacements from the radial and chord earthquake analyses were given in Tables 12 and 22. They are repeated below in Tables 37 and 38.

Table 37
Radial Earthquake Displacements

Radial Earthquake/No Backfill Model		
Superstructure Displacement		
Location	Radial (feet)	Chord (feet)
Abut. A	0.134	0.012
Pier No. 1	0.149	0.001
Midspan	0.153	0
Pier No. 2	0.149	0.001
Abut. B	0.134	0.012
Pier Displacement		
Location	Tangential (feet)	Longitudinal (feet)
Column to Shaft	0.074	0.03

Design Step 9.2 (continued)

Table 38
Chord Earthquake Displacements

Chord Earthquake/No Backfill Model		
Superstructure Displacement		
Location	Radial (feet)	Chord (feet)
Abut. A	0.032	0.128
Pier No. 1	0.013	0.14
Midspan	0	0.142
Pier No. 2	0.013	0.14
Abut. B	0.032	0.128
Pier Displacement		
Location	Tangential (feet)	Longitudinal (feet)
Column to Shaft	0.025	0.087

DESIGN STEP 10

DESIGN STRUCTURAL COMPONENTS

This section covers the design of critical superstructure and substructure elements, exclusive of the foundations, that resist seismic forces. For this example, only selected lateral force resisting systems will be discussed. These include the column and its connection to the drilled shaft.

Design Step 10.1

Column Design

Given below is the basic data for the column. See Figure 30 for details.

$f_c := 4000 \cdot psi$ Concrete strength in column

$f_{yh} := 60 \cdot ksi$ Nominal steel yield strength

$Ht_{clr} := 15 \cdot ft$ Clear height of column in transverse direction

$Hl_{clr} := 21 \cdot ft$ Clear height of column in longitudinal direction

$b_c := 3.5 \cdot ft$ Outside width of column in longitudinal direction

$d_c := 5.5 \cdot ft$ Outside depth of column in transverse direction

Determine the core dimensions of the column, assuming a 2-inch cover.

$ht_c := 42 \cdot in - 2 \cdot 2 \cdot in$ Core dimension in short direction

$ht_c = 38 \cdot in$

$hl_c := 66 \cdot in - 2 \cdot 2 \cdot in$ Core dimension in long direction

$hl_c = 62 \cdot in$

Design Step 10.1 (continued)

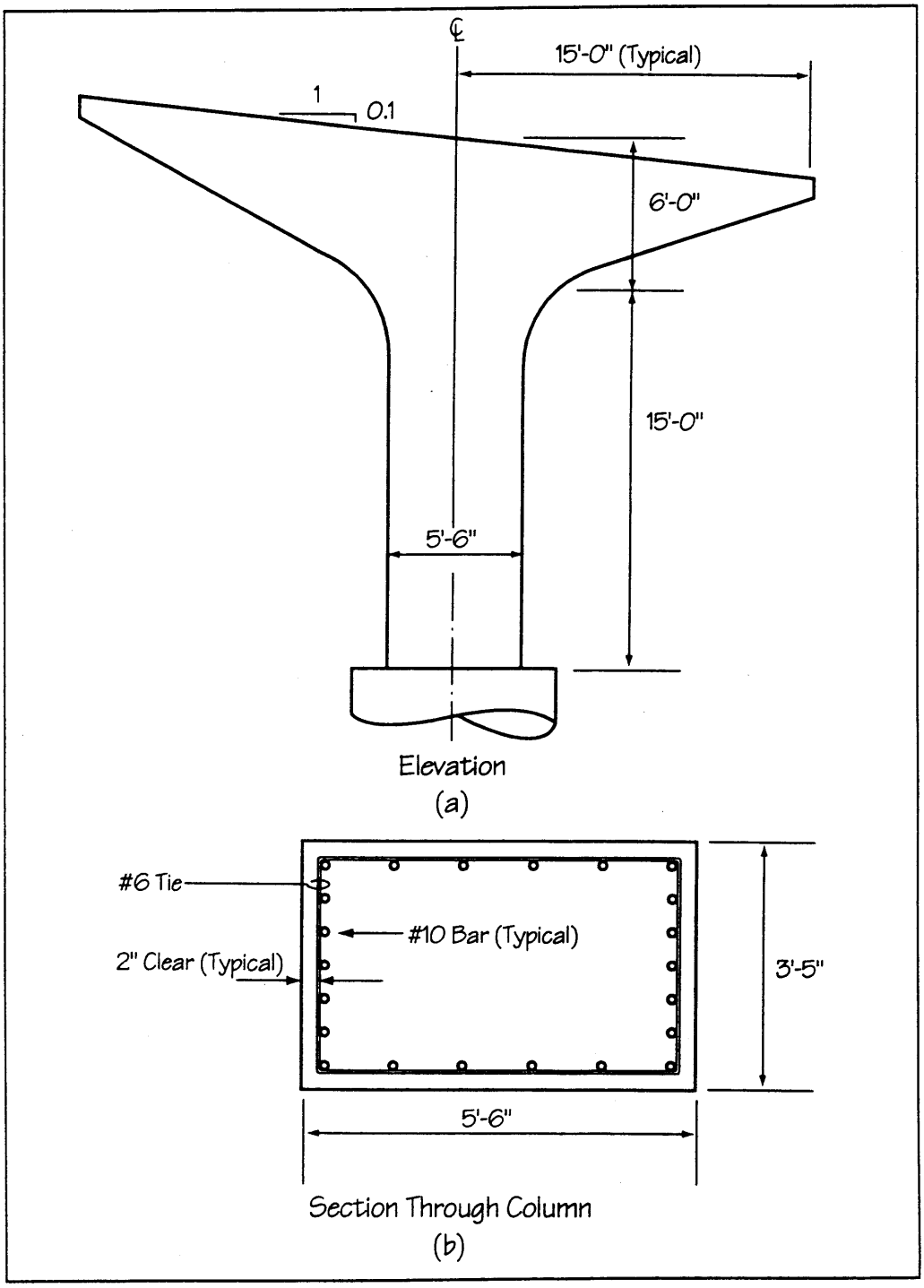

Figure 30 — Details Column

Design Step 10.1.1

Determine Longitudinal Reinforcement

Use the preliminary longitudinal reinforcement computed in Design Step 7.4.1. Use 22 #10 bars distributed as shown in Figure 30, 7 bars on each short side and 6 bars on each long side.

Design Step 10.1.2

Determine Typical Transverse Reinforcement [Division I-A, Article 7.6.2(C)]

a) The required shear strength of the column section must be at least that calculated per Division I, Article 8.16.6.1, using the ϕ value from Division I, Article 8.16.1.2 for shear.

$\phi := 0.85$ $\quad f_c := 4000$

For loading in the transverse direction

$bt_w := 42 \cdot in$ Width in transverse direction

$dt := 66 \cdot in - 2 \cdot in - 0.75 \cdot in - \frac{1.27}{2} \cdot in$ Effective depth in transverse direction

$dt = 62.62 \cdot in$

$Vp_t := 1166 \cdot kip$ Plastic shear in transverse direction

The required transverse shear strength of the section must be at least

$Vt_n := \frac{Vp_t}{\phi}$ $\quad Vt_n = 1372 \cdot kip$ Division I Eqn (8-46)

For loading in the longitudinal direction

$bl_w := 66 \cdot in$ Width in longitudinal direction

$dl := 42 \cdot in - 2 \cdot in - 0.75 \cdot in - \frac{1.27}{2} \cdot in$ Effective depth in longitudinal direction

$dl = 38.62 \cdot in$

Design Step 10.1.2 (continued)

$Vp_l := 706 \cdot kip$ Plastic shear in longitudinal direction

The required longitudinal shear strength of the section must be at least

$$Vl_n := \frac{Vp_l}{\phi} \qquad Vl_n = 831 \cdot kip$$ Division I Eqn (8-46)

b) The concrete shear strength of the column calculated per Division I, Article 8.16.6.2 applies only to the middle portion of the column. Refer to Design Step 10.1.3 for the transverse reinforcement requirements in the end regions.

In the transverse direction, the concrete shear contribution is

$$Vt_c := 2 \cdot \sqrt{f_c \cdot psi} \cdot \left(bt_w \cdot dt\right)$$ Division I Eqn (8-51)

$Vt_c = 333 \cdot kip$

In the longitudinal direction, the concrete shear contribution is

$$Vl_c := 2 \cdot \sqrt{f_c \cdot psi} \cdot \left(bl_w \cdot dl\right)$$ Division I Eqn (8-51)

$Vl_c = 322 \cdot kip$

c) The required shear strength provided by the transverse steel is calculated per Division I, Article 8.16.6.3.

In the transverse direction

$$Vl_s := Vl_n - Vl_c$$ Division I Eqn (8-47)

$Vl_s = 508 \cdot kip$

Design Step 10.1.2 (continued)

In the longitudinal direction

$Vl_s := Vl_n - Vl_c$ Division I Eqn (8-47)

$Vl_s = 508 \cdot kip$

The maximum spacing will be set at "d/4" to ensure that more than one bar crosses a potential shear crack. In Division I, this limit is invoked only if the shear required of the steel exceeds $4(fc)^{1/2}$ bd. However, it is good practice to ensure that seismic detailing meets this limit as a minimum in any case.

For the transverse direction

$st_{max} := \frac{dt}{4}$ $st_{max} = 15.7 \cdot in$

The shear reinforcement area required is then

$At_v := \frac{Vt_s \cdot st_{max}}{f_{yh} \cdot dt}$ Division I Eqn (8-53)

$At_v = 4.33 \cdot in^2$

This is a rather large area; therefore, reduce the spacing to 4 inches and recalculate. This is the maximum spacing that will be allowed in the end regions.

$At_v := \frac{Vt_s \cdot 4 \cdot in}{f_{yh} \cdot dt}$ $At_v = 1.11 \cdot in^2$

If 4 #5 legs are used, then

$At_v := 0.31 \cdot in^2 \cdot 4$ $At_v = 1.24 \cdot in^2$

Okay. Use 4 #5 bars in transverse direction

Design Step 10.1.2 (continued)

For the longitudinal direction

$sl_{max} := \frac{dl}{4}$ $sl_{max} = 9.7 \cdot in$ Try $s = 4$ in

The shear reinforcement area required is then

$Al_v := \frac{Vl_s \cdot 4 \cdot in}{f_{yh} \cdot dl}$ Division I Eqn (8-53)

$Al_v = 0.88 \cdot in^2$

Again, use 4 #5 bars spaced at 4 inches. These will provide more than adequate strength and lateral restraint for longitudinal bars.

Design Step 10.1.3

Determine Minimum End Region Transverse Reinforcement [Division I-A, Article 7.6.2(C)]

The end regions must meet the following two criteria.

- **Criteria 1 — The shear strength of the concrete, V_c, shall be in accordance with Division I, Article 8.16.6.2, when the axial load exceeds 0.1 f'_c A_{core}. As the average compression stress increases from 0 to 0.1 f'_c, the shear strength of the concrete may be assumed to increase linearly from 0 to the value given in Division I, Article 8.16.6.2.**

- **Criteria 2 — The extent of the 'End Region' extends above the footing and below the soffit of the cap beam not less than (a) the maximum cross sectional dimension of the column, (b) one-sixth of the clear height of the column, and (c) 18 inches.**

Check the implications of Criteria 1.

The core area of the concrete must first be calculated.

Recall that $ht_c = 38 \cdot in$ $hl_c = 62 \cdot in$

$A_c := ht_c \cdot hl_c$ $A_c = 2356 \cdot in^2$ Area of core

Design Step 10.1.3 (continued)

Calculate the stress in the column core. Use the axial force at the base of the flare, as given in Design Step 8.1(a), 1295 kips.

$$\sigma_{core} := \frac{1295 \cdot kip}{A_c} \qquad \sigma_{core} = 550 \cdot psi$$

$$0.1 \cdot f'_c \cdot psi = 400 \cdot psi$$

Because the axial stress on the core exceeds 0.1 f '$_c$, the full V_c value may be used for the end regions. Because the shear strength provided by the concrete is the same as that used in Design Step 10.1.2 for the middle regions, the required shear reinforcement is identical in the end regions.

Determine the controlling dimensions specified by Criteria 2.

a. Maximum cross section of the column = 66 inches
b. Hclr/6 = 21 ft / 6 = 42 inches
c. 18 inches minimum

Use 66 inches as the end region dimension.

Note that this dimension is a rough estimate of the length of column over which inelastic action or yielding may be expected. Therefore in this column, the "end regions" are as shown in Figure 31. The potential hinge zone at the base of the flare has an "end region" extending above and below the base of the flare. This design element recognizes the spread of plasticity possible when hinging occurs in the middle of a member. Note that the end regions almost encompass the entire column. For this reason, the entire height of the column could be considered an "end region."

Design Step 10.1.3 (continued)

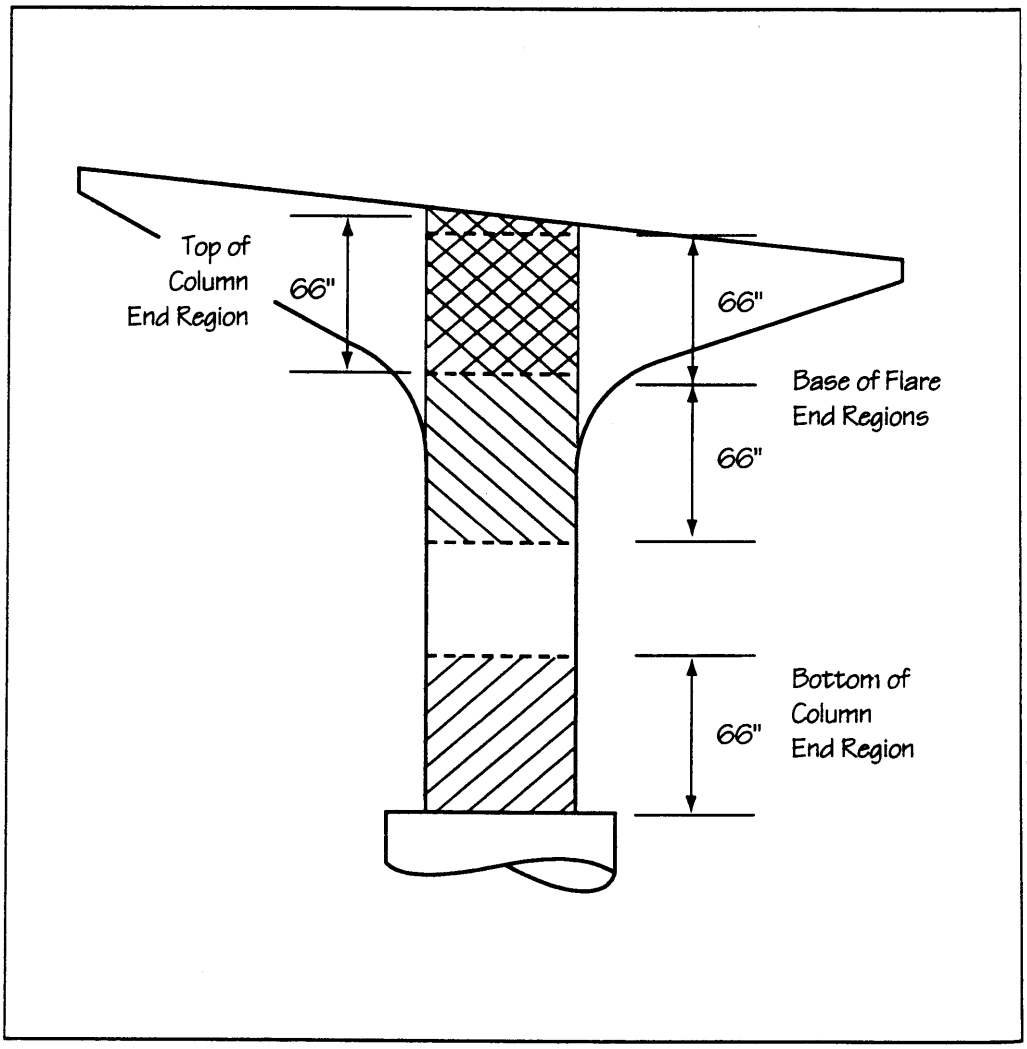

Figure 31 — End Region Geometry

Design Step 10.1.4

Determine Plastic Hinge Confinement Reinforcement [Division I-A, Article 7.6.2(D)]

The core of the column must be confined by special transverse reinforcement over the end regions determined in the previous step. In this case the full height of the column will be used, since very little of the column's length is outside the potential hinge zones.

The total gross sectional area of rectangular hoop reinforcement required is the greater of the areas given by Equations 7-6 and 7-7 in Division I-A.

For transverse reinforcement extending across the long direction of the column

$a := 4 \cdot in$ Maximum spacing of transverse reinforcement in end region

Recall that $b_c = 3.5 \cdot ft$ $d_c = 5.5 \cdot ft$ $ht_c = 38 \cdot in$

$A_g := b_c \cdot d_c$ $A_g = 2772 \cdot in^2$ Gross area of column

Also the area of the column core is $A_c = 2356 \cdot in^2$

$$At_{sh} := 0.30 \cdot a \cdot ht_c \cdot \left(\frac{f_c}{f_{yh}}\right) \cdot \left(\frac{A_g}{A_c} - 1\right)$$ Division I-A Eqn (7-6)

$At_{sh} = 0.537 \cdot in^2$

$$At_{sh} := 0.12 \cdot a \cdot ht_c \cdot \frac{f_c}{f_{yh}}$$ Division I-A Eqn (7-7)

$At_{sh} = 1.22 \cdot in^2$ Controls

Design Step 10.1.4 (continued)

If 4 #5 bars are used, then

$A_s := 1.24 \cdot in^2$ Say okay

For transverse reinforcement extending across the short dimension of the column

Recall that $hl_c = 62 \cdot in$

$$Al_{sh} := 0.30 \cdot a \cdot hl_c \cdot \left(\frac{f_c}{f_{yh}}\right) \cdot \left(\frac{A_g}{A_c} - 1\right)$$ Division I-A Eqn (7-6)

$Al_{sh} = 0.88 \cdot in^2$

$$Al_{sh} := 0.12 \cdot a \cdot hl_c \cdot \frac{f_c}{f_{yh}}$$ Division I-A Eqn (7-7)

$Al_{sh} = 1.98 \cdot in^2$ Controls

If 6 #5 bars are used, then

$A_s := 1.86 \cdot in^2$ Even though this is less than the controlling value, say okay

The reason for using a slightly smaller value is as follows: The provided area is equal to 94 percent of the required area, and plastic hinging was not predicted to occur under the design earthquake. Thus, large inelastic demands that might cause buckling of the longitudinal bars and damage to the core concrete are unlikely to be experienced.

So, use 4 #5 bars extending in the long direction, and 6 #5 bars in the short direction. Space these at 4 inches on center throughout the height of the column.

Design Step 10.1.5

Summary of Column Reinforcement

The reinforcement of the column is summarized in Figure 32.

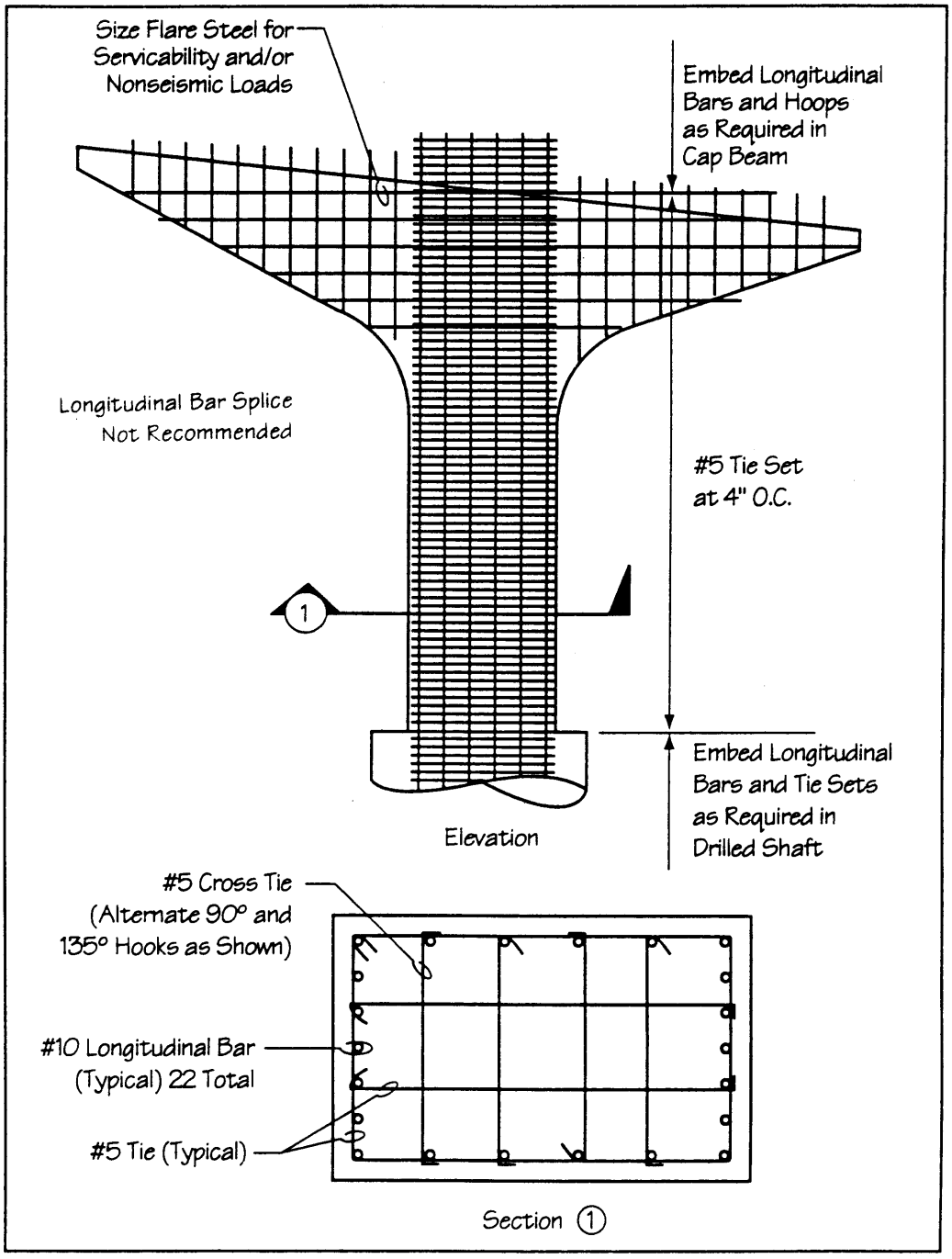

Figure 32 — Column Reinforcement

Design Step 10.2 **Connection Design**

Design Step 10.2.1 Longitudinal Linkage

Not applicable.

Design Step 10.2.2 Hold Downs

Not applicable.

Design Step 10.2.3 Connection of Column to Cap Beam
[Division I-A, Article 7.6.4]

Not addressed in this example.

Design Step 10.2.4 Connection of Column to Drilled Shaft
[Division I, Article 8.25 and Division I-A, Article 7.6.4]

The connection of the column to the drilled shaft can be based on either the plastic hinging forces or the modified elastic forces, according to Article 7.2.5(C). The longitudinal steel shall be anchored to develop 1.25 f_y to account for potential overstrength of the steel and cyclic effects. Additionally, the transverse reinforcement shall be extended a distance of one-half the maximum column dimension into the shaft, but not less than 15 inches.

In this section, the development of the longitudinal bars and the detailing of the transverse steel will be addressed.

The basic data for the drilled shaft are discussed first.

The shaft is 8 feet in diameter, in part to accommodate any misalignment that may occur during construction. Additionally, the cover used with a drilled shaft should be more generous than that used with other elements in order to allow for irregularities in the side walls. The Washington State Department of Transportation (WSDOT 1995) uses a minimum of 6 inches.

For this example use a cover of 6 inches.

WSDOT also requires the use of a concrete strength reduced from that specified, 0.6 f'_c.

Design Step 10.2.4 (continued)

In this example, assume a strength of 4000 psi in the shaft. Thus, use 2400 psi for the concrete strength used in design.

The straight development length of a #10 bar per Division I, Article 8.25, without the additional requirements of Division I-A, is as follows.

Basic data are

$f_c := 0.6 \cdot 4000$ Concrete compressive strength in shaft

$f_c = 2400$ psi

$A_b := 1.27$ Area of #10 bar

$d_b := 1.27$ Diameter of #10 bar

$f_y := 60000$ Yield stress in psi

Basic development length equation

$$L_{db} := 0.04 \cdot A_b \cdot \frac{f_y}{\sqrt{f_c}} \cdot in \qquad L_{db} = 62.2 \cdot in$$

$0.0004 \cdot d_b \cdot f_y \cdot in = 30.5 \cdot in$ Does not control

Modify length for probable steel yield stress, 1.25 f_y
(Division I-A, Article 7.6.4)

$L_d := 1.25 \cdot L_{db}$

$L_d = 77.8 \cdot in$

This is the development length required for the #10 bars. However, the column bars must effectively transfer their tension forces to the longitudinal bars of the drilled shaft. In essence, the arrangement of bars forms a noncontact splice. The geometry of the bars is shown in Figure 33. The worst-case area for tension force transfer is between the shaft bars and the column bars at

Design Step 10.2.4 (continued)

the middle of the long side. The center-to-center distance between these bars is shown as dimension A in the figure. In order to provide effective force transfer between these bars, add length A to the development length to determine the full splice length. Figure 34 illustrates conceptually why this procedure is necessary.

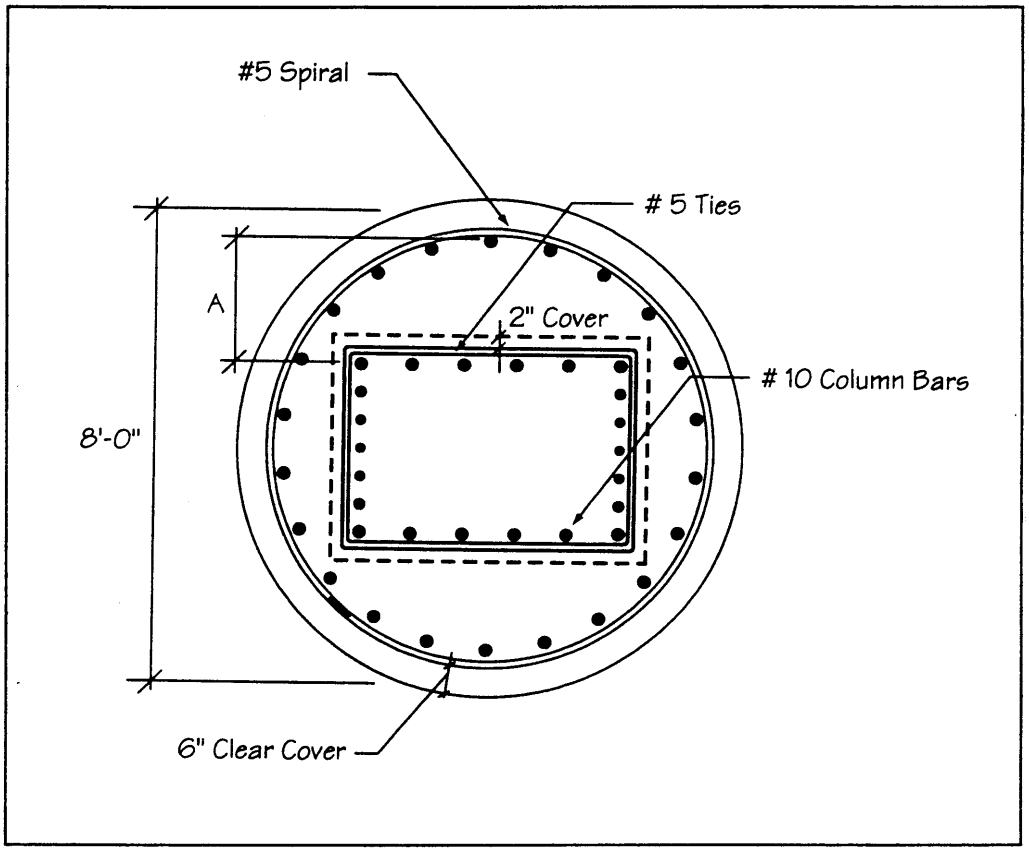

Figure 33 — Cross Section of Drilled Shaft and Column Steel

Design Step 10.2.4 (continued)

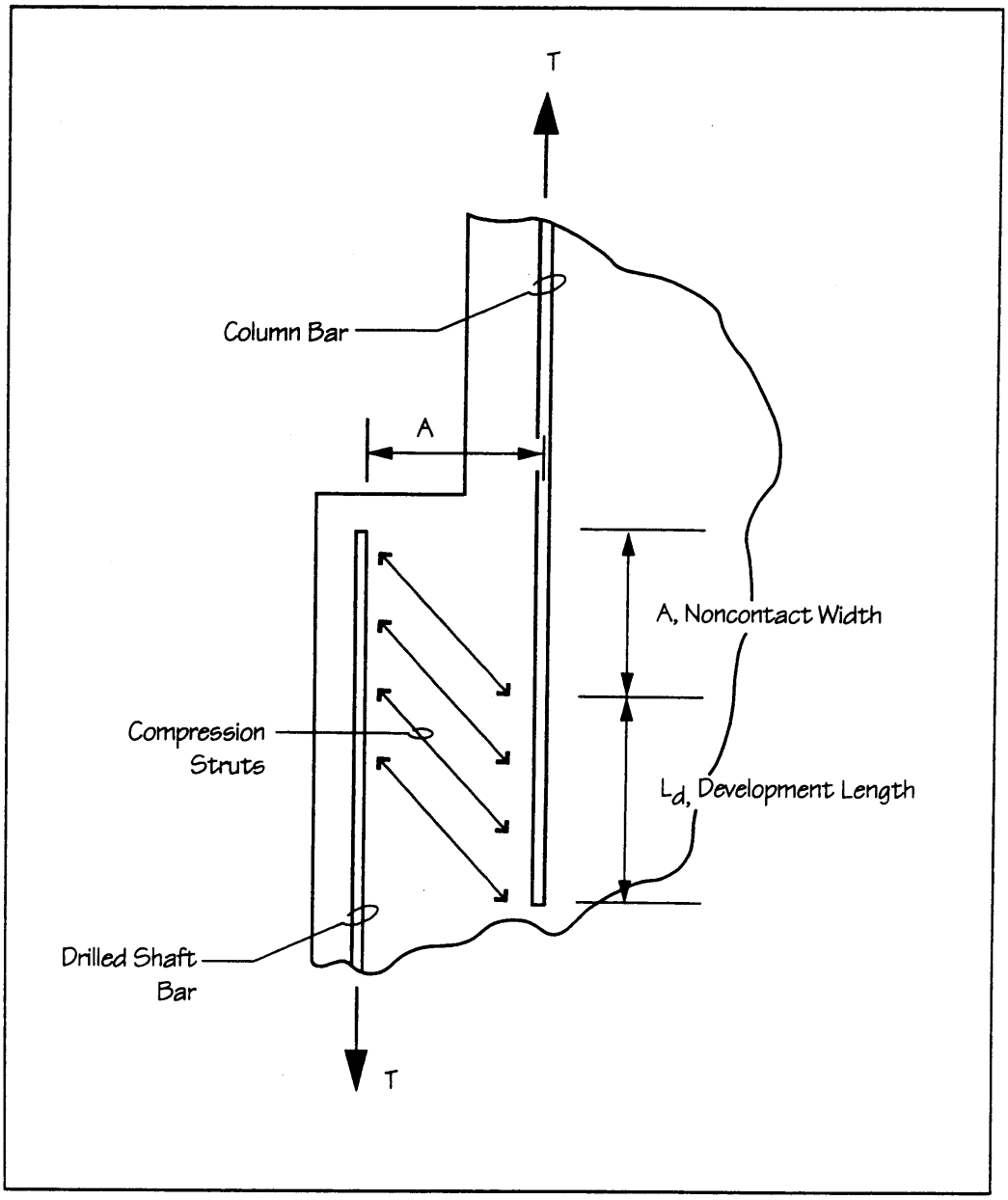

Figure 34 — Noncontact Splice Behavior

Determine the distance A.

$$A := \frac{8}{2}\cdot ft - 6\cdot in - 0.625\cdot in - \frac{1.0}{2}\cdot in - \frac{3.5}{2}\cdot ft - 2\cdot in - 0.625\cdot in - \frac{1.27}{2}\cdot in$$

Design Step 10.2.4 (continued)

These dimensions account for

- the column radius
- the shaft cover
- the shaft spiral
- half the diameter of the shaft bars
- half the column width
- the column cover
- the column ties
- half the diameter of the column bars

$A = 17 \cdot in$

Thus add this 17 inches to the development length to obtain the full splice length.

$L_{splice} := L_d + A$ $\qquad L_{splice} = 7.9 \cdot ft$

Use a splice length of 8 feet, and continue the column hoops 3 feet into the drilled shaft. See Figure 35.

Design Step 10.2.4 (continued)

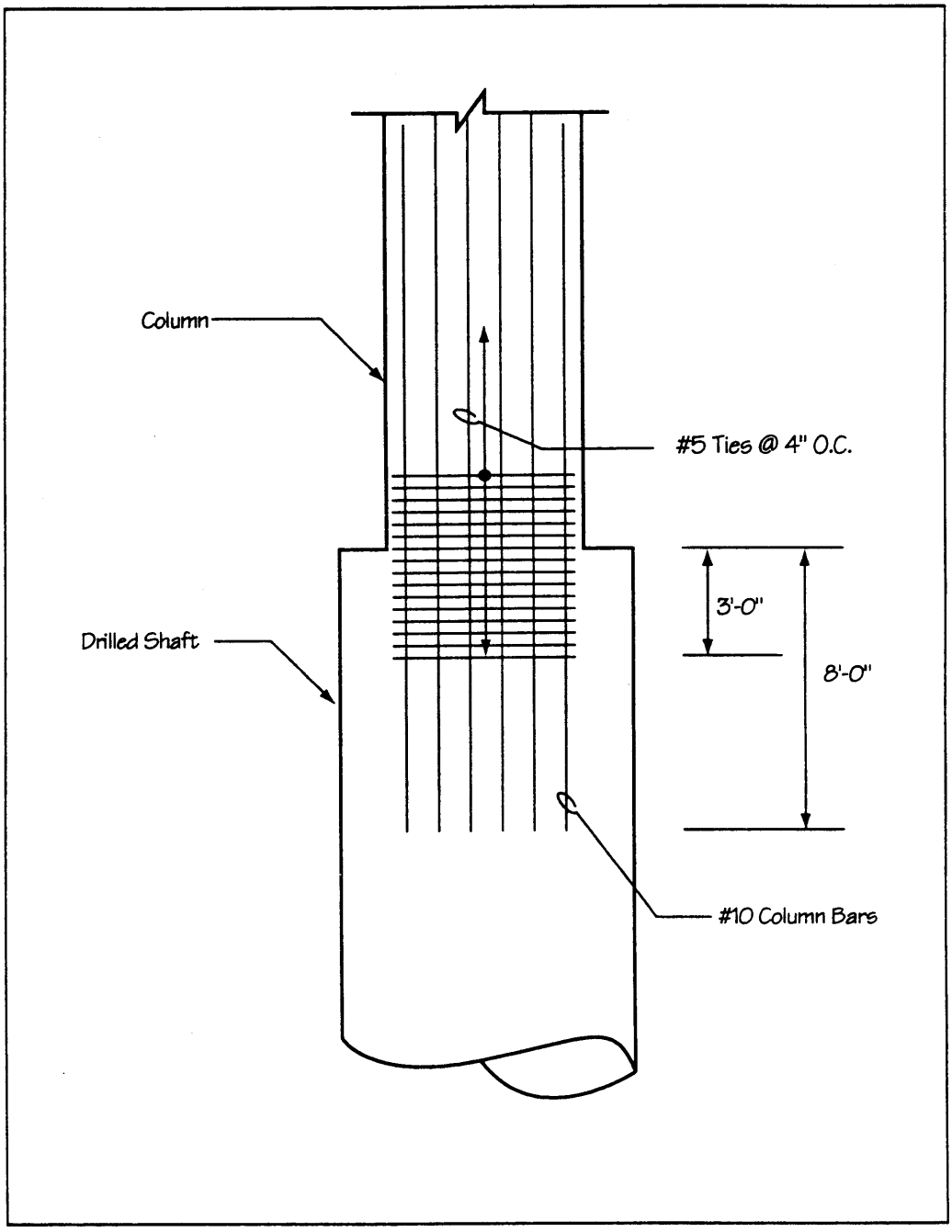

Figure 35 — Column-to-Drilled Shaft Connection

DESIGN STEP 11

DESIGN FOUNDATIONS
[Division I-A, Article 7.4.2]

In this design example, only the reinforcement in the drilled shafts will be sized.

Design Step 11.1

Design Drilled Shaft (Pier No. 1)
[Division I-A, Article 7.4.2]

Design Step 11.1.1

Longitudinal Steel

The design flexural forces for the drilled shaft are either the forces developed by plastic hinging at the base of the column or the elastic modified design forces (determined using R = 1 for the seismic forces), whichever is smaller.

In this example, the elastic modified forces are smaller, and thus the flexural steel in the drilled shaft will be based on them. The philosophy of this design is to provide for the elastic modified forces, since they are generally smaller in all cases. Because shear failure can result in the loss of axial load carrying capacity, the transverse steel is sized to carry the plastic hinging forces, even though it is unlikely that they will be developed. Such an approach provides fail safe lateral strength in the case that an actual earthquake is larger than that designed for.

Since the minimum steel provisions for columns controlled the amount of steel used in the column, minimum steel may also govern for the drilled shaft. In this case the minimum specified by FHWA (1988), 0.5 percent, will be used. Then the maximum elastic moments will be checked against the strength corresponding to this steel content.

Recall the geometry and material strengths from Design Step 10.2.4.

$f_c := 0.6 \cdot 4000 \cdot psi$ Concrete strength in shaft

$d_{sh} := 8 \cdot ft$ Diameter of shaft

$c := 6 \cdot in$ Clear cover

The controlling design forces for the shaft are listed in Table 36, and are repeated below.

Design Step 11.1.1 (continued)

For load case LC1

$Pu_1 := 1315 \cdot kip$ Axial force at top of shaft

$Mt_1 := 3043 \cdot kip \cdot ft$ Maximum transverse moment in shaft (22 feet deep)

$Ml_1 := 6052 \cdot kip \cdot ft$ Maximum longitudinal moment in shaft (22 feet deep)

$Mr_1 := \sqrt{Mt_1^2 + Ml_1^2}$ Resultant moment

$Mr_1 = 6774 \cdot kip \cdot ft$

For load case LC2

$Pu_2 := 1338 \cdot kip$ Axial force at top of shaft

$Mt_2 := 5515 \cdot kip \cdot ft$ Maximum transverse moment in shaft (22 feet deep)

$Ml_2 := 3666 \cdot kip \cdot ft$ Maximum longitudinal moment in shaft (22 feet deep)

$Mr_2 := \sqrt{Mt_2^2 + Ml_2^2}$ Resultant moment

$Mr_2 = 6622 \cdot kip \cdot ft$

Because the maximum moment occurs 22 feet down into the shaft, the axial force present at that level may be less than that at the surface. Therefore, neglect the axial force due to the shaft itself in the calculation of the flexural capacity. The ϕ factor used for the design should be based on the same criteria as the column.

$$A_g := \frac{(8 \cdot ft)^2 \cdot \pi}{4} \qquad A_g = 50.3 \cdot ft^2$$

Design Step 11.1.1 (continued)

$$\sigma_u := \frac{Pu_2}{A_g} \qquad \sigma_u = 185 \cdot psi$$

Per Division I-A, Article 7.6.2(B), $\phi = 0.5$ when the maximum axial stress exceeds $0.2 * f'_c$, and varies linearly from 0.5 to 0.9 for stresses less than $0.2 * f'_c$. See Figure 26.

$$f_c := 0.6 \cdot 4000 \cdot psi \qquad 0.2 \cdot f_c = 480 \cdot psi$$

Because the applied axial force is less than 480 psi, the value of ϕ is greater than 0.5.

$$\phi := 0.9 - \frac{\sigma_u}{0.2 \cdot f_c} \cdot (0.9 - 0.5) \qquad \phi = 0.75$$

Using the value of ϕ just determined, the required forces for the column design can be calculated as follows.

For LC1

$\frac{Pu_1}{\phi} = 1763 \cdot kip$ Required axial strength

$\frac{Mr_1}{\phi} = 9081 \cdot ft \cdot kip$ Required flexural strength

For LC2

$\frac{Pu_2}{\phi} = 1794 \cdot kip$ Required axial strength

$\frac{Mr_2}{\phi} = 8878 \cdot ft \cdot kip$ Required flexural strength

The interaction diagram for the drilled shaft with 30 #10 bars (0.53 percent steel) is shown in Figure 36. Also shown on the plot are the load cases LC1

Design Step 11.1.1 (continued)

and LC2 , adjusted for the appropriate ϕ factor. As discussed in Design Step 7, the interaction is plotted for a ϕ of unity and the loads are divided by ϕ to obtain required strengths.

Use 30 #10 bars spaced evenly on a diameter that produces 6 inches of clear cover to a #5 spiral.

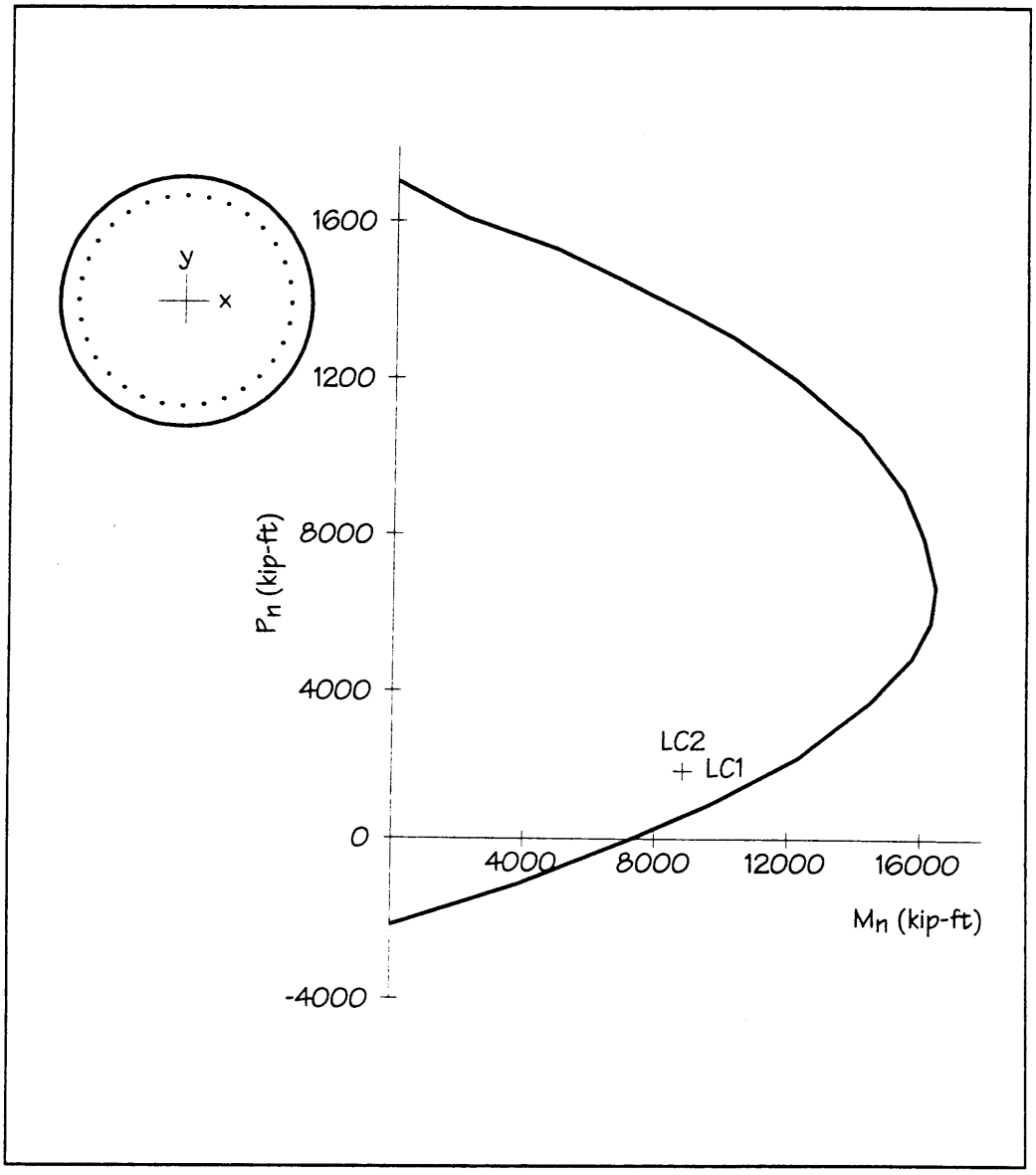

Figure 36 — Interaction Diagram for Drilled Shaft

Design Step 11.1.2

Transverse Steel
[Division I, Section 8.18.2 and Division I-A, Article 7.6.2]

For this bridge, plastic hinging is unlikely to occur during the design earthquake ground motion. Since this is the case, the shear strength design of the drilled shaft will be based on the shear determined for the column by assuming that plastic hinges form at the top of the column (or flare) and in the column just above the transition to the drilled shaft.

As discussed in Design Step 7.4.2, this shear, which corresponds to an assumed plastic hinging mechanism, is a conservative upper-bound to the actual mechanism shear.

The assumed mechanism shear is largest at the top of the shaft; thus some distribution of the shear down the length of the shaft should be used to design the shear reinforcement along the shaft. The most conservative distribution is a constant shear. However, assuming a constant shear may result in too much transverse steel and an overly conservative design. Alternatively, the elastic distribution of shear forces can be used, since they represent the next best estimate of the actual distribution.

Assume that the shear distribution in the drilled shaft at mechanism is the same as that in the shaft under fully elastic response.

a) Required Shear Strength

$f_c := 0.6 \cdot 4000 \cdot psi$ Concrete strength

$f_{yh} := 60 \cdot \frac{kip}{in^2}$ Yield stress of spiral reinforcing

$b_w := 96 \cdot in$ Outside diameter of shaft

Diameter of concrete core, measured to the outside of the transverse spiral reinforcement. Assume a 6-inch clear cover.

$d_{core} := b_w - 2 \cdot (6 \cdot in)$ $d_{core} = 84 \cdot in$

Design Step 11.1.2 (continued)

An upper-bound for the plastic hinging shear was given in Design Step 8.1(c) for the column. The forces were expressed as shears in the transverse and longitudinal directions; these are repeated below.

$Vp_t := 1166 \cdot kip$ Transverse hinging shear

$Vp_l := 706 \cdot kip$ Longitudinal hinging shear

$Vr := \sqrt{Vp_t^2 + Vp_l^2}$ Resultant hinging shear

$Vr = 1363 \cdot kip$

As discussed above, the maximum shear at the top of the shaft will be used to anchor a shear envelope that is based on the elastic seismic shear distribution. Tables 11 and 21 contain the elastic shears in the drilled shaft for the radial and chord earthquake ground motions. These shears have been repeated in Table 39 and they have been combined in the LC1 and LC2 directional load cases. The table lists the resultant shear force in the shaft. Note also that the dead load is not included, because only the earthquake shear distribution is of interest here. The two load cases, as can be seen in Table 11A, give almost identical resultant shear results, and these shear values have been plotted in Figure 37. In the figure, the elastic shear is shown "stepped," as the computer model reports the shear. This distribution is then scaled to produce a maximum of 1363 kips at the top of the shaft and smoothed to indicate an actual distribution.

Design Step 11.1.2 (continued)

Table 39
Maximum Elastic Shear Forces in Shaft

Depth (ft)	V_{tr} (kips)	V_{lr} (kips)	V_{tc} (kips)	V_{lc} (kips)	V_{R1} (kips)	V_{R2} (kips)
2	272	113	96	310	387.1	364.6
6	256	107	91	293	365.9	343.9
10	217	91	78	249	311.2	292
14	161	68	60	187	234	217.8
18	97	42	39	115	144.6	132.9
22	29	14	17	40	51.13	42.88
26	35	13	4	32	38.72	42.68
30	93	36	23	97	119.2	119.2
34	140	56	39	151	186.3	182.4
38	175	70	51	190	235	228.8
42	195	79	59	213	264.3	256.2
46	197	80	60	217	268.8	259.4
50	181	74	56	200	248.1	238.9
54	145	59	45	160	198.5	191.2
58	85	35	27	94	116.9	112.5
60	0	0	0	0	0	0

V_{tr} = Shear in Transverse Direction for Radial Earthquake

V_{lr} = Shear in Longitudinal Direction for Radial Earthquake

V_{tc} = Shear in Transverse Direction for Chord Earthquake

V_{lc} = Shear in Longitudinal Direction for Chord Earthquake

$$V_{R1} = ((1.0\ V_{lc} + 0.3\ V_{lr})^2 + (1.0\ V_{tc} + 0.3\ V_{tr})^2)^{1/2}$$

$$V_{R2} = ((0.3\ V_{lc} + 1.0\ V_{lr})^2 + (0.3\ V_{tc} + 1.0\ V_{tr})^2)^{1/2}$$

Design Step 11.1.2 (continued)

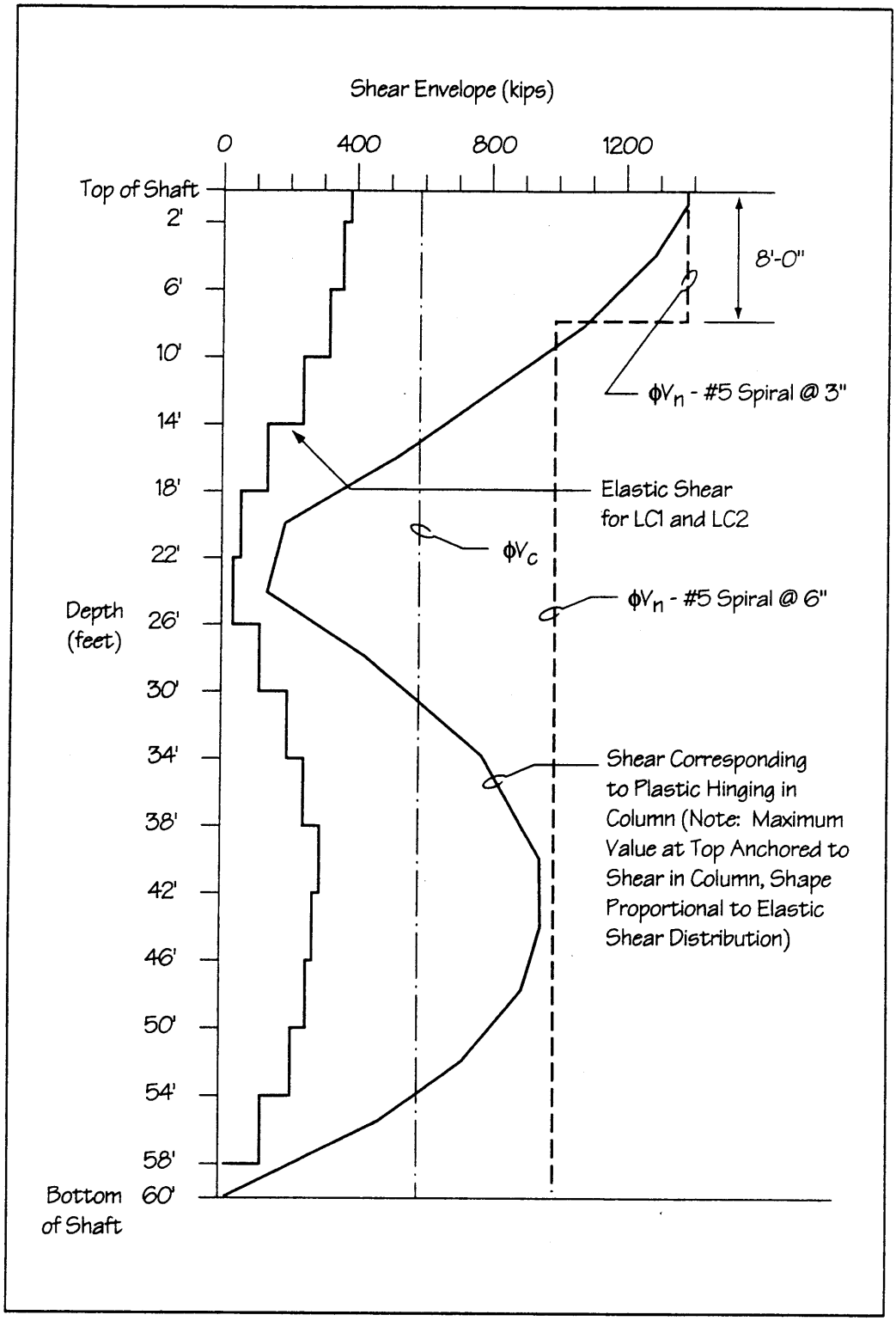

Figure 37 — Shear Envelope (kips)

Design Step 11.1.2 (continued)

The provided shear strength should be determined in accordance with Division I. This is the same procedure as was applied in Design Step 10 for the column.

$\phi := 0.85$

The maximum shear strength required is

$V_n := \frac{Vr}{\phi}$ Division I Eqn (8-46)

$V_n = 1604 \cdot kip$

For computing shear strength of circular sections, d need not be less than the distance from the extreme compression fiber to the centroid of the tension reinforcement in the opposite half of the member. Refer to Figure 38 for the variables.

$d_{core} = 84 \cdot in$ $b_w = 96 \cdot in$

The location of the #10 longitudinal bars from the center of the column is

$r_b := \frac{d_{core}}{2} - 0.625 \cdot in - \frac{1.27}{2} \cdot in$

$r_b = 40.7 \cdot in$

$z_{bar} := \frac{2}{\pi} \cdot r_b$ Centroid of tension side reinforcement (Popov, 1976)

The effective depth d of the circular section is

$d := \frac{b_w}{2} + z_{bar}$ $d = 73.9 \cdot in$

Design Step 11.1.2 (continued)

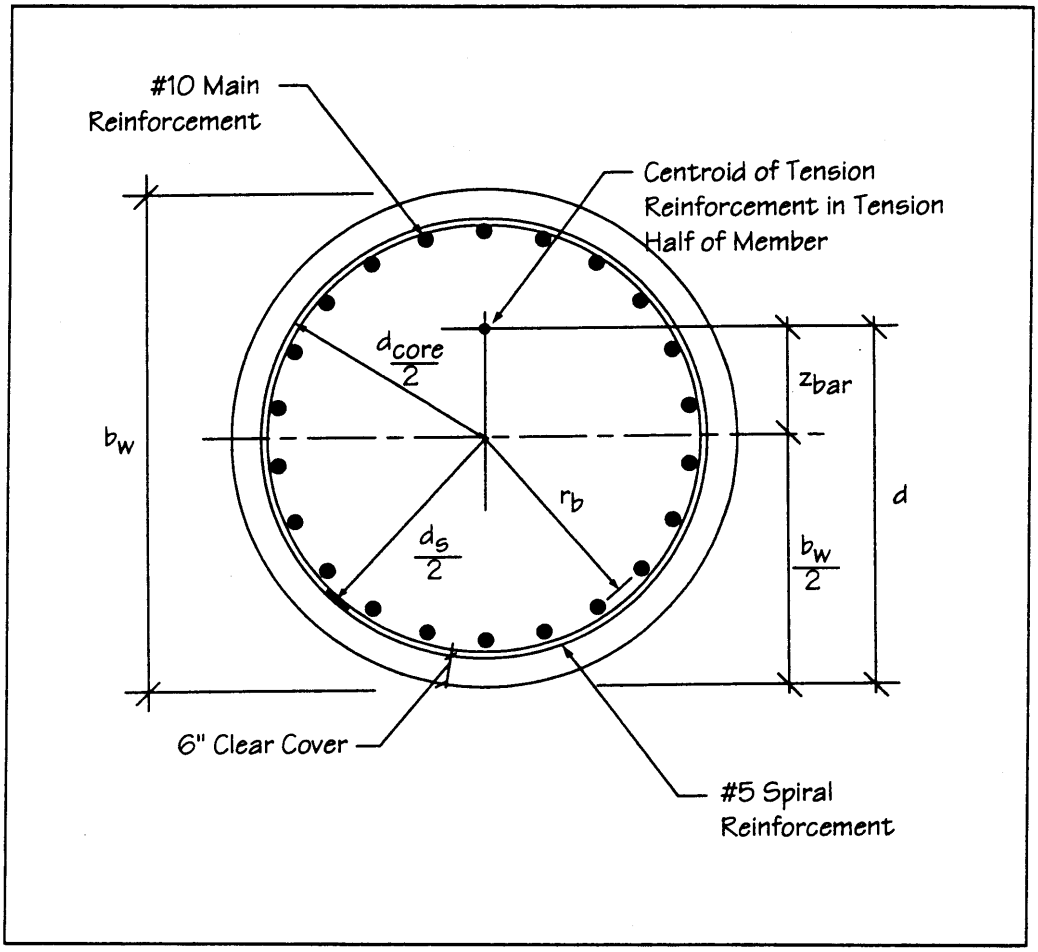

Figure 38 — Key to Column Steel Centroid

The concrete contribution to the shear strength is

$V_c := 2 \cdot \sqrt{f_c} \cdot b_w \cdot d \cdot psi$ Division I Eqn (8-51)

$V_c := 695 \cdot kip$ $\phi \cdot V_c = 591 \cdot kip$

This value is also shown in Figure 37.

Design Step 11.1.2 (continued)

The required shear strength calculated per Division I, Article 8.16.6.3, for the top of the shaft, is

$V_s := V_n - V_c$ Division I Eqn (8-47)

$V_s = 909 \cdot kip$

Try a spiral pitch of 3 inches, which will meet the requirements of Division I, Article 8.18.2.2.3.

$s := 3 \cdot in$

The resulting shear reinforcement is then

$A_v := \frac{V_s}{f_{yh}} \cdot \frac{s}{d}$ Division I Eqn (8-53)

$A_v = 0.61 \cdot in^2$ For two legs of the spiral reinforcement

Use a #5 spiral at a 3-inch pitch.

$A_{v\_provided} := 2 \cdot (0.31 \cdot in^2)$

$A_{v\_provided} = 0.62 \cdot in^2$

Determine a point where the spiral pitch can be increased to say 6 inches. Because the shaft will be placed without vibration over most of its length, a pitch greater than 3 inches is necessary to obtain proper compaction of the concrete. As shown in Figure 35, the column bars are embedded 8 feet into the shaft. This transition provides a reasonable location for changing the pitch of the spiral.

Try a spacing of 6 inches for the spiral, and keep the #5 spiral.

$s := 6 \cdot in$ $A_{v\_provided} = 0.62 \cdot in^2$

Design Step 11.1.2 (continued)

$$V_s := \frac{A_{v\_provided} \cdot f_{yh} \cdot d}{s} \qquad V_s = 458 \cdot kip$$

$$\phi \cdot V_s = 390 \cdot kip$$

Then the total shear strength provided by a #5 at 6-inch spacing

$$V_n := V_c + V_s$$

$$\phi \cdot V_n = 980 \cdot kip$$

This shear strength is represented in Figure 37 by the lower dashed line. As can be seen, the strength is adequate over nearly the entire height. A short section falls outside the strength envelope just below 8 feet. However, the actual shear demand is not known precisely enough to be concerned about this slight discrepancy.

b) *Normal Confinement*

The layout and spacing of the ties must meet the requirements of Article 8.18.2 of Division I. Even though a spiral is used in the drilled shaft, the volumetric ratio of reinforcement specified by Equation (8-63) does not need to be met unless the shaft is designed as a spiral tied column. In this case, the strength reduction factor ϕ is controlled by Division I-A requirements; therefore, the spiral versus tied distinction made in Division I is irrelevant.

Design the ties to meet the requirements of Article 8.18.2.3. A #5 spiral is used with #10 longitudinal bars, and the spacing is 6 inches. Thus the minimums listed in the article are met.

Design Step 11.1.3

Summary of Drilled Shaft Design

The final configuration and reinforcement for the drilled shaft are shown in Figure 39.

Thirty #10 longitudinal bars are used to give a reinforcement ratio of 0.53 percent. The transverse reinforcement is a #5 spiral with a 3-inch pitch over the upper 8 feet of the shaft, and a 6-inch pitch over the lower 52 feet of the shaft.

Design Step 11.1.3 (continued)

The connection of the column to shaft is as shown in Figure 35.

The 3-inch pitch for the spiral, which extends over the upper 8 feet, provides confinement of the splice between the shaft and the column steel, which provides an additional benefit to using a relatively heavy spiral in this zone of the shaft.

The 6-inch pitch over the remaining 52 feet of the drilled shaft might be considered relatively heavy reinforcement. However, the spiral provides the shear strength necessary to resist the full plastic hinging force possible in the column. While this force is a maximum at the top of the shaft, the shear, as seen in Figures 22(a) and 22(b), may still be large even at significant depths down the shaft.

Design Step 11.1.3 (continued)

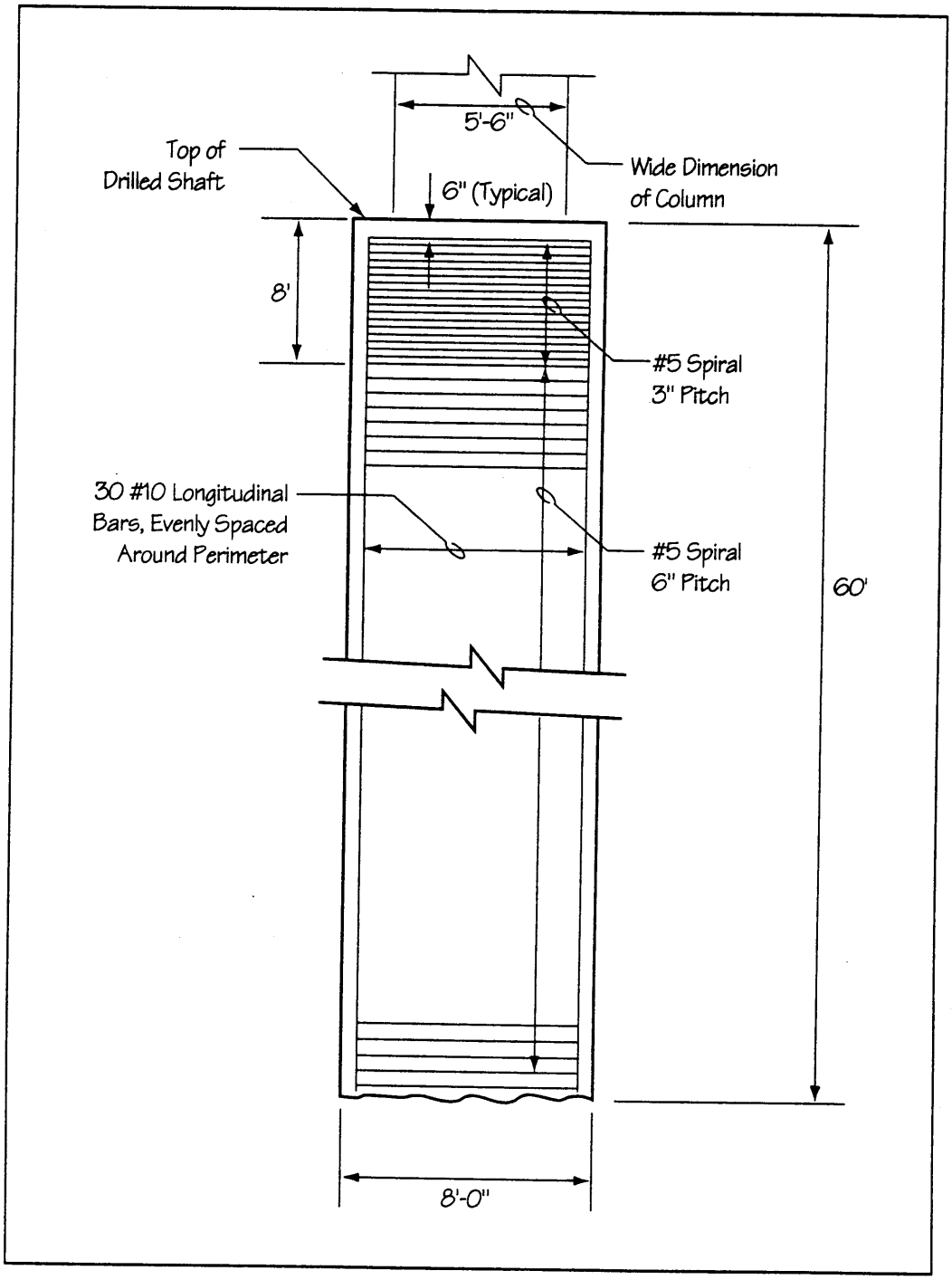

Figure 39 — Drilled Shaft Reinforcement

DESIGN STEP 12

DESIGN ABUTMENTS

In this section, the design of the pipe piles at the abutments will be discussed.

Design Step 12.1

Design Pipe Piles
[Division I-A, Article 7.4.2(C)]

The pipe piles have been considered pinned at their tops, in part to soften the pile systems and prevent them from attracting too much seismic force, and in part to relieve reinforcement congestion that would result in the end diaphragm if a full moment connection were to be used at the top of the pile.

Design Step 12.1.1

Details of End Diaphragm to Pile Connection

A common detail for producing a pinned-top pile is shown in Figure 40. The pipe is embedded beyond the lower reinforcement, but not so far as to restrain the rotation of the top of the pile. Obviously, in a large earthquake, some damage will occur adjacent to the pile at the base of the end diaphragm, although this effect should be limited to minor spalling. The functions of the various components of the detail are described below.

- The pipe is to be filled with concrete over the upper 12 feet of the pile, to prevent buckling of the pipe walls.
- The center bars provide shear transfer integrity into the pipe core concrete. By centering the bars, the moment capacity of the bars is kept to a minimum. The area of these bars must exceed 1 percent of the core area per Division I-A, Article 7.4.2(C). In this case, 4 #5 bars provide this area.
- The center bars and the hoops in the end diaphragm provide resistance to pull-out of the pile in the event of significant uplift.

Design Step 12.1.1 (continued)

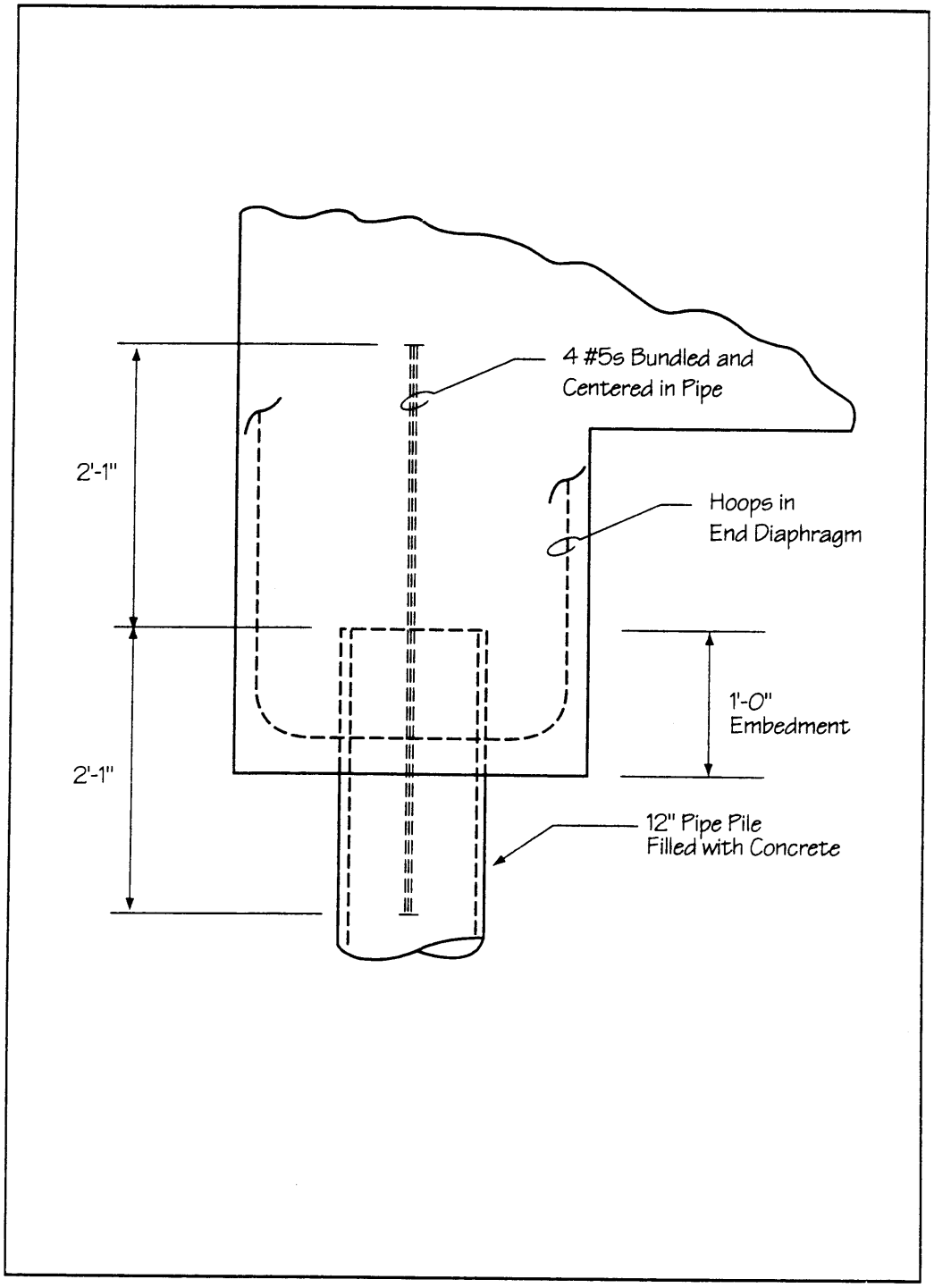

Figure 40 — Detail of Pipe Pile-to-End Diaphragm Connection

Design Step 12.1.1 (continued)

An alternative detail that could potentially be used to produce 'low damage' pin at the bottom of the end diaphragm is shown in Figure 41. The goal of the detail is to provide reliable shear transfer, while simultaneously preventing damage from occurring in the pipe or the diaphragm. The functions of the various components of the detail, in addition to those discussed above, are described below.

- The expansion joint filler wrapped around the pipe allows the lateral movement inevitable in an earthquake to occur without damaging the end diaphragm.
- The L-bars are located in the lower slab of the box girder, and turn down into the end diaphragm to provide a positive load path for longitudinal tension forces.
- The hoops around the top of the pile provide confinement in order to prevent local damage near the top of the pile.

Per Article 7.4.2(C) in Division I-A, the piles should be anchored into the footing sufficiently to develop 1.25 times the longitudinal reinforcement yield strength. Additionally, for this design, which uses 4 #5 bars centered in the pipe, the development length must be increased by 33 percent, due to the bundling of the four bars.

According to Article 8.25.1 of Division I, the basic development length of the #5 bars is

$l_{db} := 15 \cdot in$

Thus, to account for the required increase in steel yield and to account for the reduced effectiveness of bundled bars, the required development length becomes

$l_d := 1.25 \cdot 1.33 \cdot l_{db}$ $\qquad l_d = 25 \cdot in$

Thus, use 25 inches of embedment beyond the end of the pile if the hoops in the end diaphragm can assist in transferring uplift to the main box girder. Or use 25 inches beyond the soffit of box girder if the end diaphragm hoops cannot help transfer uplift.

Design Step 12.1.1 (continued)

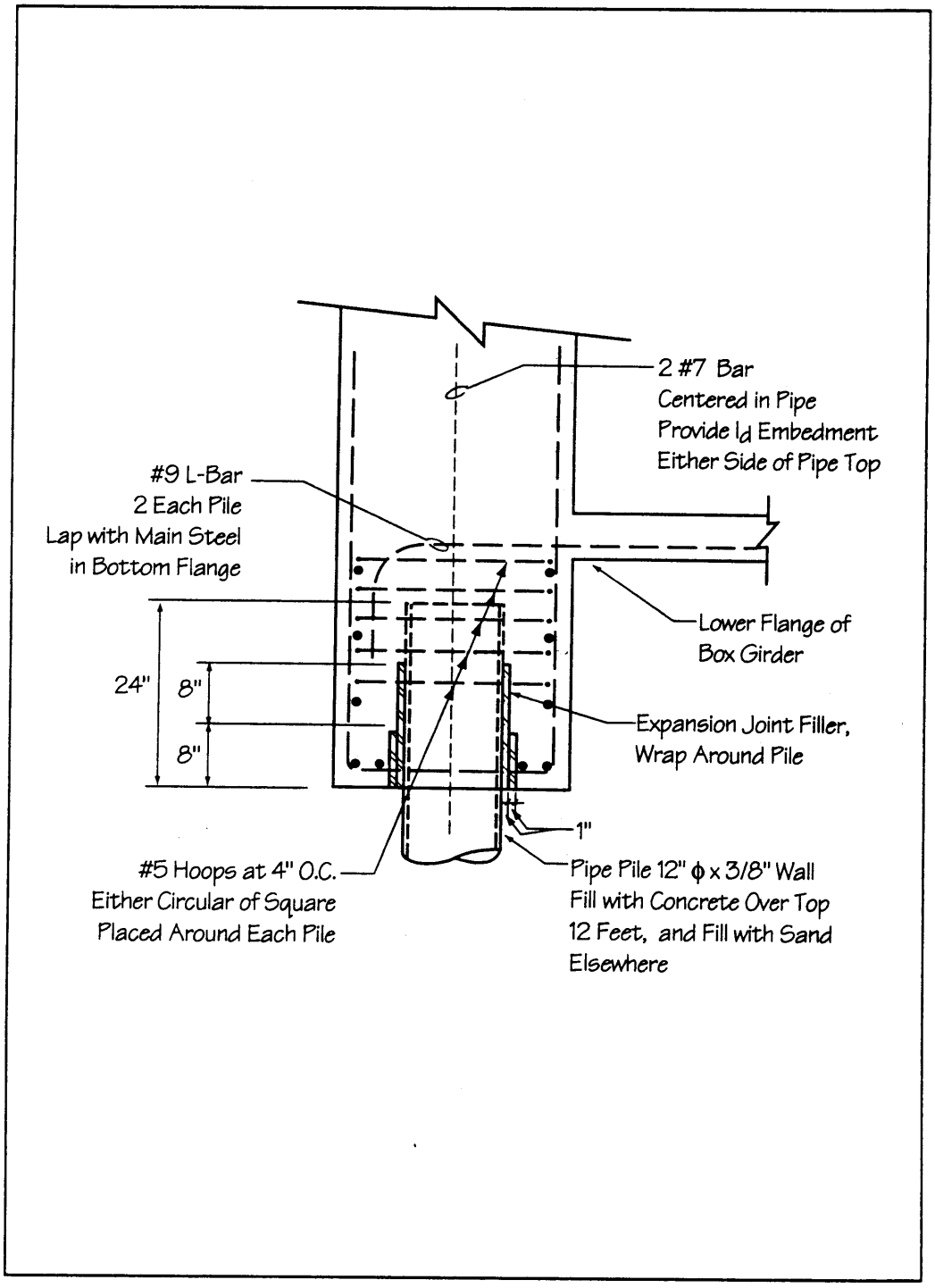

Figure 41 — Detail for Pinning Top of Pile

Design Step 12.1.2

Check of Seismic Forces in Pipe Piles

The maximum force, and hence stress, in the pipe piles should be checked.

The elastic forces induced in the piles for load cases LC1 and LC2 are the controlling design forces, and these forces are listed in Table 35. Inspection of the forces and moments, taking into account their directions, indicates that the lateral forces listed in the table can be considered alone. This means that the moments acting to produce lateral translation of the piles (moment about the vertical axis) is small and can be neglected.

Thus the lateral pile forces listed in Table 35 will be used with the coefficients discussed in Design Step 6.2.2 for the DM7 Method in order to determine the maximum pile forces and stresses. The information given in Figure 13, which is repeated here as Figure 42, will also be used.

The controlling forces from Table 35 are

For LC1

$Fgt_1 := 229 \cdot kip$ Transverse group shear

$Fgl_1 := 351 \cdot kip$ Longitudinal group shear

For LC2

$Fgt_2 := 208 \cdot kip$ Transverse group shear

$Fgl_2 := 374 \cdot kip$ Longitudinal group shear

Design Step 12.1.2 (continued)

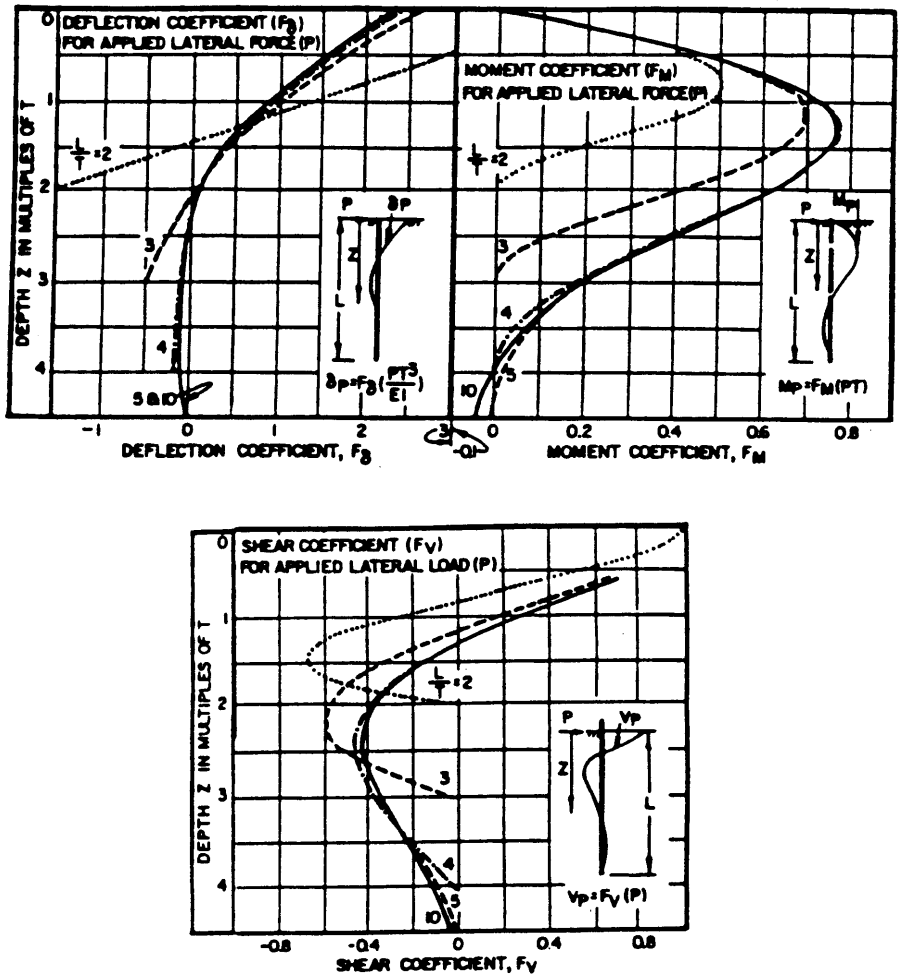

Case I. Flexible Cap or Hinged End Condition

From: NAVFAC DM7.02 (1986)

Figure 42 — Influence Value for Pile with Applied Lateral Load and Moment

From these group forces, the individual pile forces may be calculated simply by dividing by the number of piles.

For LC1

$$Ft_1 := \frac{Fgt_1}{7} \qquad Ft_1 = 32.71 \cdot kip$$

Design Step 12.1.2 (continued)

$$Fl_1 := \frac{Fgl_1}{7} \qquad Fl_1 = 50.14 \cdot kip$$

For LC2

$$Ft_2 := \frac{Fgt_2}{7} \qquad Ft_2 = 29.71 \cdot kip$$

$$Fl_2 := \frac{Fgl_2}{7} \qquad Fl_2 = 53.43 \cdot kip$$

Recall from Design Step 6.2.2 that the pile stiffness, and therefore the internal forces, are a function of the nondimensional parameter, L/T. These relationships are repeated here in the form of influence charts. See Figure 42.

Recall that the length of the pipe piles is 40 feet, and the value of T is different in the longitudinal and transverse directions due to the dependence of the subgrade modulus on pile group effects.

Also recall that

$$L := 40 \cdot ft$$

$$T_{long} := 55.1 \cdot in \qquad \frac{L}{T_{long}} = 8.7$$

$$T_{trans} := 59.2 \cdot in \qquad \frac{L}{T_{trans}} = 8.1$$

From Figure 42 for the case of applied pile shear, the moment coefficient for the two directions is given below, as taken from the upper right figure.

$$F_m := 0.77$$

This is the coefficient for the maximum moment in the pile, which occurs at a depth of about 1.25 times T. It is essentially the same for both directions.

Design Step 12.1.2 (continued)

The maximum moments in the piles can be found using the equation given in the moment figure.

These moments will be determined in each of the two basic directions, and then the resultant will be found to check the stress.

For LC1

$Ml_1 := F_m \cdot Fl_1 \cdot T_{long}$

$Mt_1 := F_m \cdot Ft_1 \cdot T_{trans}$

For LC2

$Ml_2 := F_m \cdot Fl_2 \cdot T_{long}$

$Mt_2 := F_m \cdot Ft_2 \cdot T_{trans}$

Determine the resultant moments for the two load cases.

$Mr_1 := \sqrt{Ml_1^2 + Mt_1^2}$

$Mr_2 := \sqrt{Ml_2^2 + Mt_2^2}$

$Mr_1 = 2598 \cdot kip \cdot in$

$Mr_2 = 2641 \cdot kip \cdot in$

These moments can then be used to calculate the maximum stress in the pipe pile. Given the section modulus and/or plastic section modulus. Note that the pipe alone is used to calculate the stress; the concrete fill is completely discounted. This is conservative, because the concrete was counted on in terms of stiffness, but is not used for strength.

For a 12-inch standard weight (3/8-inch-thick wall) pipe

$S := 43.8 \cdot in^3$ $Z := 57.4 \cdot in^3$

For this type of pipe, the elastic bending stress is

$fe_1 := \frac{Mr_1}{S}$ $fe_1 = 59.315 \cdot ksi$

$fe_2 := \frac{Mr_2}{S}$ $fe_2 = 60.289 \cdot ksi$

Design Step 12.1.2 (continued)

The bending stress based on the plastic section modulus is

$$fp_1 := \frac{Mr_1}{Z} \qquad fp_1 = 45.262 \cdot ksi$$

$$fp_2 := \frac{Mr_2}{Z} \qquad fp_2 = 46.005 \cdot ksi$$

Comparison of the two stress calculations for the two load cases indicates that a Grade 50 pipe with a yield stress of 50 ksi would be expected to experience some yielding (as indicated by fe being greater than 50 ksi), but a full plastic hinge will not have formed (as indicated by fp being less than 50 ksi). These calculations are based on the bending stress alone. The dead load axial stress is approximately 3 ksi, which when added to the bending stresses does not change the conclusions.

Therefore, some inelastic action will be expected. However, the intensity of inelastic behavior should be relatively low, because full plasticity is not expected and the distributed support of the soil against the pipe will spread the yielding over a significant length of pile.

A 12-inch-nominal-diameter pipe with 3/8-inch wall thickness made of Grade 50 steel will be adequate.

DESIGN STEP 13 — DESIGN SETTLEMENT SLABS

Not applicable.

DESIGN STEP 14 — REVISE STRUCTURE

Not required.

DESIGN STEP 15 SEISMIC DETAILS

DETAILS SUMMARY

Several details emphasizing the seismic issues discussed in this example are included within this section. Many of the sketches shown in this section have been introduced and discussed in greater detail in the previous design sections. The details are repeated here as a summary.

Column Reinforcement Details (Figure 43)

The vertical reinforcement is based on the minimum one percent steel requirements. The transverse reinforcement is based on the necessity of providing sufficient strength to sustain a conservative plastic hinging shear, even though significant inelastic action is not expected. This approach is rational, and the intention is to prevent brittle shear failure from ever occurring in the column. Plastic hinge zone confinement is extended over the entire height of the column, since the possibility of hinging exists over a substantial length of the column.

Column to Drilled Shaft Connection (Figure 44)

The shaft has intentionally been made larger in diameter than the column in order to allow the column reinforcement cage to pass inside the shaft cage, even if the shaft, after construction, is not centered under the superstructure. Such an allowance accounts for actual construction practice and tolerances.

The column longitudinal reinforcement is extended into the upper portion of the drilled shaft. The depth of embedment accounts both for development of the bars and the 'noncontact' configuration of the column and shaft bars. The column longitudinal steel should not be lap spliced above the connection with the drilled shaft. The transverse column steel also passes into the shaft to provide joint confinement.

Drilled Shaft Reinforcement Details (Figure 45)

The longitudinal reinforcement meets the minimum specification recommended by FHWA, 0.5 percent. The transverse steel is sized to carry the same plastic hinging shear that the column can carry. This shear demand is assumed proportional to the elastic shear distribution. Consequently, heavy spiral reinforcement is required only over the upper 8 feet of the shaft. This spiral also provides confinement for the column longitudinal steel anchorage.

DETAILS SUMMARY (continued)

The shaft spiral is opened to a 6-inch pitch below the 8-foot depth, and this pitch extends to the base of the shaft. The 6-inch pitch is considered a minimum, because the shaft concrete will likely be placed without significant external vibration for compaction. Thus, the wider spiral allows better flow of the concrete from the center of the shaft to the exterior.

Welded Splice Spiral Details (Figures 46)

The spiral in the shaft will likely be spliced either within the 6-inch pitch region or at the junction between the 3- and 6-inch pitches. This figure provides a detail for making a welded connection between the two spirals.

Pipe Pile to End Diaphragm Details (Figures 47 and 48)

The pipe piles at the abutments should behave essentially as pinned connections. The first figure provides a conventional detail for providing a pinned connection. The center of the pile is filled with concrete to prevent wall buckling of the pipe, and reinforcement, which is bundled in the center of the pipe, provides the necessary uplift capacity. The bars are centered to minimize the flexural restraint that will develop under lateral deflection of the top of the pile. Some local crushing and spalling of the end diaphragm concrete should be expected in a large earthquake.

Figure 48 provides a conceptual detail of a pinned connection that can withstand significantly larger displacement than is expected for this design. The tops of the piles are wrapped with expansion joint filler material to suppress the local concrete damage that can otherwise occur.

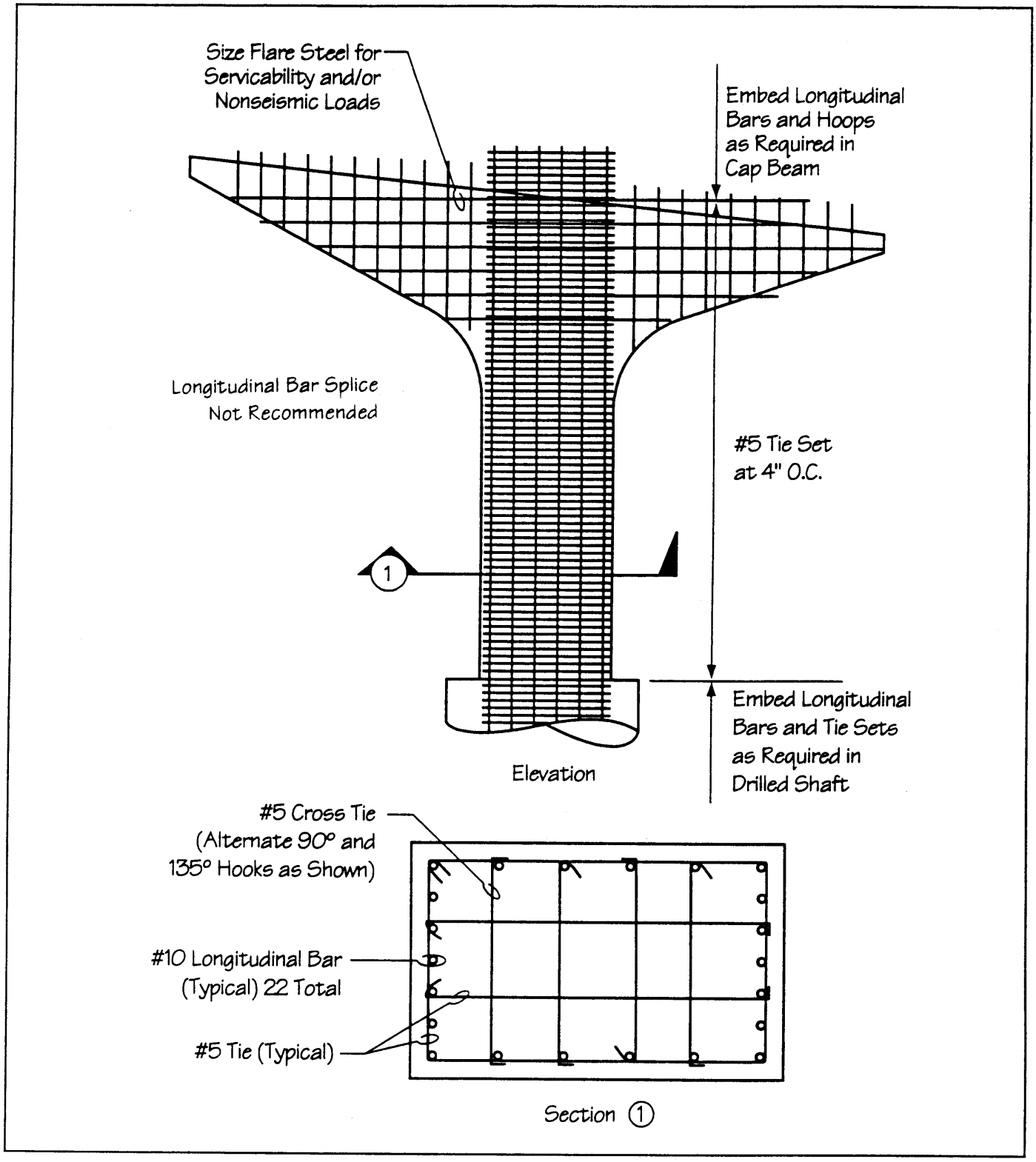

Figure 43 — Column Reinforcement Details

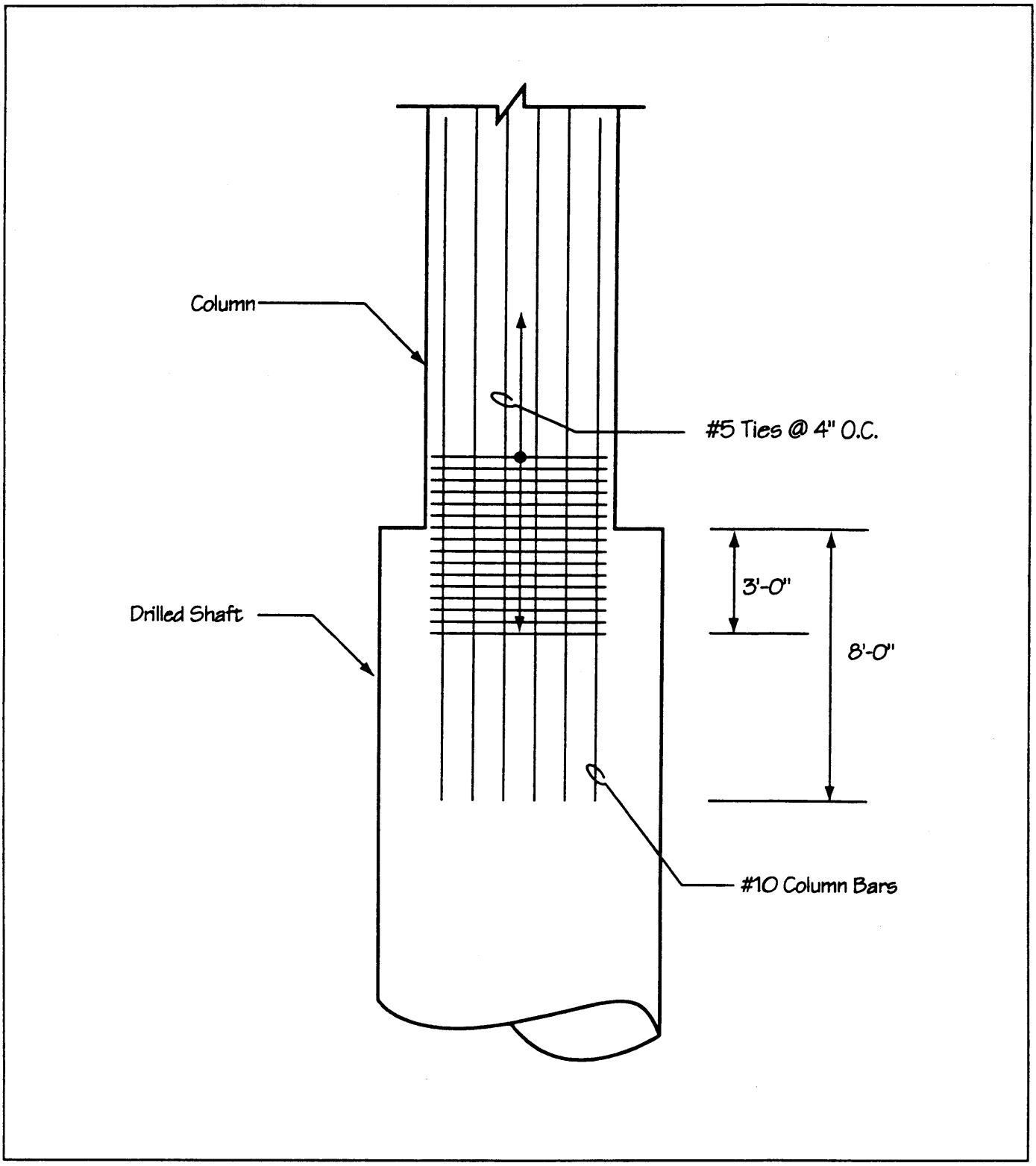

Figure 44 — Column to Drilled Shaft Connection

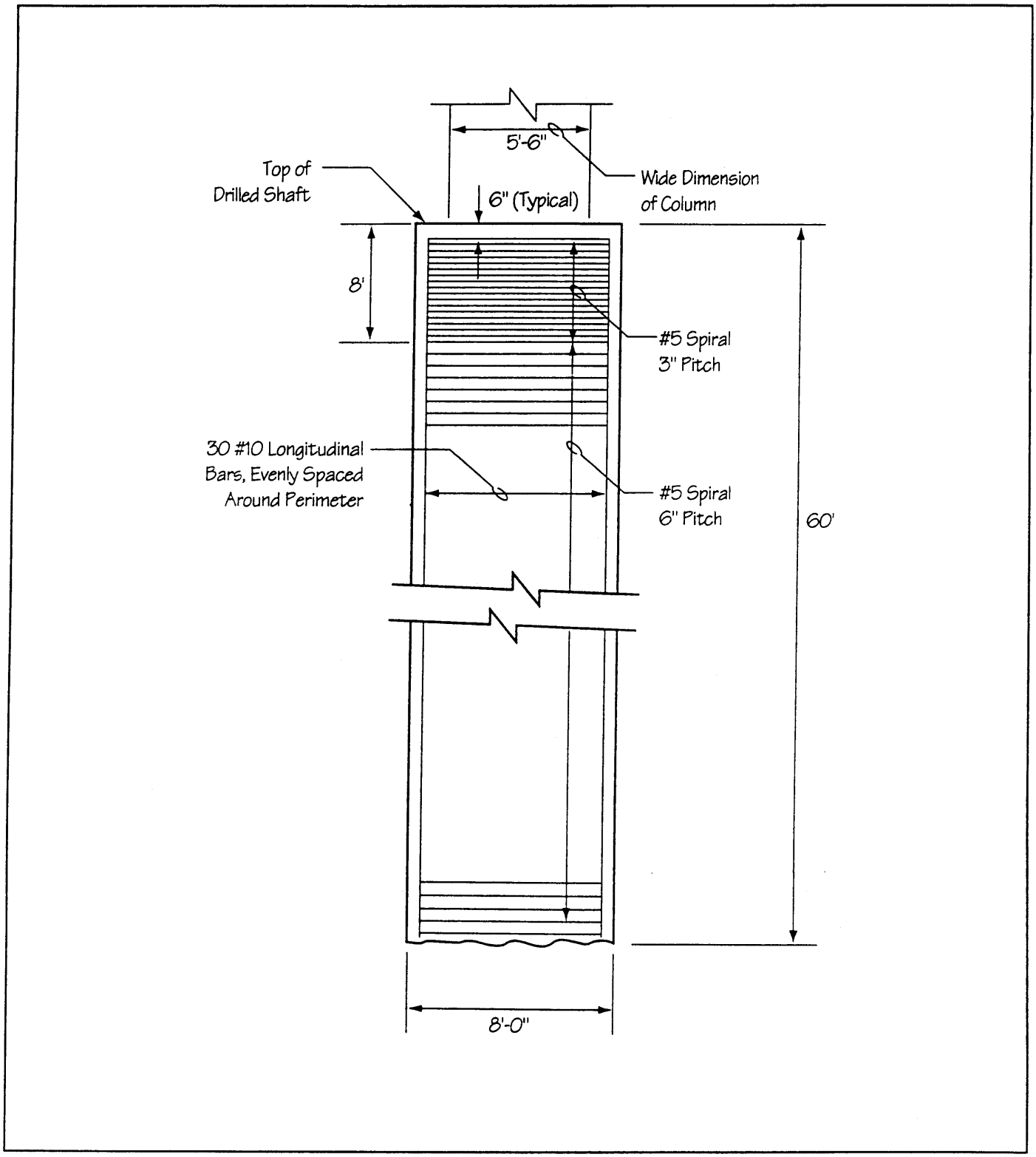

Figure 45 — Drilled Shaft Reinforcement Details

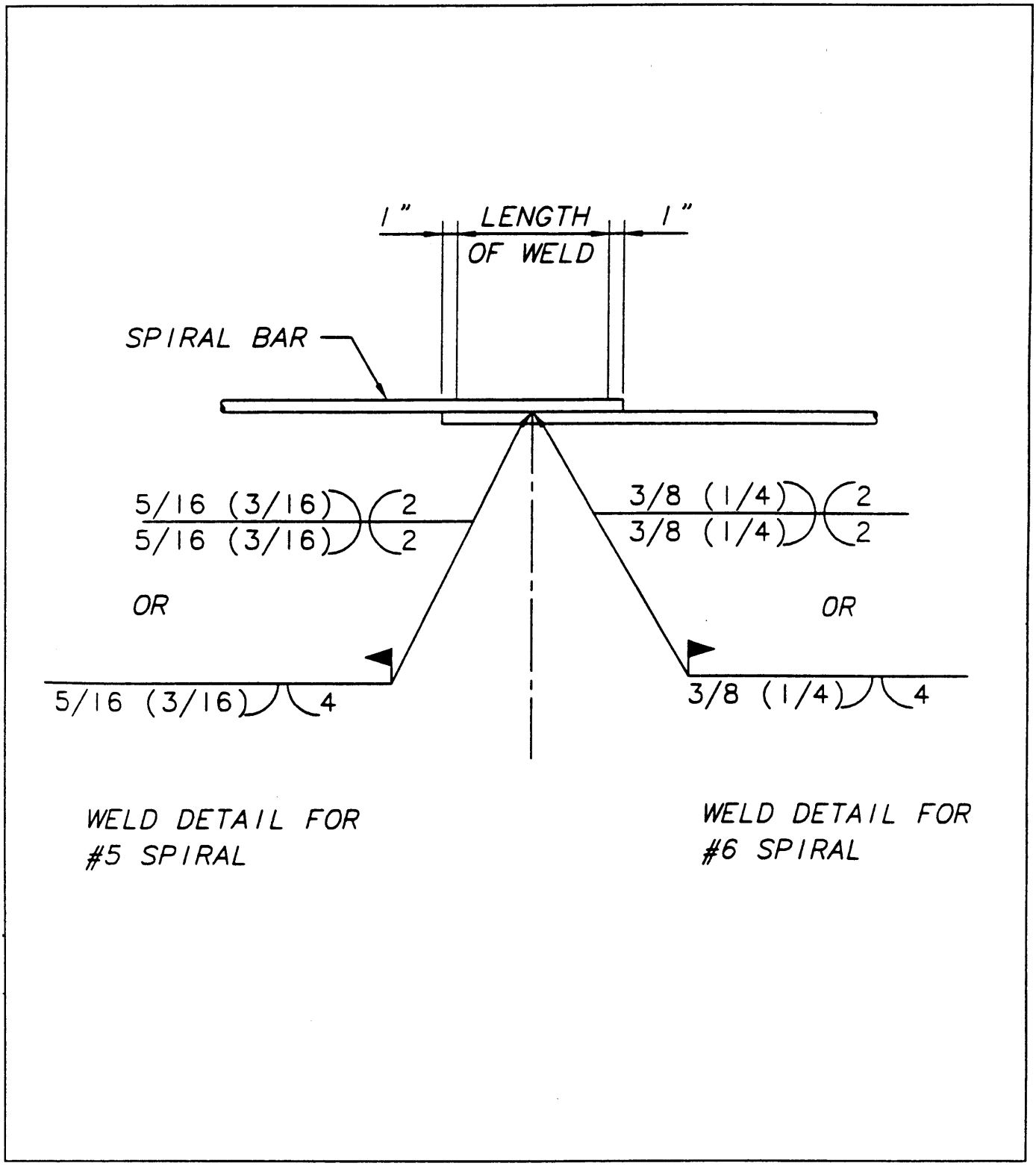

Figure 46 — Welded-Splice Spiral Detail

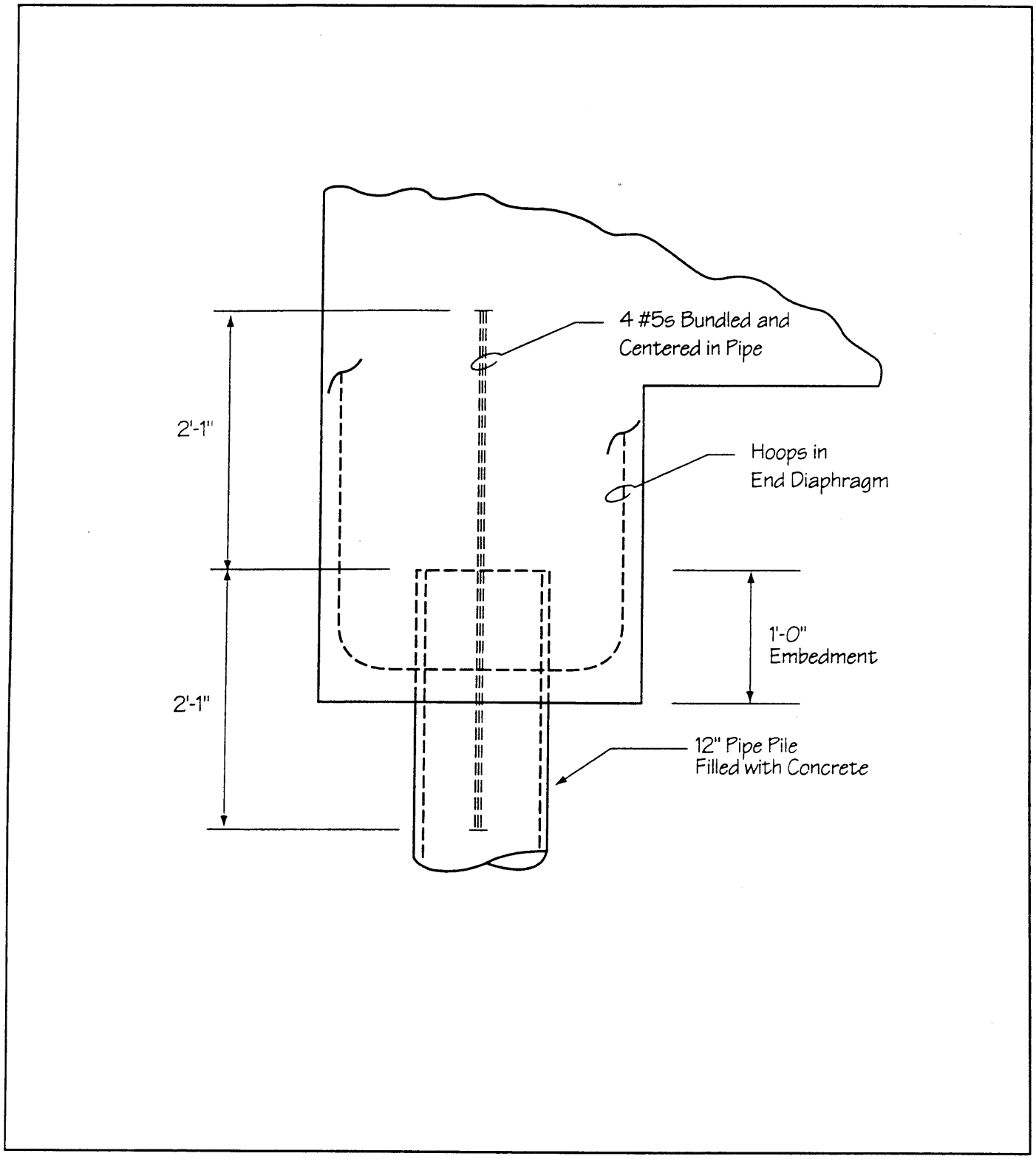

Figure 47 — Pipe Pile to End Diaphragm Connection Details

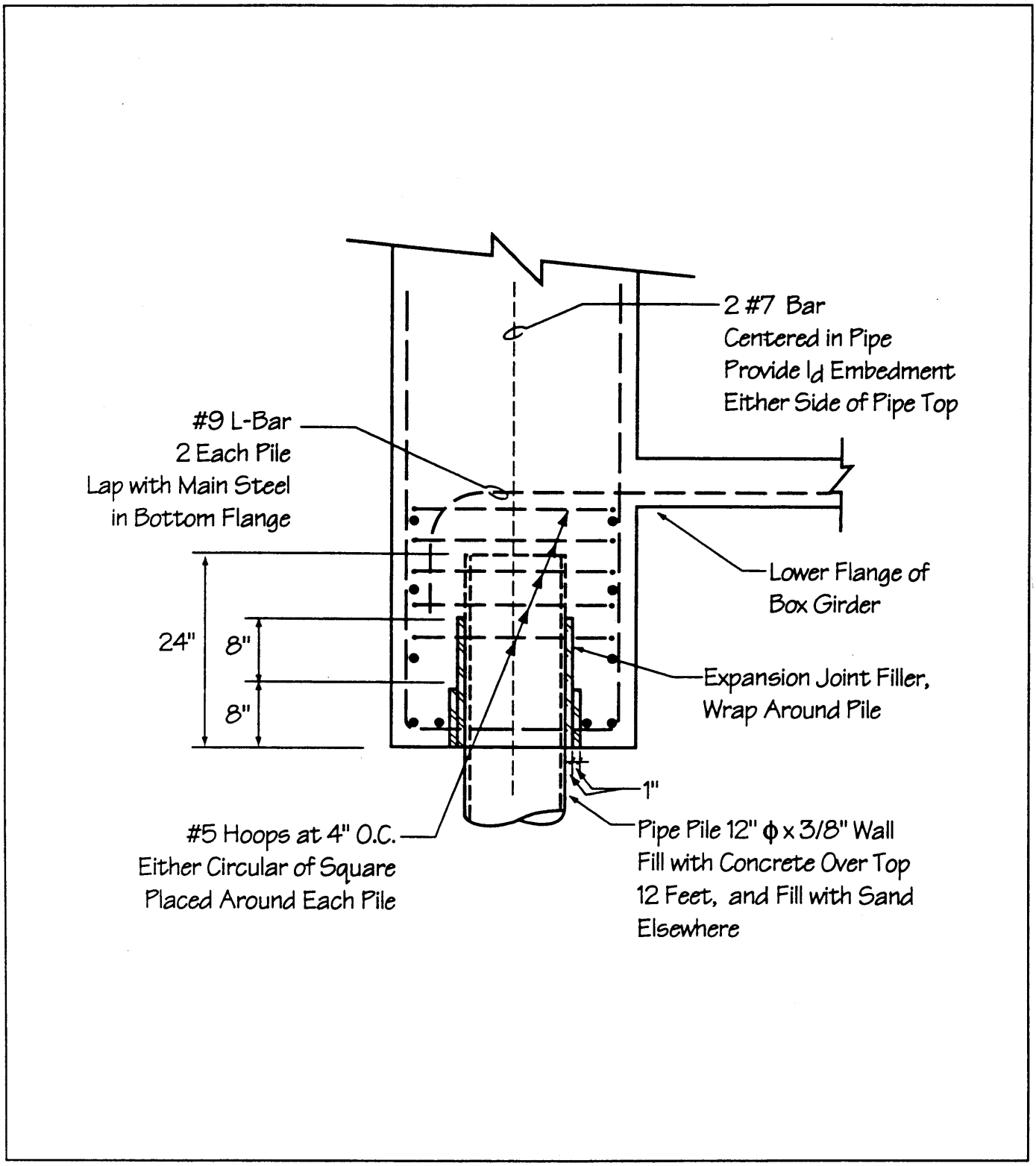

Figure 48 — Pipe Pile to End Diaphragm Connection Alternate Details

Section IV
Closing Statements

SECTION IV CLOSING STATEMENTS

SEISMIC PERFORMANCE

The seismic performance of this bridge is highly dependent on the manner in which the abutments behave. Due to the sharp curve (104-degree) and the integral abutment, the structure will experience different resistances depending on whether it is moving away from the backfill soil or into the backfill. This behavior, due to its directional dependence, is nonlinear, and therefore, the seismic behavior of the bridge can be bracketed only by using standard elastic analysis techniques.

Several models of the structure were considered; these included one without the backfill and one including the backfill. The response of the bridge when no backfill is present produces the more severe loading on the other substructure components, the piers and drilled shafts and the pipe piles at the abutments. This more severe loading case was used for the design of the various substructure elements.

The stiffnesses of the abutment pipe piles were developed using the Navy Facilities Engineering Command (NAVFAC DM7) approach to illustrate how a simple estimate of stiffness can be made. This is an easy approach for obtaining initial stiffnesses, but the method does not lend itself to adjustment for soil nonlinear effects at larger displacements. In this example, due to the stiffness of the abutment foundation elements, some nonlinearity of the soil may occur. However, this effect was not accounted for in the design, and the inclusion of the nonlinear effects would be a logical next step to take to improve the design.

The columns are founded on 60-foot-deep, 8-foot-diameter drilled shafts located in a medium-dense cohesionless soil deposit. The combination of the relatively stiff abutments, the intermediate acceleration coefficient, and the relatively flexible drilled shafts prevented any plastic hinging from occurring in the columns at the design earthquake level. This combination also prevented nonlinear action of the soil from occurring adjacent to the drilled shafts. If nonlinear response in the soil had occurred, it would not have been included in the analysis unless the soil to a depth of about two shaft diameters or more had been affected.

Due to the lack of significant inelastic demands, the columns may be reduced in cross section to perhaps produce a more efficient design. However, the columns as they are sized now, 3.5 by 5.5 feet, are relatively well proportioned relative to the rest of the structure. Other loadings,

SEISMIC PERFORMANCE (continued)

not directly considered in this example, might control how small the columns could be made. This is an area that might warrant additional consideration if another design iteration was made.

The pipe piles at the abutments attract quite a lot of load, as indicated by the fact that they experience some yielding, although they do not develop full plastic hinges. This slight yielding is deemed acceptable in this case since the chance of severe damage as a result of the piles yielding is highly unlikely. The relative stiffnesses of the abutments and piers also makes it essentially impossible to avoid these high pile forces. In fact if the same piles are fixed at their heads, the yielding problem is worsened many times, due to the increased abutment stiffness and to the concentration of bending that occurs at the end diaphragm/pile connection.

Finally the hierarchy of resistance is such that if the abutments soften significantly due to soil nonlinearity or due to shaking that is more severe than the design event, the bridge would still perform well. There is reserve capacity in the intermediate piers to accommodate extra load that might be shifted to them. Although the elastic forces controlled the design, the piers were nonetheless designed to withstand the plastic hinging shear force. This design choice was made to eliminate the possibility of brittle shear failure in the event of a larger earthquake.

Section V
References

SECTION V REFERENCES

AASHTO (1991). *Guide Specifications for Seismic Isolation Design*, American Association of State Highway and Transportation Officials, Washington, DC.

AASHTO (1993). *Standard Specifications for Highway Bridges,* American Association of State Highway and Transportation Officials, Washington, DC, 15th Edition, as Amended by the Interim Specifications, Division I-A, Commentary.

AASHTO (1994). *Proposed Revisions to the AASHTO Standard Specifications for Highway Bridges, Division I-A: Seismic Design*, National Center for Earthquake Engineering Research, Buffalo, NY.

AISC (1989). *Manual of Steel Construction, Allowable Stress Design*, Ninth Edition, American Institute of Steel Construction, Chicago, IL.

Caltrans (1989). *Bridge Design Aids Manual*, "Section 14 - Seismic, Dynamic Model Assumptions and Adjustments, October 1989," State of California, Department of Transportation, Sacramento, CA.

Conner, G.F. and Grant, W.P. (1995). "Seismic Analysis of Concrete Columns on Single Drilled Shafts," *Proceedings of the National Seismic Conference on Bridges and Highways*, Federal Highway Administration and State of California, Department of Transportation, San Diego, CA.

CSI (1994). *SAP90 Version 6.0 Beta Release*, Computers and Structures, Inc., Berkeley, CA.

FHWA (1987). *Seismic Design and Retrofit Manual for Highway Bridges*, Report No. FHWA-IP-87-6, Federal Highway Administration, National Technical Information Service, Springfield, VA.

FHWA (1988). *Drilled Shafts*, Report No. FHWA-HI-88-042, Federal Highway Administration, National Technical Information Service, Springfield, VA.

Gaylord, E.H., Gaylord, C.N., and Stallmeyer, J.E. (1992). *Design of Steel Structures*, Third Edition, McGraw-Hill, Inc., New York, NY.

REFERENCES
(continued)

Heins, C.P. (1975). *Bending and Torsional Design in Structural Members*, Lexington Books, D.C. Heath and Co., Lexington, MA.

NAVFAC (1986). *Foundations and Earth Structures*, Design Manual 7.02, Naval Facilities Engineering Command, Alexandria, VA.

PCA (1993). *PCACOL, Strength Design of Reinforced Concrete Column Sections*, Microcomputer Edition, Version 2.30, Portland Cement Association, Skokie, IL.

Popov, E.P. (1978). *Mechanics of Materials*, Prentice-Hall, Inc., Second Edition, Englewood Cliffs, NJ.

Poulos, H.G. and Davis, E.H. (1980). *Pile Foundation Analysis and Design*, John Wiley and Sons, New York, NY.

Reese, L.C. and Wang, S.H. (1993). *LPILEplus, Stress and Deformation Analysis of Piles Under Lateral Loading*, Ensoft, Inc., Austin, TX.

Scott, R.F. (1981). *Foundation Analysis*, Prentice-Hall, Englewood Cliffs, NJ.

Terzagi, K. (1955). *Evaluation of Coefficient of Subgrade Reaction, Geotechnique*, London, Vol. 5, No. 4, December.

Wang, C. and Salmon, C.G. (1992). *Reinforced Concrete Design*, Fifth Edition, Harper Collins Publishers Inc., New York, NY.

WSDOT (1995). *Bridge Design Manual*, Washington State Department of Transportation, Engineering Publications, Olympia, WA.

Young, W.C. (1989). *Roark's Formulas for Stress and Strain*, Sixth Edition, McGraw-Hill Book Company, New York, NY.

Appendix A
Geotechnical Data

APPENDIX A GEOTECHNICAL DATA

SUBSURFACE CONDITIONS

Subsurface conditions were derived from four borings, one at each abutment and interior pier. As shown in Figure A1, the subsurface conditions consist of coarse alluvial flood deposits. Although the borings extended only to depths of about 100 feet, geologic maps indicate these deposits extend to considerable depth (> 200 feet). The water table is located at the ground surface at the interior piers.

SOIL PROPERTIES

Soil properties for the subsurface materials are shown in Figure A1. These properties were estimated from empirical correlations to the standard penetration test resistance values in the borings. Laboratory tests may provide more detailed design values. New fill will be required at the abutments. The fill is anticipated to have similar properties to the native soils, as shown in Figure A1.

SOIL PROFILE TYPE

Type II — Deep cohesionless conditions where the soil depth exceeds 200 feet and the soils overlying the rock are stable deposits of sand and gravel.

SITE ACCELERATION

0.20g — Taken from AASHTO seismicity map.

FOUNDATION DESIGN

Abutments

Nominal 12-inch-diameter by 3/8-inch wall thickness closed-ended, concrete-filled pipe piles were chosen for design. These pipes are standard-weight pipes as listed by AISC (1989).

Axial capacity based on U.S. Army Corps of Engineers (1991).

Critical depth = 15 $\rho \cong$ 15 feet (for medium dense sand).

Tension

$$Q_{T\,ult} = f_s p L = K_t \sigma_{v\,avg} (\tan \delta)\, p L$$

where

$Q_{T\,ult}$ ultimate tension capacity of single pile (kips)

FOUNDATION DESIGN (continued)

K_t coefficient of lateral earth pressure (assumed as 0.67 for tension)

$\sigma_{v\ avg}$ average effective vertical stress over the length of the pile; effective stress increases linearly to the critical depth of 15 feet and is constant below this depth (ksf)

δ angle of friction between soil and steel pile (= 0.75ϕ)

p circumference of pile (3.34 feet)

L length of embedment of pile below ground surface (feet)

$Q_{T\ ult}$ = 0.67 (15′ x 0.1224kcf x 1/2) (tan 0.75 x 34) (3.34′)(15′)
+ 0.67 (15′ x 0.1224kcf)(tan 0.75 x 34)(3.34′)(25′)
= 64 kips

Compression

$Q_{C\ ult} = A_t q_t + K_c \sigma_{v\ avg} (\tan \delta)\ pL$

where

$Q_{C\ ult}$ ultimate compression capacity of single pile (kips)

K_c coefficient of lateral earth pressure (assumed as 2.0 for compression)

q_t tip resistance (ksf)
= where $N_q = 40$ for $\phi = 34°$

A_t area of tip of pile = $\pi/4\ (1.06')^2 = 0.887\ ft^2$

$Q_{C\ ult}$ = $(0.887\ ft^2)$(15′ x 0.1224kcf)(40)
+ (2.0)(15′ x 0.1224kcf x 1/2)(tan 0.75 x 34)(3.34′)(15′)
+ (2.0) (15′ x 0.1224kcf)(tan 0.75 x 34)(3.34′)(25′)
= 255 kips

Piers

60-foot-deep x 8-foot-diameter drilled shafts were chosen for design.

Axial capacity was based on Das (1995).

FOUNDATION DESIGN (continued)

Tension

$Q_{T\,ult} = K\sigma_{v\,avg}(\tan\delta)\,pL$

where

K $(1 - \sin\phi) = 0.44$

$\sigma_{v\,avg}$ $(30' \times 0.060kcf) = 1.8$ ksf

$\tan\delta$ $\tan(0.9 \times 34) = 0.59$

p $\pi(8') = 25.13'$

L $60'$

$Q_{T\,ult} = 0.44\,(1.8\text{ ksf})\,(0.59)\,(25.13')\,(60')$
$= 705$ kips

Compression

$Q_{C\,ult} = A_p q + Q_{T\,ult} = A_p\,(32\text{ ksf}) + Q_{T\,ult}$
$= \pi/4\,(8')^2\,(32\text{ ksf}) + 705$ kips
$\cong 2300$ kips

Lateral Resistance

Pile/drilled shaft stiffness values may be computed from simplified procedures (NAVFAC Design Manual 7.02, 1986) or from computer programs, such as LPILE^{plus} (Reese and Wang, 1993), that are widely used by various Departments of Transportation and design consultants.

OTHER CONCERNS

Liquefaction of the medium dense, silty sand soils was analyzed using the procedures of Seed et. al. (1984) and Seed and Harder (1990). The results indicated an adequate factor of safety against liquefaction.

Based on the proposed configuration, the abutment slopes have a static factor of safety of 1.8 and a dynamic factor of safety of 1.3, based on a pseudo-static analysis. These factors of safety are adequate.

REFERENCES

Das, B.M. (1995). *Principles of Foundation Engineering*, Third Edition, PWS Publishing Company, Boston, MA, p. 828.

Seed, H.B. and Harder, L.F., Jr. (1990). "SPT-Based Analysis of Cyclic Pore Pressure Generation and Undrained Residual Strength," Proceedings of the H. Bolton Seed Memorial Symposium, Vol. 2, edited by J. Michael Duncan, Published by BiTech Publishers, Ltd., pp. 351-376.

Seed, H.B., Tokimatsu, K., Harder, L.F., and Chung, R.M., 1984. "The Influence of SPT Procedures in Soil Liquefaction Resistance Evaluations," Berkeley, CA, University of California UCB/EERC-84/15.

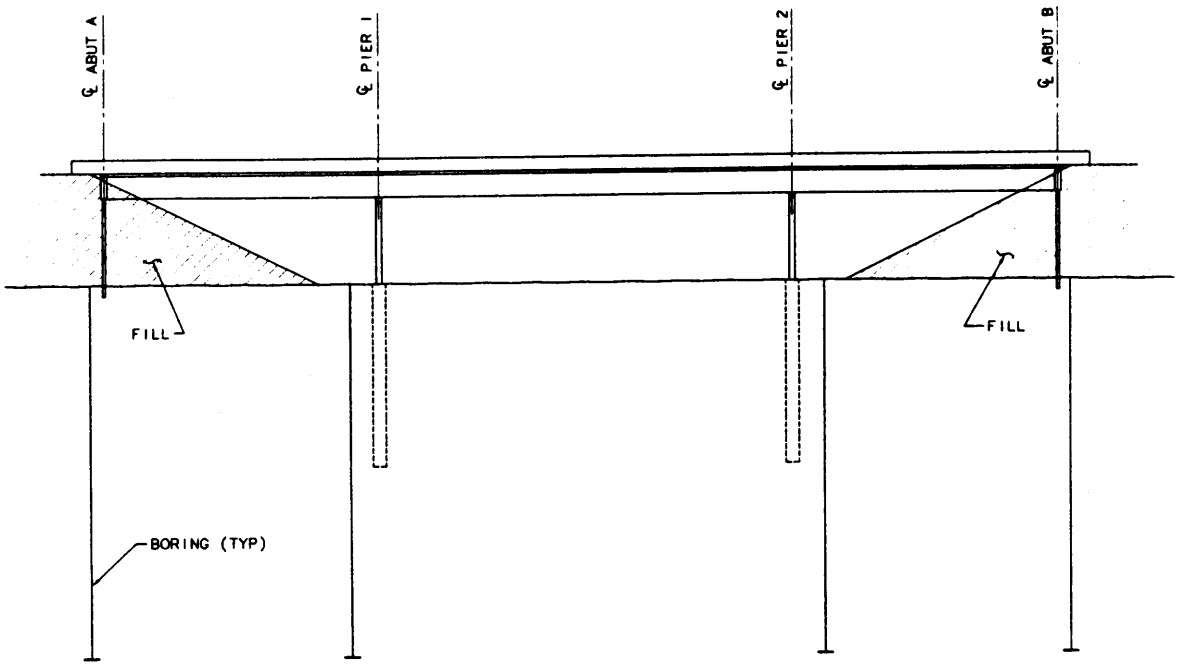

DEVELOPED ELEVATION

SOIL PROPERTIES

Stratum	Depth (ft)	Soil Description	N (bpf)	γ (pcf)	ϕ (deg)	c (pcf)	n_h (pci)
Alluvium	0 to > 100	Medium dense, silty sand	20	122.4	34	0	15
New Fill	Above grade	Medium dense sand and gravel	20	122.4	34	0	23

Where:

N standard penetration resistance (blows per foot)
γ total unit weight (pounds per cubic foot)
ϕ internal angle of friction (degrees)
c cohesion (pounds per square foot)
n_h constant of horizontal subgrade reaction (pounds per cubic foot)

Figure A1 — Subsurface Conditions

Appendix B
SAP90 V6.0 Beta Input

```
C Bridge 6 FHWA \ Input File for SAP90 Version 6.0 Beta

FHWA BRIDGE NO 6 B6SH15PA


SYSTEM

  LENGTH=FT  FORCE=KIP


COORDINATE

  NAME=CYL   X=0 Y=0 Z=0
             X=0 Y=-1 Z=0
             X=1 Y=-1 Z=0

  NAME=ABUTA X=160  Y=-4.626   Z=0
             X=0    Y=-4.626   Z=0
             X=159  Y=-4.626   Z=1

  NAME=PIER1  X=135.348  Y=-39.126   Z=85.329
              X=0        Y=-39.126   Z=0
              X=134.348  Y=-39.126   Z=85.329

  NAME=PIER2  X=50.452   Y=-39.126   Z=151.838
              X=0        Y=-39.126   Z=0
              X=49.452   Y=-39.126   Z=151.838

  NAME=ABUTB  X=-38.297  Y=-4.626   Z=155.349
              X=0        Y=-4.626   Z=0
              X=-39.297  Y=-4.626   Z=154.349

  NAME=EQK    X=0          Y=0     Z=0
              X=-0.7872    Y=0     Z=0.6167
              X=0          Y=0     Z=1


JOINT

  1         X=0        Y=0        Z=0
  1011      X=160      Y=0        Z=0
  1021      X=135.348  Y=0        Z=85.329
  1031      X=50.452   Y=0        Z=151.838
  1041      X=-38.297  Y=0        Z=155.349
  4101      X=160      Y=-4.626   Z=0
  4209      X=135.348  Y=-84.126  Z=85.329
  4210      X=135.348  Y=-82.126  Z=85.329
  4210,4224,1 X=135.348 Y=-82.126,-26.126 Z=85.329
  4225      X=135.348  Y=-24.126  Z=85.329
  4226      X=135.348  Y=-16.626  Z=85.329
  4227      X=135.348  Y=-9.126   Z=85.329
  4228      X=135.348  Y=-7.126   Z=85.329
  4229      X=135.348  Y=-5.126   Z=85.329
  4230      X=135.348  Y=-3.126   Z=85.329
  4309      X=50.452   Y=-84.126  Z=151.838
  4310      X=50.452   Y=-82.126  Z=151.838
  4310,4324,1 X=50.452 Y=-82.126,-26.126 Z=151.838
```

```
  4325      X=50.452 Y=-24.126 Z=151.838
  4326      X=50.452 Y=-16.626 Z=151.838
  4327      X=50.452 Y=-9.126 Z=151.838
  4328      X=50.452 Y=-7.126 Z=151.838
  4329      X=50.452 Y=-5.126 Z=151.838
  4330      X=50.452 Y=-3.126 Z=151.838
  4401      X=-38.297 Y=-4.626  Z=155.349


  CSYS=CYL SF=1
    1011,1018,1 CR=160 CA=0,28.2003
    1021,1028,1 CR=160 CA=32.2289,66.6958
    1031,1038,1 CR=160 CA=71.6197,99.8200


LOCAL

  ADD=4101 CSYS=ABUTA
  ADD=4209,4230,1 CSYS=PIER1
  ADD=4309,4330,1 CSYS=PIER2
  ADD=4401 CSYS=ABUTB
  ADD=1011,1018,1 CSYS=EQK
  ADD=1021,1028,1 CSYS=EQK
  ADD=1031,1038,1 CSYS=EQK
  ADD=1041 CSYS=EQK


RESTRAINTS

  ADD=4209 DOF=UY
  ADD=4309 DOF=UY


SPRING

  CSYS=ABUTA
    ADD=4101 U1=2569 U2=291700 U3=2074 R1=3.97E7 R2=3.50E5 ;no abut soil restraint
  CSYS=ABUTB
    ADD=4401 U1=2569 U2=291700 U3=2074 R1=3.97E7 R2=3.50E5 ;no abut soil restraint
  CSYS=PIER1
    ADD=4210 U1=26*232 U3=26*232
    ADD=4211 U1=26*216 U3=26*216
    ADD=4212 U1=26*200 U3=26*200
    ADD=4213 U1=26*184 U3=26*184
    ADD=4214 U1=26*168 U3=26*168
    ADD=4215 U1=26*152 U3=26*152
    ADD=4216 U1=26*136 U3=26*136
    ADD=4217 U1=26*120 U3=26*120
    ADD=4218 U1=26*104 U3=26*104
    ADD=4219 U1=26*88  U3=26*88
    ADD=4220 U1=26*72  U3=26*72
    ADD=4221 U1=26*56  U3=26*56
    ADD=4222 U1=26*40  U3=26*40
    ADD=4223 U1=26*24  U3=26*24
    ADD=4224 U1=26*8   U3=26*8
```

```
  CSYS=PIER2
    ADD=4310 U1=26*232 U3=26*232
    ADD=4311 U1=26*216 U3=26*216
    ADD=4312 U1=26*200 U3=26*200
    ADD=4313 U1=26*184 U3=26*184
    ADD=4314 U1=26*168 U3=26*168
    ADD=4315 U1=26*152 U3=26*152
    ADD=4316 U1=26*136 U3=26*136
    ADD=4317 U1=26*120 U3=26*120
    ADD=4318 U1=26*104 U3=26*104
    ADD=4319 U1=26*88  U3=26*88
    ADD=4320 U1=26*72  U3=26*72
    ADD=4321 U1=26*56  U3=26*56
    ADD=4322 U1=26*40  U3=26*40
    ADD=4323 U1=26*24  U3=26*24
    ADD=4324 U1=26*8   U3=26*8

MASS

  ADD=1021 UX=79/32.2 UY=79/32.2 UZ=79/32.2          ;pier diaphragm
  ADD=1031 UX=79/32.2 UY=79/32.2 UZ=79/32.2          ;  "
  ADD=1015 UX=15/32.2 UY=15/32.2 UZ=15/32.2          ;inter. diaphr.
  ADD=1025 UX=15/32.2 UY=15/32.2 UZ=15/32.2          ;  "
  ADD=1035 UX=15/32.2 UY=15/32.2 UZ=15/32.2          ;  "
  ADD=1011 UX=119/32.2 UY=119/32.2 UZ=119/32.2       ;abutment diaphr
  ADD=1041 UX=119/32.2 UY=119/32.2 UZ=119/32.2       ;  "
  ADD=1011 UX=5.06/32.2 UY=5.06/32.2 UZ=5.06/32.2    ;barriers
  ADD=1012,1018,1 UX=10.1/32.2 UY=10.1/32.2 UZ=10.1/32.2 ; "
  ADD=1021,1028,1 UX=12.4/32.2 UY=12.4/32.2 UZ=12.4/32.2 ; "
  ADD=1031,1038,1 UX=10.1/32.2 UY=10.1/32.2 UZ=10.1/32.2 ; "
  ADD=1041 UX=5.06/32.2 UY=5.06/32.2 UZ=5.06/32.2    ;barriers

MATERIAL

  NAME=CONC TYPE=ISO M=0.15/32.2  W=0.15  IDES=C
    E=519000  U=0.18
  NAME=SHAFT TYPE=ISO M=0.0/32.2  W=0.00  IDES=C
    E=519000  U=0.18
  NAME=RIGID TYPE=ISO M=0 W=0 IDES=C
    E=519000 U=0.18

SECTION

  NAME=SUPER MAT=CONC A=56.22 I=250,6800 J=777
  NAME=ENDDI MAT=RIGID A=10000 I=10E6,10E6 J=10E6
  NAME=RIGID MAT=RIGID A=10000 I=10E6,10E6 J=10E6
  NAME=PIER1 MAT=CONC SH=R T=3.5,28
  NAME=PIER2 MAT=CONC SH=R T=3.5,20
  NAME=PIER3 MAT=CONC SH=R T=3.5,10
  NAME=PIER4 MAT=CONC SH=R T=3.5,5.5
  NAME=SHAFT MAT=SHAFT SH=P T=8
```

```
FRAME

  CSYS=CYL

  5011 J=1011,1012 SEC=SUPER PLANE12=-CZ    ;superstructure elements
  5018 J=1018,1021 SEC=SUPER PLANE12=-CZ    ;    "
  5021 J=1021,1022 SEC=SUPER PLANE12=-CZ    ;    "
  5028 J=1028,1031 SEC=SUPER PLANE12=-CZ    ;    "
  5031 J=1031,1032 SEC=SUPER PLANE12=-CZ    ;    "
  5038 J=1038,1041 SEC=SUPER PLANE12=-CZ    ;    "

  GEN=5011,5017,1 IINC=1 JINC=1             ;generate superstructure elements
  GEN=5021,5027,1 IINC=1 JINC=1             ;    "
  GEN=5031,5037,1 IINC=1 JINC=1             ;    "

  7101 J=4101,1011 SEC=ENDDI PLANE13=-CR    ;abuta rigid link
  7401 J=4401,1041 SEC=ENDDI PLANE13=-CR    ;abutb rigid link

  7209 J=4209,4210 SEC=SHAFT PLANE13=-CR    ;pier 1 elements
  GEN=7209,7224,1 IINC=1 JINC=1
  7225 J=4225,4226 SEC=PIER4 PLANE13=-CR    ;    "
  7226 J=4226,4227 SEC=PIER4 PLANE13=-CR    ;    "
  7227 J=4227,4228 SEC=PIER3 PLANE13=-CR    ;    "
  7228 J=4228,4229 SEC=PIER2 PLANE13=-CR    ;    "
  7229 J=4229,4230 SEC=PIER1 PLANE13=-CR    ;    "
  7230 J=4230,1021 SEC=RIGID PLANE13=-CR    ;    "


  7309 J=4309,4310 SEC=SHAFT PLANE13=-CR    ; pier 2 elements
  GEN=7309,7324,1  IINC=1 JINC=1
  7325 J=4325,4326 SEC=PIER4 PLANE13=-CR    ;    "
  7326 J=4326,4327 SEC=PIER4 PLANE13=-CR    ;    "
  7327 J=4327,4328 SEC=PIER3 PLANE13=-CR    ;    "
  7328 J=4328,4329 SEC=PIER2 PLANE13=-CR    ;    "
  7329 J=4329,4330 SEC=PIER1 PLANE13=-CR    ;    "
  7330 J=4330,1031 SEC=RIGID PLANE13=-CR    ;    "


LOAD
  CSYS=0
  NAME=DL
    TYPE=GRAVITY ELEM=FRAME
      ADD=* UY=-1
    TYPE=FORCE
      ADD=1021,1031,10 UY=-79
      ADD=1015,1035,10 UY=-15
      ADD=1012,1018,1 UY=-10.1
      ADD=1021,1028,1 UY=-12.4
      ADD=1031,1038,1 UY=-10.1

  NAME=CONC
    TYPE=FORCE
      ADD=1025 UX=616.7 UZ=787.2
```

```
MODES

  TYPE=EIGEN  N=10


FUNCTION

  NAME=ACCSPEC NPL=1
    0.0    0.50
    0.4372 0.50
    0.45   0.4904
    0.5    0.4572
    0.55   0.429
    0.6    0.4048
    0.65   0.3838
    0.7    0.3653
    0.75   0.3489
    0.8    0.3342
    0.9    0.309
    1.0    0.288
    1.2    0.255
    1.4    0.2301
    1.6    0.2105
    1.8    0.1946
    2.0    0.1814
    2.4    0.1607
    2.8    0.145
    3.0    0.1385
   10.0    0.062

SPEC

  CSYS=EQK
  NAME=RADEQK   DAMP=0.05
    ACC=X   FUNC=ACCSPEC  SF=32.2
  NAME=CHRDEQK  DAMP=0.05
    ACC=Z   FUNC=ACCSPEC  SF=32.2


OUTPUT

  ELEM=JOINT  OUT=DISP,REAC  LOAD=*   SPEC=*
    ADD=1011,1041,10
    ADD=4101,4401,100
    ADD=4225,4325,100
    ADD=1025
    ADD=4210,4224,1
  ELEM=FRAME  OUT=FORCE  LOAD=*   SPEC=*
    ADD=7101,7401,100
    ADD=7209,7229,1
    ADD=7309,7329,1
```